



UNIVERSITAT DE
BARCELONA

Comprehensive Molecular Characterization of Childhood Liver Cancer: Identification of Prognostic Biomarkers

Marina Simon Coma

ADVERTIMENT. La consulta d'aquesta tesi queda condicionada a l'acceptació de les següents condicions d'ús: La difusió d'aquesta tesi per mitjà del servei TDX (www.tdx.cat) i a través del Dipòsit Digital de la UB (diposit.ub.edu) ha estat autoritzada pels titulars dels drets de propietat intel·lectual únicament per a usos privats emmarcats en activitats d'investigació i docència. No s'autoritza la seva reproducció amb finalitats de lucre ni la seva difusió i posada a disposició des d'un lloc aliè al servei TDX ni al Dipòsit Digital de la UB. No s'autoritza la presentació del seu contingut en una finestra o marc aliè a TDX o al Dipòsit Digital de la UB (framing). Aquesta reserva de drets afecta tant al resum de presentació de la tesi com als seus continguts. En la utilització o cita de parts de la tesi és obligat indicar el nom de la persona autora.

ADVERTENCIA. La consulta de esta tesis queda condicionada a la aceptación de las siguientes condiciones de uso: La difusión de esta tesis por medio del servicio TDR (www.tdx.cat) y a través del Repositorio Digital de la UB (diposit.ub.edu) ha sido autorizada por los titulares de los derechos de propiedad intelectual únicamente para usos privados enmarcados en actividades de investigación y docencia. No se autoriza su reproducción con finalidades de lucro ni su difusión y puesta a disposición desde un sitio ajeno al servicio TDR o al Repositorio Digital de la UB. No se autoriza la presentación de su contenido en una ventana o marco ajeno a TDR o al Repositorio Digital de la UB (framing). Esta reserva de derechos afecta tanto al resumen de presentación de la tesis como a sus contenidos. En la utilización o cita de partes de la tesis es obligado indicar el nombre de la persona autora.

WARNING. On having consulted this thesis you're accepting the following use conditions: Spreading this thesis by the TDX (www.tdx.cat) service and by the UB Digital Repository (diposit.ub.edu) has been authorized by the titular of the intellectual property rights only for private uses placed in investigation and teaching activities. Reproduction with lucrative aims is not authorized nor its spreading and availability from a site foreign to the TDX service or to the UB Digital Repository. Introducing its content in a window or frame foreign to the TDX service or to the UB Digital Repository is not authorized (framing). Those rights affect to the presentation summary of the thesis as well as to its contents. In the using or citation of parts of the thesis it's obliged to indicate the name of the author.



Universitat de Barcelona



Programa de Doctorat en Biomedicina
Universitat de Barcelona

Comprehensive Molecular Characterization Of Childhood Liver Cancer: Identification Of Prognostic Biomarkers

Tesi doctoral presentada per:

Marina Simon Coma

per obtenir el títol de Doctora en Biomedicina
per la Universitat de Barcelona

Directora:

Dra. Carolina Armengol Niell

Institut d'Investigació en
Ciències de la Salut Germans
Trias i Pujol

Tutor:

Dr. Oriol Bachs Valldeneu

Universitat de Barcelona

Badalona, 2017

Al papa,

*Més tenaçment que mai, m'esforço a créixer
sabent que tu creixes amb mi: projectes,
il·lusions, desigs, prenen volada
per tu i amb tu, per molt distants que et siguin,
i amb tu i per tu somnio d'acomplir-los.*

Miquel Martí i Pol

A en Raül, aquesta tesi és mig teva

TABLE OF CONTENTS

LIST OF TABLES	1
LIST OF FIGURES	3
ABBREVIATIONS	5
1. INTRODUCTION	9
1.1 Childhood cancer	11
1.2 Liver tumors in childhood: clinical and pathological features	12
1.2.1 Hepatoblastoma (HB)	13
1.2.1.1 Incidence	13
1.2.1.2 Etiology and risk factors	13
1.2.1.3 Diagnosis	14
1.2.1.4 Prognosis, clinical stratification and treatment	14
1.2.1.5 Pathology	25
1.2.2 Pediatric Hepatocellular Carcinoma (pHCC)	31
1.2.2.1 Incidence	31
1.2.2.2 Etiology and risk factors	31
1.2.2.3 Diagnosis	32
1.2.2.4 Prognosis, clinical stratification and treatment	32
1.2.2.5 Pathology	34
1.3 Biology of pediatric liver tumors	36
1.3.1 Gene mutations	37
1.3.2 Gene fusions	41
1.3.3 Copy Number Variations (CNV)	41
1.3.4 Allelic imbalances	46
1.3.5 Gene expression profiles	47
1.3.6 Proteomic markers	50
1.3.7 Epigenetic features	52
1.4 Experimental models of liver cancer: patient derived xenografts	53
2. AIMS	55
3. PATIENTS, MATERIALS AND METHODS	59
3.1 Establishment of a collection of biological samples from pediatric patients with liver cancer and healthy individuals	61
3.1.1 Patients inclusion	61
3.1.2 Biological samples obtaining and storage	62
3.1.2.1 Blood and derivatives	62
3.1.2.2 Tissue samples	62
3.1.3 Clinical and pathological data registry	63
3.1.5 Molecular characterization of the samples	63
3.2. Proteomic study	64
3.1.1 Patients, tissue and plasma samples	64
3.1.2 Protein study	66
3.1.2.1 Protein isolation and quantification	66
3.1.2.2 Proteomic analysis	66
3.1.2.2.1 Two Dimension Gel Electrophoresis	67
2D-DIGE Spot digestion and protein identification	68
3.1.2.2.2 Label-Free LC-MS and peptide identification	68
3.1.2.2.3 Mass spectrometry analysis	69
3.1.2.2.3.1 MALDI-TOF/TOF analysis	69
3.1.2.2.3.2 LTQ Orbitrap XL analysis	70
3.1.2.2.4 Database searches	70
3.1.2.3 Western Blot (WB)	71
3.1.2.4 Immunohistochemistry (IHC)	73
3.1.2.5 Enzyme-Linked ImmunoSorbent Assay (ELISA)	74
3.1.3 Bioinformatic analysis	75

3.1.3.1 Pathway analysis	75
3.1.3.2 Bioinformatics analysis of proteomic data	75
3.1.3.3. Statistical analysis	76
3.3 Genomic and RNAseq study	77
3.2.1 Patients and tissue samples	77
3.2.2 RNA Study	79
3.2.2.1 RNA isolation quantification and quality control	79
3.2.2.4 RNA sequencing	81
3.2.2.5 Retrotranscription	82
3.2.2.6 Droplet Digital PCR (ddPCR)	82
3.2.3 DNA Study	84
3.2.3.1 DNA isolation and quantification	84
3.2.3.3 Cytoscan HD Array	85
3.2.3.4 PCR	87
3.2.3.5 Quantitative real Time PCR (qRT-PCR)	88
3.2.3.6 Sanger Sequencing	90
3.2.4. Statistical analysis	90
4. RESULTS	93
4.1 Establishment of a collection of biological samples from pediatric patients with liver cancer and healthy individuals.	95
4.2. Proteomic study	99
4.2.1 Proteomic profile of HB	101
4.2.2 Deregulated proteins in aggressive HB tumors	109
4.2.3 Identification of a 3-protein signature	113
4.2.4 Assessment of the prognostic value of the 3-protein signature in an independent cohort	115
4.2.5 Plasma expression of C1QBP	125
4.2.6 Integrative analysis of the proteomic, genomic and transcriptomic data	126
4.3. Genomic and RNAseq study of pediatric liver tumors	130
4.3.1 RNA sequencing analysis	132
4.3.1.1 Fusion protein identification	132
4.3.1.2 Mutational analysis	135
4.3.1.3 Editing analysis	138
4.3.2 Comprehensive genomic study of pediatric liver tumors and recurrences	140
4.3.2.1 Copy Number Variations and allelic imbalances in primary HB and recurrences	140
4.3.2.1.3 Small overlapping regions of imbalance (SORI) analysis	146
4.3.2.4 CNV and LOH in Patient-Derived Xenografts and their primary tumors	147
4.3.2.5 CNV and LOH in pHCC	150
4.3.2.6 Correlation of main genomic imbalances and their impact on patient prognosis	152
4.3.2.6 Prognostic genomic classification in HB	154
4.3.3 Molecular classification of HB	158
5. DISCUSSION	161
6. CONCLUSIONS	179
7. REFERENCES	183
8. ACKNOWLEDGEMENTS	199

LIST OF TABLES

Table 1. Summary of the main clinical trials on HB. _____	27
Table 2. Top mutated genes in HB, NOS and HCC. _____	43
Table 3. Frequent chromosomal imbalances identified in HB. _____	47
Table 4. Chromosomal imbalances found in HB and HCC. HB data is a compilation of 16 already published studies. _____	48
Table 5. Main features of C1 and C2 HB subtypes. _____	51
Table 6. Immunohistochemical stains useful for the diagnosis of HB. _____	55
Table 7. Clinical, pathological and molecular features of the 160 patients included in the study. _____	67
Table 8. List and details of the different antibodies used for WB. _____	73
Table 9. Clinical and pathological features of the 27 patients and healthy individuals included in the ELISA study. _____	75
Table 10. Main clinical, pathological and features of the 56 patients included in the genomic and RNAseq study. _____	80
Table 11. Primers and probes used for ddPCR. _____	85
Table 12. Primers used for conventional PCR. _____	89
Table 13. Primers used for qRT-PCR. *Housekeeping gene _____	90
Table 14. Proteins identified both by DIGE and LF _____	101
Table 15. Deregulated proteins in HB. _____	102
Table 16. Deregulated proteins in HB involved in the top deregulated pathways identified by IPA. _____	105
Table 17. Top deregulated proteins in aggressive C2 tumors. _____	108
Table 18. Deregulated proteins in C2 tumors involved in EIF2 signaling pathway. _____	110
Table 19. Association of the 3 proteins with age and AFP levels at diagnosis. P-val, unpaired t-test p-value. _____	115
Table 20. Association of the 3 proteins with clinical, pathological and molecular features. _____	116
Table 21. Univariate analysis. _____	117
Table 22. Multivariate analysis. _____	120
Table 23. Correlated proteins at protein and DNA level. _____	124
Table 24. Top correlated genes at protein and RNA level in C2 vs C1 tumors. _____	125
Table 25. Fusion transcripts in HB identified by RNAseq. _____	129
Table 26. Top mutated genes validated in HB. _____	131
Table 27. Gains with CN>3 found in primary HB tumors. _____	140
Table 28. Homozygous deletions found in primary HB tumors. _____	141
Table 29. Comparison of the main genomic imbalances identified in HB, PDX and pHCC and univariate analysis. _____	149
Table 30. Association of clinical, pathological and molecular data to the genomic classification of HB. _____	152

LIST OF FIGURES

Figure 1. Incidence of pediatric tumors in Spain is similar to other European countries.	13
Figure 2. Summary of the different clinical trials conducted on HB.	17
Figure 3. PRETEXT system.	19
Figure 4. SIOPEL patient clinical stratification 2012.	21
Figure 5. Risk stratification trees CHIC-Hepatoblastoma Stratification (CHIC-HS) system.	25
Figure 6. Histological patterns of HB (López-Terrada et al., 2013).	27
Figure 7. Epithelial HB histology types.	30
Figure 8. Mixed HB histotype.	31
Figure 9. NOS histology.	32
Figure 10. pHCC histology types.	37
Figure 11. Wnt/ β -catenin pathway.	41
Figure 12. CNVs in HB reported in the literature.	45
Figure 13. Workflow followed on the proteomic study.	64
Figure 14. Workflow followed on the genomic and transcriptomic study.	77
Figure 15. Temperature scheme for retrotranscription.	82
Figure 16. Temperature scheme used for ddPCR.	83
Figure 17. PCR temperature conditions.	87
Figure 18. Temperature scheme for qRT-PCR.	89
Figure 19. Temperature scheme for Sanger sequencing.	90
Figure 20. Prospective collected samples since 2009.	96
Figure 21. Hierarchical cluster analysis of the proteomic data.	99
Figure 22. Top deregulated pathways in HB vs. NT according to the IPA analysis.	103
Figure 23. Validation of the top deregulated pathways Akt and Hippo by WB.	105
Figure 24. Deregulation of the EIF2 pathway in aggressive C2 HB.	110
Figure 25. Identification of 3 prognostic biomarkers.	111
Figure 26. 3-protein signature definition.	112
Figure 27. Representative immunohistochemical staining of the 3 protein signature.	113
Figure 28. Survival analysis of the 3 biomarkers individually and the 3-protein signature.	118
Figure 29. Clinical CHIC-HS and 3-protein signature survival analysis.	120
Figure 30. 3-protein signature survival analysis in non-treated specimens.	121
Figure 31. Plasmatic levels of C1QBP in pediatric control individuals and liver cancer patients assessed by ELISA.	122
Figure 32. CIRCOS plot of the proteomic, transcriptomic and genomic data.	125
Figure 33. Validation of the fusion events identified in HB.	129
Figure 34. CTNNB1 gene mutations and deletions.	131
Figure 35. BLCAP nt5 editing validation.	132

Figure 36. RNA editing analysis. _____	133
Figure 37. ADAR1 and ADAR2 gene expression assessed by qPCR and correlation with BLCAP and global editing. _____	134
Figure 38. Number of chromosomal and allelic imbalances in primary HB tumors. ____	136
Figure 39. Copy number variations analysis in HB. _____	137
Figure 40. Allelic imbalances in HB. _____	138
Figure 41. Number of SORIs identified per chromosome. _____	141
Figure 42. Copy number variations in primary HB tumors and their PDXs. _____	143
Figure 43. LOH in primary HB tumors and their PDXs. _____	144
Figure 44. Copy number variations and allelic imbalances in pHCC. _____	146
Figure 45. Genomic classification of HB. _____	150
Figure 46. Genomic classification validation. _____	152
Figure 47. Molecular classification of HB. _____	153

ABBREVIATIONS

2-D DIGE, Two-Dimension
Fluorescence Difference Gel
Electrophoresis

AFP, Alpha Fetoprotein
APC, Adenomatous Polyposis Coli

BAC, Bacterial Artificial
Chromosome
BLCAP, Bladder-cancer associated
protein
Bp, Base Pairs
BWS, Beckwith-Weidmann syndrome

C1QBP, complement C1q binding
protein

C5V, cisplatin + fluorouracil +
vincristine

CARBO, carboplatin

CC, carboplatin + cisplatin

CDDP, cisplatin

CITA, cisplatin + pirarubicin

CHAPS, 3-[(3-cholamidopropyl)
dimethylammonio]-1-
propanesulfonate

CHIC, Children's Hepatic tumors
International Collaboration

CHIC-HS, Children's Hepatic tumors
International Collaboration
Hepatoblastoma Stratification

pHCC, Pediatric Hepatocellular
Carcinoma

CKAP4, cytoskeleton associated
protein 4

CN, Copy Number

CNS, Central Nervous System

CNV, Copy Number Variation

COG, Children's Oncology Group

CST, Childhood Solid Tumors

CTNNB1, Catenin Beta 1

CRYL1, crystallin lambda 1

c-LOG, Childhood Liver Oncology
Group

DOXO, doxorubicin

DKK1, Dickkopf-1

DTT, Dithiothreitol

EFS, Event Free Survival

EIF2, Eukaryotic Initiation Factor-2

ELISA, Enzyme-Linked
ImmunoSorbent Assay

EpCAM, epithelial cell adhesion
molecule

EPHB4, EPH receptor B4

FA, Fractional Abundance

FAP, Familial Adenomatous
Polyposis

FFPE, Formalin-Fixed Paraffin-
Embedded

FL, Fetal Liver

FL-pHCC, Fibrolamellar
Hepatocellular Carcinoma

GEETHI, Grupo Español para el
Estudio de Tumores Hepáticos
Infantiles

GPC3, Glypican 3

GPOH, German society for Pediatric
Oncology and Hematology

HB, Hepatoblastoma

HCC, Hepatocellular Carcinoma

IA, Iodoacetamide

ICC, Intrahepatic
Cholangiocarcinoma

IEF, Isoelectric Focusing

IFO, ifosfamide

IGF2, Insulin like growth factor 2

IGTP, Health Science Research
Institute Germans Trias i Pujol

IHC, immunohistochemistry

IPA, Ingenuity Pathway Analysis

IPA, Ifosfamide + cisplatin +
doxorubicin

ISR, integrated stress response

ITEC, ifosfamide + pirarubicin +
etoposide + carboplatin

JPLT, Japanese Study Group for
Pediatric Liver Tumors

LF, nano-LC-ESI-MS/MS Label free

LI, Labeling Index

LOH, Loss of Heterozygosity

MiR, microRNA

MS, Mass Spectrometry

NFE2L2, Nuclear Factor, Erythroid 2 Like 2

NOS, Hepatocellular Malignant Neoplasm

NT, Non-tumor

nt, Nucleotide

OS, Overall Survival

PA-CI, cisplatin + *doxorubicin*

PBL, Peripheral Blood Lymphocytes

PCR, Polymerase Chain Reaction

PLADO, cisplatin + *doxorubicin*

PDX, Patient-Derived Xenograft

pHCC, Pediatric Hepatocellular Carcinoma

Ppm, Parts per Million

PRETEXT, PREtreatment EXTent of disease

qPCR, Quantitative Polymerase Chain Reaction

R, Recurrence

RMD, Rare Mutation Detection

Rpm, Revolutions Per Minute

RT, Room Temperature

RT-PCR, Retrotranscription Polymerase Chain Reaction

SCU, Small Cell Undifferentiated

SDS-PAGE, Sodium Dodecyl Sulfate Polyacrylamide Gel Electrophoresis

SEHOP, Sociedad Española de Hematología y Oncología Pediátricas

SIOPEL, Société Internationale d'Oncologie Pédiatrique – Epithelial Liver Tumor Study group

SNP, Single Nucleotide Polymorphism

SORI, Small Overlapping Region of Imbalance

STS, Soft Tissue Sarcomas

T, Tumor

TERT, Telomerase Reverse Transcriptase

TLCT, Transitional Liver Cell Tumors

TMA, Tissue Microarrays

UPD, Uniparental Disomy

VP, etoposide

Vs., Versus

WES, Whole-Exome Sequencing

YAP, Yes-associated protein

1. INTRODUCTION

1.1 Childhood cancer

Malignant tumors in children and adolescents are rare events, even though they represent approximately 1-2% of all cancers and are one of the leading causes of death from disease in this population (Crist and Larry, 1991; Grovas *et al.*, 1997; Zarzosa *et al.*, 2017). During the 80s and 90s, the curation rate for solid tumors increased as much as 50%, mostly due to the definition of histologic subtypes related to prognosis that were incorporated in the clinical staging systems, the improvement of tumor imaging techniques and the progress of chemotherapeutic treatments with decreased side effects (Crist and Larry, 1991).

In Spain, 155.5 new cases per million children among 0-14 years are diagnosed each year according to the last report of the Spanish Registry of Childhood Tumors of the Spanish Society of Pediatric Hematology and Oncology (RETI-SEHOP) (R Peris Bonet *et al.*, 2016). The incidence of the different tumor types in Spain is similar to neighbor countries such as France, Germany or the United Kingdom (Figure 1A) (Reti-Sehop, 2014).

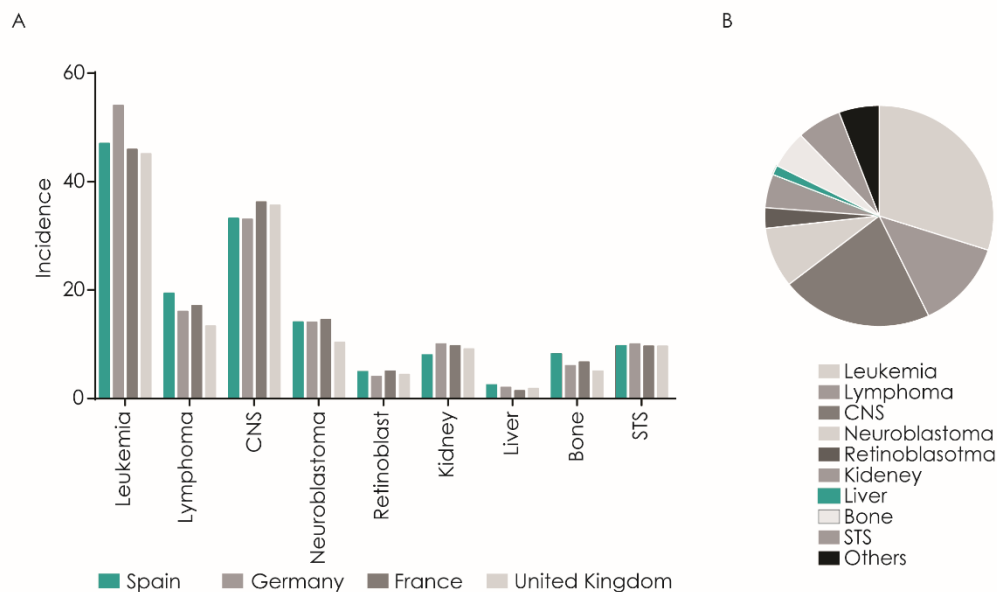


Figure 1. Incidence of pediatric tumors in Spain is similar to other European countries. Comparison of the incidence of the main childhood tumors in Spain, Germany, France and United Kingdom (A). Incidence of the different tumor types in Spain (B). Abbreviations: CNS, Central Nervous System; STS, Soft Tissue Sarcomas. Modified from the RETI-SEHOP report (Reti-Sehop, 2014).

According to the RETI-SEHOP report of 2014, °main tumors in childhood are leukemia (30%) and CNS tumors (21.5%) followed by Lymphomas (12.9%) and Neuroblastoma (8.8%). Liver tumors represent the seventh most frequent childhood cancer in Spain (*Figure 1B*).

1.2 Liver tumors in childhood: clinical and pathological features

Pediatric liver tumors can be categorized as benign or malignant and as some of the benign lesions can undergo malignant transformation, the therapeutic strategy can change (Emre, Umman and Rodriguez-Davalos, 2012). Benign lesions of the liver in childhood represent about 30% of pediatric primary liver masses and comprise hepatic hemangioendothelioma, mesenchymal hamartoma, focal nodular hyperplasia, nodular regenerative hyperplasia and hepatic adenoma (Litten and Tomlinson, 2008; Chiorean et al., 2015). Malignant tumors of the liver in children and adolescents under 18 years of age are rare events and account for 1-2% of all the pediatric malignancies (Grovas *et al.*, 1997; Litten and Tomlinson, 2008; Emre, Umman and Rodriguez-Davalos, 2012; Tanaka, Inoue and Horie, 2013). The incidence of liver cancer in infants represented 2% of malignancies by 1980 and this was doubled to 4% in 10 years (Emre, Umman and Rodriguez-Davalos, 2012). In Spain, liver tumors in children and adolescents between 0-14 years account only for 1.4% of the pediatric tumors (Reti-Sehop, 2014).

In contrast to adult liver tumors in which the predominant form is the Hepatocellular Carcinoma (HCC), the main liver tumor in children is Hepatoblastoma (HB), accounting for two thirds of the total (Litten and Tomlinson, 2008; Emre, Umman and Rodriguez-Davalos, 2012). Pediatric HCC (pHCC) is even rarer than HB and is usually diagnosed in older patients and adolescents. In addition to HB and pHCC, other liver malignancies in children include sarcomas, germ cell tumors, and rhabdoid tumors. The histology and anatomy of a pediatric liver tumor guides the treatment and prognosis (Litten and Tomlinson, 2008).

1.2.1 Hepatoblastoma (HB)

1.2.1.1 Incidence

The annual incidence of HB is of 1.5 cases/million children under 15 years (García-Miguel and López Santamaría, 2005; Spector and Birch, 2012). HB is typically diagnosed during lactation or in young patients: 68% during the first 2 years of life and 88% in children under 5 years (García-Miguel and López Santamaría, 2005). Boys are affected more commonly than girls, with a male:female ratio [1.2-3.6]:1 (Emre, Umman and Rodriguez-Davalos, 2012).

1.2.1.2 Etiology and risk factors

As HB is diagnosed at very early ages and as the highest incidence is at birth, its initiation during gestation seems to be required. The fact that HB cells resemble fetal or embryonal liver cells and antenatal or perinatal diagnosed cases also points to this early development. For this reason, events occurring around gestation appear to be key factors (Spector and Birch, 2012). Although risk factors for HB are not well characterized, it is known that the risk of developing HB increases in children suffering Beckwith-Wiedemann syndrome (BWS), hemihypertrophy, and familial adenomatous polyposis (FAP) (Darbari *et al.*, 2003).

BWS is an overgrowth syndrome characterized by gigantism, macroglossia, omphalocele, hemihypertrophy and neonatal hypoglycemia. Most cases are caused by a defect in the imprinting or uniparental disomy (UPD) of the Insulin like growth factor 2 (IGF2)-H19 locus localized in chromosome 11p15. Significantly higher rates of HB among 0-4 years BWS patients have been reported (DeBaun and Tucker, 1998; Spector and Birch, 2012).

FAP, an autosomal dominant pre-malignant disease that usually progresses to malignancy, is mainly caused by inactivating mutations in the Adenomatous polyposis coli (APC) gene, a tumor suppressor gene acting as an antagonist of the Wnt signaling pathway. Even though different studies with discordant results have been published, Hirschman *et al* identified APC mutations in 8 out of 93 HB cases

(8.6%). However, no difference in age at diagnosis was found when comparing FAP-associated vs non-FAP-associated HB, in contrast to what usually happens in cancers associated with genetic predisposing mutations (Hirschman, Pollock and Tomlinson, 2005; Spector and Birch, 2012).

Other factors associated to higher risk of HB development are extremely low weight at birth (Ikeda, Matsuyama and Tanimura, 1997; Spector, Feusner and Ross, 2004; McLaughlin *et al.*, 2006), male gender (McLaughlin *et al.*, 2006), maternal smoking (McLaughlin *et al.*, 2006; Pu *et al.*, 2009), infertility treatment (McLaughlin *et al.*, 2006) and maternal and paternal occupational exposure to metals (Buckley *et al.*, 1989).

1.2.1.3 Diagnosis

HB is diagnosed in patients with an abdominal mass, failure to thrive and anemia (Emre, Umman and Rodriguez-Davalos, 2012). Typically, patients between 6 months and 3 years of age, with alpha-fetoprotein (AFP) levels higher than normal and hepatic mass are considered as having HB and in many clinical trials the biopsy was not even compulsory (von Schweinitz *et al.*, 1997; Brown *et al.*, 2000; Perilongo *et al.*, 2004). However, biopsy is required in patients younger than 6 months because the wide different hepatic masses they can have as well as the possibility to misdiagnose an elevated AFP at this young age. It is also needed in patients older than 3 years because the risk of having a pHCC (Perilongo *et al.*, 2004).

1.2.1.4 Prognosis, clinical stratification and treatment

Over the last decades, many clinical trials have been run devoted to improve chemotherapy treatment and stratification for HB patients (*Figure 2*). These trials have been organized by the main groups working on pediatric tumors worldwide, namely, the Société Internationale d'Oncologie Pédiatrique – Epithelial Liver Tumor Study group (SIOPEL), the German Society for Pediatric Oncology and Hematology (GPOH), the Japanese Study Group for Pediatric Liver Tumors (JPLT) and the

American Pediatric Oncology Group (COG). A summary of the stratification, chemotherapy treatment and survival results can be found in *Table 1*.

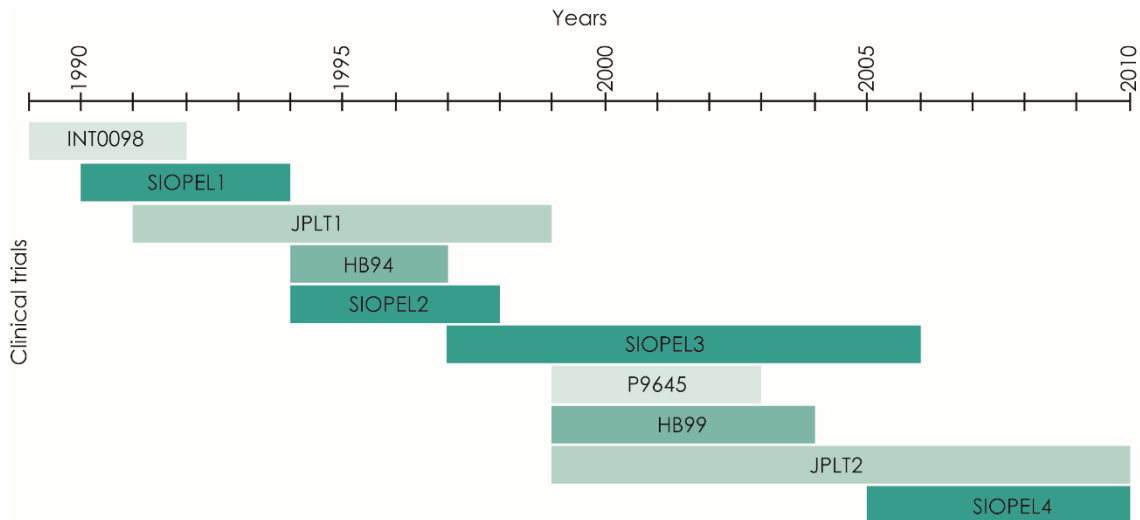


Figure 2. Summary of the different clinical trials conducted on HB. Different colors correspond to the different groups, from lighter to darker: COG, JPLT, GPOH and SIOPEL.

The American COG conducted their first randomized trial for the treatment of HB (INT0098) from 1989 to 1992. A total of 182 patients were included and randomized in 2 chemotherapeutic regimens: cisplatin, vincristine, and fluorouracil (regimen A, C5V) or cisplatin and continuous infusion doxorubicin (regimen B). Patients were stratified according to a surgical criteria after surgical resection or biopsy and before the beginning of chemotherapy: stage I, complete gross resection; stage II, microscopic residual disease; stage III, gross residual intrahepatic disease; stage IV, metastatic disease with either complete or incomplete resection. The results showed that the 5-year EFS was 91%, 100%, 64% and 25% in patients with stage I, stage II, stage III and stage IV respectively. The authors concluded that the outcome was similar for either regimen within disease stages, however, the doxorubicin- containing regimen proved more toxic and therefore, regimen A (cisplatin, vincristine, and fluorouracil) was recommended for treatment (Ortega *et al.*, 2000).

After the first trial, in 1999 the COG group started their new trial that was opened until 2003, the P9645 study. In this study patients with advanced HB, that is, stage III or IV, were randomly treated with standard therapy C5V or with cisplatin

combined with carboplatin (CC). In order to test the capacity of amifostine to reduce side effects, patients were also randomized to receive it or not. As a result, authors observed that the arm with CC had an increased risk of adverse events compared to the C5V arm, as the 1-year EFS was of 37% for patients receiving CC compared to 57% for C5V receiving patients ($p=0.017$) (Malogolowkin *et al.*, 2006).

The first trial launched by the SIOPEL group, the SIOPEL 1, was open from 1990 until 1994 and aimed to evaluate the response of HB to chemotherapy as well as the prognostic significance of different parameters. Chemotherapy regimen consisted of 4 courses of cisplatin $80\text{mg}/\text{m}^2$ administered in continuous infusion over 24h followed by doxorubicin $60\text{mg}/\text{m}^2$ in 48h continuous infusion (PLADO). In that study, in which 154 children suffering HB were enrolled, the features considered were: age, AFP levels, platelet count and histology; as well as radiologic parameters such as pretreatment extent of disease (PRETEXT) (Figure 3), lung metastases, enlarged hilar lymph nodes, vena cava or extrahepatic vena porta tumor extension and tumor focality. Results showed that PRETEXT staging was an independent prognostic factor both for event free survival (EFS) and overall survival (OS) whereas presence of metastasis was associated only with EFS (Brown *et al.*, 2000).

SIOPEL 2 trial was conducted between 1995 and 1998 in which therapy was guided according to risk. Thus, 135 HB patients were enrolled and stratified in standard risk HB (SR-HB) or high risk HB (HR-HB). SR-HB tumors were the ones involving 1, 2 or 3 liver sectors (PRETEXT I, II or III) entirely confined to the liver and without metastasis in the lung, whereas HR-HB were defined by involving the 4 hepatic sectors (PRETEXT IV) or presenting with extrahepatic disease, either metastasis, extrahepatic abdominal mass or portal/hepatic veins involvement. The aim of this study was to test the efficacy and toxicity of 2 chemotherapy regimens applied to the abovementioned groups. SR-HB patients were treated with 2 courses of cisplatin (CDDP), at a dose of $80\text{mg}/\text{m}^2$ every 14 days, delayed surgery and 2 new CDDP courses. HR-HB patients were given CDDP alternating every 14 days with carboplatin (CARBO), $500\text{mg}/\text{m}^2$, and doxorubicin (DOXO), $60\text{mg}/\text{m}^2$. Two courses of CARBO/DOXO and one of CDDP were given postoperatively to HR-HB patients. The 3-year OS for the SR-HB patients was 91% compared to the 53% of the HR-HB. The

results of the study confirmed that the treatment based on CDDP monotherapy together with surgery was effective for SR-HB, but there was a need of improving the survival for HR-HB patients (Perilongo *et al.*, 2004).

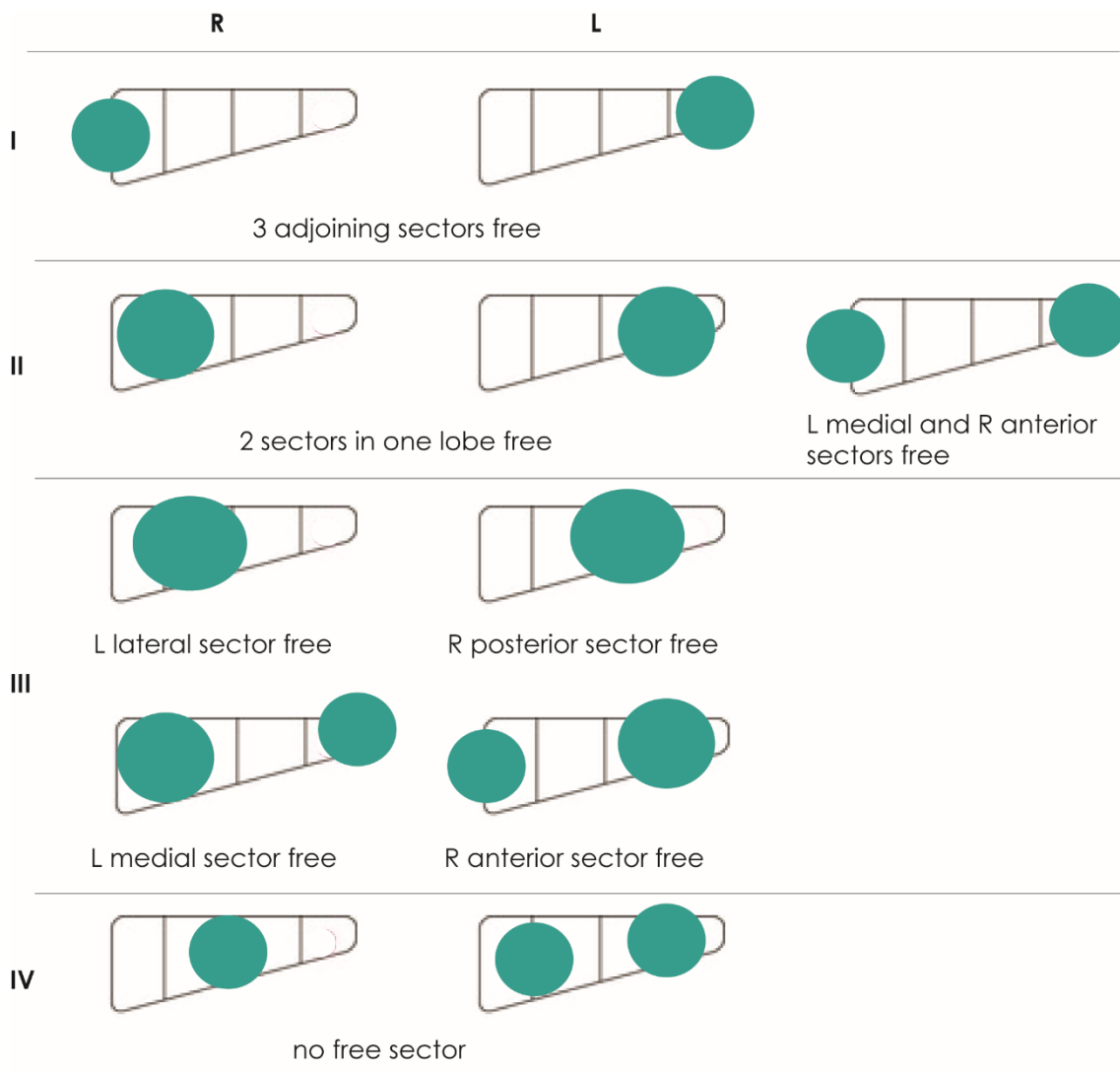


Figure 3. PRETEXT system. In the PRETEXT system, the liver according to its surgical anatomy was divided into four sections, namely an anterior and a posterior sector on the right and a medial and a lateral sector on the left. Thus, based on tumor extension within the liver, four groups were identified as follows: PRETEXT I, three adjoining sectors free (tumor only in one sector); PRETEXT II, 2 adjoining sectors free (tumor involves 2 sectors); PRETEXT III, one sector or two non-adjoining sectors free (tumor involves two or three sectors); and PRETEXT IV, no free sector (tumor in all four sectors). Adapted from (Brown *et al.*, 2000).

Introduction

The SIOPEL 3 trial, based on the SIOPEL 2, run between 1998 and 2004 and was focused to the treatment of HR-HB. As for the previous study, HR-HB was defined as tumor in all liver sections (e.g. Pretreatment Extension IV [PRETEXT-IV]), or vascular invasion (portal vein [P], three hepatic veins [V]), or intra-abdominal extrahepatic extension (E), or metastatic disease. Patients with AFP less than 100 ng/mL at diagnosis or tumor rupture were also considered as HR-HB. Patients were initially treated with alternating cycles of cisplatin and the combination of carboplatin plus doxorubicin. After seven cycles, tumor resectability was assessed; if feasible, complete resection was performed, followed by the remaining three cycles. If the tumor was unresectable, patients were treated with another three cycles followed by, if was feasible, complete tumor resection. For patients whose primary tumors remained unresectable, total hepatectomy with liver transplantation had to be considered at this point. Regardless of the time point of surgery, a maximum of 10 cycles were given. The results of this study showed that the 3-year EFS was 48%±13% and the OS 53%±13%, similar to that obtained in the SIOPEL 2 (3-year OS for HR-HB=53%). Also, the applied treatment was efficient for patients with metastatic disease as in 50% of the children the lung lesions disappeared with chemotherapy and in another 20% achieved partial response (Zsíros *et al.*, 2010).

Based on the results of the SIOPEL 2 and 3 trials, the researchers proposed a new stratification system including the following prognostic parameters: PRETEXT stage, age>5years, AFP>10⁶ ng/mL, multifocal tumors, presence of metastasis, AFP<100 ng/mL and Small Cell Undifferentiated (SCU) histology (Figure 4). The evaluation of the new stratification system showed that the 3-year EFS was 90%, 71% and 49% for stratum Good, Intermediate and Poor, respectively. A similar trend was observed regarding OS (Maibach *et al.*, 2012).

The SIOPEL 4 trial run from 2005 to 2009. The study was focused in the improvement of HR-HB patient's treatment by chemotherapy intensification based on weekly preoperative administration of cisplatin together with monthly doxorubicin and radical surgery. A total of 61 evaluable patients were included and were classified as high risk according to the above mentioned criteria used in the SIOPEL 3. All patients were given preoperative chemotherapy followed by

surgical removal of the remaining tumor lesions when possible. Patients whose tumor remained unresectable were given additional preoperative treatment before surgery. After surgery, patients received postoperative chemotherapy. At the completion of the study, the 3-year EFS was 76% and OS was 83%. The results implied a significant improvement of patient outcome for HR-HB (SIOPEL3 3-year EFS was 48% and the OS 53%), but it is even better for metastatic patients, as 95% of the patients had a complete remission vs 50% from the previous trial (Zsiros *et al.*, 2013).

Prognostic Strata	Prognostic factors							
	PRETEXT 1/2/3	PRETEXT 4	Age > 5 years	AFP > 1.2x10 ⁶	Multi-focal	M+	AFP < 100	SCU
Good	+	-	-	-	-	-	-	-
Intermediate	+/-	at least one				-	-	-
Poor	+/-	+/-	+/-	+/-	+/-	at least one		

Figure 4. SIOPEL patient clinical stratification 2012. Based on the SIOPEL 2 and 3 results, the SIOPEL group established a new classification in which Stratum 1 was defined by HB completely confined to the liver AND involving at the most 3 hepatic sections (PRETEXT I, II and III) AND none of the other risk factors; Stratum 2 included patients with at least one of the following features: age above 5 years, PRETEXT IV, AFP higher than 1.2x10⁶ ng/mL AND none of the risk factors considered for stratum 3; Stratum 3 patients must present one or more of the following factors: metastases, AFP below 100ng/mL OR small cell undifferentiated histology. +, factor must be present; -, factor must be absent; +/-, factor may be present or absent. Modified from (Maibach *et al.*, 2012).

The JPLT have also conducted clinical trials devoted to the improvement of the treatment for HB patients. First, the JPLT-1 was run from 1991 to 1999 and 134 patients with HB were included. Patients were stratified according to the extent of disease, which is slightly different from the PRETEXT system. Thus, patients were classified as: stage I, the tumor occupied one segment of the liver; stage II, the tumor occupied 2 segments of the liver; stage IIIA, the tumor occupied 3 segments of the liver, stage IIIB, the tumor occupied 4 segments of the liver; and stage IV, metastatic disease was present. When the liver tumor that occupied 1 or 2 segments extended to the inferior vena cava or the portal vein, stage was defined as IIIA. Stage I or II patients were divided in 2 arms: 91A1, patients received one course of preoperative

intraarterial chemotherapy and then postoperative intravenous chemotherapy, and in protocol 91A2 patients underwent initial primary surgery, which was followed by intravenous chemotherapy. The chemotherapy regimen consisted of repeated courses of Cisplatin (CDDP) and tetrahydropyranil (THP) as well as one shot of Adriamycin. Patients with stage IIIA, IIIB or IV were treated with intraarterial or intravenous chemotherapy randomly. EFS/OS at 3 years was of: stage I 88.9%/100%, stage II 84.2%/100%, stage IIIA 67.5%/76.6%, stage IIIB 25.4%/50.3% and stage IV 40.6%/64.8%. Overall, the 3-years EFS was of 66% and the OS of 77.8%. Interestingly, the authors also observed a trend to better outcome for patients diagnosed under 1 year of age, although it was not a significant result.

In the JPLT-2 study, opened from 1998 to 2008 and including 212 patients, patients were stratified according to PRETEXT I, PRETEXT II-IV or metastatic disease. PRETEXT I patients were treated with primary resection followed by low doses of cisplatin-pirarubicin (CITA) consisting in at least 2 courses of 80mg/m² cisplatin on day 1 followed by 30mg/m² pirarubicin on days 2 and 3. Otherwise, patients received preoperative CITA, followed by surgery and postoperative chemotherapy. Ifosfamide, pirarubicin, etoposide, and carboplatin (ITEC) were given as a salvage treatment. High-dose chemotherapy with hematopoietic stem cell transplantation (SCT) was reserved for patients with metastatic diseases. The OS for the 212 HB cases was 82.4% at 3 years, and 80.9% at 5 years. The EFS was 69.9% at 3 years, and 62.4% at 5 years. The 5-year OS of non- metastatic PRETEXT I, II, III, and IV cases was 100, 87.1, 89.7, and 71.2%, respectively, and the 5-year EFS was 78.3, 76.2, 72.2, and 68.3%, respectively. The outcome of patients with metastatic diseases was poor, with a 5-year OS of 43.9% (EFS 20.8%) (Hishiki *et al.*, 2011).

The GPOH have conducted 2 clinical trials, HB89 and HB94, mainly devoted to improve the chemotherapeutic treatment of pediatric patients with liver tumors. The HB89 trial was conducted between 1988 and 1993 and 72 patients with HB were enrolled. The staging criteria stratified patients into 4 distinct groups and was based on tumor involvement after surgical resection: stage I, tumor was completely resected; stage II, there was microscopic residual tumor; stage III, gross residual tumor; stage IV, distant metastases. Response criteria was based on tumor size and

AFP levels. Patients with small tumors confined to one liver lobe, were operated without previous chemotherapy treatment, larger tumors involving both lobes and those with metastases were only biopsied. All patients were treated with chemotherapy and thereafter tumors were resected when possible. Also, in the same study, the authors introduced a new chemotherapy regimen, combining cisplatin, doxorubicin and ifosfamide. At the completion of the study, the authors concluded that chemotherapy consistent of ifosfamide, cisplatin and doxorubicin was effective and associated with low acute toxicity. Moreover, combined with delayed surgery in advanced tumors, they achieved a cure rate of 75% (von Schweinitz *et al.*, 1997).

After the observation that some HBs were able to develop drug resistance after treatment with ifosfamide, cisplatin and doxorubicin, the GPOH group launched the HB94 study introducing new treatment modalities. Basically, intensity of postoperative chemotherapy was reduced for stage I HB and a new combination of etoposide and carboplatin was used for advanced or recurrent tumors. The authors also studied the implication of different clinical and pathological prognostic factors. In these study, 69 children with HB were included. As in the previous protocol, patients with tumors confined to one lobe were resected before chemotherapy treatment and the same postsurgical staging system was followed (von Schweinitz *et al.*, 1997; Fuchs *et al.*, 2002). The results showed that vascular invasion ($p=0.0039$), metastasis ($p<0.0001$) and AFP serum levels below 100ng/mL ($p=0.0005$) were significantly associated with worse disease free survival. After a median follow-up of 58 months, 77% of patients were alive (Fuchs *et al.*, 2002).

From 1999 to 2004, the GPOH run the HB 99 trial, which included 100 patients with HB. Patients were treated according to risk: SR-HB with PLADO and HR-HB CDDP/CARBO/DOXO. As a result of this approach, the 3-year survival EFS was of 90% and OS of 88% for SR-HB and an EFS of 52% and OS of 55% for HR-HB patients (Czauderna *et al.*, 2014).

More recently, in 2017, the Children's Hepatic tumors International Collaboration (CHIC) has published the new stratification system based on the

Introduction

analysis of the largest cohort of patients comprising 1605 patients treated in 8 multicenter HB trials over 25 years. These study have been possible thanks to the contribution of the 4 major groups: the SIOPEL, COG, the GPOH, and the JPLT. As a result, the new stratification system named Children's Hepatic tumors International Collaboration Hepatoblastoma Stratification (CHIC-HS) consists in 5 clinically relevant backbone groups on the basis of established prognostic factors: PRETEXT I/II, PRETEXT III, PRETEXT IV, metastatic disease, and AFP levels below 100ng/mL at diagnosis. Finally, patients are stratified in very low, low, intermediate or high risk and treated according (*Figure 5*) (Meyers et al., 2017).

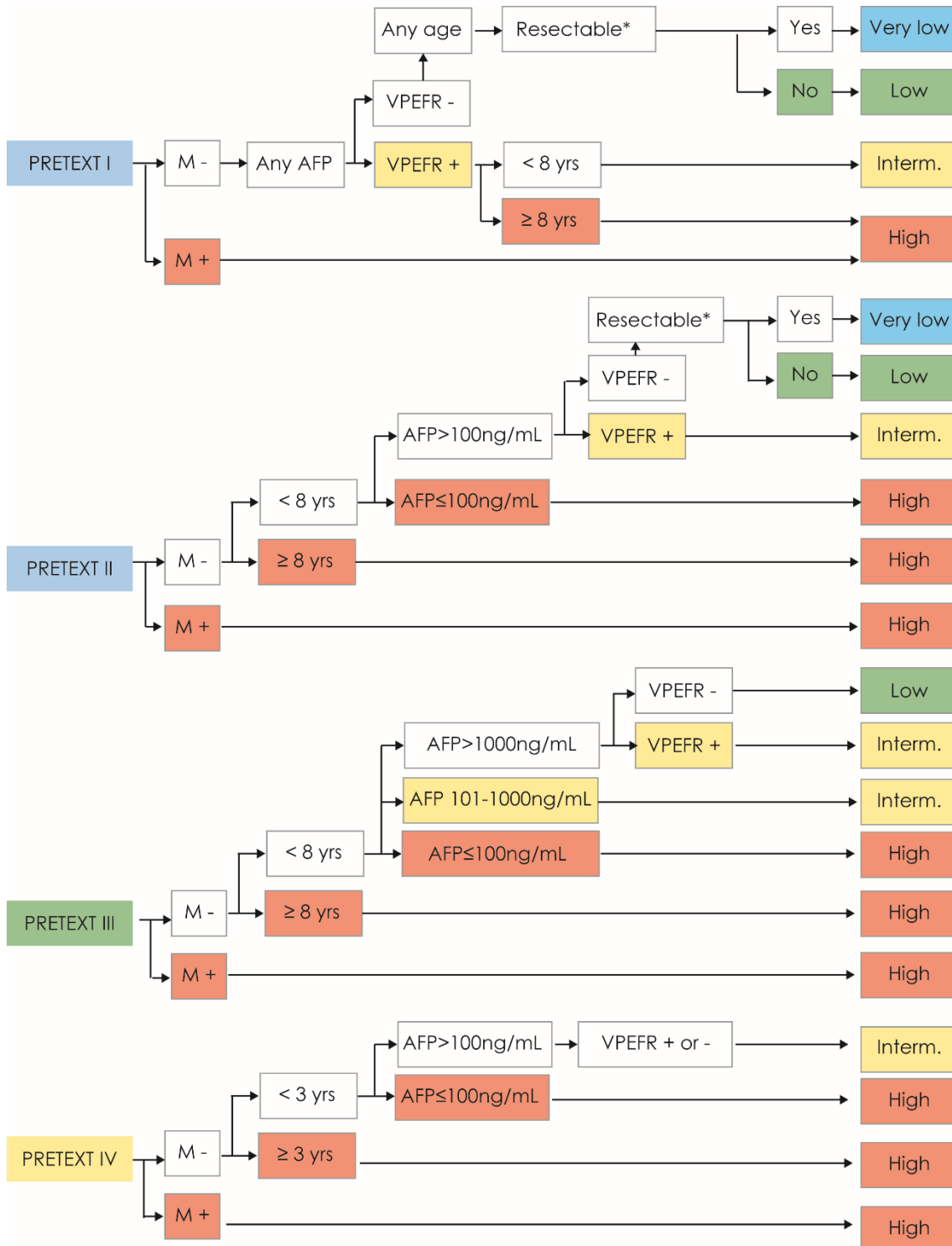


Figure 5. Risk stratification trees CHIC-Hepatoblastoma Stratification (CHIC-HS) system. Individual risk stratification trees are used depending on the PRETEXT stage. *, resectable at diagnosis. Abbreviations: M, metastasis; AFP, a-fetoprotein; Interim., intermediate; Yrs, years. Modified from (Meyers et al., 2017).

Table 1. Summary of the main clinical trials on HB. N, number of patients; SR-HB, standard risk HB; HR-HB, high risk HB; Met, metastasis; IPA, Ifosfamide + cisplatin + doxorubicin; PA-CI, cisplatin + doxorubicin; C5V, cisplatin + fluorouracil + vincristine; CDDP, cisplatin; DOXO, doxorubicin; CC, carboplatin + cisplatin; PLADO, cisplatin + doxorubicin; IFO, ifosfamide; VP, etoposide; CARBO, carboplatin; CITA, cisplatin + pirarubicin; ITEC, ifosfamide + pirarubicin + etoposide + carboplatin; yrs, years; EFS, event-free survival; OS, overall survival; DFS, disease-free survival; PFS, progression-free survival.

Study	Stratification	N	Chemotherapy	Surgery	Survival results
HB89 (GPOH) 1988-1993	I, tumor completely resected;	21	2-4 courses of IPA ± 2 courses of PA-CI	Primary surgery for small tumors confined to one lobe After 2 IPA courses for larger tumors or tumors with met	I, DFS=100% II, DFS= 50% III, DFS= 71% IV, DFS= 29%
	II, microscopic residual tumor;	6			
	III, gross residual tumor;	38			
	IV, distant metastases.	7			
INT-0098 (COG) 1989-1992	I, tumor completely resected; II, microscopic residual tumor; III, gross residual tumor; IV, distant metastases.	182	C5V or CDDP/DOXO		I, 5-yr EFS=91% II, 5-yr EFS=100% III, 5-yr EFS=64% IV, 5-yr EFS=25%
SIOPEL I (SIOPEL) 1990-1994	All patients treated equally	154	4-6 courses of PLADO	After 4-6 courses	5-yr OS = 75% 5-yr EFS = 66%
JPLT-1 (JPLT) 1991-1999	I, tumor in one segment	9	Stage I/II, 2 courses of CDDP + THP- Adriamycin Stage IIIA, IIIB, IV, CDDP +THP- Adriamycin	Stage I/II, after 1 course or primary surgery Stage IIIA, IIIB, IV, after CDDP+THP- Adriamycin	I, EFS/OS=89%/100% II, EFS/OS=84%/100% III, EFS/OS=68%/77% IIIB, EFS/OS=25%/50% IV, EFS/OS=40%/65%
	II, tumor in 2 segments	32			
	IIIA, tumor in 3 segments	48			
	IIIB, tumor in 4 segments	25			
	IV, metastatic	20			
HB94 (GPOH) 1994-1998	I, tumor completely resected;	27	Stage I/II, IFO/CDDP/DOXO Stage II/IV, IFO/CDDP/ DOXO+ VP/CARBO		I, 4-yr EFS/OS=89%/96% II, 4-yr EFS/OS=100%/100% III, 4-yr EFS/OS=68%/76% IV, 4-yr EFS/OS=21%/36%
	II, microscopic residual tumor;	3			
	III, gross residual tumor;	25			
	IV, distant metastases.	14			
SIOPEL II (SIOPEL) 1995-1998	SR-HB (PRETEXT I, II, or III)	67	6 courses of CDDP	After 4 courses	3-yr OS=91% 3-yr PFS= 89%
	HR-HB (PRETEXT IV or metastasis or extrahepatic or vascular involvement	58	6 courses of CARBO + DOXO and 4 courses of CDDP	After 4 courses CARBO/DOXO and 3 CDDP	3-yr OS=53% 3-yr PFS= 48%
SIOPEL III-HR (SIOPEL) 1998-2004	HR-HB (PRETEXT IV or metastasis or extrahepatic or vascular involvement or AFP<100ng/ml or tumor rupture)	151	10 courses of CDDP and CARBO+DOXO	After 7 courses	3-yr OS=53% 3-yr EFS=48%
JPLT-2 (JPLT) 1998-2008	PRETEXT I	16	I, CITA II-IV, CITA + CITA or ITEC	I, primary resection II-IV, after CITA	I, 5-yr EFS/OS=78%/100 % II, 5-yr EFS/OS=76%/87% III, 5-yr EFS/OS=72%/90% IV, 5-yr EFS/OS=68%/71% Met, 5-yr EFS/OS=21%/44%
	PRETEXT II	64			
	PRETEXT III	83			
	PRETEXT IV	49			
HB99 (GPOH) 1999-1998	SR	58	SR, PLADO HR, CDDP/CARBO/DOXO		SR, 3-yr EFS/OS=90%/81% HR, 3-yr EFS/OS=52%/55%
	HR	42			
P9645 (COG) 1999-2003	III, gross residual tumor; IV, distant metastases.	192	4-6 courses of C5V or CC ± amifostine	After II-IV courses	C5V, 3-yr EFS/OS= 60%/74% CC, 3-yr EFS/OS=38%/56%
SIOPEL 4 (SIOPEL) 2005-2009	HR-HB (PRETEXT IV or metastasis or extrahepatic or vascular involvement or AFP<100ng/ml or tumor rupture)	62	8 courses CDDP and 3 DOXO + 2-3 CARBO and 2-3 DOXO	After 8 courses CDDP and 3 DOXO	Whole group: 3-yr OS= 83% 3-yr EFS= 76% Patients with M: 3-yr OS= 79% 3-yr EFS= 77%

1.2.1.5 Pathology

Historically, it has been difficult to define the different patterns found in pediatric liver tumors due to their variability and rarity. In 2011, pathologists, oncologists and surgeons from the main groups worldwide (COG, SIOPEL, GPOH and JPLT) were reunited in an International Pathology Symposium in Los Angeles. From these symposium resulted a revision of the histology of pediatric liver malignancies which will be used as a guide in the future cooperative trials (López-Terrada *et al.*, 2013; Tanaka, Inoue and Horie, 2013).

HB is an embryonal tumor that arises from a hepatocyte precursor and usually recapitulates stages of liver development, thus the histopathology of HB reproduces different stages of liver development (Zimmermann, 2005). HB is a heterogeneous disease and tumors often show mixtures of different histologic compounds such as epithelial, mesenchymal, undifferentiated and others. Generally, HB tumors can be classified between epithelial or mixed (López-Terrada *et al.*, 2013; Tanaka, Inoue and Horie, 2013). The differences and subtypes of each histological pattern are explained below and summarized in *Figure 6*.

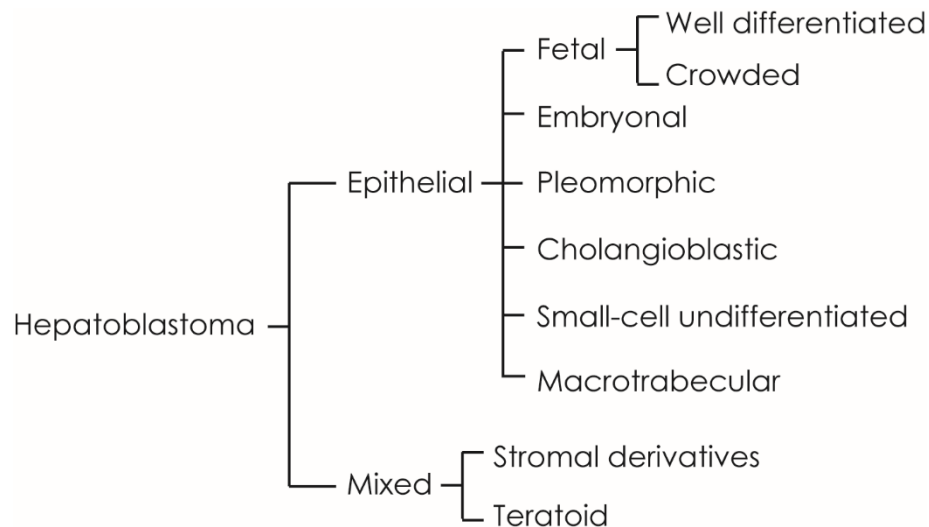


Figure 6. Histological patterns of HB (López-Terrada *et al.*, 2013).

Epithelial HB

Well differentiated fetal HB: These cells recapitulate fetal hepatocytes with tumor cells smaller than hepatocytes and are characterized by having a central and small nucleoli and glycogen or lipids which make their cytoplasm appear clear. These tumors usually contain clusters of hematopoietic precursors and mitosis are infrequent (*Figure 7A*) (Haas et al., 1989; López-Terrada et al., 2013; Tanaka, Inoue and Horie, 2013).

Crowded fetal HB: This pattern is also known as mitotically active fetal (defined as more than two mitoses per 10 high-power fields, x400 microscopic fields). In comparison to the well differentiated cells, these present higher nuclear/cytoplasmic ratio and bigger nuclei. It typically presents mixed with the well differentiated fetal pattern and embryonal (*Figure 7B*) (López-Terrada et al., 2013; Tanaka, Inoue and Horie, 2013).

Embryonal: Is the most common pattern, which resembles the liver at weeks 6-8 of gestation. Embryonal HB cells are round or angulated, with limited cytoplasm and with a nuclear-cytoplasmic ratio to some extent higher than the healthy hepatocytes. Mitosis are more frequent than in fetal histotype (*Figure 7C*) (Haas et al., 1989; López-Terrada et al., 2013; Tanaka, Inoue and Horie, 2013).

Pleomorphic component in epithelial HB: It is an uncommon pattern that typically appears in post-chemotherapy specimens and metastases. Its cells are similar to fetal or embryonal hepatocytes because their polygonal shape. However, nuclear features can differ from the well-differentiated or crowded fetal patterns, presenting irregular shape and large nucleoli. This HB type can be confused as an HCC when it presents with a macrotrabecular pattern of growth (*Figure 7D*) (López-Terrada et al., 2013; Tanaka, Inoue and Horie, 2013).

Cholangioblastic HB: This pattern results from the neoplastic cells differentiated to cholangiocytes and forming small ducts. It expresses cholangiocyte lineage markers such as cytokeratins 7 and 19. It can be surrounding the hepatocellular component of the tumor. Its cells use to be cuboidal with a round nuclei (*Figure 7E*) (López-Terrada et al., 2013; Tanaka, Inoue and Horie, 2013).

Macrotrabecular HB: Cells in this pattern can be fetal, embryonal or pleomorphic and can be similar to the hepatocellular carcinoma ones. The growth pattern is characterized by bigger cells that grow in plates that can be pure or combined with other patterns. This pattern is present in less than 5% of patients (*Figure 7F*) (Haas *et al.*, 1989; López-Terrada *et al.*, 2013; Tanaka, Inoue and Horie, 2013).

Small-cell undifferentiated (SCU) HB: This pattern was first defined as anaplastic (Kasai and Watanabe, 1970) and contain small and undifferentiated cells that sometimes express cytokeratin and vimentin, which reflects neither epithelial nor stromal differentiation. These cells can grow in a diffuse pattern but often form clusters with epithelial cell types. In less than 5% of the HBs the whole tumor is constituted of this type of cells. It is interesting to note that some SCU HBs may present typical features of malignant rhabdoid tumors, as the lack of INI1 nuclear expression. The proper identification of these variant it is crucial, as patients could benefit from chemotherapy regimens designed for malignant rhabdoid tumors instead of HB (*Figure 7G*) (Haas *et al.*, 1989; López-Terrada *et al.*, 2013; Tanaka, Inoue and Horie, 2013).

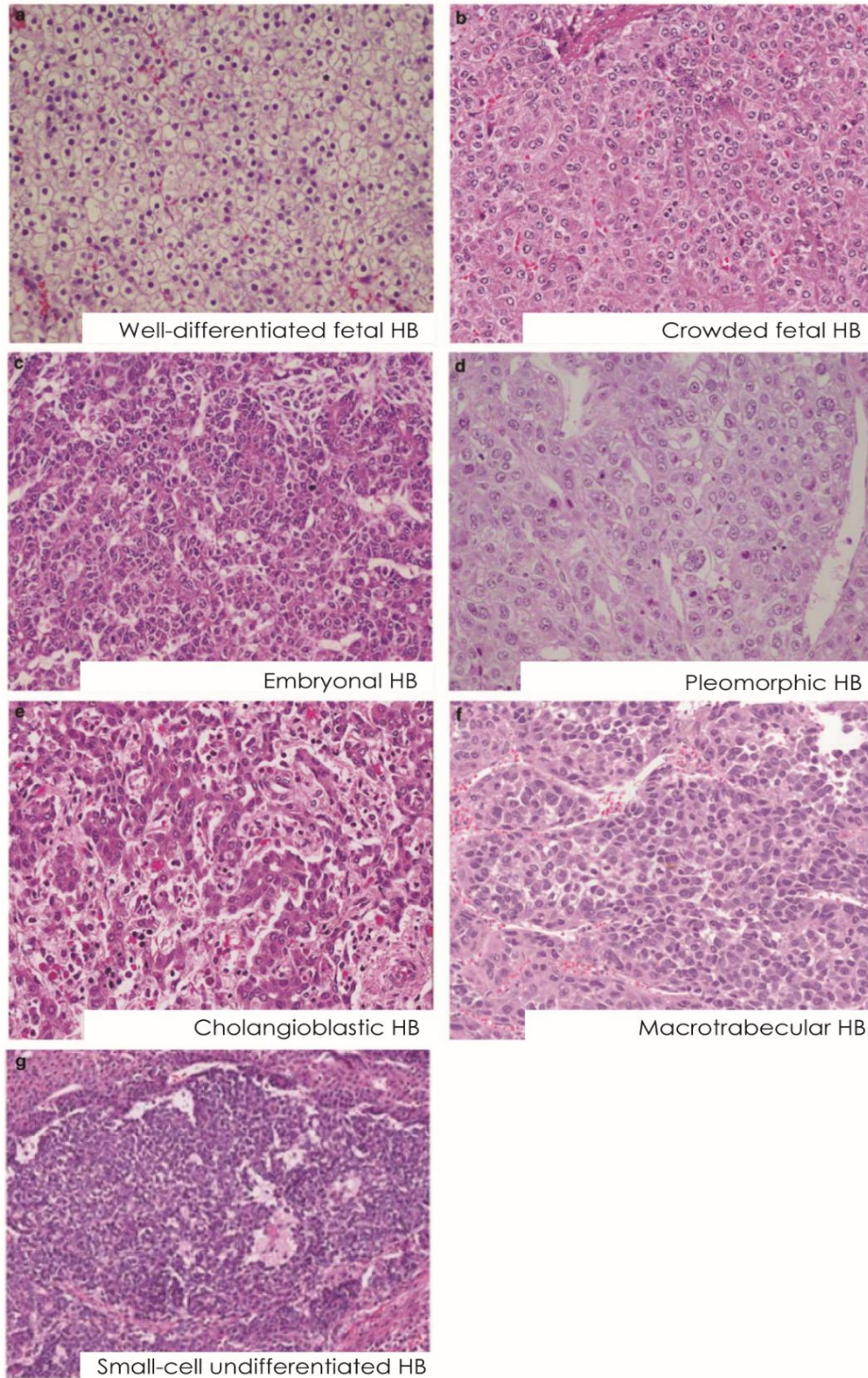


Figure 7. Epithelial HB histology types. Well-differentiated fetal pattern (a); crowded (mitotically active) fetal pattern (b); embryonal HB (c); pleomorphic HB (d); Cholangioblastic HB (e); macrotrabecular pattern (f); HB with small-cell component. Adapted from (López-Terrada *et al.*, 2013).

Mixed HB

Around 20-30% of HB tumors besides the epithelial component, they also have stromal components, which can include osteoid, skeletal, muscle and cartilage. Additionally, when heterologous components (for example neuroectodermal derivatives or melanin-containing cells) are present, tumors are classified as teratoid. Tumors showing stromal or teratoid components are both called mixed HB (Figure 8) (López-Terrada *et al.*, 2013; Tanaka, Inoue and Horie, 2013).

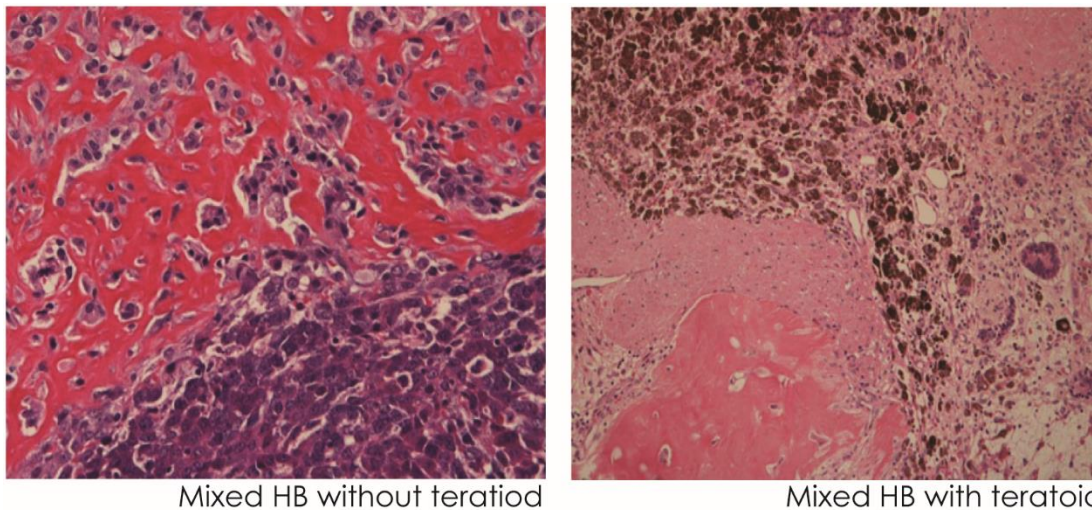


Figure 8. Mixed HB histotype. Mixed epithelial and mesenchymal HB without teratoid features. Area showing osteoid formation and embryonal epithelial pattern (bottom) (Left). Mixed epithelial and mesenchymal HB with teratoid features. Area showing accumulation of melanin-containing cells and osteoid (bottom) (Right). Adapted from (Tanaka, Inoue and Horie, 2013).

It has been matter of discussion in many publications whether the different histotypes may be related with the outcome. In their series of 71 patients, von Schweinitz *et al.*, found that pure fetal or predominantly fetal compared to tumors with predominant embryonal pattern was associated with significant better outcome, while no differences were found between mixed and epithelial tumors (von Schweinitz *et al.*, 1997). In fact, pure and well differentiated HB is a surgically curable tumor, and according to COG protocols, chemotherapy is not necessary when it can be completely resected at diagnosis (López-Terrada *et al.*, 2013; Tanaka, Inoue and Horie, 2013). Importantly, the SCU pattern of HB often present with normal or low levels of serum AFP and have been associated with poor patient outcome and increased risk of death (Ortega *et al.*, 2000; Fuchs *et al.*, 2002;

Trobaugh-Lotrario *et al.*, 2009; Haas, Feusner and Finegold, 2011). Interestingly, different pathway deregulation in the distinct histotypes have been identified. Therefore, Wnt activation predominates in embryonal and mixed types while Notch activation, which is needed for cholangiocytic differentiation, is highest in pure fetal HB (López-Terrada *et al.*, 2009).

In few tumors histological pattern makes it difficult to reach an agreed diagnostic due to a mixture of features typical of both HB and pHCC. These tumors were first named transitional liver cell tumors, but this category has been recently named as hepatocellular malignant neoplasm (NOS) (Figure 9). Usually, these tumors show a mixture of HB-like cells resembling fetal, fetal-pleomorphic and/or embryonal cells, HCC-like cells and poorly differentiated cells that grow in highly invasive patterns (Figure 9). NOS tumors are a pathological entity but they are not considered a different tumor from a clinical point of view. This malignancy was described for the first time by Prokurat *et al.*, who reported 7 cases presented in older children and adolescents (mean age=10 years, ranging from 5 to 17). The histological pattern presented made it difficult to diagnose an HB or HCC, mostly presenting macrotrabecular HB features and patients were treated as HBs obtaining poor survival results. (Prokurat *et al.*, 2002).

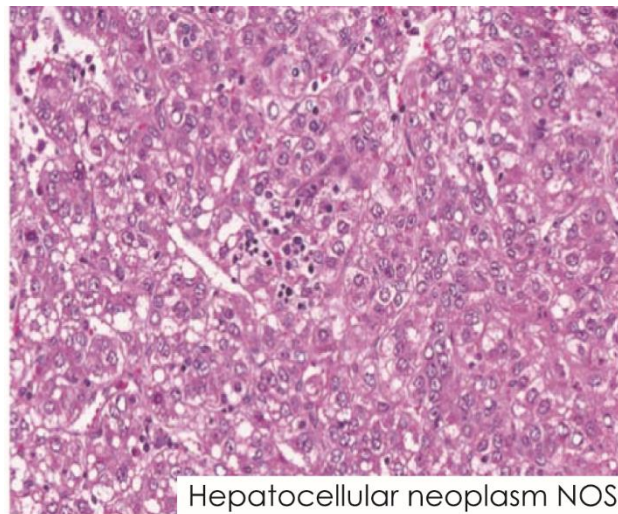


Figure 9. NOS histology.

1.2.2 Pediatric Hepatocellular Carcinoma (pHCC)

1.2.2.1 Incidence

pHCC is the second most common liver tumor in children being most of the cases diagnosed after 10 years of age and it is the main hepatic tumor in adolescents (Czauderna *et al.*, 2002). pHCC is even more rare than HB during childhood with an incidence of 0.5-1 cases per million children (Litten and Tomlinson, 2008) and represents 20% of all the malignant childhood liver tumors (Weinberg and Finegold, 1983). In areas where hepatitis B is endemic, such as sub-Saharan Africa and some areas in Asia, the incidence of HCC in pediatric population is 4 times higher than in Western countries. As happens with HB, boys are more affected than girls, with a male/female ratio 2:1 (Emre, Umman and Rodriguez-Davalos, 2012).

1.2.2.2 Etiology and risk factors

In contrast to adult HCC, most of pHCC patients are not associated with cirrhosis or other chronic liver disease caused by inborn metabolic errors such as glycogen storage disease type III, tyrosinemia type I, Wilson disease, or biliary atresia (Czauderna *et al.*, 2002; Schmid and Schweinitz, 2017). However, the high incidence of the hepatitis infection in many Asiatic countries leads to higher incidence of pHCC, although the introduction of the hepatitis B vaccine in Southeast Asia has reduced the incidence of liver tumors (Chen *et al.*, 1998; Litten and Tomlinson, 2008).

The work published by Czauderna *et al.* in 2002 was the first large series of pHCC treated in a uniform way, following the SIOPEL 1 protocol. In this study, 39 patients from 30 different countries were enrolled and 38% of them had underlying liver disease. Etiologies vary from hepatitis B and hepatic cirrhosis in 13 patients, tyrosinemia in one patient and biliary cirrhosis in one patient. These results revealed that in contrast to what occurs in adult HCC, most cases (62%) in children are de novo, not related to liver damage (Czauderna *et al.*, 2002). In contrast to the findings published by Czauderna *et al.*, in a study conducted in Taiwan, HBV infection was found in 100% of the 56 pHCC studied (Chen *et al.*, 2005). Showing that the etiology of these tumors can vary depending on the area.

1.2.2.3 Diagnosis

Patients with pHCC are usually older than HB patients, being mostly diagnosed after 3 years of age and rarely below 6. Patients suffering pHCC commonly present with hepatomegaly, sometimes associated with abdominal pain or other nonspecific symptoms such as epigastralgia, nausea, fatigue or anorexia. As it has been said before, it often develops in the presence of underlying liver disease. The fact that this tumor do not become a limitation to children's daily life, makes it difficult to diagnose at early stages, and around 80% of patients are diagnosed with advanced or metastatic disease (Chen *et al.*, 1998; Czauderna *et al.*, 2002; Perilongo *et al.*, 2004).

1.2.2.4 Prognosis, clinical stratification and treatment

Given the low incidence of pHCC it is really difficult to conduct clinical trials. In contrast to adult HCC, about 50% of pHCC patients respond to chemotherapy as shown by decrease of AFP levels and/or tumor shrinkage. So, main treatment options are focused on the use of systemic drugs and tumor resection. However, pHCC remains a dismal disease in a huge proportion of patients, mainly the ones with unresectable disease, in which the 3-year survival is less than 20%. (Schmid and Schweinitz, 2017).

In a retrospective study, Chen *et al.*, studied 55 patients with HCC treated between 1979 and 1996 in Taiwan. Patients were divided into 3 groups as follows; resectable, chemotherapeutic and untreated. Despite these patients were treated with many different chemotherapeutic regimens including different drugs such as mitomycin, doxorubicin, 5-fluorouracil, vincristine, cyclophosphamide, cisplatin and carboplatin in various combinations, the authors reported a failure in most of the patients with poor results at survival. Thus, the median survival was of 23, 3 and 2 months for the resectable, chemotherapeutic and untreated groups respectively (Chen *et al.*, 1998). Another paper of Chen *et al.* studied a cohort of 73 patients with pHCC treated between 1979 and 1997. Primary resection was achieved in 16.4% of the patients, but tumor recurrence occurred in more than 50% of them. The overall

survival at 5-years was of 30% for stage I patients (completely resected at initial surgery) and 0-5% for stage III (unresectable, tumor spillage or resection with gross residual disease but not metastatic) and IV (metastatic disease, regardless of the status of primary tumor) (Chen *et al.*, 2005).

During the INT-0098 trial (1989-1992) promoted by the American COG, patients suffering pHCC were also enrolled. Forty-six patients with pHCC were randomly assigned to chemotherapy regimen with cisplatin + vincristine + fluorouracil or cisplatin + continuous infusion doxorubicin. Patients were stratified according to postsurgical criteria, and the results of the analysis showed that the 5-year EFS/OS was of 88%/88%, 8%/23% and 0%/10% for stage I, III and IV respectively (no patients with stage II were enrolled). Thus, the global 5-year EFS for pHCC patients was of 19%. Moreover, no significant differences were found between patients receiving both chemotherapy regimens regarding EFS and OS (Katzenstein *et al.*, 2002).

From 1990 to 1994, taking advantage of the SIOPEL 1 trial, the SIOPEL group also include patients suffering pHCC. Thirty-nine children with pHCC were included and treated with preoperative chemotherapy consisting on 4-6 courses of PLADO (cisplatin + doxorubicin). If after 4 courses of PLADO the tumor was resectable, partial hepatectomy was performed and after surgery, 2 additional courses of PLADO were given. For PRETEXT I patients, primary surgery was allowed. The OS at 5 years was of 28% and the EFS was of 17%. Unfortunately, chemotherapy only showed partial responses in 50% of the cases, even though some cases with partial response remained unresectable. Thus, response to chemotherapy and presence of metastasis are adverse prognostic factors for pHCC, and complete resection of the tumor is the only chance of cure for these patients (Czauderna *et al.*, 2002).

Later on, in the SIOPEL 2 and 3 trials (1994-2006), patients with pHCC were also included and treated with superPLADO regimen (carboplatin + cisplatin + doxorubicin). When possible, primary resection was performed. The aim of these trials was to evaluate if an intensive preoperative chemotherapy was able to improve response rate and resection rate for pHCC patients. Eighty-five patients

with pHCC were included in the trials and 40% of them responded to chemotherapy. Unfortunately, as in the previous report, the 5-year OS was of 22%, showing again that a complete resection is needed for long-term outcome (Murawski *et al.*, 2016). Altogether, these results point out that pHCC cannot be treated following the same standards than HB, which responds to chemotherapy, and that the unique chance of cure for these patients is a complete resection at early stages.

1.2.2.5 Pathology

pHCC includes a biologically diverse group of neoplasms sometimes associated with underlying liver disease. However, pHCC developing in a healthy liver can be similar to HB and sometimes immunohistochemical stains together with histopathology are not enough to distinguish between them (López-Terrada *et al.*, 2013; Tanaka, Inoue and Horie, 2013). Apart from the classic pHCC, the fibrolamellar (FL-HCC) histologic variant is also frequent, especially in young adolescents.

HCC in adults usually develops in a background of liver fibrosis and cirrhosis through a multistep process of malignant transformation of cirrhotic nodules and premalignant lesions. These pre-malignant nodules can be classified in low grade or high grade depending on their similarity with healthy tissue. HCC is usually a hypervascularized tumor that depending on the similarity to non-tumor hepatocytes, can be pathologically classified in three different degrees of differentiation: well, moderate or poorly differentiated. It can also present diverse histological patterns such as trabecular, acinar or solid pattern (Paradis, 2013). Despite the etiology of pHCC depends on the area, most of the patients in contrast to adult HCC, pHCC are not associated to liver damage (see 1.2.2.2 *Etiology and risk factors for further details*). pHCC is histologically similar to the adult form and it differs from HB by the presence of tumor cells larger than normal hepatocytes in surrounding liver, broad cellular trabeculae, nuclear pleomorphism, nucleolar prominence and frequently tumor giant cells (Craig *et al.*, 1980). The macrotrabecular pattern of HCC presented in non-cirrhotic liver is very easily confused with HB (López-Terrada *et al.*, 2013) (Figure 10).

Fibrolamellar pHCC (FL-pHCC) is a different histological variant that account for around 30% of all pHCC diagnosed in patients under 20 years of age, commonly without cirrhosis or underlying liver disease. FL-pHCC is characterized by well-differentiated neoplastic hepatocytes and large and eosinophilic hepatocytes with prominent nucleoli within lamellar fibrotic tissue. Interestingly, tumor cells express biliary markers including CK7 and CK19, hepatocytic and hepatic progenitor markers, don't produce AFP and have fewer genomic alterations than classic pHCC (Tanaka, Inoue and Horie, 2013; Zen *et al.*, 2014). Although FL-HCC is not clinically different from classic HCC, when resectable, patients have better survival, perhaps because the fact that it mostly develops in a healthy liver, however in patients with advanced disease FL-HCC do not have favorable prognosis (Katzenstein *et al.*, 2003; Weeda *et al.*, 2013).

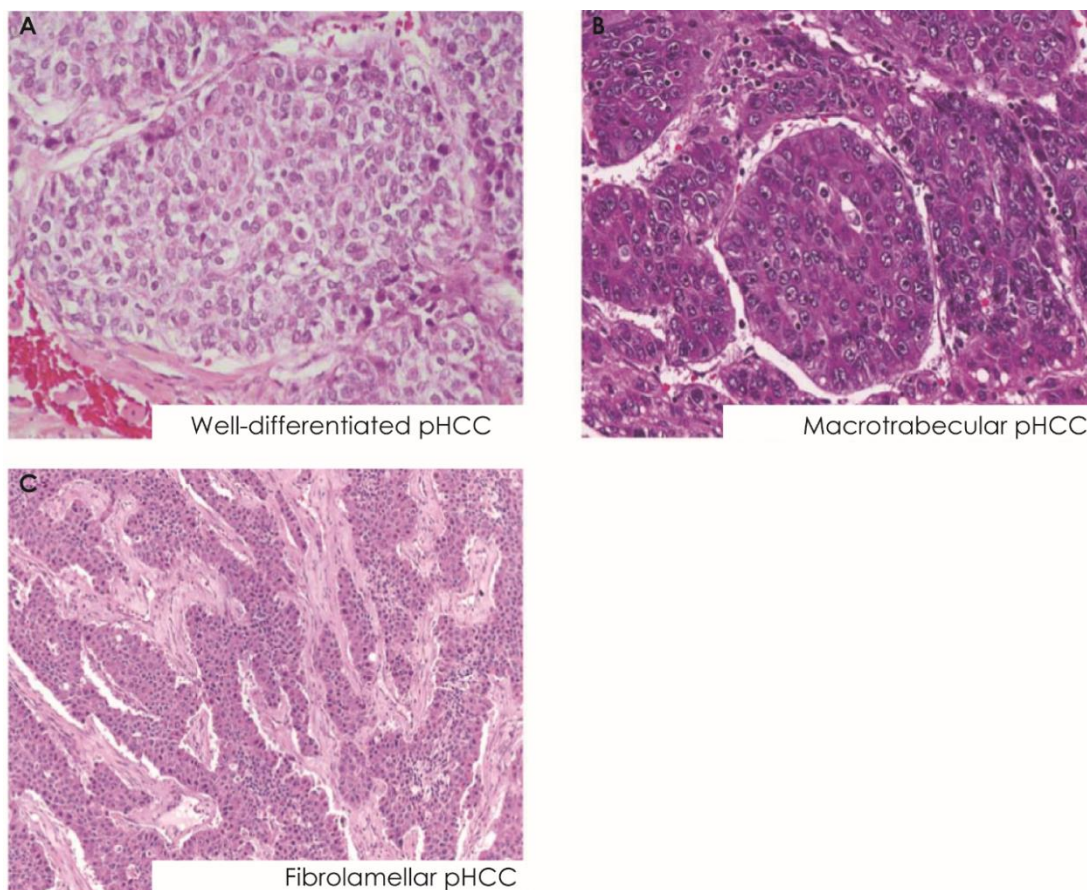


Figure 10. pHCC histology types. Well-differentiated pHCC in a Hepatitis B virus infected patient (A); Macrotrabecular pattern pHCC (B); Fibrolamellar variant of pHCC (C). Pictures from (López-Terrada *et al.*, 2013).

1.3 Biology of pediatric liver tumors

The development of a tumor is a combined and multistep process that results in a clonal expansion of cells that have accumulated the most advantageous set of genetic and epigenetic aberrations. Genetic aberrations includes point mutations, chromosomal rearrangements, chromosomal imbalances, alteration of microsatellite sequences and epigenetic changes such as methylation and histone acetylation among others (Pinkel and Albertson, 2005). However, in order for the normal cells to become tumorigenic, they have to acquire specific abilities, also known as hallmarks, such as resisting cell death, sustaining proliferative signaling, and evading growth suppressors, inducing angiogenesis, enabling replicative immortality, activating invasion and metastasis, deregulating cellular energetics and avoiding immune destruction. Even though these capabilities are key for cancer development, cancer cells need two important enabling characteristics: genome instability and mutations as well as tumor-promoting inflammation. (Hanahan and Weinberg, 2000, 2011).

Childhood solid tumors (CST) are believed to develop from progenitor cells in developing tissues or organs, allowing these cells to develop with fewer defects in key regulatory processes as compared to adult cancers. Also, in contrast to what happens in mature tissues, the progeny of cells in developing tissues are more dividing cells, often with high migratory capabilities and resistant to apoptosis. These differences can explain why, in general, CSTs are more susceptible to chemotherapy treatments. Some CSTs, such as HB, are known as embryonal tumors because they arise from immature tissues and the microscopic appearance resembles tissues in the developing embryo and fetus (Scotting, Walker and Perilongo, 2005; Zimmermann, 2005). A part of the morphologic similarities between cancer cells and their homologues in the developing embryo, in some cases the CSTs can mimic their functions. It is the case of HB, that usually secrete high levels of AFP, which is a serum protein normally produced by the healthy fetal liver cells during development (Scotting, Walker and Perilongo, 2005; Vogelstein *et al.*, 2013).

1.3.1 Gene mutations

Point mutations in certain genes can have key roles in the tumorigenesis, especially the ones activating oncogenes or inactivating tumor suppressor genes. Interestingly, constitutive activation of key signaling pathways are caused by somatic mutations in many tumors, such as constitutive activation of the Raf-MAPK pathway in 40% of melanomas (Hanahan and Weinberg, 2011). Interestingly, not all the mutations present in a tumor are drivers, thus, we can distinguish between trunk mutations, which appear at the onset of the disease and are transforming drivers; branch mutations, that appear during the natural history of the tumors possibly due to the pressure of the therapies; and passenger mutations, which are the most abundant and less relevant in tumorigenesis (Greenman *et al.*, 2007; Llovet *et al.*, 2016).

Several studies have been published aiming to describe the mutational profile of HB, mainly based in whole-exome sequencing (WES). As a results, it has been described that each HB tumor contain 4.5 mutations (range from 0 to 24) (Eichenmüller *et al.*, 2014; Jia *et al.*, 2014; Sumazin *et al.*, 2017) and 30% of the mutated genes in HB are related to transcription, 20% to chromatin organization and 20% to chromosome organization (Eichenmüller *et al.*, 2014).

The main hallmark of HB is the high rate of the β -catenin (CTNNB1) gene mutations and deletions. The most common aberrations of the CTNNB1 gene includes in frame deletions of the exon 3 as well as punctual mutations (Koch *et al.*, 1999; Jeng *et al.*, 2000; Wei *et al.*, 2000; Taniguchi *et al.*, 2002; Cairo *et al.*, 2008; Eichenmüller *et al.*, 2014; Jia *et al.*, 2014). All these alterations lead to modifications of the degradation domain of the protein, which makes it insensitive to targeting for proteasomal degradation causing an accumulation in the nucleus and stimulation of target genes transcription. The Wnt/ β -catenin pathway is a regulator of cell proliferation and differentiation during the early development and later during the growth and maintenance of several tissues. Over activation of this pathway have already been described as the main molecular driver in HB tumors. Interestingly, the APC gene, whose mutations cause the FAP syndrome, codifies for a protein that is part of a complex that regulates cytoplasmic level of β -catenin. Even though,

several components of the Wnt/ β -catenin pathway have been reported to be mutated in many cancers as well as in HB (Figure 11), CTNNB1 gene (which codifies for β -catenin protein) is reported to be mutated in 19-89% of cases, being the main causal of the pathway deregulation. Interestingly, HB cells show an aberrant IHC staining of CTNNB1, which is accumulated into the nucleus and the cytoplasm of tumor cells, as compared to the normal hepatocyte staining, which is mainly into the cell membrane. However, this altered expression of CTNNB1 is shown more frequent than CTNNB1 mutations (Miao *et al.*, 2003), suggesting that other components of the pathway are altered in HB that contributes to the CTNNB1 accumulation and pathway over-activation. Thus, mutations affecting other genes than CTNNB1 from the Wnt/ β -catenin pathway have been described in AXIN 1 (2-10%) and 2 gens (3%) (Taniguchi *et al.*, 2002; Miao *et al.*, 2003; Koch *et al.*, 2004; Cairo *et al.*, 2008) as well as in APC gene (8-61%) (Kurahashi *et al.*, 1995; Oda *et al.*, 1996). Despite the higher incidence of HB cases in FAP patients, germline mutations of the APC gene in sporadic HB are very low (Harvey *et al.*, 2008).

In spite of the fact that CTNNB1 mutations are key molecular drivers of HB and that in some cases are the unique mutational event in this tumor type, *in vivo* experiments demonstrated that mutations of CTNNB1 alone are not enough to foster the development of liver tumors (Harada *et al.*, 2002). Different results are obtained when β -catenin is stabilized in an early fetal progenitor population of cells, in which Wnt pathway activation is enough to drive carcinogenesis and to develop both HCC and HB in this mice model (Mokkapati *et al.*, 2014).

NFE2L2 mutations have been found in 9-10% of HB tumors (Eichenmüller *et al.*, 2014; Sumazin *et al.*, 2017) and it has been postulated that alterations of this activation could be the complementary event leading to liver tumorigenesis. Thus, the described mutations stabilize the protein by preventing its KEAP1-mediated degradation and lead to a constitutive activation of the pathway. However, pathway activation is found more frequently than NFE2L2 mutations, suggesting that other mechanisms could exist. Interestingly, overexpression of the NFE2L2 target gene NQO1 is frequently found in HB samples and is associated with metastasis,

vascular invasion and C2 phenotype, suggesting that NFE2L2 activation could be a prognostic factor for HB (Eichenmüller *et al.*, 2014).

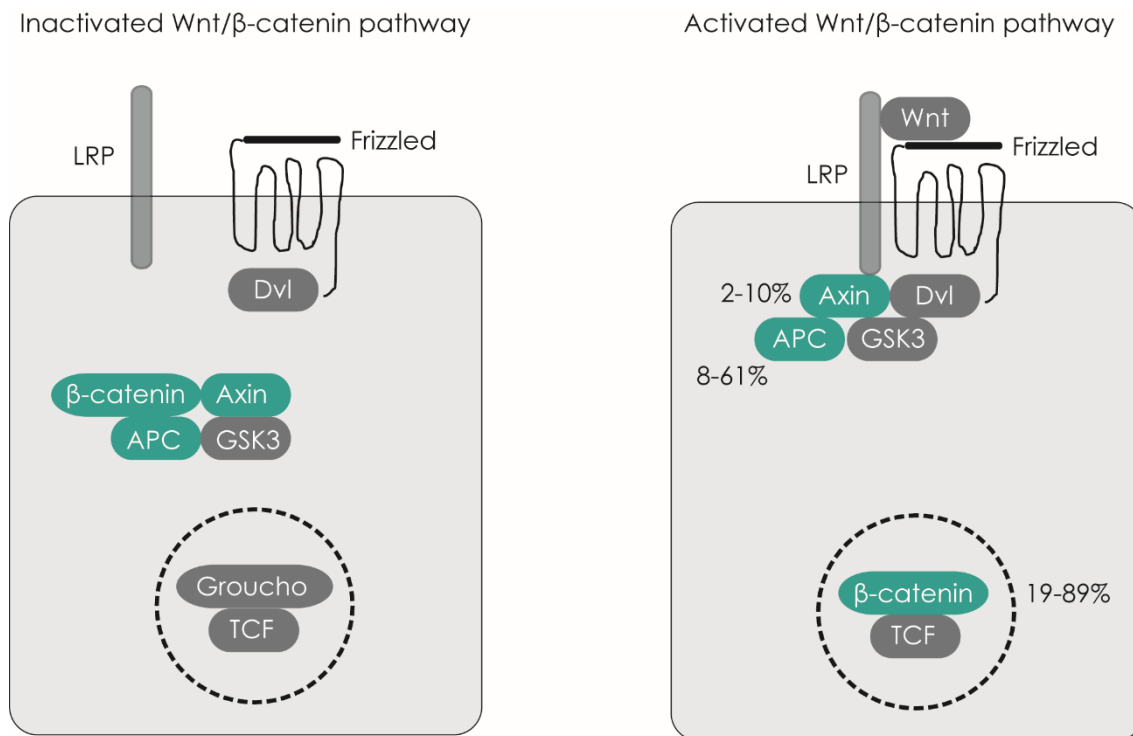


Figure 11. Wnt/β-catenin pathway. In the absence of Wnt, Axin, APC and GSK3 forms a multiprotein complex in the cytoplasm which binds and phosphorylates β-catenin targeting it for proteasomal degradation. In the nucleus (dotted circle), T cell factor (TCF) is in inactive state bound to the repressor Groucho (left). When Wnt binds to its receptor induces the association of Axin with the phosphorylated lipoprotein receptor-related protein (LRP). It causes the separation of the destruction complex and β-catenin is stabilized and translocated to the nucleus, where it binds to TCF and induces target genes transcription, including cyclin D1 and c-myc (right). Components of the pathway mutated in HB are highlighted in blue and the reported frequency of mutations is indicated. Modified from (Nusse and Lim, 1997)

In the study published by Eichenmüller *et al.*, in which whole-exome sequencing (WES) was performed in 3 NOS tumors, 27.3 (range: 11-48) mutations per tumor genome were identified, thus the mutation rate is much higher than in HB. Interestingly the authors found no correlation between number of mutations and patient age, suggesting than other factors than longer exposure time to genotoxic agents contributed to the more complexity of the NOS tumors. NOS tumors also

presented main mutations in transcription regulators. In the same study, the authors found mutations in the promoter of telomerase reverse transcriptase (TERT), previously described as the earliest genetic event in adult HCC tumors (Nault *et al.*, 2013; Schulze *et al.*, 2015), as mutated in 2/3 NOS patients but it was not present in any of the HB studied (Eichenmüller *et al.*, 2014). These promoter mutations are related with an increased TERT transcription leading to TERT reactivation (Nault *et al.*, 2013).

Pediatric cancers normally contain less mutations than adult tumors (Vogelstein *et al.*, 2013), thus is not surprising that in contrast to what happens in HB, adult HCC is a much more unstable tumor harboring 64 non-silent mutations per tumor (Schulze *et al.*, 2015). Main mutated genes in HCC described so far are TERT (54-60%), TP53 (12-48%), CTNNB1 (11-37%), ARID2 (3-18%), AXIN1 (5-15%), and CDKN2A (2-12%) (Guichard *et al.*, 2012; Schulze *et al.*, 2015; Llovet *et al.*, 2016). However, no reports on mutational profile of pHCC have been published. A comparison of the main gene mutations frequencies in HB, NOS and HCC is shown in Table 2.

Table 2. Top mutated genes in HB, NOS and HCC.

Gene	HB (%)	NOS (%)	HCC (%)	References
CTNNB1	19-89	100	11-37	(Koch <i>et al.</i> , 1999; Jeng <i>et al.</i> , 2000; Wei <i>et al.</i> , 2000; Taniguchi <i>et al.</i> , 2002; Cairo <i>et al.</i> , 2008; Curia <i>et al.</i> , 2008; Eichenmüller <i>et al.</i> , 2014; Jia <i>et al.</i> , 2014; Llovet <i>et al.</i> , 2016; Sumazin <i>et al.</i> , 2017)
NFE2L2	9-10	66	3-6	(Eichenmüller <i>et al.</i> , 2014; Llovet <i>et al.</i> , 2016; Sumazin <i>et al.</i> , 2017)
APC	8-61	-	1-2	(Kurahashi <i>et al.</i> , 1995; Oda <i>et al.</i> , 1996; Koch <i>et al.</i> , 1999; Jeng <i>et al.</i> , 2000; Wei <i>et al.</i> , 2000; Cairo <i>et al.</i> , 2008; Llovet <i>et al.</i> , 2016)
AXIN1	2-10	-	5-15	(Taniguchi <i>et al.</i> , 2002; Miao <i>et al.</i> , 2003; Eichenmüller <i>et al.</i> , 2014; Llovet <i>et al.</i> , 2016)
AXIN2	3-5	-	-	
P53	24	-	12-48	(Curia <i>et al.</i> , 2008; Llovet <i>et al.</i> , 2016)
TERT*	0	66	54-66	(Eichenmüller <i>et al.</i> , 2014; Llovet <i>et al.</i> , 2016)

*promoter mutation

1.3.2 Gene fusions

Gene fusions result from chromosomal rearrangements namely inversions, insertions, translocations or deletions that lead to a juxtaposition of two genes that were previously further. These genes could be located in the same or in two different chromosomes and the effect of the fusion transcript can vary depending on the coding or regulatory sequences affected, modifying the function of one or both genes. Thus, gene fusions can have an important role in tumor development and progression when they involve and activate oncogenes or inactivate tumor suppressor genes. Importantly, recurrent gene fusions, such as the BCR-ABL in leukemia, are key events in pediatric tumors (Dupain *et al.*, 2017). However, no fusion events have been described so far for HB or classic pHCC. Contrarily, FL-HCC is characterized by the presence of the DNAJB1-PRKACA chimeric transcript, which is a key molecular driver present in 79-100% patients (Honeyman *et al.*, 2014; Cornella *et al.*, 2015; Darcy *et al.*, 2015). This fusion results from a deletion of ~400kb on chromosome 19 and contains the first exon of DNAJB1 and exons 2-10 of PRKACA. The resulting chimera is a product of an in-frame fusion between the amino-terminal domain of the chaperone DNAJB1 and the catalytic domain of the protein kinase A. It has been proved that this fusion retains the kinase activity of the PRKACA protein (Honeyman *et al.*, 2014). Interestingly, this fusion protein is exclusively identified in FL-HCC but not in HCC, cholangiocarcinoma, hepatic adenomas or HB (Graham *et al.*, 2015).

1.3.3 Copy Number Variations (CNV)

The copy number variations (CNV) profile of tumors can be important for diagnosis and also can provide prognostic information as have been described for many tumor types such as prostate cancer, breast cancer, gastric cancer and lymphoma (Pinkel and Albertson, 2005).

Traditionally, karyotyping was used to study the chromosomal imbalances pattern since its development in the 1970s. Later on, the cytogenetic analysis of banding patterns was replaced by the fluorescence in situ hybridization (FISH)

technique, which is based in the use of fluorescently-labeled probes to locate the positions of specific DNA sequences or chromosomes and requires the use of cells undergoing division as well as pre-designed specific probes of the region to interrogate. To overcome these limitations, the comparative genomic hybridization (CGH) technique was developed to provide a genome-wide screening of CNVs using 2 genomes, test and reference, that are differently labeled and competitively hybridized to metaphase chromosomes. Afterward, a new method combining array technology and CGH was developed called array comparative genomic hybridization (aCGH) (Lucito *et al.*, 2003). aCGH is based on the comparative hybridization of 2 labelled samples, test and reference, to a set of hybridization probes. The size of the probes used determines the resolution of the technique. Finally, single nucleotide polymorphisms (SNP) arrays provide a high-resolution tool to identify CNVs. SNP platforms use probes specific to single-nucleotides that distinguish alleles and allow the identification of regions with loss of heterozygosity (LOH) (Alkan, Coe and Eichler, 2011).

Although HB is a rare tumor, several works have been published aiming to identify recurrent CNVs. In a retrospective study of 111 HB tumor karyotypes was reported that 50% of specimens had numerical aberrations and the main abnormalities identified were trisomies of chromosomes 2 (23%), 20 (22%) and 8 (19%) (Tomlinson *et al.*, 2005). Moreover, the CNV profile of 319 patients have been reported in 16 studies have been published and are reviewed in Table 3. The techniques used in these reports vary from FISH, CGH, aCGH or, more recently, SNP arrays. It has been shown that HB cells are often diploid (fetal type) or hyperdiploid (Buendia, 2002). In the different works, the number of patients with aberrations was variable, however, 63-100% of the reported cases showed CNVs, meaning that in around 15% of HBs do not harbor significant chromosomal aberrations. It is important to note that given to the different techniques used and their different resolution, the results could vary from a report to another. HB tumors are characterized by presenting more gains than losses and usually CNVs involve whole chromosomes or chromosomal arms. The most frequent reported CNVs are gains of chromosome 1q (125/319, 39%), 2q (120/319, 38%), 2p (74/319, 23%), 20q (74/319, 23%), 20p (68/319,

21%), 8q (61/319, 19%), 8p (55/319, 17%), 17 (31/319, 10%) as well as losses of chromosomes 4q (34/319, 11%) and 1p (27/319, 8%) (Figure 12). Interestingly, there is evidence suggesting that gains of chromosome 8q and 20 are predictors of poor outcome in HB (Weber *et al.*, 2000; Sainati *et al.*, 2002).

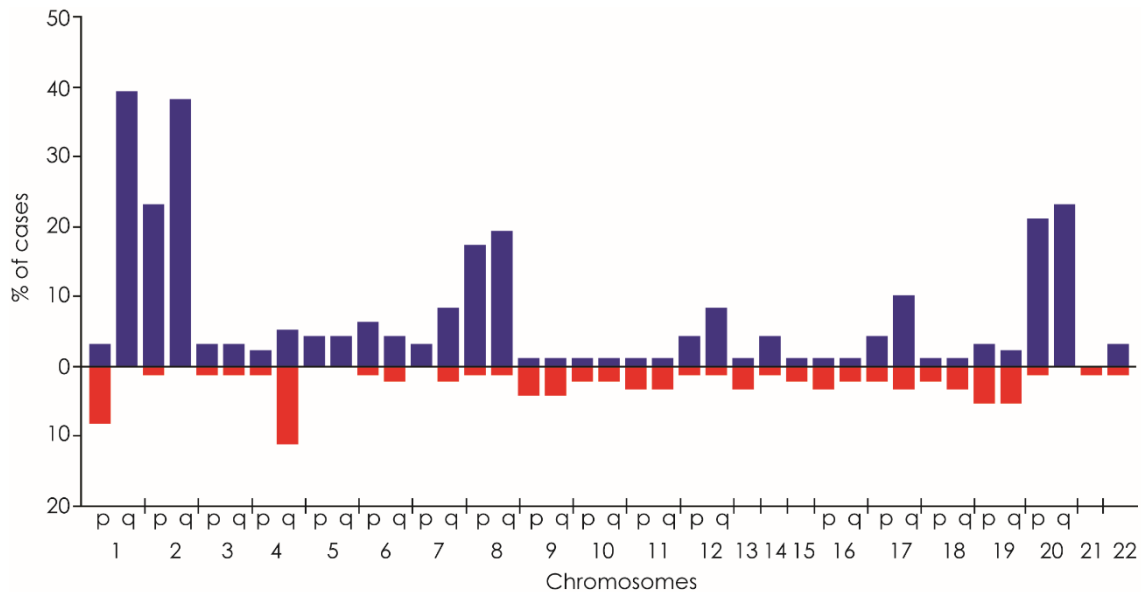


Figure 12. CNVs in HB reported in the literature. The CNV profile of 319 HB patients published in 16 studies. The percentage of described patients with chromosomal gains (blue) or losses (red) is represented in the graph. Each bar represents a chromosomal arm (p and q), except for acrocentric chromosomes (chromosomes 13, 14, 15, 21, 22 and Y). (Steenman *et al.*, 1999; Weber *et al.*, 2000; Gray, Kytölä, *et al.*, 2000; Hu *et al.*, 2000; Parada *et al.*, 2000; Kumon *et al.*, 2001; Mullarkey *et al.*, 2001; Surace *et al.*, 2002; Sainati *et al.*, 2002; Terracciano *et al.*, 2003; Adesina *et al.*, 2007; Suzuki *et al.*, 2008; Stejskalová *et al.*, 2009; T. T.-L. Chen *et al.*, 2009; Arai *et al.*, 2010; Eichenmüller *et al.*, 2014; Sumazin *et al.*, 2017).

Table 3. Frequent chromosomal imbalances identified in HB.

Study	N	% CNV	Techniques	Frequent CNVs (>20%)
(Steenman <i>et al.</i> , 1999)	16	94	CGH	+2q (75%), +1q (63%), +1p (56%), +7q (38%), +8q (31%), +17q (31%), +3 (25%), +5q (2%), +20 (25%)
(Gray, Kytölä, <i>et al.</i> , 2000)	18	78	CGH	-1p (44%), +1q (28%), -13 (28%), +2q (22%), -16p (22%)
(Hu <i>et al.</i> , 2000)	10	90	CGH	-9 (100%), +12q (100%), +8p (100%), +1q (60%), +2q (30%), +20 (30%), -11 (20%), -4 (20%)
(Weber <i>et al.</i> , 2000)	34	71	CGH	+2q (44%), +1q (41%), +2p (29%), +20 (24%)
(Parada <i>et al.</i> , 2000)	7	86	G-banding & FISH	+1q (43%), +8 (43%), +2 (29%)
(Kumon <i>et al.</i> , 2001)	38	71	CGH & FISH	+1q (45%), +2 (37%), +20 (24%), +8 (21%)
(Mullarkey <i>et al.</i> , 2001)	1		CGH	+1q, +2q, +20, +8q, +12q, +17q, +7, -17p
(Sainati <i>et al.</i> , 2002; Surace <i>et al.</i> , 2002)	10	70	FISH & cytogenetics	+1q (50%), +20 (50%), +8 (40%), +2 (30%)
(Terracciano <i>et al.</i> , 2003)	31	97	CGH	+4q (32%), +2q (23%), -4q (23%), -1p (23%)
(Adesina <i>et al.</i> , 2007)	16	100	aCGH	+5p (44%), +2 (38%), +8 (38%), +1q (31%), +20 (25%)
(Suzuki <i>et al.</i> , 2008)	17	88	SNP array	+14 (53%), +2 (47%), +1q (47%), +8 (29%), +7q (29%), +20 (24%), +17q (24%), -11p (24%)
(Stejskalová <i>et al.</i> , 2009)	9	100	aCGH & cytogenetics & FISH	+2 (56%), +20 (56%), +8 (44%), +1q (33%), +5 (22%)
(T. T.-L. Chen <i>et al.</i> , 2009)	1		aCGH & cytogenetics	+1, +3, +5, +7, +12, +16q, +17, +19q, +20, +21, -11q
(Arai <i>et al.</i> , 2010)	56	66	SNP array	+1q (50%), +2q (43%), +20q (20%)
(Eichenmüller <i>et al.</i> , 2014)	12	67	WES	+2q (67%), +1q (50%), +20 (42%), +17 (25%), +12 (25%), -4q (25%)
(Sumazin <i>et al.</i> , 2017)	43	63	SNP array	+1q (30%), -19p (30%), -19q (28%), +2p (23%), +20q (21%)

Abbreviations: N, number of patients included in each study; CNV, Copy number variation; CGH, comparative genomic hybridization; aCGH, array comparative genomic hybridization; FISH, Fluorescence in situ hybridization; SNP, single nucleotide polymorphism; WES, Whole exome sequencing.

Until now, few reports regarding the CNV profile of pHCC are available, however several reports on adult HCC indicated that these tumors had multiple chromosomal aberrations, being the most frequent gains of chromosomes 1q, 8q, 17q and 20 and losses of 1p, 4q, 8p, 13q, 16q and 17p and only 6-10% of tumors show no CNVs (Buendia, 2002; Patil et al., 2005; Kim et al., 2008). Interestingly, recurrent gain in 8q have been associated with microvascular invasion (Kim et al., 2008) and gain of 17q with poor outcome (Zhang et al., 2015).

Thus, chromosomal profiles of HB and HCC display notable differences in the type and number of CNVs. A comparison between HB and HCC chromosomal alterations is summarized in *Table 4*.

Table 4. Chromosomal imbalances found in HB and HCC. HB data is a compilation of 16 already published studies. pHCC data is from a single report (Tan et al., 2016). HCC data was obtained from (Patil et al., 2005; Kim et al., 2008).

CNV	HB (%)	pHCC (%)	HCC (%)
N	319	17	125
None	0-37	-	6-10
-1p	3-44	29-35	10-32
+1q	28-63	65-76	59-65
+2q	19-75	29-47	-
-4q	2-25	29-59	43-45
-8p	-	35-53	41-48
+8q	6-44	41	39-49
-13q	-	29-35	25-37
-16q	-	29-41	37-43
-17p	-	29-41	40-51
+17/17q	-	41-59	21-22
+20	10-56	35-59	31-34

1.3.4 Allelic imbalances

Allelic imbalances are copy-neutral alterations in which two copies of a chromosome or a part of it are from the same origin, which leads to a loss of heterozygosity (LOH). LOH can originate through homologous recombination event or because the retained chromosome was duplicated after a loss. This imbalances can trigger the development of a tumor if the LOH implies a loss of the wild-type allele in individuals with a germline mutation in a tumor suppressor gene such as RB1 in retinoblastoma or BRCA1 in breast and ovarian cancer (Cavenee *et al.*, 1983; Merajver *et al.*, 1995; Ryland *et al.*, 2015). This “second hit” hypothesis was first proposed by Knudson based on his studies in retinoblastoma (Knudson, 1971).

LOH of the 11p15 locus harboring IGF2 and H19 genes is commonly found in sporadic HB cases (Hartmann *et al.*, 2000). IGF2, an essential fetal growth factor with proliferative and antiapoptotic effects, is commonly overexpressed in HB at mRNA level and, of the 4 different possible promoters, is mainly produced of P3 (Gray, Eriksson, *et al.*, 2000; Hartmann *et al.*, 2000) in contrast to the adult liver, in which P1 is dominant. It is thought that the mechanism leading to this alterations could be a defect on the imprinting (Magrelli *et al.*, 2009). It has been described that other genes of the IGF-axis are altered, for example H19, previously described as a tumor suppressor gene, is decreased in HB as well as IGF1R, a receptor which binds IGF1 and mediates its degradation, found mainly downregulated or expressed at similar levels to non-tumor tissue (Gray, Eriksson, *et al.*, 2000). Interestingly, overexpression of IGF2 have also been reported in adult HCC which seems to be due to demethylation of the fetal promoter. Moreover, high levels of IGF2 accelerates liver tumor development in mice and treatment with and antibody anti IGF1 and IGF2 increases survival of these mice (Martinez-Quetglas *et al.*, 2016). Defects of imprinting of 11p15 locus are one of the main causes of the Beckwith-Wiedemann Syndrome, which is highly associated with the risk of tumor development, including HB (DeBaun and Tucker, 1998).

1.3.5 Gene expression profiles

During the last decades, gene expression profiling has been very used and has contributed to the discovery of molecular biomarkers and therapeutic targets as well as specific signatures for several tumors (Casamassimi *et al.*, 2017).

HB shows a general overexpression of many developmental genes, including imprinted genes such as IGF2, PEG3, PEG10, BEX1, MEG3, and NDN, which are abundantly expressed in fetal liver (Cairo *et al.*, 2008) as well as the oncogene PLAG1 (Zatkova *et al.*, 2004). Other studies have identified genes involved in many signaling pathways such as NFE2L2 targets (Eichenmüller *et al.*, 2014); up-regulation of target genes of the hedgehog pathway which is implicated in embryonic development of the liver and also its regeneration in the adult. Moreover, inhibition of this pathway in vitro leads to decreased cell viability of HB cell lines (Eichenmüller *et al.*, 2009); Yes-associated protein (YAP) target genes, survivin, CTGF and Cyclin D1, involved in cell proliferation, are overexpressed in poor prognosis HB (Sumazin *et al.*, 2017). YAP is the main effector of the Hippo pathway and is inversely correlated with pathway activation. The Hippo signaling pathway is an important regulator of cell proliferation and organ size. Hippo pathway activation leads to phosphorylation of YAP and its localization into the cytoplasm, where it remains inactive. Conversely, pathway inactivation leads to YAP accumulation into the nucleus and target gene transcription by TEAD transcription factor. Low levels of YAP phosphorylation suggesting pathway activation as well as target genes overexpression have been shown in HCC and HB (H. Li *et al.*, 2012). Interestingly, colocalization in the nucleus of YAP and β -catenin have been found in HB but not in HCC (Tao *et al.*, 2015). It has been proved that inactivation of Hippo pathway in vivo is enough to dedifferentiate adult hepatocytes into progenitor-like cells (Yimlamai *et al.*, 2014).

Interestingly, studies based on gene expression arrays have been useful to establish HB classifications and to define gene expression signatures correlated to patient outcome. The first classification, identified by unsupervised analysis of transcriptomic data, was published by Cairo *et al.* and is based in a 16-gene signature which distinguish between 2 groups of tumors called C1 and C2. While the

C1 subclass resembles liver features at late stages of intrauterine liver, and is characterized by presenting mostly fetal histotype, lower chromosomal instability and lower proliferation rate, the C2 recapitulates earliest stages of liver development with a predominantly embryonal histotype associated with an enrichment in hepatic progenitor markers such as cytokeratin 19 and EpCAM, high number of chromosomal aberrations and higher proliferation rate. Interestingly, the C2 phenotype is associated with advanced tumor stage (vascular invasion, distant metastasis at diagnosis and PRETEXT IV) as well as worse patient outcome (Cairo *et al.*, 2008). Main C1 and C2 features are summarized in Table 5. Importantly, specific miR expression profiles regulated by Myc have been reported in HB (Cairo *et al.*, 2010).

Table 5. Main features of C1 and C2 HB subtypes. Modified from (Cairo *et al.*, 2008).

Features	C1	C2
Wnt pathway-related mutations	85%	77%
Overexpressed β -catenin targets	Liver perivenous genes	Proliferation and antiapoptotic genes
Hepatic progenitor markers	AFP+ Ep-CAM+ KRT19 -	AFP+++ Ep-CAM+++ KRT19 +
Liver developmental stage	Late fetal/postnatal	Early fetal
Proliferation rate	Low	High
Gene signatures	Hepatic perivenous metabolism	Cell cycle, mitotic checkpoint, Myc signaling
Chromosomal instability	Low	High
Specific chromosomal changes	-	+2p, +8q
Histologic main component	Fetal, pure fetal	Embryonal, crowded fetal, macrotrabecular
Tumor stage	Early	Advanced
Disease outcome	Favorable	Unfavorable

More recently, Sumazin *et al.* published a new classification based in transcriptomic data distinguishing into 3 HB subtypes: low risk group was defined by low Wnt signaling activity and low expression of LIN28B and HMGA2 whereas high risk group was characterized by high NFE2L2 activity and high expression of LIN28B, HMGA2, SALL4 and AFP. Patients who were not predicted to be at low or high risk were considered as intermediate-risk group. Interestingly, this classification was significantly correlated with patients survival and AFP, LIN28B and HMGA2 can be assessed by IHQ (Sumazin *et al.*, 2017).

Specific deregulated genes in HB as compared to HCC have also been described, comprising the overexpressed MIG6, TGF β 1, DLK1, IGF2 and PEG10 and downexpressed IFI27 and LGAL24 (Luo *et al.*, 2006).

HCC transcriptomic signatures have also been identified. In 2007 Boyault *et al.* identified a 16-gene signature that defined 6 different subclasses, named G1-G6 that had different pathway activation as well as mutations and etiologies (Boyault *et al.*, 2007). Later on, in 2010 Hoshida *et al.*, that differentiated 3 subclasses, named S1, S2 and S3 that had different pathway activation, gene expression and pathologic features (Hoshida and Toffanin, 2010).

Transcriptomic studies of FL-HCC have shown overexpression of many oncogenes, some of them related to other cancers, such as ErbB2 from the EGF pathway (Malouf *et al.*, 2014; Simon *et al.*, 2015; Sorenson *et al.*, 2017), cell cycle regulators AURKA and E2F3, CYP19A1 from the estrogen synthesis pathway (Simon *et al.*, 2015), IGF2BP1 (Sorenson *et al.*, 2017) and specific neuroendocrine genes (Malouf *et al.*, 2014).

MicroRNAs (miRs) are small non-coding RNA (22-25 nt) evolutionary conserved that regulate gene expression by regulating mRNA posttranscriptionally, aligning with the 3'-untranslated region and targeting mRNA for degradation or inhibiting translation. Thus, miRs have important roles in the regulation of embryogenesis, metabolism, cell proliferation, apoptosis and differentiation and can also be implicated in many pathogenic processes, such as carcinogenesis as they can target oncogenes or tumor suppressor genes. A huge number of studies

have reported deregulation of specific miRs in tumors versus normal tissues (Olson *et al.*, 2009; Garzon, Marcucci and Croce, 2010).

Particular miRs have been identified to be deregulated in HB as compared to non-tumor tissue (He *et al.*, 2016; Sumazin *et al.*, 2017) as well as in HCC vs HB (Magrelli *et al.*, 2009) and also miR-492 has been proven to modulate PLAG1 expression and to be codified within the coding sequence of the keratin 19 (KRT19) gene (von Frowein *et al.*, 2011). Moreover, a specific 4 miR signature regulated by Myc have been defined in undifferentiated aggressive HB. Importantly, this signature of 4 miRs have demonstrated prognostic value also in HCC (Cairo *et al.*, 2010). Recently, a new study has proposed mir-4510 as a tumor suppressor due to its inhibition of GPC3 in HCC as well as HB cells and supports its putative role as a candidate for miRNA-replacement therapy for patients with liver cancer (Cartier *et al.*, 2017).

1.3.6 Proteomic markers

AFP is the most abundant plasma protein and it is produced by yolk sac and the liver during fetal development. Its plasma levels decrease quickly after birth and normal adult levels are typically reached by the age of 8 to 12 months. Thus, AFP expression in adult are often associated to liver cancer. AFP is thought to be the fetal counterpart of serum albumin and it binds copper, nickel, fatty acids and bilirubin. Importantly, it has been traditionally used as tumor marker for HB patients (von Schweinitz *et al.*, 1997; Fuchs *et al.*, 2002; Maibach *et al.*, 2012; López-Terrada *et al.*, 2013) because most patients show elevated levels at presentations except of 5-10% who have low or normal AFP levels (De loris *et al.*, 2008). Additionally, very high (AFP>10⁶ ng/mL) (Maibach *et al.*, 2012) or very low levels (AFP<100ng/mL) (Perilongo G, Shafford E, 2000; De loris *et al.*, 2008) have also been correlated with reduced overall survival. Interestingly, pHCC patients with high levels (>20ng/mL) have worse outcome than patients with normal levels (Katzenstein *et al.*, 2002) and FL-pHCC patients show normal levels of AFP (Craig *et al.*, 1980; Czauderna *et al.*, 2002). Even though AFP levels seems not to be a good marker to differentiate HB from pHCC, it

seems to be useful as a predictor of recurrence in case its preoperative levels were elevated (Chen *et al.*, 2005) and as a chemotherapy treatment response marker (Koh *et al.*, 2011).

The glutamate-ammonia ligase (GLUL), which is a target gene of the Wnt pathway, have also been reported to be upregulated in HB as well as in well differentiated and less aggressive C1 subtype as compared to non-tumor liver at both gene and protein level (Cairo *et al.*, 2008). Glypican 3 (GPC3) is an oncofetal protein overexpressed in both HB and HCC (Luo *et al.*, 2006). Despite the fact that GPC3 staining is exclusively observed in tumor tissue with complete negativity in non-tumor liver and that it can be found in serum of HCC patients, GPC3 serum levels are not associated with prognostic features in HB (Zhou *et al.*, 2017). Interestingly, epithelial cell adhesion molecule (EpCAM) which is expressed in bile ducts and ductules and lesser in periportal hepatocytes, have been identified by immunohistochemical (IHC) studies in 35% of adult HCCs (Yamashita *et al.*, 2008; Bae *et al.*, 2012). It has been suggested that this EpCAM-positive cells could be cancer stem cells with potential of self-renewal and tumorigenesis in xenografts (Yamashita *et al.*, 2009; Kimura *et al.*, 2010). Interestingly, in an IHC study of EpCAM expression including 12 pHCC, 20 adult HCC, 14 FL-HCC and 15 HB, revealed that it was expressed in 100% of pHCC whereas in only 15% of adult HCC (Zen *et al.*, 2014). Expression in and most of the FL-HCC and HB (Ruck *et al.*, 2000; Ward *et al.*, 2010). Other immunohistochemical markers useful for the identification of HB are listed in *Table 6*.

Activation of the PI3K/Akt pathway have been reported in HB, mainly by confirmed over-expression of p(Ser473)-Akt, and rarely due to PI3KCA mutations found in 2% of HB. In vitro experiments confirmed that growth of human HB cells depends on an activated PI3K/Akt pathway. Interestingly, IGF2 is a potent ligand of the IGF-I receptor, which transduces its signal mostly by the PI3K/Akt pathway. Thus overexpressed IGF2 in HB could explain PI3K/Akt pathway activation. Remarkably, GSK-3 β , a downstream target of PI3K, is involved in β -catenin degradation, and is highly phosphorylated in HB, which indicates activation of the pathway (Hartmann

et al., 2009). Although GSK-3 β is a common effector of both pathways, it seems that its regulation is not mediated by the same phosphorylation events (Wu, 2010).

Table 6. Immunohistochemical stains useful for the diagnosis of HB. Modified from (López-Terrada *et al.*, 2013).

	Well differentiated	Crowded	Pleomorphic	Embryonal	SCU	Mesenchymal	Cholangioblastic
GPC3	Finely granular	+++ coarse	++ coarse	+++ coarse/rare-	-, rare +	-	-
B-catenin	Variably +/+++ N or normal	+ /+++ N	+ /+++ N	+ /+++ N, can be -	+++ N	+++ N on osteoid/blastema/- in teratoid elements	Variable/positive nuclei
GS	+++	+++	Variable	Variable, can be -	-	-	-
Hep Par	+++	+++	Variable	Usually -	-	-	-
Cyclin D1	-	+ /++	+ /+++	+ /+++	+ /++	Variable/- in teratoid	
CK7	-	-		-	- /+	Variable/weak in blastema	+++
CK19	-	-	-	-	+ /++ variable	- /weak in blastema	+++
CD34	+ Endo	+ Endo					
Vimentin	-	-	-	-	+ /++	+++	Usually -
INI1	+++	+++	+++	+++	- pure SCU; variable when mixed	+++	+++

Abbreviations: N, nuclear.

1.3.7 Epigenetic features

Epigenetics refers to the inheritance of patterns of DNA and RNA activity that do not depend on the nucleotide sequence. Main epigenetic events are CpG islands methylation and histone modifications such as acetylation. CpG island hypermethylation blocks transcription, thus it can inactivate tumor suppressor genes or modify gene expression profiles. It has also been observed hypermethylation of promotor regions of specific miRNAs that act as gene regulators related to cancer and metastasis (Esteller, 2011).

Imprinted genes are expressed in a parent-of-origin way and are characterized by DNA methylation on one of the two parental alleles, thus, there are maternally methylated or paternally methylated genes. Importantly, many

imprinted genes regulate cell growth and differentiation, and for this reason, disrupting of imprinting may lead diseases like cancer, and specifically, HB (Rumbajan *et al.*, 2013). For example, hypermethylation of H19/IGF2 imprinting domain at the 11p15.5 locus is the cause of the BWS and is also observed in 29% sporadic HB. Loss of the maternally-expressed tumor suppressor gene H19 and the duplication of the IGF2 paternal allele could lead to an imbalance between growth-inhibiting and growth-promoting stimuli and contribute to tumor development (Albrecht *et al.*, 1994; Hartmann *et al.*, 2000).

In HB, no methylation array studies have been published yet, however several studies reported epigenetic silencing of SFRP1 and APC genes, both of them negative regulators of the Wnt pathway (Shih *et al.*, 2007; Sakamoto *et al.*, 2010) (see 1.2.3.1 *Gene mutations for details about Wnt/ β -catenin pathway*), HHIP which is a negative regulator of the Hedgehog pathway (Eichenmüller *et al.*, 2009), the JAK/STAT regulator SOCS1 (Nagai *et al.*, 2003; Honda *et al.*, 2008; Sakamoto *et al.*, 2010), the apoptosis regulator CASP8 (Honda *et al.*, 2008) and tumor suppressor RASSF1A (Honda *et al.*, 2008; Sakamoto *et al.*, 2010) and IGF2 (33%), and hypermethylation in GNASXL (40%) and RB1 (41%) (Rumbajan *et al.*, 2013). As many of these methylation events have been described as markers for several clinicopathological aspects of HB, it has been suggested that the aberrant promoter methylation detection in serum DNA could be used for the detection of high-risk patients (Tomlinson and Kappler, 2012).

1.4 Experimental models of liver cancer: patient derived xenografts

Using preclinical models is mandatory for translational research and it is even more important in childhood liver tumors due to its rarity. Although the use of cell lines led to important knowledge in the field of cancer biology, they are not the best model since are adapted to grow in an artificial environment and accumulate genetic changes during its culture (Zarzosa *et al.*, 2017). The first murine models mimicking human tumors were developed by the subcutaneous injection of cell lines, either established or primary isolated from tumor samples. Later on, the

implantation of tumor tissue fragments in mice to generate patient derived-xenografts (PDX) was developed. Importantly, engrafted tissue maintains the original tumor heterogeneity and the associated stroma, contributing to a better model for the study of tumor biology as compared to cell culture. Interestingly, the model perpetuation by different passages, allow to stabilize the tumor phenotype and to use it to test different drugs (Hoffman, 1999). First PDX models were generated by heterotopically tumor transplantation, mostly implanted subcutaneously in the back of the mice, but these tumors have many inconveniences such as less ability to develop metastasis. Thus, orthotopic PDX, that is, tumor engrafted in the same organ of origin, better resemble patient tumor progression and response to treatment, but its achievement is more complicated than heterotopic PDX (Zarzosa *et al.*, 2017).

The use and characterization of PDX is required in order to deep in the knowledge of pediatric liver tumors and to test new therapeutic options. The first evidence of HB could be engrafted and grown in immunocompromised mice as PDX models was reported by Fuchs *et al.* in 1996. In their study, 4/6 tumors grew in the mice and despite fetal tissue could also be observed in the successful PDX, only tumors with embryonal components could progress. This seems to indicate that the growth of HB xenografts depends on the presence of an immature phenotype. Interestingly, the grafted tumors showed high AFP levels as the primary tumors did (Fuchs *et al.*, 1996). More recently, Bissig-Choisat *et al.* were able to develop orthotopic PDX from 4 HB, 1 pHCC and 1 NOS. These PDX resembled the histology, genetic and biological features of the primary tumors, including the metastatic behavior (Bissig-Choisat *et al.*, 2016). To our knowledge, no reports on orthotopic PDX form pediatric liver tumors have been reported. PDX generation form adult HCC have been reported, both heterotopically (Xin *et al.*, 2014) and orthotopically (Armengol *et al.*, 2004).

2. AIMS

The global aim of this thesis was to perform a molecular characterization of childhood liver cancer by using omic and next generation sequencing techniques in order to deep in the knowledge of the mechanisms implicated in the development and progression of pediatric liver cancer, and to contribute to an improvement on patient stratification and clinical management. To do so, we established the follow specific aims:

1. To establish a highly clinically annotated collection of tumor samples of pediatric patients with liver cancer.
2. To study the proteomic profile of HB tumors in order to identify deregulated pathways and prognostic biomarkers at proteomic level that could be easily applied at the clinical practice.
3. To increase the molecular knowledge of pediatric liver cancer (HB, pHCC and NOS) through the integration of different data obtained from 2 different approaches:
 - a. RNAseq study in order to identify fusion proteins and mutations.
 - b. Genomic study to identify recurrent chromosomal and allelic imbalances associated to prognosis

3. PATIENTS, MATERIALS AND METHODS

3.1 Establishment of a collection of biological samples from pediatric patients with liver cancer and healthy individuals

With the purpose of creating the first collection of biological samples from pediatric patients with liver cancer in Spain, the Childhood Liver Oncology Group (c-LOG) has been collecting samples since its creation in 2009 in collaboration with the Grupo Español para el Estudio de Tumores Hepáticos Infantiles (GEETHI) and supported by the Sociedad Española de Hematología y Oncología Pediátricas (SEHOP) and the SIOPEL group. This huge work implies the coordination of a multidisciplinary team of surgeons, pathologists, pediatric oncologists and nurses from the participating hospitals,

This collection together with additional samples obtained from international collaborations is the basis of the translational research of the cLOG group and specifically, of the present PhD thesis.

The study was approved by the Biomedical Research Committee of the Health Science Research Institute Germans Trias i Pujol (IGTP), and patient informed consent was obtained at each medical center at the time of sample collection in accordance with European Union guidelines for biomedical research. Finally, collected samples were processed and stored at the IGTP.

3.1.1 Patients inclusion

From 2009 onwards, biological samples from patients diagnosed with a liver tumor in the main hospitals in Spain (mainly Hospital Universitari Vall d'Hebron (Barcelona), Hospital Universitario La Paz (Madrid) and Hospital Universitari I Politècnic La Fe (Valencia)) were obtained.

Frozen and FFPE tissue samples as well as plasma and peripheral blood monocytes (PBL) were collected from pediatric patients suspected with a liver tumor. The diagnosis was obtained by an expert pathologist after tumor biopsy. Samples from patients with a final diagnosis of a benign tumor lesion were also included in the collection. PBL from the parents of the patients were also obtained.

Furthermore, plasma samples from healthy children undergoing minor surgical operations non-related with liver damage or cancer were obtained from the Hospital Universitari Vall d'Hebron from July to December 2015.

3.1.2 Biological samples obtaining and storage

3.1.2.1 Blood and derivatives

Blood samples were obtained at the time of diagnosis before chemotherapy treatment when possible, by specialized nurses in the respective hospitals using standard blood collection tubes. When possible, blood samples were obtained by taking advantage of an already programmed blood extraction. Due to the young age of the patients, the volume of blood obtained was variable (5-10mL).

Immediately after blood extraction, plasma samples were obtained by centrifuging blood at 2000g for 10 minutes at 4°C and taking the supernatant. The plasma obtained was aliquoted and immediately frozen at -80°C or stored with dry ice until sample shipment. Once at the IGTP, plasma samples were stored at -80°C until its use.

Peripheral Blood Lymphocytes (PBL) were isolated from by centrifuging the blood at 2000rpm (revolutions per minute) for 10 minutes and taking the interphase (cellular phase).

From healthy patients, only plasma samples were obtained, also following the same protocol explained above.

3.1.2.2 Tissue samples

Tissue samples were obtained from biopsy, surgical resection or liver transplant procedures by expert pathologists.

At the time of diagnostic biopsy, surgeons were asked to perform an extra tru-cut passage in order to obtain tumor tissue sample for research purposes, only when possible.

From surgical specimens, tumor tissue as well as non-tumor liver tissue were obtained. Pathologists were asked to prepare:

- 1-3 pieces of tumor tissue (depending on tumor size) in cryotubes for its immediate freezing
- 2 pieces of tumor tissue to be kept fresh in complete cell culture media
- Formalin-fixed Paraffin-embedded (FFPE) blocks
- 1-3 pieces of non-tumor liver tissue in cryotubes for its immediate freezing
- 1 piece of non-tumor liver tissue to be kept fresh in cell culture

All the tissue samples had to be snap-frozen with liquid nitrogen or dry ice and stored at -80°C until its shipment, except fresh samples, which had to be preserved and shipped at RT.

In order to assess protein expression in large series of patients, we developed 11 tissue microarrays (TMA) by using FFPE tissues from this collection including samples of 144 patients, 104 tumors, 40 biopsies and 42 NT samples.

3.1.3 Clinical and pathological data registry

Parallel to the sample obtaining, clinical, pathological and familiar data were also obtained from the patients included in the study.

Pediatric oncologists and pathologists were asked to complete specific forms designed for the study in order to collect all the clinical, familiar and pathological data associated and to send them back to the IGTP.

3.1.5 Molecular characterization of the samples

At molecular level, frozen tumors were annotated according to the 16-gene signature by qPCR and β -catenin gene mutations as previously reported (Cairo et al., 2008). For FFPE tumors, nuclear accumulation of β -catenin and ki67 staining was analyzed by immunohistochemistry.

3.2. Proteomic study

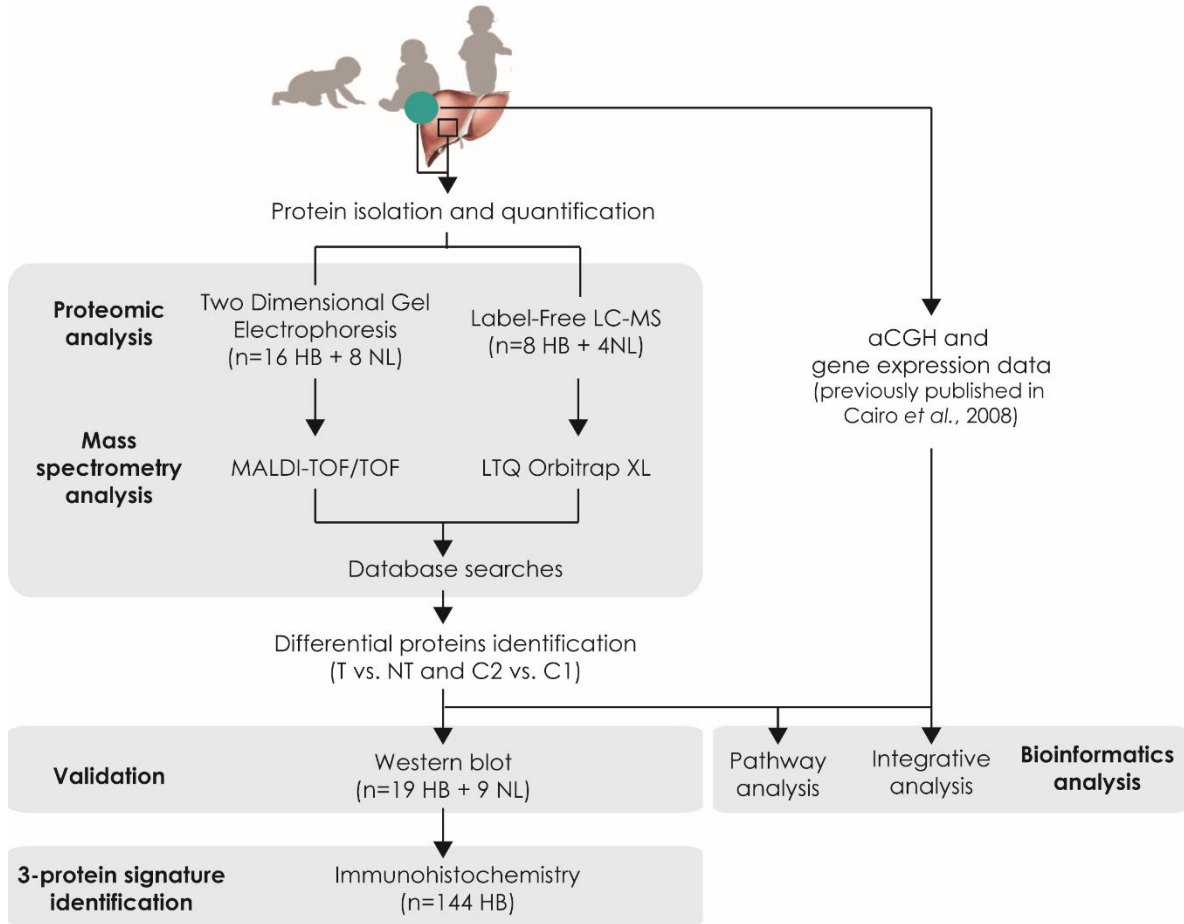


Figure 13. Workflow followed on the proteomic study.

3.1.1 Patients, tissue and plasma samples

The proteomic study includes samples from 160 patients included in 2 sets of samples (discovery and validation set). The discovery set comprised frozen tumor samples from 16 patients previously analyzed by Affymetrix HG-U133A microarrays (Cairo *et al.*, 2008) together with 8 NT, cell lines and FL. As control, 2 human fetal livers at different gestational ages obtained from the Biobank of the Hospital Universitari Vall d'Hebron (Barcelona) were also included in the study. For the validation set, a total of 186 samples including 104 surgical specimens and 40 biopsies from 133 patients with HB, 6 NOS and 5 pHCC in non-cirrhotic liver, as well

as adjacent non-tumor liver from 42 patients were analyzed. Those samples used for the validation set were included in 11 TMAs.

Table 7 summarizes the main clinical and pathological features of the 160 childhood patients with liver cancer included in the study. Regarding the discovery set, we studied 16 tumors which were previously characterized (Cairo *et al.*, 2008) as C1 (n=11) and C2 (n=5). Patients received chemotherapy treatment prior to surgery, most being enrolled in clinical trials of the SIOPEL group (Perilongo G, Shafford E, 2000). Fifty-six (9/16) percent of the patients had PRETEXT III or IV tumor, 31% (5/16) presented with metastasis at diagnosis and 56% (9/16) had vascular invasion. Eighty-one percent of the tumors (13/16) presented an epithelial histology. Mean follow-up was of 45.7 months with a cancer-related death incidence of 37.5%.

Regarding the validation set, 99 patients received chemotherapy treatment prior to surgery, most being enrolled in clinical trials of the SIOPEL group (Perilongo G, Shafford E, 2000). Seventy-four (57%) of the HB patients had PRETEXT III or IV tumor, 114 (85%) presented with metastasis at diagnosis and 103 (79%) had vascular invasion. A pathological examination of all the tumor specimens was performed by national expert pathologists (L. G. and M. G.). Eighty two of the tumors (60%) presented an epithelial histology and ninety one (70%) of them a main predominant fetal component. Regarding the pHCC, 2 patients (50%) presented with metastasis at diagnosis and 67% has vascular invasion. Mean follow-up was of 87 months with 14 cancer-related deaths for HB patients and 44 months and 3 cancer-related deaths for pHCC.

Table 7. Clinical, pathological and molecular features of the 160 patients included in the study.

	Discovery set		Validation set	
	HB (n=16)	HB (n=139)	HB (n=139)	pHCC (n=5)
• Age, months (median, [range])	29 [12-204]	13 [0.29-159]	123 [118.179]	
• Serum AFP, ng/mL (range)	448-1.708.400	11-7.627.330	NA	
• Preoperative chemotherapy (Y/N)	15/1	96/43	3/2	
• Tumor stage				
PRETEXT stage (I/II/III/IV/NA)	1/6/6/3/0	11/45/50/24/9	0/0/0/2/3	
Metastasis at diagnosis (Y/N/NA) (%Y)	5/11/0 (31.25%)	20/114/5 (15%)	2/2/1 (50%)	
Vascular Invasion (Y/N/NA) (%Y)	9/7/0 (56.25%)	28/103/8 (21%)	2/1/2 (67%)	
• Histology				
Epithelial/Mixed /NA	13/3/0	82/55/2	-	
MEC: Fetal/Non-Fetal*/NA	10/6/0	91/40/8	-	
SCU histology (%)	0	5 (4%)	-	
NOS tumors (%)	0	6 (4%)	-	
• 16-gene Subtype (C1/C2)	11/5	-	-	
• Follow-up, months (mean)	45.7	87.1	43.7	
Tumor recurrence (Y/N)	1/15	13/126	0/5	
Outcome: cancer-related deaths (%)	6 (37.5%)	14 (11%)	3 (60%)	

* Non fetal includes: Embryonal, crowded fetal, macrotrabecular and SCU
NA, non-available; MEC, Main Epithelial Component

3.1.2 Protein study

3.1.2.1 Protein isolation and quantification

Liver tumor and non-tumor tissue samples in lysis buffer (7M urea; 2M thiourea; 2% CHAPS; 65mM DTT; 1% protease inhibitor; 0.6% benzonase) were homogenized by using FastPrep®-24 Instrument (MP Biomedicals). Then, homogenized samples were ultracentrifugated at 32.000 rpm for 50 minutes, the supernatant was collected and its protein concentration was determined using the Bio-Rad Protein Assay (Bio-Rad).

3.1.2.2 Proteomic analysis

All the proteomics experimental work and analysis has been done at the Proteomics Facility of Cic bioGUNE Center for Cooperative Research in Biosciences (Derio, Bizkaia) by Dr Mikel Azkargorta under supervision of Dr Felix Elortza.

The proteomic profiling of 16 HB tumor (11 C1 and 5 C2 subtypes) and 8 non-tumor liver tissues was studied by Two-Dimension Fluorescence Difference Gel Electrophoresis (2-D DIGE). Moreover, 8 tumor (4 C1 and 4 C2 subtypes) and 4 non-tumor samples were selected for nano-LC-ESI-MS/MS Label free (LF) analysis.

3.1.2.2.1 Two Dimension Gel Electrophoresis

Protein extracts were precipitated using 2D Clean-Up kit (GE Healthcare) and resuspended in Cell Lysis-Buffer, containing 7M Urea, 2M Thiourea, 4% CHAPS, 30mM Tris. Samples were incubated for 1h at RT under agitation, and protein content was quantified using the Bio-Rad Protein Assay (Bio-Rad). Proteins were labeled following manufacturer's instructions (GE Healthcare). Each sample was labeled with Cy3 or Cy5 cyanine dyes used in a ratio of 400 pmol dyes for each 50 µg protein. Samples of different HB subclasses and non-tumor tissues were randomly labeled to avoid dye biases. Cy2 dye was specifically used for labeling the internal standard (mixture of the different samples present in the study). Prior to the analysis, Cy3- and Cy5-labeled sample pairs were mixed together with a Cy2-labeled internal standard aliquot in equal proportions (50ug each). A buffer containing DTT and ampholytes was added to these mixtures, to a final concentration of 7M Urea, 2M Thiourea, 4% CHAPS, 15mM Tris, 65mM DTT, 1% ampholytes. The 150 µg protein mixtures were loaded and run in 24cm pH 4-7 strips (GE Healthcare) for isoelectric focusing (IEF). After the IEF, strips were incubated in equilibration buffer (6M Urea, 100 mM Tris pH 6.8, 30% (w/v) glycerol, 2% (w/v) SDS) with 2% DTT for 15 min, and in the same buffer with 2.5% IA instead of DTT for another 15 min. Second dimension (SDS-PAGE) was carried out in an Ettan Dalt Six chamber (GE Healthcare) using 12% polyacrylamide gels. Gels were run at 1W/gel for 30 min, 5 W/gel for another 30 min, and finally at 17 w/gel for approximately 3h. Images were acquired in a Typhoon Trio scanner (GE Healthcare) following manufacturer's recommendations and analyzed using REDFIN software (Ludesi). Spot volume normalization against the internal standard was automatically performed. Spots with a volume >100 and present in all the gels in each comparison were considered for the analysis. After the ANOVA test performed by the software, spots with a $p < 0.05$ and a ratio >1.5 in either direction

were considered as significantly deregulated, and therefore excised from the gel. For this purpose, a gel with 300µg protein was run, matched to the analyzed set, and picked using the automatic Ettan Spot Picker (GE Healthcare). These spots were digested and submitted to mass spectrometry analysis.

2D-DIGE Spot digestion and protein identification

Gel spots were reduced and alkylated prior to their digestion with trypsin. Thus, spots were washed and incubated with DTT (10 mM in 50 mM ammonium bicarbonate, 30 µl) at 56 °C for 20 min, followed by an incubation in IA (50 mM in 50 mM ammonium bicarbonate, 30 µl) for another 20 min in the dark. Then, spots were washed in ammonium bicarbonate, dried by adding excess of acetonitrile and incubated with trypsin (12.5 µg/mL in 50 mM ammonium bicarbonate, 10 µl) for 20 minutes in ice. After rehydration, the trypsin supernatant was discarded, spots were covered with 50 mM ammonium bicarbonate, and incubated overnight at 37 °C. After digestion, supernatant was collected and acidic peptides were further extracted with trifluoroacetic acid (TFA) 0.1 % and pooled with the previously released peptides. Samples were dried out in a RVC2 25 speedvac concentrator (Christ) and submitted to MALDI-TOF/TOF analysis (see 3.1.2.2.3.1 MALDI-TOF/TOF analysis). When no confident identification was obtained with MALDI-TOF/TOF, peptides were analyzed in an LTQ Orbitrap XL ETD mass spectrometer (Thermo Finnigan), (see 3.1.2.2.3.2 LTQ Orbitrap XL analysis).

3.1.2.2.2 Label-Free LC-MS and peptide identification

Fifty µg of protein extracts were precipitated and resuspended in 6M Urea. Then, the sample was reduced (5mM DTT for 45 min), alkylated (25mM IAA for 45 min), and diluted to a final concentration of 1M Urea. For protein digestion, trypsin was added to a trypsin:protein ratio of 1:10. The mixture was incubated overnight at 37°C, dried out in a RVC2 25 speedvac concentrator (Christ) and resuspended in 0.1% FA. The equivalent of 300ng of each sample was submitted to Liquid Chromatography-MS label-free analysis. LTQ Orbitrap XL mass spectrometer (Thermo Finnigan) was used for this purpose. The Progenesis LC-MS (version

4.0.4265.42984, Nonlinear Dynamics) was employed for the label-free differential protein expression analysis.

Progenesis LC-MS (version 4.0.4265.42984, Nonlinear Dynamics) was utilized for the label-free differential protein expression analysis. One of the runs was adopted as the reference to which the precursor masses in all other samples were aligned to. Only features comprising charges of 2+ and 3+ were selected. The raw abundances of each feature were automatically normalized and logarithmized against the reference run. Samples were grouped in accordance to the comparison being performed, and an ANOVA analysis was performed. Features with an ANOVA p-value ≤ 0.05 and a ratio >1.5 in either direction were only further considered. A peak list containing the information of these significantly different features was generated and exported to the Mascot search engine (Matrix Science Ltd.) The generated .mgf file was searched against Uniprot/Swissprot human database. The list of identified peptides was imported in Progenesis LC-MS and the previously quantified features were matched to the corresponding peptides. Non-conflicting peptides (peptides occurring in only one protein) were specifically chosen for quantitative purposes, and only proteins with at least two quantified non-conflicting peptides were selected. The significance of expression changes was again tested at protein level, and proteins not satisfying the ANOVA p-value ≤ 0.05 and Ratio >1.5 in either direction criteria were filtered out.

3.1.2.2.3 Mass spectrometry analysis

3.1.2.2.3.1 MALDI-TOF/TOF analysis

Dried peptides were resuspended in 0.1 % TFA, desalted using in-house Poros R2+R3 micro-columns, eluted in α -Cyano-4-hydroxycinnamic acid (HCCA) (prepared in 10:30 acetonitrile:TFA 0.1 %), and spotted on a MALDI Ground Steel 384 plate (Bruker Daltonics). The spots were allowed to dry out prior to the analysis. MS and MS/MS analysis were performed on an Autoflex III Smartbeam TOF/TOF (Bruker), equipped with a LIFT and a reflectron. Peptide ionization was carried out using 200 Hz pulses of a 360 nm solid-state laser. Mass resolution was kept above 7500 for the entire mass window. One thousand and four hundred scans were carried out for the

peptide mass fingerprint (PMF) analysis, and the parental ions were selected manually. Peptide fragment fingerprinting (MS/MS) analysis was performed using 400 scans for the parental ions and 1600 scans for the fragments.

3.1.2.2.3.2 LTQ Orbitrap XL analysis

Peptide separation was performed on a nanoACQUITY UPLC System (Waters) on-line connected to an LTQ Orbitrap XL mass spectrometer (Thermo Electron). An aliquot of each sample was loaded onto a Symmetry 300 C18 UPLC Trap column (180 μm x 20 mm, 5 μm (Waters)). The precolumn was connected to a BEH130 C18 column (75 μm x 200 mm, 1.7 μm (Waters)), and equilibrated in 3% acetonitrile and 0.1% FA. Peptides were eluted directly into the LTQ Orbitrap XL mass spectrometer through a nanoelectrospray capillary source (ProxeonBiosystems), at 300 nl/min and using a 30 min linear gradient of 3–50% acetonitrile for DIGE spots, or a 60 min linear gradient of 3–50% acetonitrile for LF samples. The mass spectrometer automatically switched between MS and MS/MS acquisition in DDA mode. Full MS scan survey spectra (m/z 400–2000) were acquired in the orbitrap with mass resolution of 30000 at m/z 400. After each survey scan, the six most intense ions above 1000 counts were sequentially subjected to collision-induced dissociation (CID) in the linear ion trap. Precursors with charge states of 2 and 3 were specifically selected for CID. Peptides were excluded from further analysis during 60 s using the dynamic exclusion feature.

3.1.2.2.4 Database searches

MALDI data was processed using FlexAnalysis v3.0 (Bruker Daltonics). The resulting mass lists were generated by BioTools v2.1 (Bruker Daltonics) and the database searches were performed by Mascot v2.1 (Matrix Science) search engine against Uniprot/SwissProt database (version 2013_07, 540,546 entries) using Mascot version 2.2.07. Carbamidomethyl was chosen as fixed modification. Peptide mass tolerance of 30 ppm and 0.7 Da of fragment mass tolerance were chosen along with up to one missed cleavages.

LTQ Orbitrap XL searches were performed using Mascot search engine v2.1 (Matrix Science) with Proteome Discoverer 1.2. (Thermo Electron).

Carbamidomethylation of cysteines was set as fixed modification, and oxidation of methionines as variable modification. 5 ppm of peptide mass tolerance, 0.5 Da fragment mass tolerance, and 2 missed cleavages were allowed. Spectra were searched against Uniprot/Swissprot database version 2013_07. Regarding LF searches, only peptides with a false discovery rate of <5% were selected for further analysis. For the 2D-DIGE protein identification, only proteins identified as unique in a given spot were used for further statistical analysis.

3.1.2.3 Western Blot (WB)

The 8 putative prognostic biomarkers identified by proteomics as well as key proteins of significant pathways were validated by SDS-PAGE electrophoresis and Western blotting analysis. To do so, 50 µg of protein extracts were resolved in SDS-10% polyacrylamide gels (SDS-12% for DERM) under reducing conditions, and electrophoretically transferred to nitrocellulose membranes (Bio-Rad Laboratories, UK). The membranes were then blocked with Starting Block TBS blocking buffer (Pierce) for 1h at RT and incubated overnight at 4°C with indicated primary antibodies diluted in blocking buffer. The membranes were subsequently incubated with the appropriate fluorescently-coupled secondary antibodies (IRDye 800Cw-conjugated goat anti mouse IgG or IRDye680Cw-conjugated goat anti rabbit IgG 926-32210 and 926-68021 respectively, Li-Cor), diluted in blocking buffer for 60 min at RT. Three 15 minutes washings between steps were performed with TBS-0.01% Tween 20 (phosphorylation markers) or PVS-0.01% Tween 20 (non-phosphorylation markers). Tubulin antibody was used as a loading control in all the experiments. Bound antibody was detected with an Odyssey Infrared Imager and densitometric analysis was performed by using the Odyssey V.3 software (LI-COR). A reference sample was included in all the membranes used and fold change of the biomarkers expression was calculated using it as a control. The different antibodies used for WB are listed in *Table 8*.

Table 8. List and details of the different antibodies used for WB.

Protein	Type	Working dilution	Reference	Brand
ALB	mAb	1:5000	A 6684	Sigma-Aldrich, St Louis, MO, USA
Akt	mAb	1:2000	4691	Cell signal
Akt (Phospho-Ser473)	mAb	1:2000	4060	Cell signal
CRYL1	poAb	1:1000	HPA040403	Sigma-Aldrich, St Louis, MO, USA
CKAP4	poAb	1:500	HPA000792	Sigma-Aldrich, St Louis, MO, USA
C1QBP	poAb	1:250	HPA026483	Sigma-Aldrich, St Louis, MO, USA
DERM	poAb	1:285	10537-1-AP	ProteinTech/AntibodyBCN
EIF	mAb	1:1000	NBP2-02669	Bio-Techne, Minneapolis, MN, United States
pEIF 2a	mAb	1:1000	04-342	Millipore, Billerica, MA, USA
GLUL	mAb	1:2000	610517	BD Transduction Laboratories, Lexington, KY, USA
TMPSD	poAb	1:2500	PA5-30935	Thermo Fisher Scientific
TP53	mAb	1:200	Sc-47698	Santa Cruz Biotechnology, Dallas, TX, USA
TUBULIN	mAb	1:10000	T6074	Sigma-Aldrich, St Louis, MO, USA
TXNL1	poAb	1:250	HPA002828	Sigma-Aldrich, St Louis, MO, USA
YAP	mAb	1:1000	WH0010413M1	Sigma-Aldrich, St Louis, MO, USA
YAP (Phospho-Ser127)	poAb	1:1000	SAB4301450	Sigma-Aldrich, St Louis, MO, USA

3.1.2.4 Immunohistochemistry (IHC)

The expression of the 3 significant biomarkers, C1QBP, CKAP4 and CRYL was assessed in 144 FFPE pediatric liver tumors and 42 non-tumorous livers included in 4-micron sections mounted on silanized DAKO glass slides of 6 different Tissue Microarrays (TMA) by IHC. The same tumors were also characterized according to its proliferation degree (Ki67) and β -catenin status.

For immunostaining, tissue sections were deparaffinised and rehydrated in water. Antigen retrieval was performed in a DAKO PT link (Agilent, Santa Clara, CA; USA). Slides were incubated with the same antibodies previously used for WB at the following working dilutions: C1QBP and CKAP4 (1: 100), and CRYL (1: 200) for 60 min. Prediluted mAB antibodies for Ki67 (#M7240) and β -catenin (#M3539) all from Agilent Technologies, were also used. Staining was detected with Dako Envision Plus kit. Slides were counterstained with Hematoxylin and coverslipped with DPX mountant for microscopy (VWR Int).

The expression of prognostic biomarkers determined by IHC was calculated by examining two cores and defined according to percentage of stained hepatocytes (0=no stained cells, 1=1-4%, 2=5-19%, 3=20-39%, 4=40-59%, 5=60-79%, 6=80-100% of positive cells) and intensity 0, no staining; 1, low; 2, moderate and 3, intense staining). Percentage scores were multiplied by intensity scores to yield an overall score. Finally, by using NL staining as a reference, the cut-offs of alteration were established.

Proliferating activity was assessed by Ki67 labeling index (LI) defined as the percentage of nuclear positive cells in the observed field. Afterward, tumors were classified as low Ki67 (LI < 5%) and high proliferating Ki67 (LI > 5%). Nuclear and/or cytoplasmic β -Catenin and nuclear TP53 scores of >3 were considered as positive.

3.1.2.5 Enzyme-Linked ImmunoSorbent Assay (ELISA)

In order to quantify the plasmatic levels of C1QBP, a commercial ELISA kit was used: Enzyme-linked Immunosorbent Assay kit for Hyaluronan Binding Protein 1 (HABP1) (Cloud-Clone Corp, Katy, TX, USA).

Plasma samples from 20 patients with liver cancer and 7 healthy patients were diluted 1/100 and 1/200 in PBS. Samples were analyzed in triplicates and following manufacturer instructions. Absorbance values were determined with a spectrophotometer Varioskan Flash (Termofisher Scientific) at 450 nm.

Main clinical and pathological features of the 27 childhood patients with liver cancer and healthy individuals included in the study are listed in *Table 9*. Patients with liver cancer were classified as good (n=10) or poor outcome (n=10). Patients with bad prognosis features (poor) were classified if presented metastasis and/or multifocality and/or PRETEXT IV and/or AFP >10⁶ ng/mL and/or more than 3 years and/or pHCC. The patients classified as “good prognosis” did not meet the mentioned criteria.

Table 9. Clinical and pathological features of the 27 patients and healthy individuals included in the ELISA study.

	Healthy individuals (n=7)	Liver cancer patients (n=20)
• Age, months (median, [range])	27 [4-50]	14 [0.2-144]
• Serum AFP, ng/mL (range)	-	710-1374186
• Tumor stage		
PRETEXT stage (I/II/III/IV/NA)	-	2/8/6/4
Metastasis at diagnosis (Y/N/NA)	-	4/15/1
Vascular Invasion (Y/N/NA)	-	-
• Histology		
HB: Epithelial/Mixed Tumors/NA Tumors	-	10/9
MEC: Fetal/Non-Fetal*/NA	-	10/6/3
SCU histology	-	1
pHCC	-	1
• Follow-up, months (mean)	-	38
Outcome: cancer-related deaths	-	1 (5%)

*Non fetal includes: embryonal, macrotrabecular and fetal atypical.
NA, non-available; MEC, Main Epithelial Component

3.1.3 Bioinformatic analysis

3.1.3.1 Pathway analysis

In order to identify the deregulated pathways in HB and specially, in the C2 aggressive cases, we used the software Ingenuity® Pathway Analysis (IPA®) which allows to search and analyze *omic* data, such us proteomics, and to identify deregulated pathways, targets or biomarkers. The data analyzed comprised the deregulated proteins in the T vs NT, C2 vs C1, C1 vs NT and C2 vs NT comparisons ($p < 0.05$, $-1.5 \leq FC \leq +1.5$). IPA software calculated an activation z-score, which determines whether an upstream transcriptional regulator has significantly more activated predictions ($z > 0$) than inhibited predictions ($z < 0$).

After loading the different lists, a core analysis was run using IKB as a reference set. Direct and indirect relationships were considered. Only experimentally observed interactions were contemplated and evidences found in all species and tissues and cell lines were taken into account.

3.1.3.2 Bioinformatics analysis of proteomic data

The bioinformatics analysis was done in collaboration with Lara Nonell from the Microarray Analysis Services (SAM) in the Institut Hospital del Mar d'Investigacions mèdiques (IMIM).

Unsupervised and supervised analysis of proteomic data

Hierarchical clustering was performed with Pearson's correlation distance and Complete as linkage method and also Principal component analysis were applied to assess sample aggregation.

Integrative study

The integration of DNA, RNA and protein data was performed with two different methodologies. The first approach was conducted with regression techniques by using DR Integrator (DRI) (Salari, Tibshirani and Pollack, 2009) (<http://CRAN.R-project.org/package=DRI>), a methodology that requires the same set of samples and also the same set of genes to be analyzed. To integrate two data

sets with the objective of comparing two conditions represented in both data sets, it computes a moderated t-test for each set and then it combines both results to create a common score. For this purpose DNA data was transformed to obtain a data set with genes instead of BACs. This was performed by taking raw data and, for each present gene taking the mean value of the corresponding matching BACs. Control samples were estimated by taking the distribution of DNA controls and resampling to obtain 2 new control samples. Protein data were analyzed on one side through DIGE and on the other side through LF by completing it with DIGE data (only complementary proteins). In order to complete LF data with DIGE, they were previously scaled and joined. Once all data was prepared, DRI was executed in 3 steps, first integrating DNA and RNA, then DNA and protein and finally RNA and protein.

3.1.3.3. Statistical analysis

In order to study the significant bivariate differences, t-student, chi-square or Fisher tests were used according to convenience. To study the impact on patient event free survival (EFS) or overall survival (OS) of the different biomarkers studied and the 3-protein signature, the Kaplan–Meier method was used to estimate survival curves, and the log-rank test was used to compare them. Cox regression was used to assess the impact of the different classifications in patient event free survival. Statistical analysis was performed with the GraphPad Prism 7 for Windows, GraphPad Software (La Jolla, CA, USA) and the IBM SPSS statistics for Windows, version 15 (Chicago, IL, USA). Fisher exact test calculated with the online tool <http://vassarstats.net/fisher2x3.html> for tables other than 2x2.

3.3 Genomic and RNAseq study

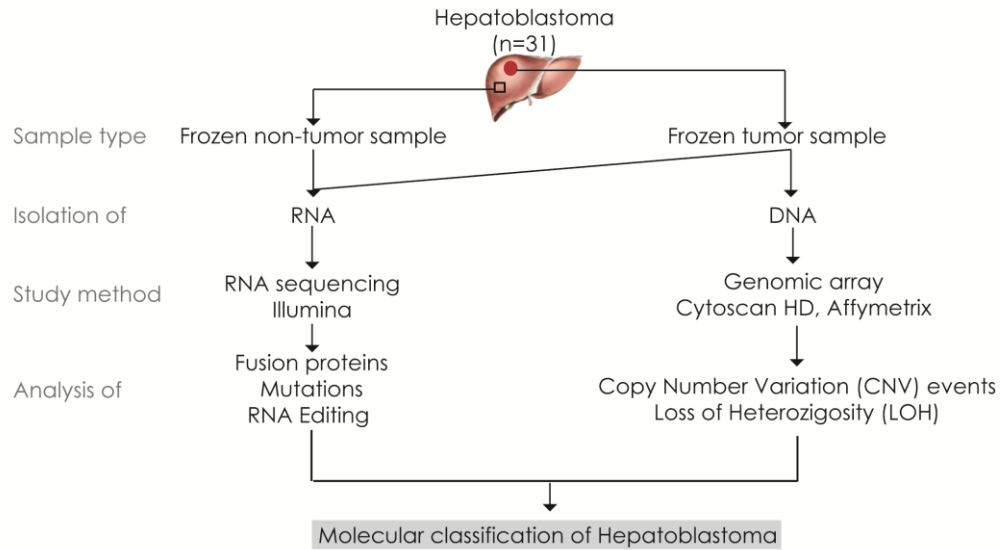


Figure 14. Workflow followed on the genomic and RNAseq study.

3.2.1 Patients and tissue samples

For this study, we analyzed 81 frozen tissue samples of 31 patients with HB by three different techniques: RNA sequencing (Illumina platform and CytoSCAN array (Affymetrix)). Samples included primary tumors (n=31), non-tumor liver (N=31), recurrences (n=2) and Patient Derived Xenografts (PDX) samples from 31 HB patients and 4 pHCC were included in the discovery set, whereas frozen tumor samples from additional 21 patients with HB were used for the validation set. Moreover, 11 PDX samples were included in the study including 1 orthotopic PDX obtained from a case of our Spanish collection thanks to Dr A. Villanueva and 12 subcutaneous PDX obtained in collaboration with Dr S. Cairo of the XenTECH Company.

Table 10 summarizes the main clinical and pathological data of the 52 patients with liver cancer included in this study. Regarding to patients from the discovery set, 100% received chemotherapy treatment prior to surgery, most being enrolled in clinical trials of the SIOPEL group (Perilongo G, Shafford E, 2000). Mean age was of 16 months and 62% presented tumors with an advance PRETEXT stage (III or IV). Twenty-nine percent of patients presented with metastasis at diagnosis and

42% with vascular invasion. Thirty-nine percent of patients were classified as high risk according to the CHIC-HS classification (Meyers *et al.*, 2017). Mean follow-up was of 36 months and 16% of patients died of cancer.

In relation to the 4 pHCC included in the discovery set, mean age was 201 months and 1 of them received preoperative chemotherapy treatment. No one presented metastasis at diagnosis but 75% had vascular invasion. Mean follow-up was of 100.7 months with 1 cancer-related death.

Concerning the validation set, 88% of the patients received chemotherapy treatment prior to surgery, most being enrolled in clinical trials of the SIOPEL group (Perilongo G, Shafford E, 2000). Mean age was of 21 months and 47% presented tumors with an advance PRETEXT stage (III or IV). Seventeen percent of patients presented with metastasis at diagnosis and 23% with vascular invasion. Thirty-five percent of patients were classified as high risk according to the CHIC-HS classification (Meyers *et al.*, 2017). Mean follow-up was of 3.5 months. Expert pathologists (L. Guerra, R. Ortega and M. Garrido) reviewed the histology of all the tumor specimens.

Table 10. Main clinical, pathological and features of the 56 patients included in the genomic and RNAseq study.

	Discovery set		Validation set
	HB (n=31)	pHCC (n=5)	HB (n=21)
• Age, months (median, [range])	16 [1-180]	214 [58-320]	21 [1-126]
• Serum AFP, ng/mL (range)	663-2.186.461	-	300-1.708.400
• Preoperative chemotherapy (Y/N/NA)	31/0/0	1/4/0	15/2/4
• Tumor stage			
PRETEXT stage (I/II/III/IV/NA)	2/9/13/5/2	-	0/9/4/4/4
Metastasis at diagnosis (Y/N/NA) (%Y)	9/21/1 (29%)	1/4/0 (20%)	3/14/4 (17%)
Vascular Invasion (Y/N/NA) (%Y)	13/17/1 (42%)	3/2/0 (60%)	4/13/4 (23%)
• Histology			
- HB: Epithelial/Mixed /NA	12/15/4	-	10/3/8
Main component: Fetal/Non-Fetal*	11/16/4	-	11/0/10
SCU histology	3	-	2
- NOS	2	-	-
- Fibrolamellar HCC	-	3	-
• Clinical classification CHIC-HS (VL/L/I/H/NA)	9/6/4/12/NA	-	8/3/2/4/4
• Follow-up, months (mean, [range])	36 [1-152]	89 [18-106]	35,5 [3,5-120]
Tumor recurrence (Y/N) (%Y)	15/26 (16%)	3/2 (60%)	0
Outcome: cancer-related deaths (%)	5 (16%)	1 (20%)	0

*Non-fetal includes: Crowded fetal and embryonal

NA, non-available; PRETEXT, pretreatment extent of disease; SCU, small cell undifferentiated; NOS, hepatocellular malignant neoplasm; VL, very low; L, low; I, intermediate; H, high risk.

3.2.2 RNA Study

3.2.2.1 RNA isolation quantification and quality control

Total RNA from frozen tissue was isolated with the mirVana™ mirRNA Isolation kit (Thermo Fisher Scientific) following manufacturer's instructions. This protocol is useful to isolate RNA molecules from tissues and cells by using a method based on a glass fiber filter and allows an enrichment of small molecules of RNA (< 200 nt).

To ensure no RNA degradation occurred during tissue manipulation, tissue was not defrosted until lysis buffer addition. To do so, we used a frozen mortar and liquid nitrogen was continuously added. Tissue samples were broken until a piece of

20-30 mg was obtained and then kept at -80°C until RNA isolation procedure was performed.

Tissue lysis and homogenization was carried out with the Fastprep system and the Lysing Matrix type D tubes (MP Biomedicals, Santa Ana, California, USA) that enable tissue disruption of difficult samples and performance in cold conditions. After adding 600uL of Lysis Buffer, tubes were placed in the Fastprep instrument and 3 runs of 40sec at 6m/s were done. Samples were kept on ice during instrument resting between runs. Then, the homogenate was transferred into a new tube and additional 600uL of Lysis Buffer were added to the Lysing Matrix tube and the 3 runs repeated, this step allows maximum tissue homogenization and RNA recovery. After that, the homogenate was transferred to the same tube than previously.

Once the tissue was completely homogenized, the organic extraction was performed by adding 1/10 volumes of miRNA Homogenate Additive and incubating on ice for 10 minutes. A volume of Acid-Phenol:Chloroform was added to each sample, mixed and centrifuged at 10.000 g for 5 min at RT. After centrifugation, the aqueous phase (upper) was transferred into a new tube and 1.25 volumes of ethanol 100% at RT were added. The total volume of lysate/ethanol was filtered by adding up to 700 µl and centrifuging 15 sec at 10.000 g at RT. The filter was washed once adding 700 µl of miRNA Wash Solution 1 twice adding 500 µl of Wash Solution 2/3 and centrifuged 10 sec at 10.000g. Finally, the RNA elution was performed by adding 100 µl of pre-heated (95°C) nuclease-free water (Thermo Fisher Scientific) to the filter, incubating the tubes 1 min at RT and centrifuging 30 sec at 10.000g.

After RNA elution, DNase digestion was performed to eliminate possible contaminating DNA with the DNA-free™ kit (Thermo Fisher Scientific) following manufacturer's instructions. Briefly, eluted RNA was separated in 2 tubes of 50uL each (ideal volume reaction) and 5uL of rDNase buffer and 1uL of rDNase I enzyme added. RNA samples were incubated for 30 min at 37°C. After that, 5 µL of rDNase I inactivator reagent was added and mixed by vortex. Samples were incubated 2 min at RT. Samples were centrifuged 1,5 min at 10000 g and the supernatant was

carefully removed without disturbing the pellet and transferred into a new tube (the 2 tubes of 50 μ L were putted together).

RNA was stored at -80°C until its use. RNA quantification and contaminant analysis was performed by spectrophotometry (Nanodrop ND-2000, Thermo Scientific). The A260/280 ratio, which may indicate the presence of protein, should be >1.7 and the A260/230 ratio, an indicator of residual phenol, guanidine, magnetic beads, carbohydrates or proteins, should be >1.3 .

The integrity was checked with the Agilent 2100 Bioanalyzer (Agilent Technologies, Santa Clara, USA). Only samples with good RNA integrity (RNA integrity number -RIN- above 7) were subsequently used in sequencing experiments.

3.2.2.4 RNA sequencing

RNA sequencing technique and bioinformatics analysis was performed at the genomics core facility of the Ichan School of Medicine at Mount Sinai (NY, USA) by Dr Nicholas Akers and Dr Bojan Losic in collaboration with Dr Josep Maria Llovet's team.

The RNA-seq analysis was only preformed on HB patients, including tumor, non-tumor, recurrences and PDX tissue samples.

RNA-seq was conducted on poly-A enriched RNA, 100 bp single reads on an Illumina HiSeq2500 instrument. Raw sequencing reads were mapped to the GRCh37 reference genome (USCS) using STAR (2.4.2g1). Raw library size differences between samples were treated with the weighted trimmed mean method (Robinson and Oshlack, 2010). RNA fusions were detected by filtering chimeric STAR alignments (see <http://starchip.readthedocs.io/en/latest/>). Mapped RNA-seq reads were subject to splitting, trimming, local indel realignment, and base-score recalibration pre-proessing with the IndelRealigner, TableRecalibration tools from GATK (Piskol, Ramaswami and Li, 2013) under the GATK Best Practices for RNA-seq paradigm (*The*

GATK *Best Practices for variant calling on RNAseq, in full detail*, 2014). MuTect (Cibulskis *et al.*, 2013) was then used with default settings to quantify somatic mutation burden.

3.2.2.5 Retrotranscription

Total RNA (1 µg) was reverse-transcribed using the RNA to cDNA EcoDry Premix (double primed) kit (Takara Bio Inc., Shiga, Japan) according to manufacturer's instructions. RNA was diluted in 20 µl of RNase DNase Free water and mixed with the lyophilized EcoDry Premix containing SMART™ MMLV Reverse Transcriptase, Random hexamers and oligo(dT)₁₈ primers, MgCl₂ (6 mM final concentration), BSA, DTT, dNTP Mix, reaction buffer, cryoprotectant and stabilizers. Samples were incubated in a thermocycler at 41°C for 60', at 70°C for 10' with a final step of 4°C (Figure 15).

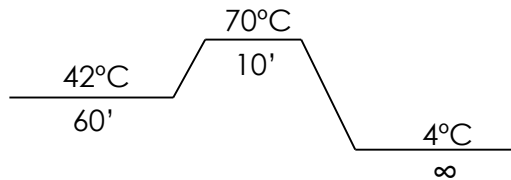


Figure 15. Temperature scheme for retrotranscription using the RNA to cDNA EcoDry Premix (double primed) kit (Takara Bio Inc., Shiga, Japan).

3.2.2.6 Droplet Digital PCR (ddPCR)

ddPCR (Bio-Rad, Hercules, California, USA) system combines water-oil emulsion droplet technology with microfluidics. First, ddPCR reactions are prepared in a similar manner as real-time PCR reactions that use TaqMan hydrolysis probes labeled with FAM and HEX reporter fluorophores. After the mix is prepared, samples are placed into a droplet generator, which partitions each sample into 20,000 nanoliter-sized droplets. In this way, target and background DNA are distributed randomly into the droplets. Droplet generation produces uniform in size and volume droplets for the samples, enabling precise target quantification. Then, droplets are transferred to a 96-well plate and PCR amplification is carried out within each droplet using a thermal cycler. Following PCR, droplets are streamed in a single file on a droplet reader, which analyzes each droplet individually using a two-color

detection system to detect FAM and HEX. Positive droplets, which contain at least one copy of the target DNA molecule, exhibit increased fluorescence compared to negative droplets.

In order to quantify the level of BLCAP nt5 editing in different RNA samples a Rare Mutation Detection (RMD) experiment was performed. RMD method is useful when a biomarker exists within a background of highly abundant counterpart that differs by only a single nucleotide. In this assay, a single primer pair and 2 probes labeled with FAM (unknown, nt5 edited) and HEX (reference, nt5 wt) are used.

Briefly, RNA from T, NT, R, PDX and cell lines was isolated and reverse-transcribed as previously described (see sections 3.2.2.1 and 3.2.2.5) cDNA was diluted 1/25 and for each sample, 8,8 μ l of cDNA were mixed with 1,1 μ l of FAM-labeled probe, 1,1 μ l of HEX-labeled probe and 11 μ l of Super Mix. Then 20 μ l of the mixture transferred in the assigned wells of the cartridge as well as 70 μ l of oil. After that, droplets were generated using the QX200 droplet generator and 40 μ l were transferred to a 96-well plate. Once all the droplets were generated and transferred to the plate, it was sealed and a PCR was performed (see conditions in *Figure 16* and primers/probes used in *Table 11*). After PCR amplification, droplets fluorescence was read with the QX200 reader.

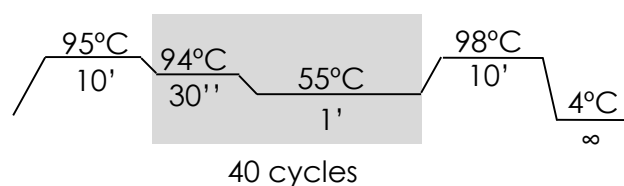


Figure 16. Temperature scheme used for ddPCR.

Table 11. Primers and probes used for ddPCR.

Primer/probe	Sequence 5'-3'
Forward Primer	CTTGGTGAAGGCCCTG
Reverse Primer	CTGCCCCGTCCTCCT
Wt nt5 probe (HEX)	ATCATGTaTTGCCTCCAGT
Edited nt5 probe (FAM)	TCATGTgTTGCCTCCAG

ddPCR data was analyzed with the QuantaSoft™ software and the fractional abundance (FA) of the edited nt5 of BLCAP was automatically calculated (FA= a/a+b, where a=HEX and b=FAM).

3.2.3 DNA Study

3.2.3.1 DNA isolation and quantification

Total DNA from frozen tissue and PBLs was isolated with the MagMAX™ DNA Multi-Sample Kit (Thermo Fisher Scientific) following manufacturer's instructions. This protocol uses MagMAX™ magnetic bead-based nucleic acid isolation technology to produce high yields of purified DNA, free from inhibitors that may affect downstream reactions.

For PBLs, The cellular phase was transferred into a fresh tube and 2 volumes of Erythrocytes Lysis Buffer (ELB) were added, samples were incubated RT for 30 minutes in the roller and centrifuged at 2000 rpm for 10 min. The pellet was resuspended with ELB, incubated 3' at RT and centrifuged at 3000 rpm for 5 minutes. The PBLs were aliquoted and stored at -80°C until its use.

Frozen tissue was defrosted and disaggregated using a scalpel. Sample homogenization was performed by adding 184 µL of PK Buffer and 16 µL of proteinase K to the defrosted tissue or the PBL sample. Once the samples was completely homogenized, 200 µL of Multi-sample DNA Lysis Buffer was added to each sample and mixed properly. Then, 300 µL of 100% Isopropanol was added and the tubes were shaken for 3' at speed 2 on a vortex adaptor. Then, 40 µL of DNA

binding beads at 4 mg/mL were added and tubes were shaken for 3' at speed 2. After that, tubes were placed in the magnetic stand for 5' or longer times to allow the beads to pellet against the magnet. Then, samples were washed using 300 µL of Wash Solution 1 and 300 µL of Wash Solution 2. After washing, the supernatant was discarded without disturbing the beads. The tubes were left uncapped to allow them to air-dry for 3' on the magnetic stand. Then, tubes were removed from the magnetic stand and 100 µL of RNase were added and tubes shaken 2' at speed 2 on the vortex adaptor. After RNase digestion, samples were washed again with the Wash Solution 2 and tubes were air-dried uncapped for 3'. DNA was eluted by adding 200 µL of DNA Elution Buffer 1, mixing the samples by vortex and incubating them 5' at 70°C. After the incubation, tubes were shaken for 5' at speed 2 on the vortex adaptor. Then, 200 µL of DNA Elution Buffer 2 was added and tubes were shaken by vortex until resuspended. After that, the tubes were placed in the magnet stand until the solution was clear and the eluted DNA was transferred to a new tube.

DNA quantification and contaminant analysis was performed by spectrophotometry (Nanodrop ND-2000, Thermo Fisher Scientific) and was stored at -20°C until use. DNA integrity was assessed by running it in a 1% agarose gel. DNA fragments had to be bigger than 500bp.

Only DNA samples meeting the above mentioned criteria were subsequently used in microarray and experiments.

Cytoscan HD array was performed by Dr Mar Mallo from the Affymetrix Array Platform in the Institut Contra la Leucèmia Josep Carreras under the supervision of Dr Francesc Solé.

3.2.3.3 Cytoscan HD Array

The Cytoscan HD (Affymetrix, Thermo Fisher Scientific) array is a cytogenetic and copy number array useful to analyze DNA gains and losses (CNVs) as well as LOH in the whole genome in a single determination. Detection is performed thanks to numerous probes targeting the genome and differently from the Comparative

Genomic Hybridization (CGH), this arrays also contain probes detecting single nucleotide polymorphisms (SNPs) that allow the detection of LOH.

The Cytoscan HD array contain 2,6 millions of probes, from which 750.000 are detecting SNPs.

Cytoscan HD array was performed by following manufacturer's instruction (Cytoscan™ Assay User Manual, P/N 703038 Rev. 3) by using 250ng of DNA (5µL at $\geq 50\text{ng}/\mu\text{L}$). Briefly, DNA samples were digested by using the restriction enzyme NspI and then ligated by enzymatic reaction including the adaptors to DNA generated fragments. After that, the PCR amplification was carried out with a unique primer targeting to the adaptors. PCR product was assessed by 2% agarose gel and it had to be 150bp-2000bp and quantified by spectrophotometry using the Nanodrop ND-2000 (Thermo Fisher Scientific). Then, the PCR product was fragmented again by enzymatic reaction and generated fragments were assessed in a high resolution agarose gel (3-4%) with an expected size of between 25 and 125bp. Fragments were labeled with biotin and denaturalized previously to the hybridization to the microarray performed during 16-18°C in the hybridization oven with rotation. After this step, the microarray was placed on the fluidics station for the washing step. Immediately after the washing, the microarray was stained with streptavidin-ficoeritrin which binds to the biotin. The staining process included a signal amplification step in which an anti-streptavidin and anti-IgG conjugated to biotin antibodies. Lastly, the microarray was scanned with a laser detecting fluorescence. The signal distribution pattern was recorded in .DAT and .CEL files. The .CEL file was used to generate a .CYCHP file which was used for the analysis by using the Chromosome Analysis Suit (ChAS) software.

From the 3 quality parameters included in the ChAS software (snpQC >15 ; mapPD ≤ 0.25 ; waviness ≤ 0.12), samples had to pass the mapPD restriction to be included in the final analysis. The obtained data was manually curated in order to remove false annotated CNVs or LOH by filtering by number of probes >25 and size $>50\text{kb}$ for CNVs and $>2\text{Mb}$ or $>25\text{Mb}$ for telomere and interstitial LOH respectively.

Integrative Genome Viewer was used to visualize CNV and LOH data and to calculate frequencies.

3.2.3.4 PCR

To confirm the mutations and fusion proteins events identified by RNAseq, conventional PCR was performed using the PCR Master Mix 2X (Thermo Fisher Scientific) containing 0.05 U/ μ L Taq DNA polymerase, reaction buffer, 4 mM MgCl₂, 0.4 mM of each dNTP (dATP, dCTP, dGTP and dTTP).

Two μ L of diluted DNA or cDNA was mixed with 12,5 μ L of PCR Master Mix(2X), 0,5 μ L of 10 μ M Forward primer, 0,5 μ L of 10 μ M Reverse primer and 9,5 μ L of RNase DNase free water. Conditions of the PCR amplification are shown in *Figure 17*. After the reaction, PCR product was run in a 2% agarose gel. All the primers used are listed in *Table 12*.

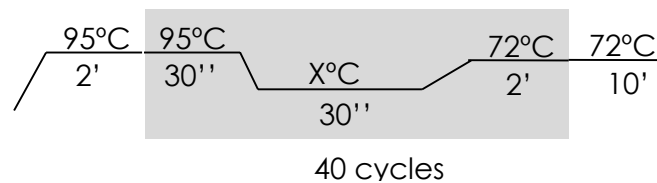


Figure 17. PCR temperature conditions. X, annealing temperature depends on the primer pair used, see *table 12*.

Table 12. Primers used for conventional PCR.

Gene/Event	Product Length (bp)	Melting Temp. (°C)	Primer location	Sequences (5'-3')
AUH-genomic	300	58	Exon 10	F: TTTATAGCGAGGGGGCCTTT R: GGGGGCTTTCTCTAGCCTGT
BLCAP	653	58	Exon 2	F: AGGGTTGAAGAAAGCGGAGG R: AGTAATGAGGCGAGAGGGGT
CTNNB1	517	55	Exon 1-4	F1: GCGTGGACAATGGCTACTCAAG R1: TATTAACCACCACCTGGTCCTC
	1043	55	Exon 1-6	R2 ¹ : TTCAGCACTCTGCTGTGGTCC
	208	55	Exon 1-3	R3 ² : CCCACTCATAACAGGACTTGGGAGG
DNAJC15-TPT1	200	58	Exon 6 Exon 4	F: GTGTGGTCCTTAAGCATCAATGT R: GGGAAACTTGAAGAACAGAGACC
EPHB4	414	62	Intron (exon 5/6)	F: TCTGCCTGACTCCCTGGTCTC R: CTCAGTGACATCTCTCCCGCC
	680	62	Intron (exon 10/12)	F: GGACATGGTGGGTGCCCCT R: ACCTCGCCAAACTCACCTTC
NFE2L2	502	62	Intron (exon 2/3)	F: CGTGTAGCCGATTACCGAGT R: GACTGGGCTCTCGATGTGAC
TERF2-genomic	300	58	Exon 2-4	F: CCACTGGAATCAGCTATCAATG R: AAGATGAGAAAAGGGGATTAGAAC
TERT	200	58	Promoter	F: CAGCGCTGCCTGAAACTC R: GTCCTGCCCCCTTCACCTT
TMEM163-SLC25A16	200	58	Intron UTR3P	F: TAAGCCGTATCAAACAGTCCATGA R: TTCGCTGTATCCCTCTCAAGC

¹Reverse primer to be used with F1, as already published (Cairo et al, 2008)

²Primer used for PCR product sequencing. Abbreviations: F, forward; R, reverse.

3.2.3.5 Quantitative real Time PCR (qRT-PCR)

Concisely, RNA was obtained and reverse-transcribed following the previous description (see sections 3.2.2.1 and 3.2.2.5). cDNA samples were diluted 1/50 with Molecular Biology Grade Water (Applichem) and 5µL of diluted cDNA were mixed with 5µL of SYBR® Select Master Mix (Applied Biosystems-Thermo Fisher Scientific) together with 10µL of specific primers. The SYBR® Select Master Mix contains SYBR® GreenER™ Dye, AmpliTaq® DNA polymerase, Heat-labile Uracile-DNA Glycosylase (UDG), ROX™ dye Passive Reference, dNTP blend containing dUTP/dTTP and optimized buffer components. Expression levels were determined in triplicate using

a 7900HT Fast Real-Time PCR System (Applied Biosystems-Thermo Fisher Scientific) in a 384-well plate. qRT-PCR conditions are shown in *Figure 18*. All the primer pairs used are listed in *Table 13*.

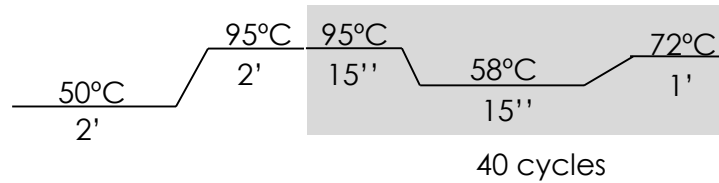


Figure 18. Temperature scheme for qRT-PCR.

The expression of the different genes of interest (GOI) was calculated using the expression levels of RHOT2 gene as a reference, applying the Delta Ct method as follows:

$$\Delta Ct = Ct_{GOI} - Ct_{RHOT2}$$

$$\text{Gene expression} = 2^{-\Delta Ct}$$

To confirm the specificity of the reaction, melting curves were carried out during the same qRT-PCR reaction and only primers with a single peak were considered.

Table 13. Primers used for qRT-PCR. *Housekeeping gene

Gene	Forward primer (5'- 3')	Reverse primer (5` - 3')
ADAR1	CCATCAGCGGGCTGTTAGAA	GGGAAACTCTCGGCCATTGA
ADAR2	GCGTTGTA CTGTCGCTGGAT	ATGAAGGCTGTGAACAGACGC
BLCAP	CTCCTGGAACGGAAGCCTTG	GGAGCAGTGGTACAGGAAACA
DLK1	AGGATGACAATGTTTGCAGGTG	TCTCTATCACAGAGCTCCCCGT
LGR5	CCCTGTGAACACCTGCTTGA	GCATGTTCACTGCTGCGATG
RHOT2*	CTGCGGACTATCTCTCCCCTC	AAAAGGCTTTGCAGCTCCAC

Gene expression was also assessed by Human Transcriptome Array 2.0 (Affymetrix) (data is not included in this thesis).

3.2.3.6 Sanger Sequencing

Sanger sequencing was used to characterize CTNNB1 gene status and to confirm the mutations and fusion proteins found by RNA sequencing. The kit used was BigDye® Terminator v3.1 Cycle Sequencing Kit (Thermo Fisher Scientific).

First, 5µL of PCR product were incubated with 2µL illustra ExoProStar 1-Step (GE Healthcare Life Sciences) for 45min at 37°C and 15min at 80°C. This reagent contains a mix of illustra Alkaline Phosphatase and Exonuclease A to remove unincorporated primers and nucleotides from the amplification reaction before sequencing. After purification, 2µL of purified PCR product were mixed with 2µL of BigDye Buffer, 1µL of BigDye, 1.6µL of 1µM primer and 3.4µL of DNase RNase free water. Sequencing reaction temperature scheme is shown in *Figure 19*.

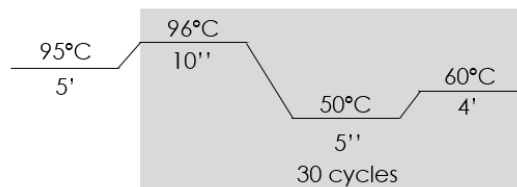


Figure 19. Temperature scheme for Sanger sequencing.

Finally, sequences were run in a Genetic Analyzer ABI 3130 using the Data Collection v3.0 software and analyzed with the Sequencing Analysis v5.3.1 package.

3.2.4. Statistical analysis

All statistical methods used for this project are detailed in section 3.1.3.3. Statistical analysis.

For the Small Overlapping Regions of Imbalance (SORIs) analysis an algorithm was made using R and Rcpp package (Eddelbuettel, 2013) in order to detect common alterations of the type gain, loss, and loss of heterozygosity (LOH) in different samples. As a result, intersections with altered regions present in at least

two samples were annotated. A table was constructed with the intersections and the state of each sample in that region defined as gain, loss, LOH or no altered. In order to find a relationship between the states of these altered regions and the reported clinical variables for each sample, a Fisher's exact test was used. FDR Adjusted p-values were obtained for each comparison. To find a possible interaction between intersected regions, Fisher's exact test was applied again comparing sample states of those regions.

4. RESULTS

4.1 Establishment of a collection of biological samples from pediatric patients with liver cancer and healthy individuals.

Results

We have created a collection of highly annotated biological samples of childhood liver cancer registered at the Instituto de Salud Carlos III (ISCIII, ref C.0000226).

Overall, samples from 66 patients have been prospectively collected since 2009 (mean of 8 patients per year) including 51 HB, 6 pHCC, 4 hamartomas and 1 of each of cholangiocarcinoma, sarcoma, benign vascular tumor, rhabdoid tumor and liver with tyrosinemia. These patients have been treated in 14 different hospitals within Spain, mainly in Hospital Universitario La Paz (n=25) and Hospital Universitari Vall d'Hebron (n=18) (*Figure 20*).

Retrospective samples from 163 patients have been obtained thanks to national and international collaborations with Hospital La Paz (38 patients), Dr. Marie Annick Buendia (32 patients), the SIOPEL group (26 patients), Hong Kong Hospital (21 patients), Bicêtre Hospital (14 patients), Dr. Stefano Cairo (11 patients), Vall d'Hebron Hospital (10 patients), Virgen Del Rocío Hospital (8 patients) and Reina Sofía Hospital (3 patients). Complete clinical data was obtained from almost all cases.

Additionally, 12 PDX samples have been obtained thanks to a collaboration with Dr. Stefano Cairo from Xentech.

Results

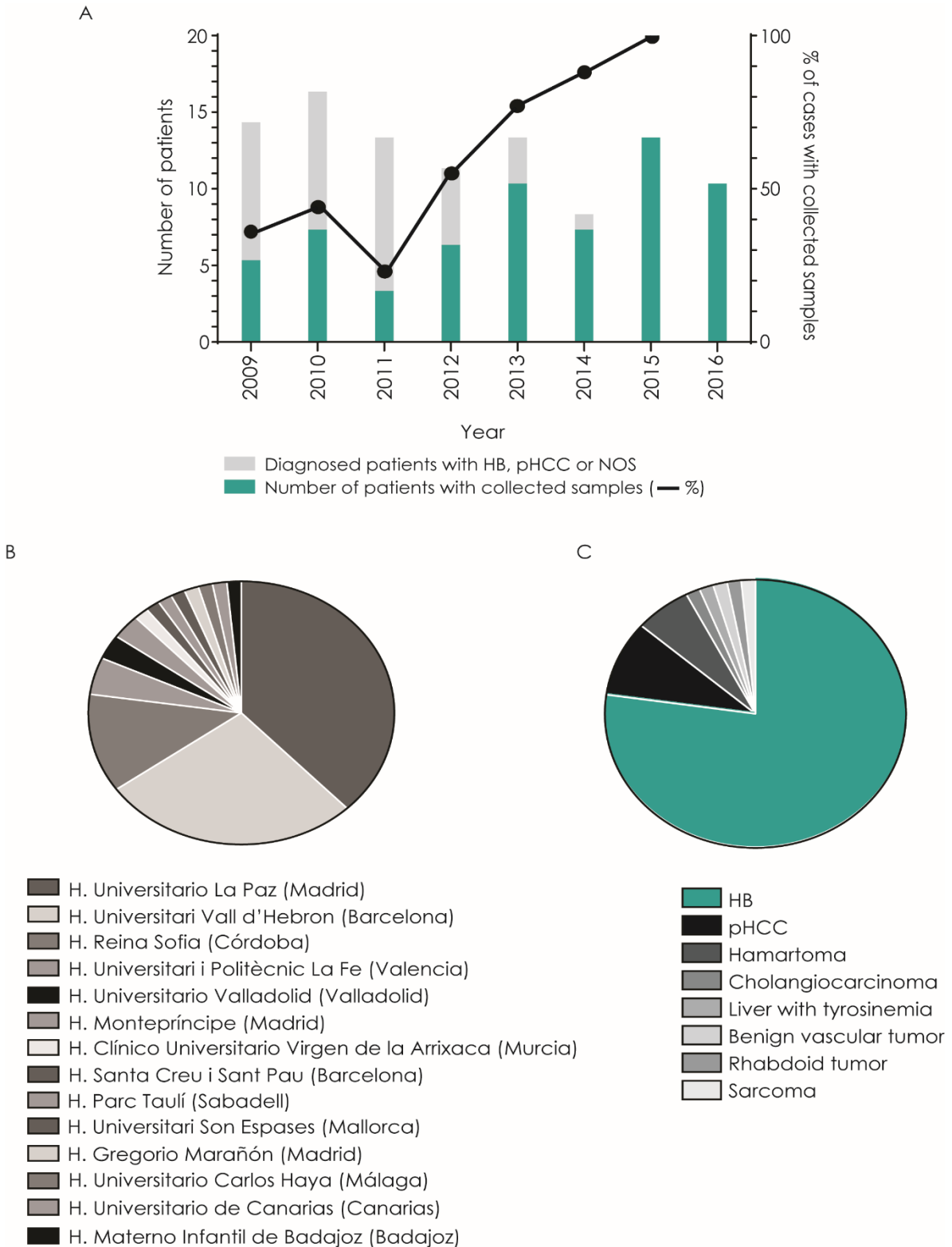


Figure 20. Prospective collected samples since 2009. Bar graph represents the number of patients diagnosed and enrolled per year in Spain (A). Plot of the different hospitals of origin of the samples (B). Different tumor types from which samples have been collected (C). Pie graph legends are listed from bigger to lower.

4.2. Proteomic study

4.2.1 Proteomic profile of HB

With the aim to define the proteome of the HB and identify putative prognostic factors at protein level as well main deregulated pathways, we performed the first comprehensive proteomic study on tissue samples obtained from HB patients. To accomplish this, 16 clinical, pathological and molecular annotated tumors (see clinical and pathological features in *Table 7*) as well as 8 non tumor liver tissues were studied by two high-throughput techniques of quantitative proteomics: two-dimensional difference gel electrophoresis (2D-DIGE) and Label-free LC-MS (LF).

The unsupervised analysis of 2D-DIGE data revealed two main hierarchical clusters of tumor and non-tumor samples (Fisher's Exact test, $p=0.0013$, *Figure 21A*). The cluster of tumors was in turn subdivided in 2 groups strongly associated with the previously defined C1/C2 classification (Cairo *et al.*, 2008) (Fisher's Exact test, $p=0.0151$) as one of the tumor clusters was composed exclusively with C1-tumors (100% of the samples were classified as C1) whereas the second cluster mainly included C2-tumors (80% of the samples). The experimental replicates of 3 different samples (HB48, HB49 and HB59) resulted in similar protein profiles, indicating high robustness of 2D-DIGE proteomic data (*Figure 21A*). Then, we selected 8 tumor and 4 non-tumor samples for LF analysis. The unsupervised study of the LF proteomic data showed again the 3 different groups of samples: non-tumor, C1 and C2 tumors (*Figure 21B*). It is worthy to highlight that 3 of the tumor samples were "wrongly-grouped" in the 2D-DIGE cluster. The fact that 2 C1 tumors clustered with NT samples may be explained by the low tumor cell content present in these tissue samples, while the C1 tumor located in the C2 cluster could be explained by the fact that some tumors are difficult to classify using the 16-gene signature, as they present a mixed gene and protein expression profiles. Thus, the "pure" samples were selected for the LF analysis, which is reflected in the unsupervised cluster.

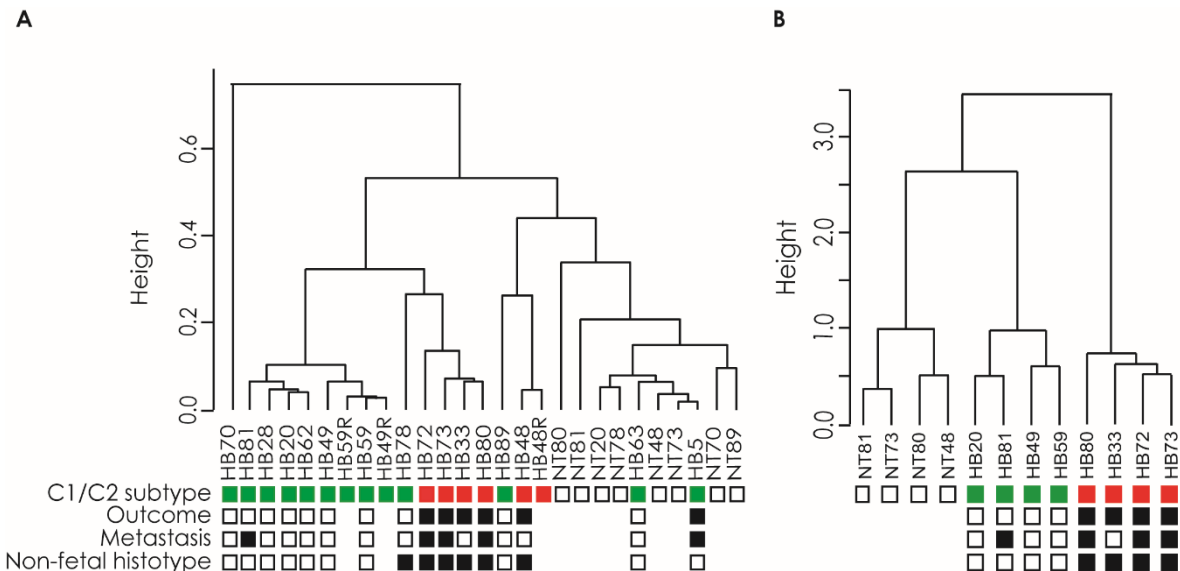


Figure 21. Hierarchical cluster analysis of the proteomic data. Representative unsupervised hierarchical clustering (Pearson distance; Linkage method: Complete) of protein expression profiles obtained from 277 DIGE spots corresponding to the top 50% highest coefficient of variation (CV) spots of 16 HBs and 8 non tumor samples (A). Representative unsupervised hierarchical clustering of protein expression profiles obtained from 390 LF proteins (50% CV) of 8 HBs and 4 non tumor samples (B). Abbreviations: T, tumor; NT, non-tumor (white squares); R, experimental replicate. Tumor samples were classified according to the 16-gene signature (Cairo *et al.*, 2008) as C1 and C2 (green and red squares, respectively). Black boxes in the rows above the heat maps indicate (from top to bottom): dead of the disease, metastasis at diagnosis, and non-fetal histotype.

In order to identify the deregulated proteins in HB, we compared the proteomic profiles of tumor and non-tumor samples. The 2 tumor samples that shared part of their protein profiling with the non-tumor samples were excluded of this analysis. The supervised analysis comparing T vs. NT revealed a total of 231 differentially expressed proteins ($p < 0.05$ and $FC \pm 1.5$); among them, 25 proteins were identified by 2D-DIGE, 178 proteins by LF and 28 were identified by both techniques. The two approaches were highly complementary since only 12% of the proteins were identified with the two proteomic techniques (fold change obtained by both techniques for common proteins is shown in *Table 14*). An important source of variability is the fact that not all the samples have been analyzed by LF, as only 4 samples of each group (NT, C1 and C2) were analyzed with this technique.

Table 14. Proteins identified both by DIGE and LF. FC, fold change. For DIGE, if a protein have been identified in more than 1 spot, the range is shown and the number of spots in which the protein have been identified. Grey indicate discordant results.

PROTEIN	FC DIGE (N. spots)	FC LF
GPDA	0.4	0.2
ACTB	1.6-1.9 (5)	0.2
EST1	0.4	0.2
FTCD	0.40 (2)	0.2
ACDSB	0.6-0.7 (2)	0.2
GRP75	1.6	0.3
CNDP2	0.5	0.3
ALDH2	0.4-0.5 (3)	0.3
AL1A1	0.6	0.4
ECHM	0.5	0.4
ANXA5	1.8-2 (2)	2.3
CATD	1.6	2.4
ENOA	0.6-0.7 (2)	2.5
HSP7C	1.6-1.9 (2)	2.6
APOA1	2.0	2.7
CATB	1.8	2.9
A1AT	1.8	3.0
HS90B	2.1	3.0
HS90A	1.9	3.3
GELS	3.3	3.4
HSP71	2.2	3.6
ALBU	1.8-2.9 (10)	3.7
1433Z	2.3	3.8
LMNB1	2.4	4.0
VIME	1.8-4.1 (6)	4.1
HBB	1.9-3.6 (3)	5.0
GSTP1	2.1	6.2
CH60	1.6	7.4

Three of the proteins identified by both techniques –ACTB, GRP75 and ENOA– showed discordances between both techniques, probably because of different isoforms and were excluded from further analysis. In total, 127 proteins were found to be up- and 101 proteins down-regulated in HB tumor as compared to non-tumor tissues. Top differently expressed proteins in HB are listed in *Table 15*.

Table 15. Top deregulated proteins in HB. T/NT, T vs. NT is fold change; Criteria: LF p-value<0.0005; DIGE p-value<0.001; (*) When a protein was found by both techniques, LF FC was chosen. Abbreviations: Tech, Technique; Ref, References related to cancer.

Tech.	Gene	Gene Description	T/NT	Ref.
<i>Up-regulated proteins in HB</i>				
	VIM	Vimentin	4,1	(O'Brien, Finlay and Gilbert-Barness, 1989)
	HBB	Hemoglobin, beta	3,6	(Khan <i>et al.</i> , 2013)
	ENO2	Enolase 2 (gamma, neuronal)	2,7	(T. Zhang <i>et al.</i> , 2013)
	KRT6A	Keratin 6A	2,6	
	LMNB1	Lamin B1	2,4	(Sun <i>et al.</i> , 2010)
2DE	HDGF	Hepatoma-derived growth factor (high-mobility group protein 1-like)	2,2	(Yoshida <i>et al.</i> , 2006; Tsang <i>et al.</i> , 2009)
	UBA5	Ubiquitin-activating enzyme E1-domain containing 1	2,1	
	COL6A1	Collagen, type VI, alpha 1	2,1	
	HSPA8	Heat shock 70kDa protein 8	1,9	(Yang <i>et al.</i> , 2015)
	SERPINA1	Serpin peptidase inhibitor, clade A (alpha-1 antiproteinase, antitrypsin), member 1	1,8	(Qin <i>et al.</i> , 2013)
	YWHAG	Tyrosine 3-monooxygenase/tryptophan 5-monooxygenase activation protein, gamma polypeptide	1,7	(T. Liu <i>et al.</i> , 2013)
	TUB5	Tubulin, beta	1,6	
	FBLN1	Fibulin 1	20,8	(Kanda <i>et al.</i> , 2011)
	FLNA	Filamin A, alpha (actin binding protein 280)	10,59	(Ai <i>et al.</i> , 2011)
	RAN	RAN, member RAS oncogene family	5,3	(Lu <i>et al.</i> , 2013)
	ITGB1	Integrin, beta 1 (fibronectin receptor, beta polypeptide, antigen CD29 includes MDF2, MSK12)	5,2	(Ishikawa <i>et al.</i> , 2011; Zha <i>et al.</i> , 2014)
LF	YWHAQ	Tyrosine 3-monooxygenase/tryptophan 5-monooxygenase activation protein, theta polypeptide	4,2	
	YWHAZ*	Tyrosine 3-monooxygenase/tryptophan 5-monooxygenase activation protein, zeta polypeptide	3,8	(Huang <i>et al.</i> , no date; Liu <i>et al.</i> , 2014)
	CLIC1	Chloride intracellular channel 1	3,2	(R. Li <i>et al.</i> , 2012; Megger <i>et al.</i> , 2013; S. Zhang <i>et al.</i> , 2013; Wei <i>et al.</i> , 2015)

Tech.	Gene	Gene Description	T/NT	Ref.
<i>Down-regulated proteins in HB</i>				
2DE	ECHS1	Enoyl Coenzyme A hydratase, short chain, 1, mitochondrial	-2,1	(Hu <i>et al.</i> , 2004)
	ALDH2	Aldehyde dehydrogenase 2 family (mitochondrial)	-2,5	(Cairo <i>et al.</i> , 2008)
	SELENBP1	Selenium binding protein 1	-2,9	(Raucci <i>et al.</i> , 2011; Stasio <i>et al.</i> , 2011; Rusolo <i>et al.</i> , 2013)
LF	CYB5A	Cytochrome b5 type A (microsomal)	-3,3	(Khan <i>et al.</i> , 2013)
	HSD17B10	Hydroxysteroid (17-beta) dehydrogenase 10	-4,3	
	PRDX4	Peroxiredoxin 4	-4,5	
	FTCD*	Formiminotransferase cyclodeaminase	-4,6	(Yu <i>et al.</i> , 2014)
	UGP2	UDP-glucose pyrophosphorylase 2	-4,8	(Tan <i>et al.</i> , 2014)
	ASS1	Argininosuccinate synthetase 1	-6,4	(Tan <i>et al.</i> , 2014)
	FBP1	Fructose-1,6-bisphosphatase 1	-6,5	(Chen <i>et al.</i> , 2011)
	HRSP12	Heat-responsive protein 12	-7,9	(Chong <i>et al.</i> , 2008)
	ALDOB	Aldolase B, fructose-bisphosphate	-10,1	(Peng <i>et al.</i> , 2008)
	BHMT	Betaine-homocysteine methyltransferase	-10,5	(Megger <i>et al.</i> , 2013; Review, 2013)
	GNMT	Glycine N-methyltransferase	-12,7	(Liu <i>et al.</i> , 2003)
	ENO3	Enolase 3 (beta, muscle)	-13,9	
	AKR7A3	Aldo-keto reductase family 7, member A3 (aflatoxin aldehyde reductase)	-30,5	(Albrethsen <i>et al.</i> , 2011)

Results

The Ingenuity Pathway Analysis by using the list of proteins significantly deregulated in tumors (n=228; $p < 0.05$; $FC \pm 1.5$) revealed an activation of the PI3K/Akt, integrin, ILK, Rho and PAK signaling as well as an inactivation of HIPPO signaling pathway (Figure 22). Proteins identified by DIGE and/or LF as deregulated in HB vs NT and involved in the deregulated pathways according to IPA analysis are listed in Table 16.

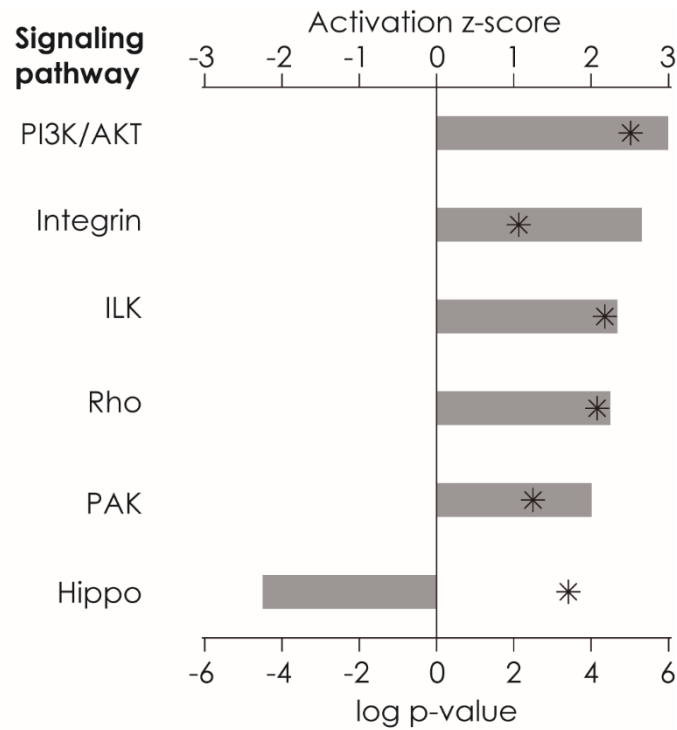


Figure 22. Top deregulated pathways in HB vs. NT according to the IPA analysis. Grey bars represent the activation z-score ($z\text{-score} \geq \pm 2$) and * represent the log p-value ($\log p\text{-value} > 2$).

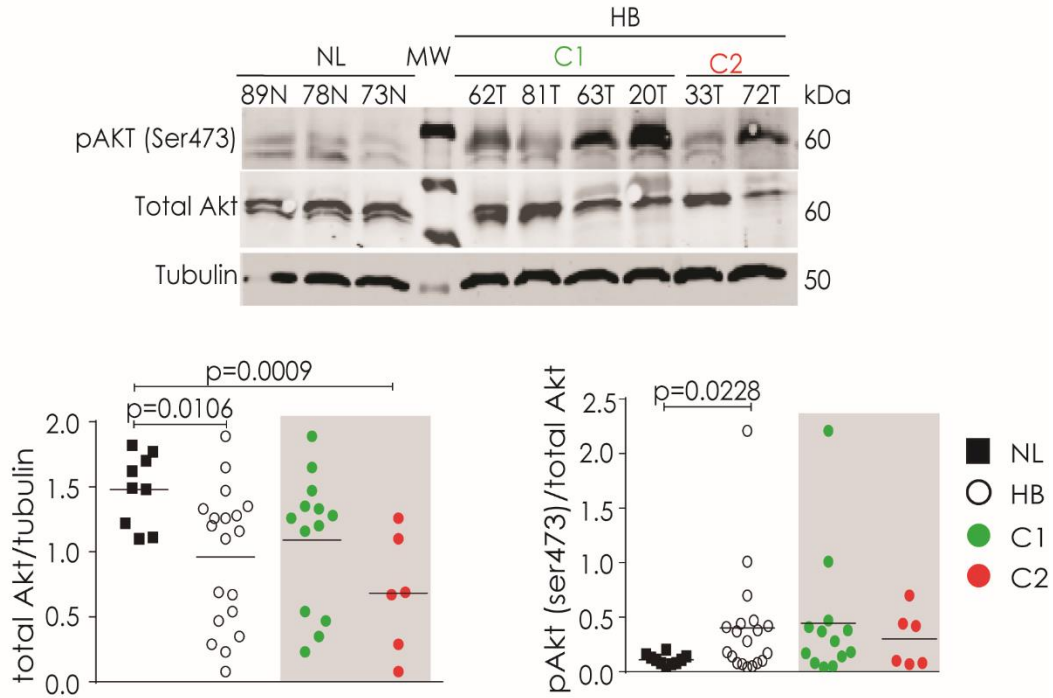
Table 16. Deregulated proteins in HB involved in the top deregulated pathways identified by IPA.

Protein	Hippo	PI3K/Akt	Integrin	ILK	RhoA	PAK	HB vs NL FC	Loc.	Type(s)
YWHAB	x	x					2,8	C	transcription regulator
YWHAE	x	x					2,7	C	other
YWHAG	x	x					1,7	C	other
YWHAQ	x	x					4,2	C	other
YWHAZ	x	x					3,8	C	enzyme
ITGB1		x	x	x		x	5,2	PM	transmembrane receptor
HSP90AA1		x					3,3	C	enzyme
HSP90AB1		x					3,1	C	enzyme
HSP90B1		x					1,6	C	other
SKP1	x						4,1	N	transcription regulator
CFL1				x	x	x	5,3	N	other
MYL6				x	x	x	2,8	C	other
FLNA				x			10,6	C	other
FN1				x			4,7	ES	enzyme
MYH9				x			3,5	C	enzyme
VIM				x			4,1	C	other
MYL9			x	x	x	x	5,0	C	other
MYL12A			x		x	x	1,9	C	other
ACTA2			x	x	x		8,4	C	other
ACTN4			x	x			2,5	C	transcription regulator
CAPNS1			x				2,3	C	peptidase
CTTN			x				4,3	PM	other

Abbreviations: Loc., location; C, cytoplasm; PM, plasma membrane; N, nucleus; ES, extracellular space.

From the top deregulated pathways, PI3K/Akt and Hippo were selected for validation by WB (Figure 23). Total Akt was under expressed in HB vs NT (t-test $p=0.0106$) and was even more repressed in aggressive C2 tumors (t-test $p=0.0009$). In contrast, phosphorylation of Akt at Ser473 was higher in HB vs NT (, t-test $p=0.0228$). Regarding Hippo pathway, total YAP was overexpressed in HB vs NT (t-test $p=0.0015$). The overexpression of YAP is higher in C2 tumors than in C1 vs NT (t-test $p=0.0428$ and $p=0.0153$, respectively). Phosphorylation of YAP at Ser127 is higher in HB than in NT (t-test $p=0.0256$).

A



B

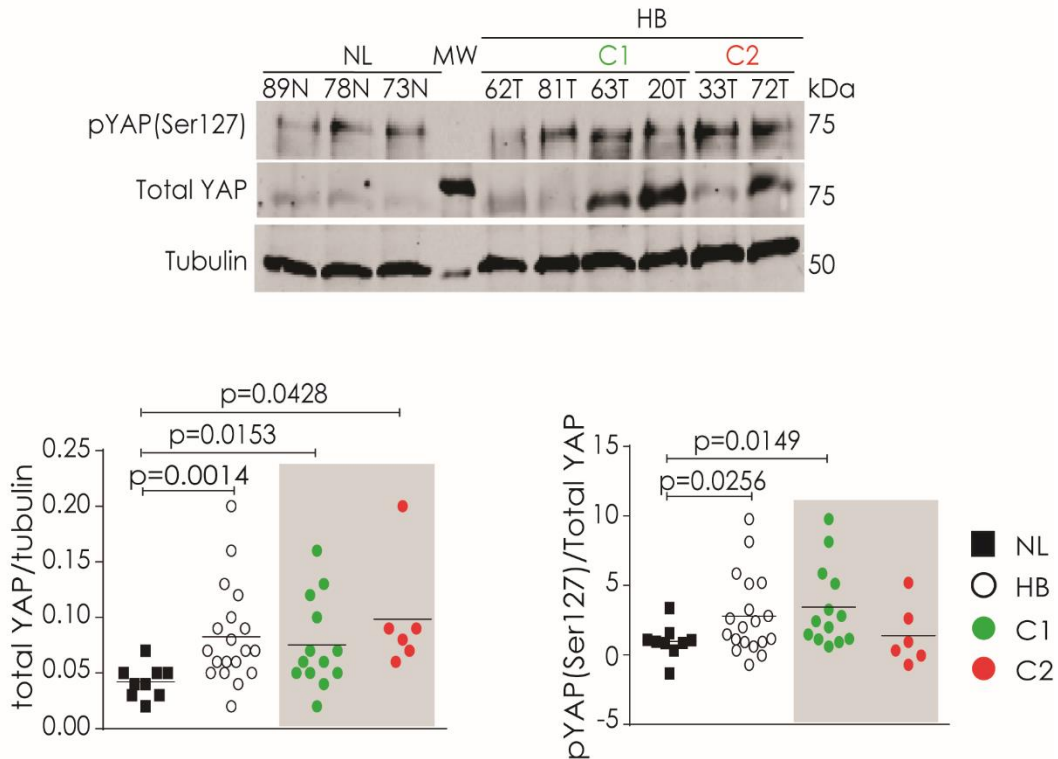


Figure 23. Validation of the top deregulated pathways Akt and Hippo by WB using specific antibodies and tubulin as a loading control in 9NL and 19HB (13C1 and 6C2). Representative WB images of a single experiment and quantification of the WB results for Akt (A). Representative WB images of a single experiment and quantification of the WB results for Yap (B).

4.2.2 Deregulated proteins in aggressive HB tumors

In an attempt to identify proteins deregulated in aggressive tumors, we performed a supervised analysis by comparing the proteomic profiles of the two prognostic subtypes (C1 and C2) previously reported. By using the two different proteomic approaches, we were able to detect 230 differentially expressed proteins between C2 and C1 ($FC \pm 1.5$, $p < 0.05$), 108 down and 124 upregulated. Among them, 20 (9%) were identified by 2D-DIGE, 216 (94%) by LF and 6 (3%) in both techniques. Overall, 2 proteins showed discordant results between both techniques, GRP75 which was found as down-regulated in C2 vs C1 ($FC = -1.61$, $p\text{-value} = 0.0027$) by DIGE and up-regulated by LF ($FC = 3.70$, $p\text{-value} = 0.01$). Proteins with discordant results were excluded of further analysis. The second discordant protein was ALB, which was identified as overexpressed by LF as well as in 10 out of 11 spots by DIGE but in an additional spot it was found to be downregulated. Common identified proteins were CO6A1 ($FC\ LF = -12$; $FC\ DIGE = -2$, mean of 3 spots), ENOA ($FC\ LF = 2.8$; $FC\ DIGE = 1.7$), HDGF ($FC\ LF = 3$; $FC\ DIGE = 1.6$) and ACTB ($FC\ LF = -7.4$; $FC\ DIGE = -1.8$, mean of 5 spots). The top deregulated proteins differently expressed in the 2 HB subclasses identified by the two techniques are summarized in *Table 17*.

Table 17. Top deregulated proteins in aggressive C2 tumors. Criteria: p-value<0.0005 in all comparisons except for C1 or C2 vs NL DIGE data (p-value<0.001); Proteins identified by both techniques. Abbreviations: Tech =Technique; FC = Fold Change; NL= Normal Liver; Ref = References related to liver cancer; Bold indicates proteins selected for WB validation.

Tech	Gene	Gene description	C2/C1	Ref
<i>Up-regulated proteins in aggressive C2 tumors</i>				
	TMPRSS13	Transmembraneprotease, serine 13	3.54	(Hashimoto <i>et al.</i> , 2010)
	HSP90AB1	Heat shock protein 90kDa alpha (cytosolic), class B member 1	1.83	
2DE	HSP90AA1	Heat shock protein 90kDa alpha (cytosolic), class A member 1	1.65	(Negroni <i>et al.</i> , 2014)
	HDGF	Hepatoma-derived growth factor (high-mobility group protein 1-like)	1.56	(Yoshida <i>et al.</i> , 2006; Tsang <i>et al.</i> , 2009)
	NCL	Nucleolin	8.87	(Chen <i>et al.</i> , 2015)
	NPM1	Nucleophosmin (nucleolar phosphoprotein B23, numatrin)	6.99	(Cairo <i>et al.</i> , 2008)
	C1QBP	Complement component 1, q subcomponent binding protein	6.40	
	SSB	Sjogrens syndrome antigen B (autoantigen La)	6.39	
	CKAP4	Cytoskeleton-associated protein 4	5.47	(Li, Liu, <i>et al.</i> , 2014; Li, Tang, <i>et al.</i> , 2014)
LF	EIF5AL1	Eukaryotic translation initiation factor 5A-like 1	4.93	
	SFPQ	Splicing factor proline/glutamine-rich (polypyrimidine tract binding protein associated)	4.31	
	FKBP1A	FK506 binding protein 1A, 12kDa	3.83	
	HNRNPM	Heterogeneous nuclear ribonucleoprotein M	3.11	
	P4HB	Procollagen-proline, 2-oxoglutarate 4-dioxygenase (proline 4-hydroxylase), beta polypeptide	3.11	(Negroni <i>et al.</i> , 2014)
	SOD2	Superoxide dismutase 2, mitochondrial	2.99	
	HSPA8	Heat shock 70kDa protein 8	2.82	(Yang <i>et al.</i> , 2015)
	SERPINA1	Serpin peptidase inhibitor, clade A (alpha-1 antitrypsin), member 1	2.53	(Qin <i>et al.</i> , 2013)

Tech	Gene	Gene description	C2/C1	Ref
<i>Down-regulated proteins in aggressive C2 tumors</i>				
2DE	ACTB	Actin, beta	-2.18	(Waxman and Wurmbach, 2007)
	ALB	Albumin	-3.35	
	TXNL1	Thioredoxin-like 1	-6.96	
LF	GRHPR	Glyoxylatereductase/hydroxypyruvatereductase	-3.94	(Pan et al., 2013)
	LAP3	Leucineaminopeptidase 3	-5.33	(Tian et al., 2014)
	ADH1A	Alcohol dehydrogenase 1A (class I), alphapolyptide	-5.35	(Dannenb erg et al., 2006)
	GGT5	Gamma-glutamyltransferase 5	-6.61	
	BDH1	3-hydroxybutyrate dehydrogenase, type 1	-6.85	
	IDH2	Isocitrate dehydrogenase 2 (NADP+), mitochondrial	-7.21	(Sia et al., 2013; Zhang et al., 2014)
	ALDH2	Aldehyde dehydrogenase 2 family (mitochondrial)	-7.68	(Cairo et al., 2008)
	PYGL	Phosphorylase, glycogen; liver (Hers disease, glycogen storage disease type VI)	-7.82	
	COL6A2	Collagen, type VI, alpha 2	-8.21	(Lai et al., 2011)
	COL6A3	Collagen, type VI, alpha 3	-10.00	(Lai et al., 2011)
	CRYL1	Crystallin, lambda 1	-11.04	(Patil et al., 2005; Cheng et al., 2010)
	COL6A1	Collagen, type VI, alpha 1	-12.13	
	ADH1B	Alcohol dehydrogenase 1B (class I), beta polypeptide	-14.09	(Dannenb erg et al., 2006)
	DPT	Dermatopontin	-24.44	(Li et al., 2009)
	GLUL	Glutamate-ammonia ligase (glutamine synthetase)	-28.30	(López-Terrada et al., 2009)
FBN1	Fibrillin 1	-32.05		
DPT	Dermatopontin	-24.44	(Li et al., 2009)	
GLUL	Glutamate-ammonia ligase (glutamine synthetase)	-28.30	(López-Terrada et al., 2009)	
FBN1	Fibrillin 1	-32.05		

The Ingenuity Pathway Analysis including the top deregulated proteins in C2 vs C1 tumors (n=229; p<0.05; FC±1.5), revealed a strong over-activation of the eukaryotic initiation factor-2 (EIF2) signaling pathway (Activation z-score=2; p-value=1.22 10⁻⁶) in the aggressive C2 tumors. No other significant pathways were found with the selected criteria. Proteins from the EIF2 pathway identified as deregulated in C2 vs C1 comparison are listed in *Table 18*.

Table 18. Deregulated proteins in C2 tumors involved in EIF2 signaling pathway.

Symbol	C2 vs C1 FC	Location	Type(s)
RPS16	5,55	C	other
RPS21	5,28	C	other
RPS12	4,11	C	other
RPL5	4,03	C	other
RPS28	3,82	C	other
RPLP2	3,79	C	other
RPL23A	3,62	O	other
RPL12	3,44	N	other
RPSA	2,59	C	translation regulator
RPS27A	2,55	C	other
RPS3A	2,46	N	other
EIF3B	1,73	C	translation regulator
EIF3H	1,72	C	other
EIF3I	1,72	C	translation regulator
RPL8	1,72	O	other
RPL10A	1,67	N	other
RPL36	1,66	C	other
EIF2S2	1,66	C	translation regulator
RPL22	1,66	N	other
PPP1CC	1,59	N	phosphatase
RPL23	1,58	C	other
EIF3F	1,54	C	translation regulator
EIF3E	1,53	C	other

Abbreviations: EIF, eukaryotic translation initiation factor; PPP, protein phosphatase; RP, ribosomal protein; C, cytoplasm; N, nucleus; O, other

Different phosphorylation of EIF2 between the 2 tumor prognostic subclasses was further validated by Western blot using the 19 (13 C1 and 6 C2) tumor samples revealing a decrease in the pEIF-2 α (Ser51)/total EIF in C2 HB as compared to NL (FC=-1,7; p=0.0010) (*Figure 24*).

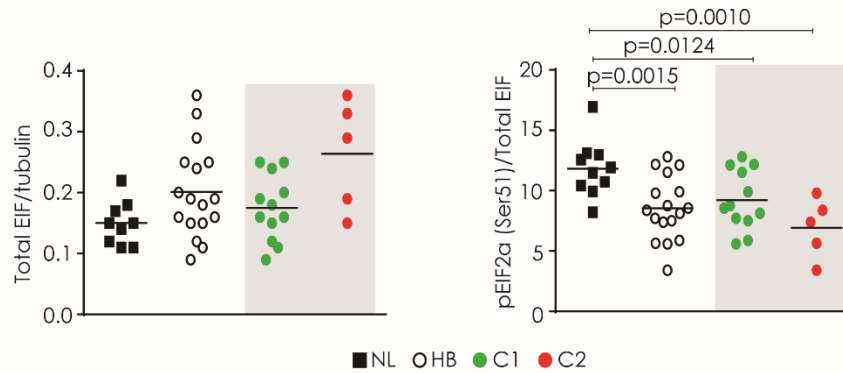


Figure 24. Deregulation of the EIF2 pathway in aggressive C2 HB.

4.2.3 Identification of a 3-protein signature

To select among the differentially expressed proteins between the C1 and C2 tumors the candidates to be validated as prognostic biomarkers, we focused on those proteins differentially expressed between both tumor subtypes ($FC_{\pm} 2.5$, $p < 0.008$) but also between tumor and non-tumor tissues ($FC_{\pm} 1.5$, $p < 0.05$). This was done with the purpose to facilitate their assessment in any pathology department by using the non-tumor liver as a control of protein expression. So, we selected 8 putative prognostic markers (ALBU, DERM, GLUL, TXNL, TMPRSS13, C1QBP, CRYL1 and CKAP4) for further validation by WB. The quantified protein expression of these markers in C1 and C2 tumors as well in non-tumor samples is shown in *Figure 25A*. After quantification of the specific protein bands, 3 out of the 8 initial proteins, cytoskeleton associated protein 4 (CKAP4), complement C1q binding protein (C1QBP) and crystallin lambda 1 (CRYL1) were found to be significantly deregulated in the aggressive C2 tumor subtype as compared with the non-tumor liver and were selected for further validation study by using immunohistochemistry in an independent set of samples (protein expression assessed by WB is shown in *Figure*

25B). In order to confirm its correlation with patient survival, WB data was used to classify patients as having 0, 1, 2 or 3 of the biomarkers altered taking into account NL intensity. The Kaplan-Meier survival analysis, showed that tumors with no altered biomarkers had an EFS probability of 100% as compared to patients with at least one altered biomarker (Log-rank p-value=0.0027; Figure 25C).

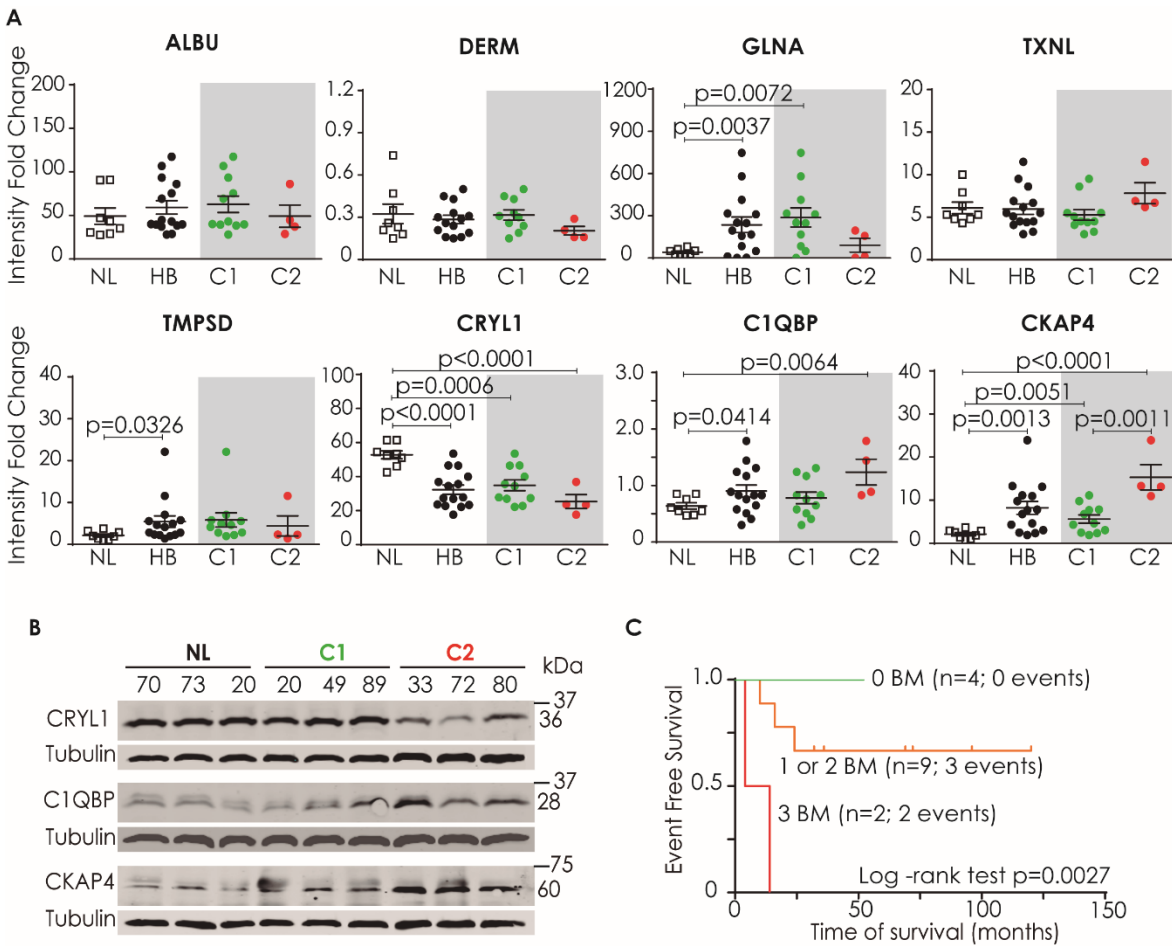


Figure 25. Identification of 3 prognostic biomarkers. Prognostic value of eight proteins was assessed by Western blot in the discovery set of samples. Protein expression quantified from WB of the 8 putative biomarkers. NL, Normal liver (white boxes); HB, Hepatoblastoma (black circles) (A). Representative Western blot of 3 NL and 6 HB (3 C1 and 3 C2) from the 3 selected prognostic biomarkers (B). Kaplan-Meier plot of Event Free Survival for 15 patients classified according the 3 prognostic biomarkers expression by Western Blot (C).

4.2.4 Assessment of the prognostic value of the 3-protein signature in an independent cohort

The immunostaining of C1QBP, CKAP4 and CRYL1 was assessed in 11 tissue microarrays from 144 childhood liver cancer patients, including 133 with HB, 6 with NOS and 5 with HCC in non-cirrhotic liver and additionally in 44 NL samples. CKAP4 showed a cytoplasmic, finely granular staining pattern, on both non tumoral hepatocytes and tumoral cells, with different intensities (negative, weak and strong). Most cases showed a similar and diffuse intensity all over the examined tissue. No staining of nuclei or other tissue cells was seen. C1QBP showed also a cytoplasmic, granular pattern, with a more varied shade of intensities (negative, weak, moderate and intense). Focal staining of tumoral nuclei was sometimes noted. Non tumoral liver was either negative or showed a faintly positive cytoplasmic staining of hepatocytes. No staining of other tissue elements was noted. CRYL1 stained both cytoplasm and nuclei of tumoral cells. The intensity of staining was negative, weak, moderate or intense. Non tumoral hepatocytes showed a similar pattern of staining with a tendency to increase nuclei intensity in periportal areas. No staining of other tissue elements was noted. Representative staining for each marker is shown in Figure 27.

In order to define the value of the 3-protein signature for every tumor, a score was calculated for each protein taking into account the global score (percentage of positive cells x intensity of the staining). Then, we defined C1QBP and CKAP4 biomarkers as “altered” when their staining score was two-fold higher than the staining of the adjacent non-tumor liver whereas CRYL1 tumor staining was defined as “altered” when no staining was observed. An overview of the 3-protein signature definition is shown in *Figure 26*.

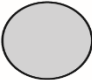
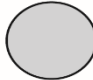
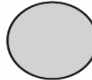
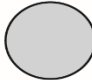











Protein	NL staining	Cutoff alteration	Situations			
			T1	T2	T3	T4
CKAP4		≥12				
NL score	[0-6]					
C1QBP		≥12				
NL score	[0-6]					
CRYL1		=0				
NL score	[6-12]					
3-protein score			0	1	2	3

Figure 26. 3-protein signature definition. After calculating the staining score for each biomarker, a cutoff of alteration was established by using NL staining as a reference. Thus, CKAP4 and C1QBP were considered as altered when score ≥12 (2 times NL maximum value) and CRYL1 when no expression was detected. T1, T2, T3 and T4 represent different tumors with different staining of the 3 biomarkers. Grey means low expression, black high expression and white, no expression. Red circles means altered biomarker. The 3-protein score is obtained by adding the number of biomarkers altered for each tumor (3-protein score rank: 0-3).

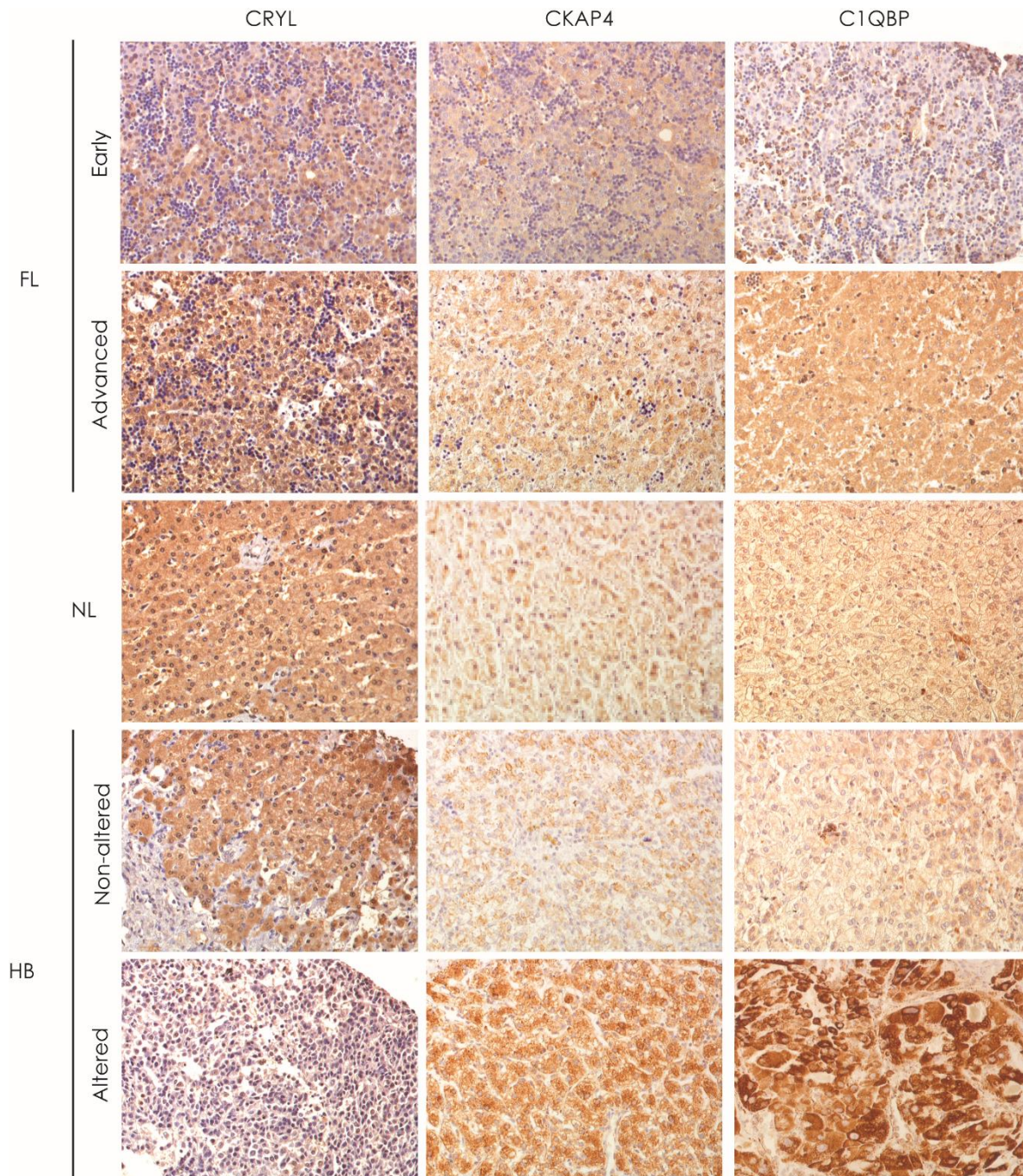


Figure 27. Representative immunohistochemical staining of the 3 protein signature. Protein expression was determined by immunohistochemistry in an independent series of tumor samples from 144 patients. A representative image of NL staining as well as tumors with normal and altered expression and fetal liver at two different developmental stages is shown. Abbreviations: FL, Fetal Liver; NL, Normal liver; HB, Hepatoblastoma.

First, we studied the association of the different biomarkers and the simplified 3-protein signature (grouping patients with at least 1 altered biomarker) with clinical, pathological and molecular parameters (*Table 19 and Table 20*) and the results showed that CKAP4 and CRYL1 were associated with patient outcome (CKAP4 vs EFS $p=0.022$, chi-square test; CRYL1 vs OS $p=0.026$, chi-square test) whereas C1QBP was not associated with EFS neither OS despite a trend on its impact. Interestingly, besides its association with EFS and/or OS, the 3 biomarkers and the 3-protein signature were significantly associated with an epithelial or mixed histology and non-fetal main epithelial component. The unpaired t-test showed that C1QBP and the 3-protein signature are significantly associated with higher age at diagnosis.

The impact of the presence of the altered biomarkers and different clinical features to patient survival was evaluated by Kaplan-Meier curves (*Table 21*). The results of the univariate analysis revealed that the 3-protein signature, CKAP4 overexpression, age >3 and 8 years at diagnosis, AFP <100ng/mL, metastasis at diagnosis, vascular invasion, mixed histology and main epithelial component no pure fetal were associated with worse patient event-free survival.

Table 19. Association of the 3 proteins with age and AFP levels at diagnosis. P-val, unpaired t-test p-value.

	Mean age (months)			Mean AFP (ng/mL)		
	No	Yes	P-val	No	Yes	P-val
CKAP4 ≥ 12	23.3	35.1	0.071	318899.6	509619.8	0.275
C1QBP ≥ 12	22.2	34.6	0.044	298323.9	517847.6	0.204
CRYL1 =0	26.5	48.3	0.186	397619.2	464417.9	0.819
3-PROTEIN SIGN ≥ 1	17.4	33.7	0.001	374861.5	425628.9	0.742

Table 20. Association of the 3 proteins with clinical, pathological and molecular features. P-val, chi-square p-value.

		CKAP4≥12			C1QBP≥12			CRYL1=0			3 PROTEIN SIGNATURE		
		N	Y	p-val	N	Y	p-val	N	Y	p-val	0	1/2/3	p-val
Event free survival	No events	63	50	0.022	59	55	0.063	104	10	0.140	42	73	0.005
	R/DOD	8	18		9	19		22	5		2	26	
Overall survival	Alive	63	54	0.237	60	58	0.188	108	10	0.026	41	78	0.001
	DOD	5	11		5	13		12	5		0	18	
VPEFR ¹	No	23	22	0.796	28	18	0.052	43	3	0.358	17	29	0.360
	Yes	46	40		38	50		77	10		26	63	
Age > 3 years	No	67	58	0.138	63	65	0.499	115	12	0.416	43	86	0.198
	Yes	5	10		6	9		12	3		2	13	
Age > 8 years	No	67	58	0.138	63	65	0.499	115	12	0.416	43	86	0.198
	Yes	5	10		6	9		12	3		2	13	
AFP<100 ng/mL	No	67	57	0.421	62	65	0.469	114	12	1.000	41	87	0.841
	Yes	0	2		2	0		2	0		0	2	
AFP100-1000ng/mL	No	62	55	0.882	58	62	0.289	108	11	0.853	37	84	0.623
	Yes	5	4		6	3		8	1		4	5	
AFP>10 ⁶ ng/mL	No	61	52	0.592	59	57	0.579	106	9	0.074	36	81	0.801
	Yes	6	7		5	8		10	3		5	8	
Metastasis	No	59	53	0.818	57	57	0.435	104	10	0.344	38	77	0.778
	Yes	11	11		9	13		18	4		6	16	
Vascular invasion	No	53	49	0.854	51	52	0.713	94	9	0.650	33	71	0.868
	Yes	14	14		16	14		25	4		10	20	
Multifocality	No	32	27	0.797	35	25	0.051	57	3	0.189	23	37	0.214
	Yes	39	36		32	45		66	10		21	57	
Histology	E	34	45	0.043	32	49	0.012	71	9	0.036	17	65	0.001
	M	35	19		35	20		52	3		27	28	
Main Epith. Comp.	PF	54	35	0.010	52	38	0.008	86	4	0.029	37	54	0.004
	Other	14	25		13	27		32	7		6	34	
ki67 staining	<5%	51	27	<0.0001	44	34	0.032	69	9	0.676	36	42	<0.0001
	>5%	21	41		25	40		58	6		9	57	

¹, VPEFR, presence of at least one of the following characteristics: involvement of vena cava, involvement of portal veins, extrahepatic disease, multifocal tumor, tumor rupture (Meyers *et al.*, 2017). Abbreviations: R, recurrence; DOD, death related to cancer; N, no; Y, yes; E, epithelial; M, mixed; Main Epith. Comp., Main epithelial component; PF, pure fetal.

Table 21. Univariate analysis.

Variable		Total	R or DOD (%)	Log-rank p-val
3-Protein Signature	0	44	2 (4)	0.005
	123	99	26 (26)	
CKAP4 \geq 12	No	71	8 (11)	0.016
	Yes	72	20 (28)	
C1QBP \geq 12	No	68	9 (13)	0.102
	Yes	75	19 (25)	
CRYL1=0	No	126	22 (17)	0.069
	Yes	15	5 (33)	
VPEFR ¹	No	46	6 (13)	0.398
	Yes	88	18 (20)	
Age > 3 years	No	128	18 (14)	<0.0001
	Yes	15	10 (67)	
Age > 8 years	No	128	18 (14)	<0.0001
	Yes	15	10 (67)	
AFP<100 ng/mL	No	128	21 (16)	0.001
	Yes	2	2 (100)	
AFP 100-1000 ng/mL	No	121	22 (18)	0.699
	Yes	9	1 (11)	
AFP>10 ⁶ ng/mL	No	117	23 (19)	0.080
	Yes	13	0 (0)	
Metastasis	No	114	15 (13)	<0.0001
	Yes	22	10 (45)	
Vascular invasion	No	104	15 (14)	0.047
	Yes	29	9 (45)	
Multifocality	No	59	9 (61)	0.622
	Yes	78	16 (20)	
Histology	E	81	21 (46)	0.006
	M	55	4 (7)	
Main Epith. Comp.	PF	90	13 (14)	0.037
	Other	40	11 (27)	
β -catenin nuclear staining	No	60	11 (18)	0.247
	Yes	17	5 (29)	
ki67 staining	<5%	78	13 (17)	0.443
	>5%	65	15 (23)	

¹, VPEFR, presence of at least one of the following characteristics: involvement of vena cava, involvement of portal veins, extrahepatic disease, multifocal tumor, tumor rupture (Meyers et al., 2017). Abbreviations: R, recurrence; DOD, death related to cancer; N, no; Y, yes; E, epithelial; M, mixed; Main Epith. Comp., Main epithelial component; PF, pure fetal.

Interestingly, the combination of the 3 biomarkers showed a stronger impact on patient survival than the 3 biomarkers independently (*Figure 28*) having an additive effect predicting EFS, thus EFS at 150 months was 96, 74, 78 or 50% depending if the tumors had 0, 1, 2 or 3 biomarkers altered (Log-rank $p=0.0041$). The impact was even stronger in the OS analysis, in which OS probability at 150 months was of 100, 81, 88 or 50% for tumors with 0, 1, 2 or 3 altered biomarker respectively. As the survival analysis showed that having 1 or 2 altered biomarkers lead to similar EFS and OS probabilities (EFS: 74 vs 78%; OS: 81 vs 88%), we defined a simplified 3-protein signature grouping patients with 1 or 2 altered biomarkers. The Kaplan-Meier curves showed that the group with best outcome included patients with tumors with an expression of the biomarkers similar to the adjacent non-tumor liver (global score=0) with 96% probabilities of EFS at 150 months, a second group with an intermediate outcome had patients with tumors that had an alteration of 1 or 2 biomarkers having 76% probabilities of EFS at 150 months and finally, a third group of patients with worse prognosis was characterized by having tumors with all biomarkers altered (global score=3) showing an EFS probability of 50% (*Figure 28*). This robust association of the 3-protein signature to EFS is even stronger in the analysis of OS, in which patients had 100, 85 or 50% of OS probabilities depending on having 0, 1/2 or 3 altered biomarkers (Log-rank $p<0.0001$). Interestingly, only 2/6 (33%) analyzed NOS tumors had no altered biomarkers (3-protein score=0) and 4/6 (66%) had at least 1 altered biomarker (2/6 had 2-3 altered biomarkers). Regarding the pHCC, all had at least one altered biomarker (1/5 had 1 altered biomarkers whereas 4/5 had 2 or 3 altered biomarkers).

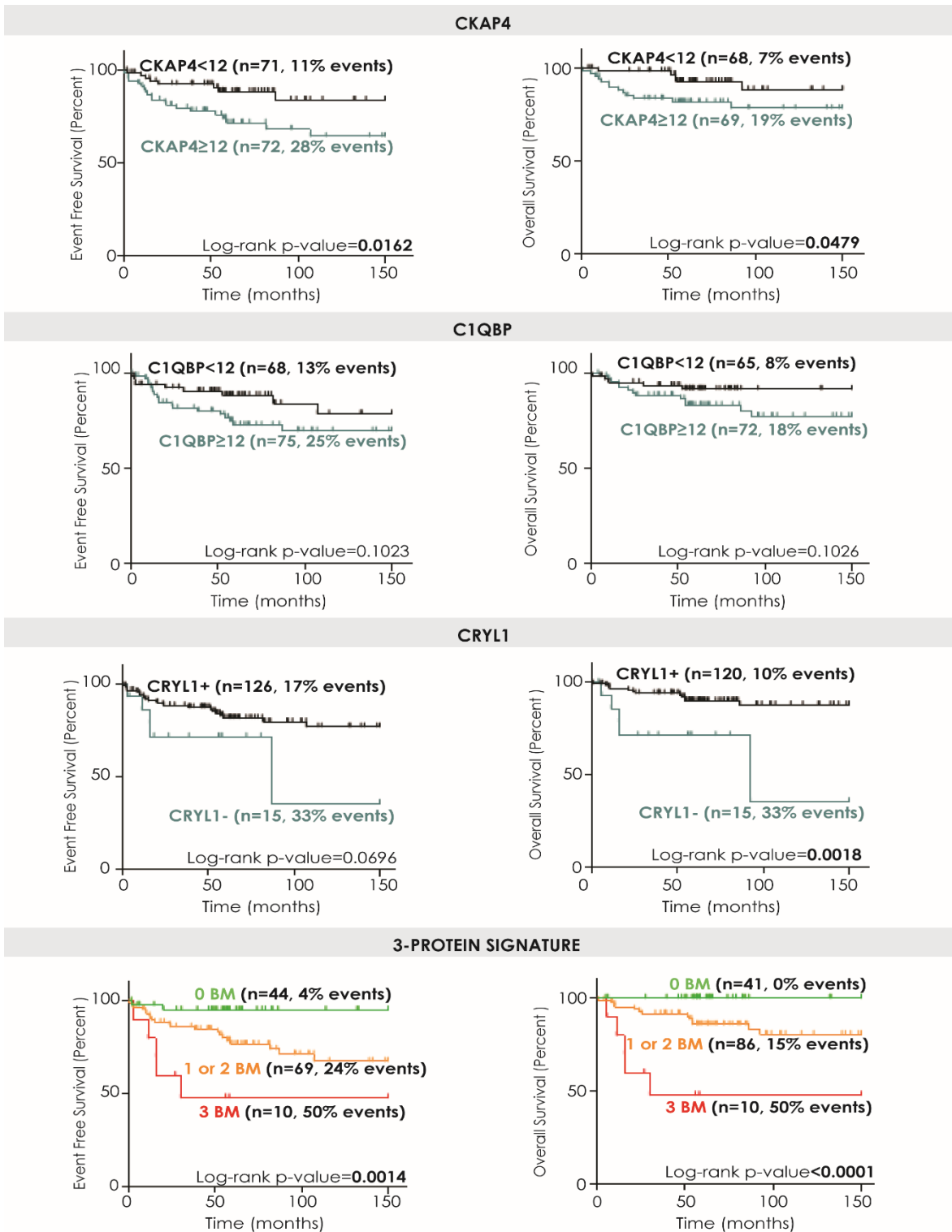


Figure 28. Survival analysis of the 3 biomarkers individually and the 3-protein signature. Kaplan-Meier plots of the 3 biomarkers individually and the 3-protein signature associated to EFS and OS.

Once we confirmed the impact of the 3-protein signature with the patient outcome, we were interested in evaluating its utility to be used for improving HB management. From our validation cohort of 144 patients, 128 patients had the clinical data to be classified with the current clinical stratification CHIC-HS (Meyers *et al.*, 2017), although very low and low patients were both considered as low risk. The survival analysis confirmed that the CHIC-HS is significantly associated with patient outcome in our cohort. Thus, patients classified as low risk had a 93% probabilities of EFS, compared to 76% of intermediate patients or 53% of high risk patients (Log-rank $p < 0.0001$) (Figure 29).

In order to assess the impact or overlapping of the 3-protein signature with the clinical classification, each group of patients was in turn sub classified with the 3-protein signature. Interestingly, the results showed that the 3-protein signature was useful to improve the classification of intermediate patients, as the deregulation of the 3 proteins led to a 50% EFS probabilities compared to patients with no altered biomarkers, who had an EFS probability of 100% (Log-rank $p = 0.0011$). This effect was also seen in the OS analysis as intermediate patients with a 3-protein score=0 had 100% OS probabilities in contrast to patients with a score=1 or 2 who had 92% OS probabilities or score=3 who had 50% OS probabilities (Log-rank $p = 0.0002$). The sub classification with the 3-protein signature for the low and high risk showed no significant impact of the signature on patient EFS or OS, despite a trend towards improving classification could be observed (Figure 29).

Interestingly, the multivariate analysis identified the 3-protein signature as an independent prognostic factor of pediatric patients with liver cancer together with the CHIC-HS clinical stratification (Table 22).

Table 22. Multivariate analysis.

Variable	HR	IC (95%)	p-value
CHIC-HS	3.29	1.7-6.3	<0.0001
3-protein signature	2.54	1.27-5.10	0.0009

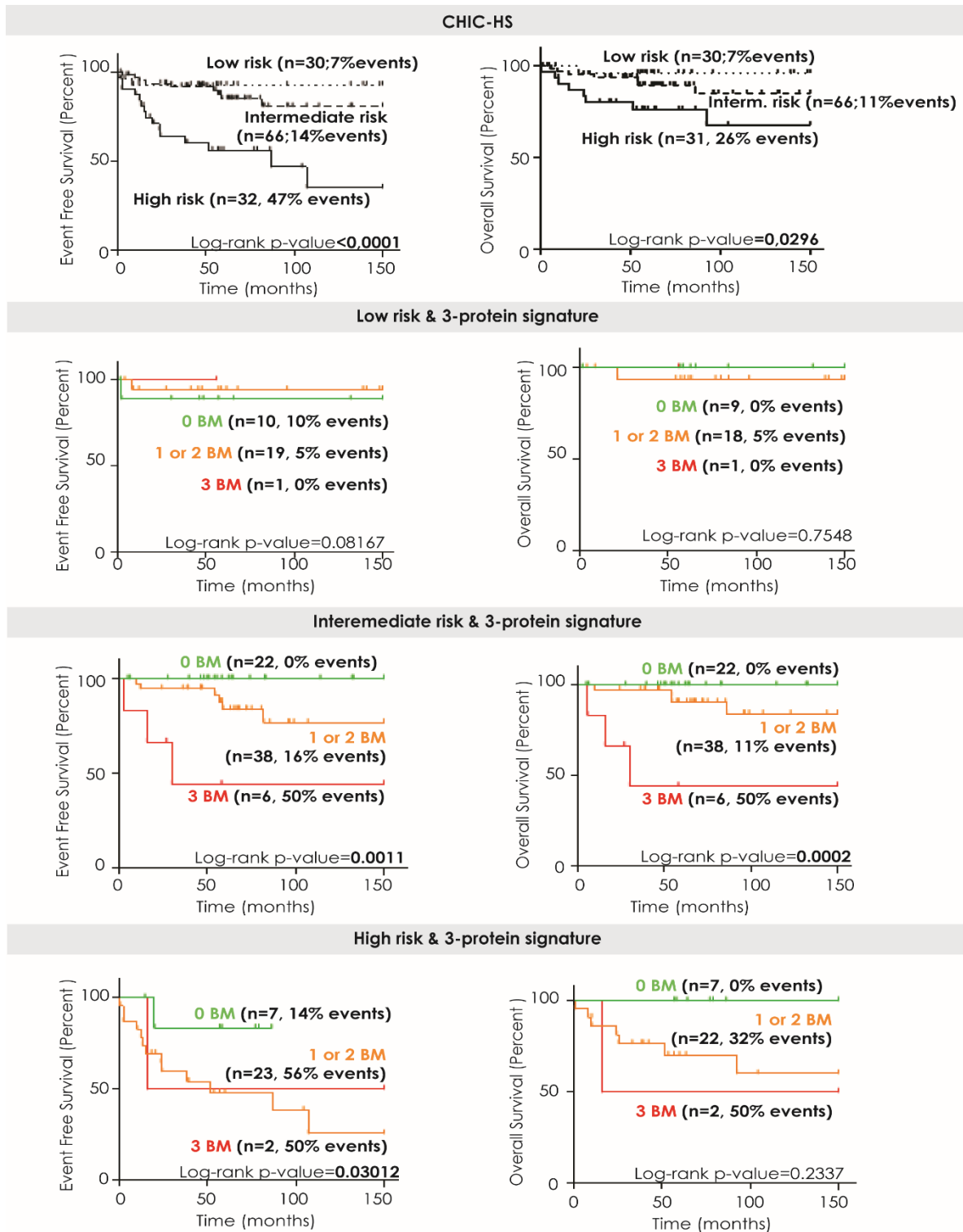


Figure 29. Clinical CHIC-HS and 3-protein signature survival analysis. One hundred and twenty eight patients were classified according to the last clinical stratification system CHIC-HS (Meyers *et al.*, 2017). Then low, intermediate and high risk patients were sub classified using the 3 protein-signature. *Interm.*, intermediate.

We wanted to assess the potential of the 3-protein signature to predict survival in non-treated specimens. The Kaplan-Meier analysis revealed that, despite not being significant, there is an association with both, EFS and OS. Interestingly, patients with zero altered biomarkers had 100% probabilities of EFS and OS, compared to patients with at least 1 altered biomarkers (*Figure 30*).

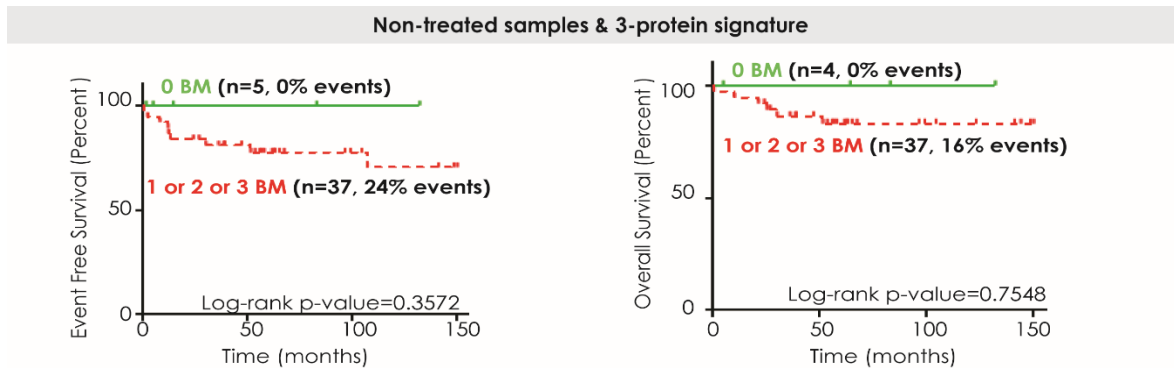


Figure 30. 3-protein signature survival analysis in non-treated specimens. Simplified 3-protein signature (grouping patients as 0 vs. at least 1 altered biomarkers) and its association with patient EFS (left) and OS (right) is represented.

4.2.5 Plasma expression of C1QBP

In order to assess the plasmatic levels of C1QBP, an ELISA was performed using 20 plasma samples from patients with liver cancer (10 with good prognosis and 10 with bad prognosis features, including 1 pHCC) and 7 healthy patients. Patients with bad prognosis features (poor) were classified if presented metastasis and/or multifocality and/or PRETEXT IV and/or AFP >10⁶ ng/mL and/or more than 3 years and/or pHCC. The patients classified as “good prognosis” did not have any of the above mentioned criteria associated to poor outcome.

Patients with poor outcome features had higher concentrations of C1QBP than healthy individuals (t-test p-value =0.0343) (*Figure 31*). Interestingly, high levels of C1QBP ([C1QBP]>15ng/mL) were also associated with multifocal tumors (Fisher test p=0.035).

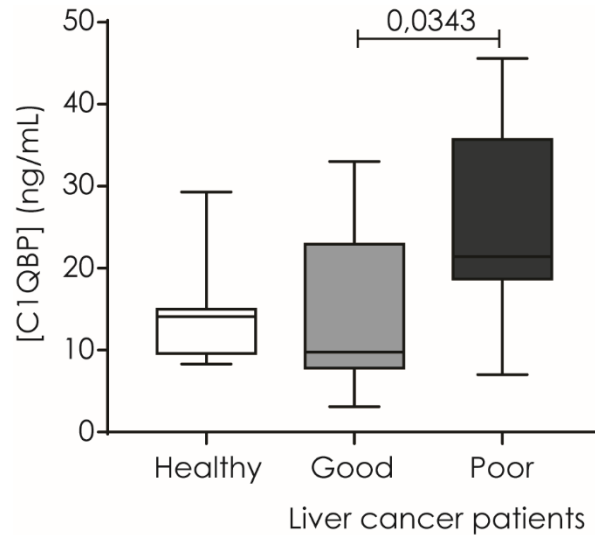


Figure 31. Plasmatic levels of C1QBP in pediatric control individuals and liver cancer patients assessed by ELISA.

4.2.6 Integrative analysis of the proteomic, genomic and transcriptomic data

In order to complete the proteomic characterization of aggressive tumors, proteomic data was correlated with previously published gene expression and copy number variation data (Cairo *et al.*, 2008). To do so, the DNA-RNA Integrator (DRI) was used. DRI allows the correlation of 2 paired data sets (originally DNA and RNA) to identify correlations between the 2 types of data analyzed (for example DNA copy number and gene expression). So, the DRI method was applied in order to find correlations between RNA and protein and also DNA and protein. The proteins, gens and BACs identified in the C2 vs. C1 comparison were used.

Sixteen genes were found correlated at protein and DNA level, 10 of them positively correlated and 6 negatively correlated (Table 23).

Table 23. Correlated proteins at protein and DNA level. Fdr p-value<0.05; ¹, also correlated at RNA and protein level.

Gene name	chr.p	dna.score.p	rna.score.p	correlation.p
SSB ¹	2	4.533	6.848	7.535
NCL ¹	2	3.508	4.147	6.475
HNRNPA3 ¹	2	3.071	3.126	6.088
STAU1	20	3.082	2.903	5.638
RBM8A	1	2.847	3.278	5.319
TPD52L2 ¹	20	4.585	3.082	5.154
CA2	8	4.368	2.998	5.055
EIF6	20	3.66	2.838	5.039
FN1	2	4.062	2.804	4.739
DBI ¹	2	2.666	4.214	4.353
ACTR2	19	-2.11	-2.79	-3.705
GANAB	11	-2.018	-2.141	-3.921
DAK	11	-2.018	-2.084	-3.973
WDR1	4	-2.132	-2.366	-4.051
TYMP	22	-2.284	-2.289	-4.562
NIT2 ¹	3	-3.831	-3.713	-7.311

One hundred and twenty-seven genes showed correlation at protein and RNA level, 70 of them were positively correlated and 57 negatively correlated. Top correlated genes are shown in *Table 24*. Interestingly, 2 of the proteins of the 3-protein signature showed significant correlation between gene and protein expression, C1QBP and CRYL1.

Among the 230 deregulated proteins in aggressive C2 tumors, 6 proteins (3%) were identified as correlated both at protein and DNA level and protein and RNA: Sjogren syndrome antigen B (SSB), nucleolin (NCL) and nitrilase family member 2 (NIT2), diazepam binding inhibitor, acyl-CoA binding protein (DBI), heterogeneous nuclear ribonucleoprotein A3 (HNRNPA3) and tumor protein D52 like 2 (TPD52L2). Interestingly, 4 of them (SSB, DBI, NCL and HNRNPA3) are codified in chromosome 2 and are positively correlated, reflecting the fact that aggressive tumors have a gain of this chromosome and suggesting that this gain is causing an increase of the gene expression and protein translation. TPD52L2, which is located in chromosome 20, is also positively correlated. On the other hand, NIT2 is codified in chromosome 3 and

it is negatively correlated in the 2 comparisons, suggesting that a DNA loss of this gene is producing a decrease in gene expression which is translated into a decrease in the protein expression too.

Table 24. Top correlated genes at protein and RNA level in C2 vs C1 tumors. Fdr p-value<0.01. *, 3 protein-signature; 1, also correlated at DNA and protein level.

Gene name	chr	dna.score.p	rna.score.p	correlation.p
C1QBP*	17	5.630	7.422	9.900
CYC1	8	4.309	4.663	8.291
SSB ¹	2	4.818	6.848	8.208
HSPE1	15	7.780	4.995	8.201
DBI ¹	2	4.844	4.214	7.880
MIF	22	3.796	3.589	6.981
NPM1	1	3.928	5.114	6.945
NCL ¹	2	6.389	4.147	6.840
CMPK1	1	4.051	6.281	6.663
SSR1	6	3.386	3.565	6.603
TPD52	8	3.897	6.157	6.364
YBX1	1	3.693	5.574	6.140
C14orf166	14	3.585	5.139	6.086
SUB1	5	3.205	4.160	5.673
TPD52L2 ¹	20	2.871	3.082	5.545
CALU	7	3.208	2.856	5.399
CHCHD3	1	2.768	3.145	5.203
PLIN3	19	3.099	4.694	5.144
TXN	17	2.640	2.845	5.088
HSPD1	12	7.171	3.433	5.076
HNRNPK	3	2.642	2.964	4.997
RPL36	19	3.456	2.759	4.961
EIF3I	1	2.945	4.363	4.933
RPS16	1	2.527	2.681	4.910
HNRNPA3 ¹	2	2.648	3.126	4.892
SPTBN1	2	-2.823	-3.638	-5.013
ALAD	9	-4.880	-3.111	-5.094
ACTN4	19	-2.661	-2.861	-5.137
SULT2A1	19	-4.622	-3.126	-5.241
CRYL1*	13	-2.969	-3.858	-5.255
BDH1	3	-2.786	-3.070	-5.316
BGN	X	-2.808	-2.792	-5.568
ACAA1	3	-2.838	-2.830	-5.653
PBLD	10	-3.329	-4.739	-5.668
ACADVL	17	-3.266	-3.199	-6.331
ADH6	4	-4.424	-9.752	-6.430
ALB	4	-4.454	-3.830	-7.123
NIT2 ¹	3	-3.897	-3.713	-7.251
CAT	11	-4.990	-4.074	-7.400
C4BPA	1	-4.299	-5.350	-7.752

Finally, in order to visualize the different data (DNA, RNA and protein) we represented a CIRCOS plot (Figure 32). The CIRCOS plot shows the high incidence of chromosomes 1q, 2 and 8 gains. Chromosome 2 shows the highest number of significant positive correlated genes at proteins and DNA level.

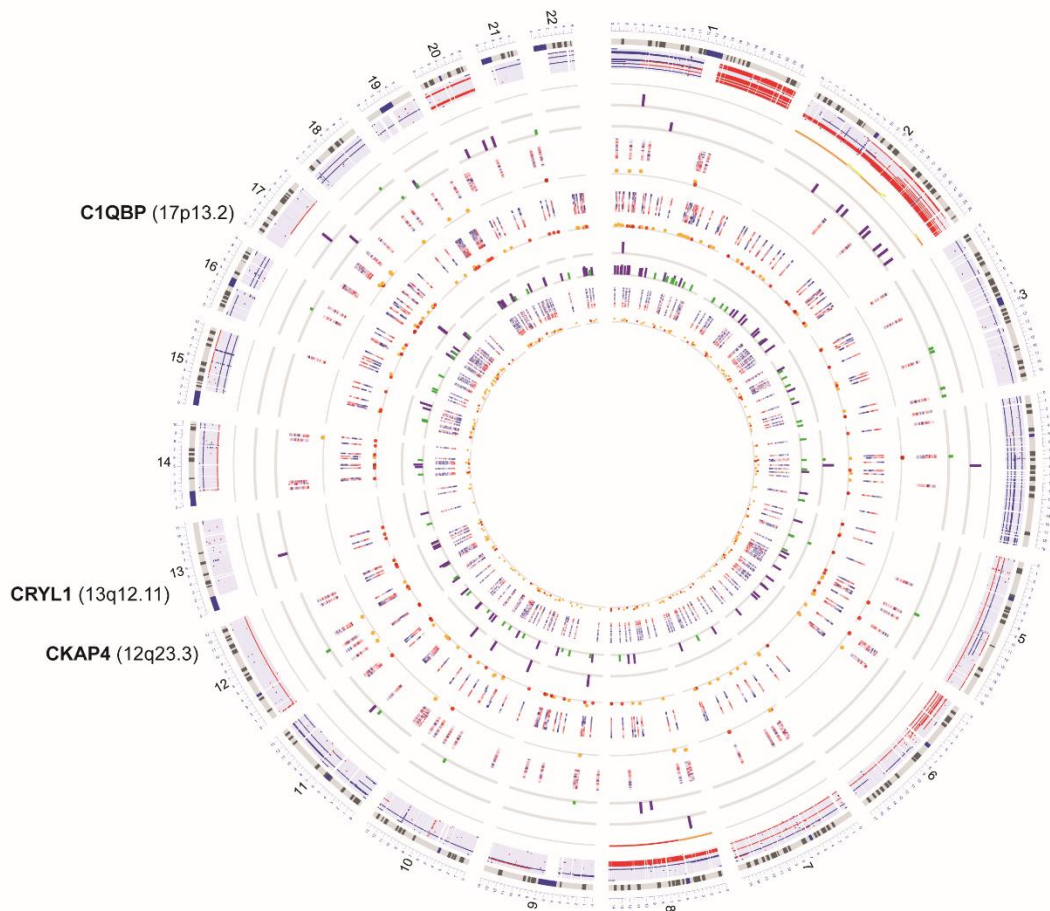


Figure 32. CIRCOS plot of the proteomic, transcriptomic and genomic data. Significant copy number gains and losses, differently expressed proteins and genes and DRI data from the C2 vs C1 comparison was represented in a CIRCOS plot. From outer to inner tracks: chromosomes; cytobands; aCGH gains (red) and losses (blue) for each sample; p-value of the aCGH C2 vs C1; DRI DNA-RNA correlation; heatmap of the proteins identified by DIGE and p-value; heatmap of the proteins identified by LF and p-value; DRI DIGE and RNA correlation; DRI LF and RNA correlation; heatmap of the differently expressed genes and p-value. DRI: purple, positive correlation; green, negative correlation; heatmap: blue, higher expression; red, lower expression. P-values: from yellow (higher p-value) to red (lower p-value).

4.3. Genomic and RNAseq study of pediatric liver tumors

4.3.1 RNA sequencing analysis

The RNAseq study was performed in a cohort of 31 pediatric patients with HB as well as 2 recurrences and 13 PDX, including paired NT. To notice that this series is particularly enriched with aggressive tumors according to the CHIC-HS (38% high risk patients). *Table 9* depicted the main clinical and pathological features of the patients included in the study.

4.3.1.1 Fusion protein identification

In order to identify putative fusion proteins in HB, RNAseq data was analyzed to find out new fusion transcripts events. A total of 13 fusion transcripts with perfect alignment were identified exclusively in tumor samples (*Table 25*). Eight out of thirteen (61%) of the events were intrachromosomal, whereas the other 39% involved 2 different chromosomes. Three out of thirteen (23%) involved immunoglobulin domains, where chromosomal rearrangements typically occur and for this reason these events were excluded of the validation. The remaining 10 events were studied to know if they could be translated in to protein in order to select the fusion events which could generate a functional chimera protein. As a result of this analysis, 4 fusion transcript events were selected and further validated by RT-PCR and Sanger Sequencing. Two out of the four selected events were intrachromosomal rearrangements involving chromosomes 13 and 16 and the other 2 were interchromosomal involving chromosomes 2 and 10, and 9 and 10, respectively. The gel electrophoresis of the PCR product showed a unique product with the specific size in the 4 primary tumors and their 2 paired PDX (*Figure 33A*). Sanger sequencing and nucleotide blast of the PCR products confirmed the presence of the fusion events (*Figure 33B*).

Table 25. Fusion transcripts in HB identified by RNAseq. Bold indicates events selected for validation.

Event	gene1	gene2	NT	HB	PDX
chr2:89161075_chr2:89185669_+_-	IgKappa	abParts	0	4	0
chr2:89161436_chr2:89185669_+_-	abParts	abParts	0	2	0
chr16:57905554_chr16:69418482_-_+	TERF2	genomic	0	1	1
chr1:149576701_chr1:145004782_+_+	LINC00623	LOC100288142	0	1	0
chr2:14494287_chr2:153572508_-_+	BC035112	PRPF40A	0	1	0
chr3:117716028_chr3:116163803_-_-	genomic	LSAMP	0	1	0
chr2:89160771_chr2:89185669_+_-	Ig kappa//abParts	abParts	0	1	0
chr13:43681313_chr13:45913631_-_+	DNAJC15	TPT1	0	1	0
chr12:20704504_chr21:27228076_+_+	PDE3A	genomic	0	2	0
chr1:148932921_chr4:4193800_+_+	LOC645166	OTOP1	0	1	1
chr2:135252042_chr10:70243176_-_+	TMEM163	SLC25A16	0	1	0
chr4:74277730_chr10:135346189_-_+	ALB	CYP2E1	0	1	0
chr9:93976735_chr10:103529680_+_+	AUH	genomic	0	1	1

Finally, in order to study whether these fusion transcripts could be relevant in HB tumorigenesis, the 4 fusion events validated were investigated in an additional set of 21 primary tumors with no positive findings, having a final incidence of 2% (1/52).

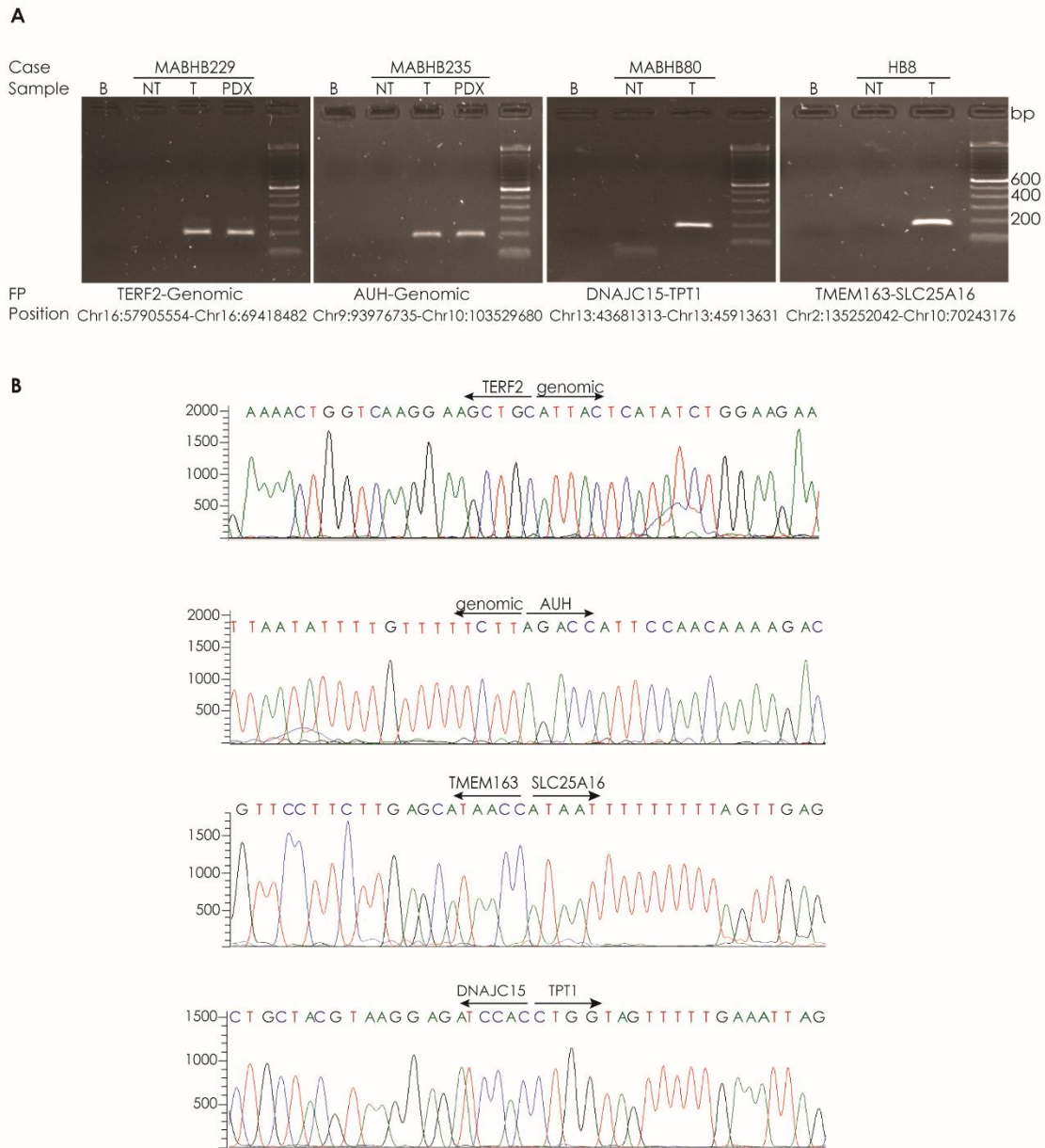


Figure 33. Validation of the fusion events identified in HB. Gel electrophoresis of the PCR product of the 4 selected fusion transcripts in tumor samples from which were identified as well as in their corresponding non-tumor and PDX samples (A). Resulting sequences of the 4 fusion transcripts in representative positive tumor samples (B).

4.3.1.2 Mutational analysis

In order to identify new mutation events in Hepatoblastoma, RNAseq data was interrogated for nucleotide changes leading to a change of amino acid (missense events) or introducing a stop codon. RNAseq results showed that the top mutated gene was Catenin Beta 1 (CTNNB1) identified as mutated in 10 cases, followed by Bladder-cancer associated protein (BLCAP) (n=9), Nuclear Factor, Erythroid 2 Like 2 (NFEL2) (n=2) and EPH receptor B4 (EPHB4) (n=2). Mutations were further validated by PCR and Sanger sequencing in the same 31 patients and in an independent cohort of 21 patients. The study was completed by sequencing the TERT promoter region, already known to be altered in NOS tumors. The results revealed that top mutated gene was CTNNB1 in 75% of tumors, followed by EPHB4, NFE2L2 and telomerase reverse transcriptase (TERT) in 6, 4 and 3% of the cases, respectively (*Table 26*). Interestingly, all the cases with NFE2L2 and EPHB4 mutations belong to the aggressive C2 subtype, while the TERT promoter mutations was identified in a NOS tumor.

Table 26. Top mutated genes validated in HB. *For CTNNB1, results from RNAseq, PCR, electrophoresis and Sanger sequencing are shown.

Gene	Training set	Validation set	%	% of C2 tumors with the mutation
CTNNB1	22/31*	17/21	75	59
NFE2L2	3/31	0/21	6	100
EPHB4	2/31	0/21	4	100
TERT	1/27	-	3	0

The analysis of CTNNB1 mutations was completed by electrophoresis and Sanger sequencing in order to find out deletions. Main aberration in CTNNB1 gene were deletions of the third exon in 50% (26/52) of the tumors, not detected by RNAseq but found by Sanger sequencing, followed by punctual mutations also in exon 3 in 25% (13/52) of the patients. Main mutation was D32Y (4/52, 8%), followed by I35S (2/52, 4%) and Y30S, D32N, D32V, G34V, S37F, T41I and S45P (1/52, 2%).

Importantly, 7 out of the 13 tumors harboring punctual mutations had a change in the Asparagine 32 (Figure 34).

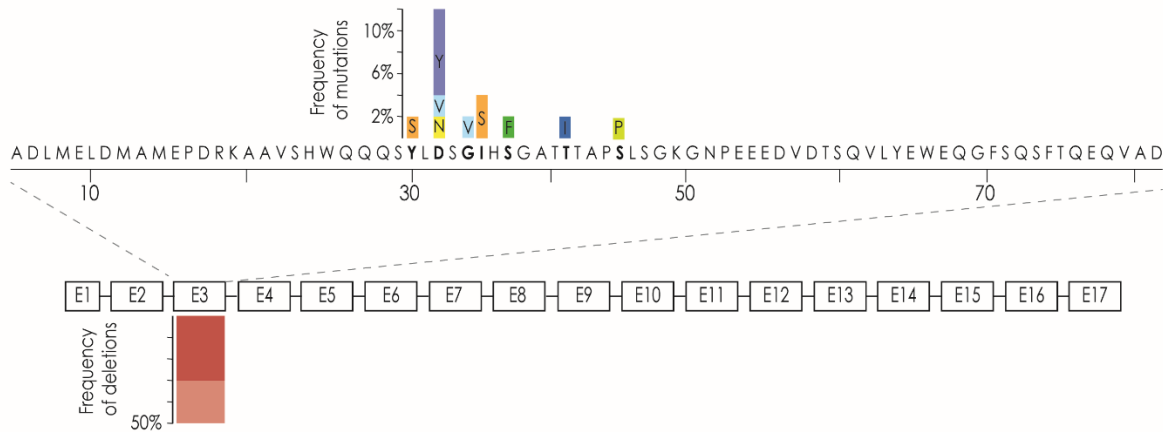


Figure 34. CTNNB1 gene mutations and deletions. All the punctual mutations were found in the third exon. Colored squares above the sequence show the frequency of the different nucleotide changes. Red squares below the protein scheme represent the % of tumors with exon 3 deletions (dark red, whole exon; light red, part of the exon).

The 3 samples harboring NFE2L2 mutations had three different changes: G31A, D77G and G81S. All of them were located in the second exon of the gene. The 2 samples with EPHB4 mutations had G368V and F594V mutations, in the 6 and 11 exons located in the extracellular and cytoplasmic domains respectively. Finally, one NOS (MABHB26) sample had a mutation in the promoter of TERT (146G>A).

Regarding BLCAP, identified by RNAseq as mutated in 9 primary tumor samples, it had several mutated sites: nucleotides 5 (A<G), 14 (A<G) and 44 (A<G). However, Sanger sequencing of the BLCAP gene revealed that all the samples were wt at DNA level. Nevertheless, further Sanger sequencing of the BLCAP mRNA of the same tumors showed the presence of a double peak in the nucleotide 5, suggesting an editing event. Moreover, BLCAP mRNA in non-tumor samples showed the presence of the mutated nucleotide as in tumor samples but with low peak intensity (Figure 35A).

As editing of BLCAP in nucleotides 14 and 44 was not detected by Sanger and editing of the nt5 of the BLCAP has already been reported in cancer (Galeano *et al.*, 2010; Hu *et al.*, 2015), only nt5 was selected for further validation. Thus, in order

to quantify the levels of nt5 BLCAP editing we performed droplet digital PCR (ddPCR). The results confirmed the over-editing of nt5 in T vs. NT samples ($p < 0.0001$, t-test; *Figure 35B*). The statistical analysis comparing paired T and NT samples, confirmed the over editing of BLCAP in 18 out of 31 (58%) analyzed pairs ($p < 0.0001$, $FC > 1.5$, paired t-test). Only in 2 out of 31 tumor samples there was a decrease in nt5 editing ($FC = -1.5$ and -1.6). Additionally, gene expression of BLCAP was assessed by qRT-PCR and the results show a decreased expression in HB vs. NT samples ($p = 0.076$, t-test; *Figure 35C*).

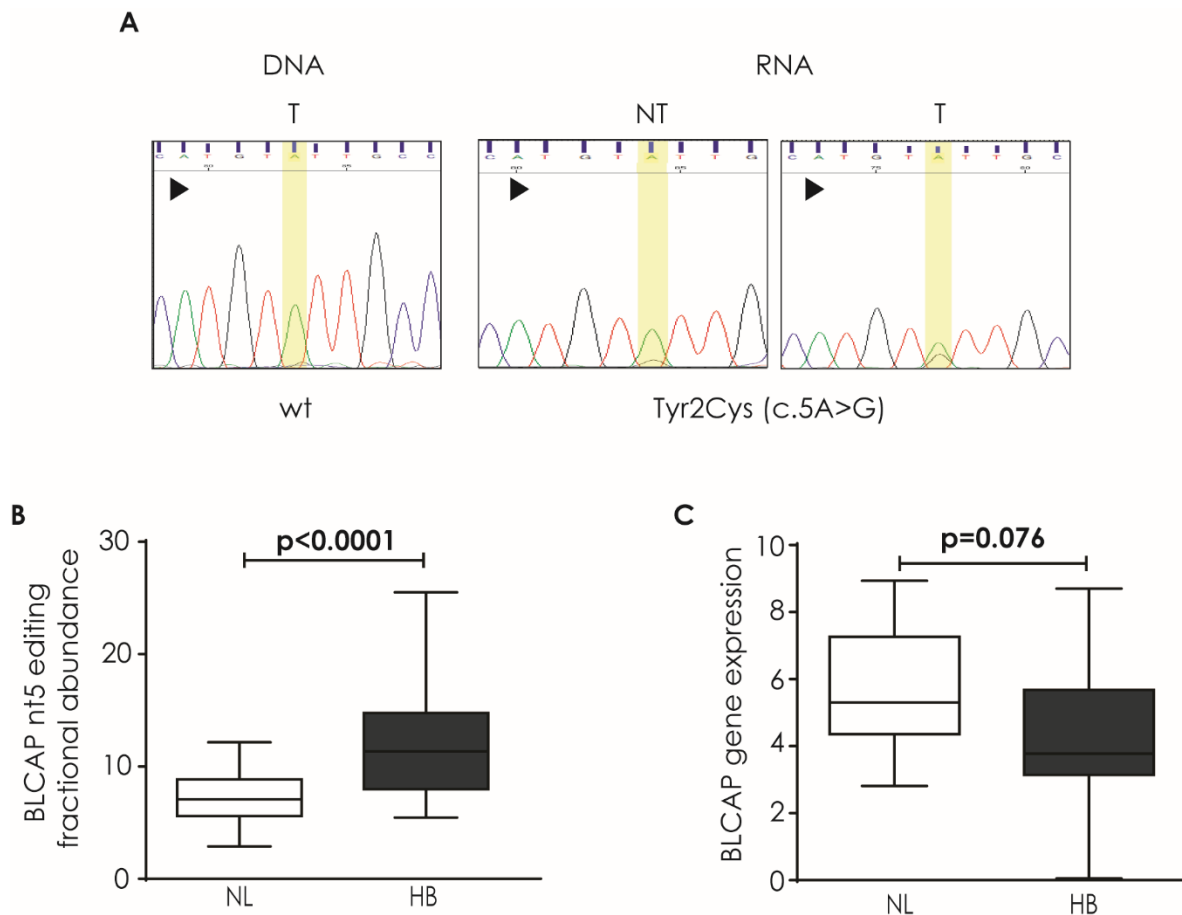


Figure 35. BLCAP nt5 editing validation. DNA and RNA sequences of the 10 first nucleotides of BLCAP. Nucleotide 5 is highlighted in yellow. Arrows indicate start codon. (A) Fractional abundance of nt5 editing of BLCAP in 31 NT and 31 HB samples quantified by ddPCR (B). BLCAP gene expression assessed by qPCR in 21 NT and 30HB (C).

4.3.1.3 Editing analysis

From the discovery of the altered editing of nt5 of BLCAP, we aimed to investigate the global editing in HB by using RNA sequencing data. The analysis showed that 98% of the edited sites were localized in repetitive ALU elements and mostly in non-coding regions (Figure 36A). Interestingly, in contrast of the BLCAP situation, we observed a global decrease in RNA editing in tumors as compared to non-tumor samples for both non-ALU and ALU sites ($p=0.0006$; $p=0.0040$, respectively, t-test; Figure 36B).

Remarkably, the editing index was correlated with patient survival (log rank test $p=0.0440$), as patients with an editing index higher than 0.202 (mean tumor editing index) which is similar to the editing index in non-tumor samples, had 100% OS probabilities as compared to patients with editing index lower than 0.202 who had 72% of OS (Figure 36C).

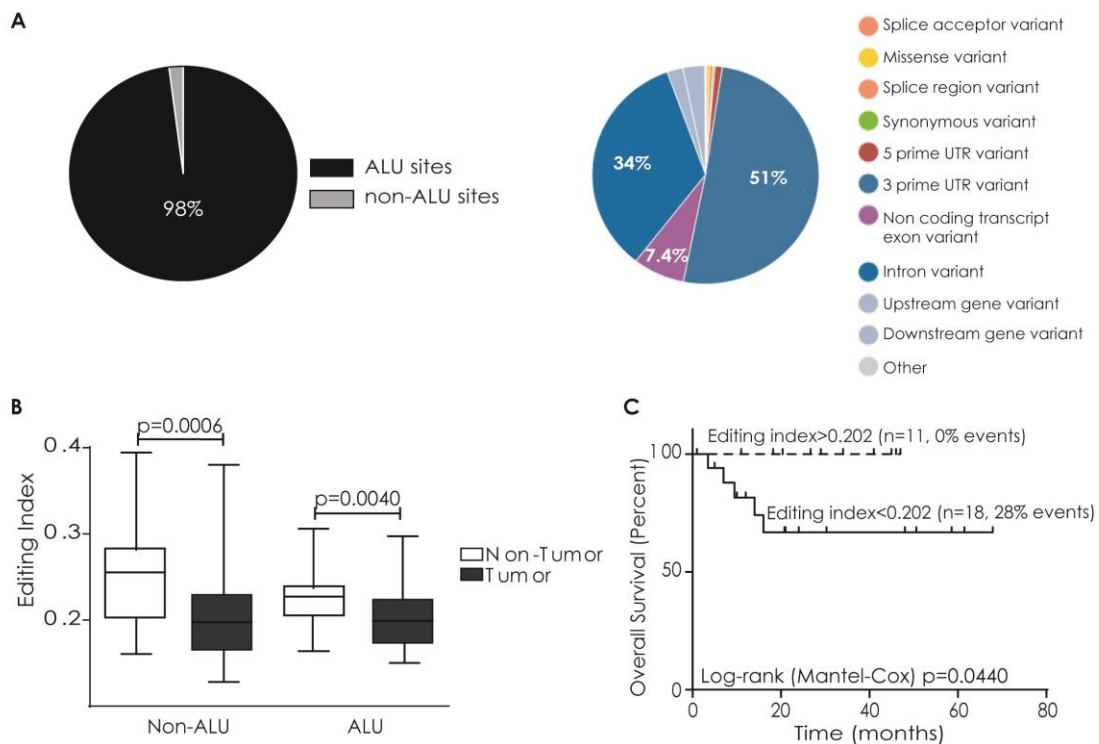


Figure 36. RNA editing analysis. RNA editing was mainly present in ALU elements and non-coding regions (A). Editing index in 31NT and 31T samples in ALU and non-ALU elements (B). Kaplan-Meier curves of the patients stratified in normal index (>0.202) or low editing index (<0.202) (C).

Since RNA editing is regulated by ADAR enzymes (Nishikura, 2010), the expression of ADAR1 and ADAR2 genes was assessed by qPCR in 27 HB samples and 26 NT samples and the results showed an overexpression of ADAR2 in tumor samples as compared to non-tumor samples (t-test $p=0.0003$) whereas no significant difference was seen in ADAR1 levels (Figure 37A). Interestingly ADAR2 gene expression was positively correlated with BLCAP nt5 editing ($p=0.0008$, $r^2=0.1991$, linear regression) but not ADAR1 ($p=0.2007$, linear regression) (Figure 37B).

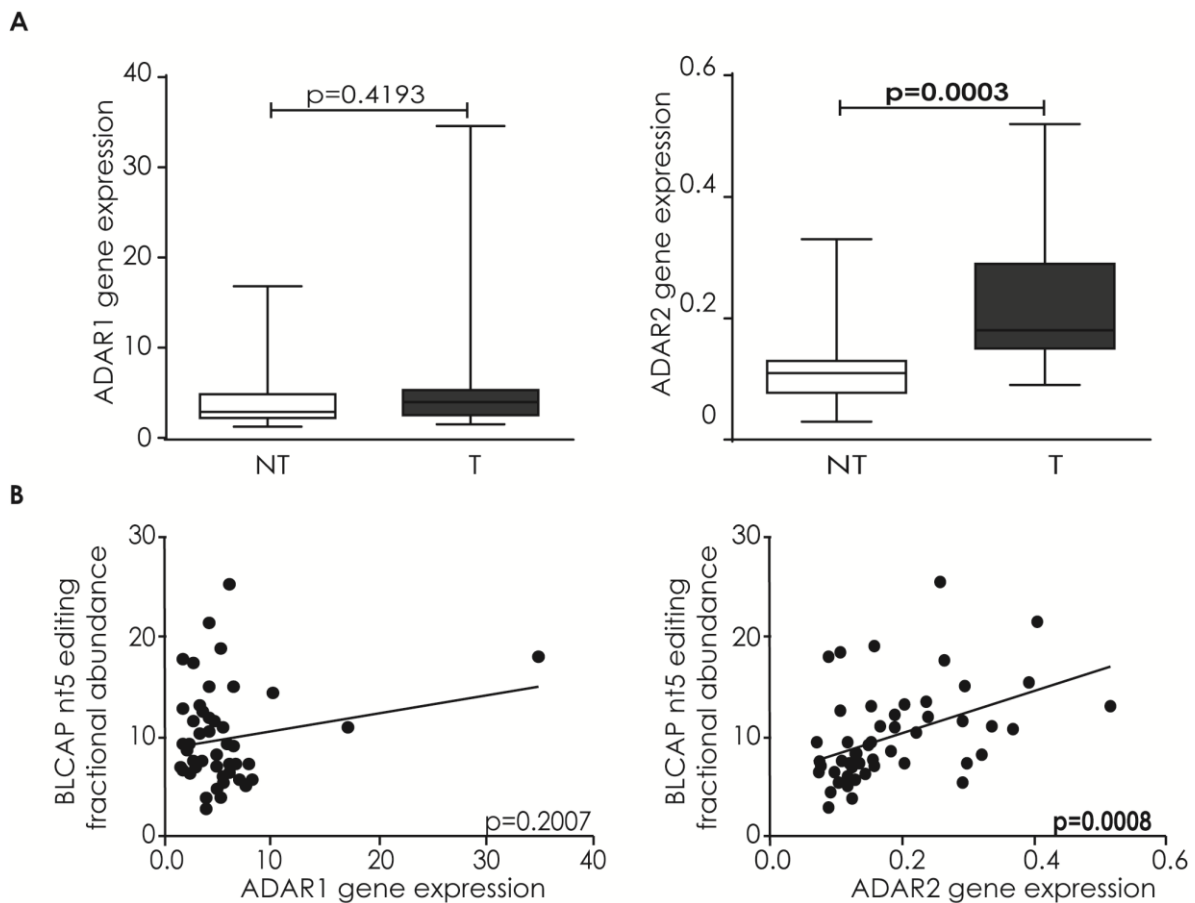


Figure 37. ADAR1 and ADAR2 gene expression assessed by qPCR and correlation with BLCAP and global editing. ADAR1 and ADAR2 gene expression in 27 NT and 27 HB samples (A). Correlation of the ADAR1 and ADAR2 gene expression with BLCAP nt4 editing (B).

4.3.2 Comprehensive genomic study of pediatric liver tumors and recurrences

The genomic study was performed in a cohort of 31 pediatric patients with HB as well as 2 recurrences, 13 PDX and 4 pHCC. To notice that this series is particularly enriched with aggressive tumors according to the CHIC-HS (38% high risk patients). *Table 9* depicted the main clinical and pathological features of the patients included in the study.

Cytoscan HD array was used to characterize chromosomal and allelic imbalances found in HB. Differently from other arrays commonly used in cancer research, Cytoscan HD was designed to interrogate all the genome with high coverage, without an enrichment of probes only in previously described regions related to cancer. This array, contains a total of 6,876,796 probes including 749,157 markers of SNPs, and is able to detect focal aberrations in new regions due to its high sensitivity.

4.3.2.1 Copy Number Variations and allelic imbalances in primary HB and recurrences

The array data obtained showed that the main copy number variations (CNV) in HB were gains of whole chromosomes or chromosomal arms, while chromosomal losses are less frequently observed and focal aberrations are rare events. Allelic imbalances or loss of heterozygosity (LOH) in HB were present across all the chromosomes. From the 31 tumors analyzed, 5 (16%) had 0 gains, 12 tumors had 1-4 gains, 9(29%) between 5-10 and 5 (16%) more than 10. Regarding losses, 5 samples (16%) had 0 gains, 16 (52%) had 1-4, 9 (21%) showed 5-10 and only 1 tumor (3%) showed more than 10 losses. Primary tumors had a mean of 4.5 LOH [0-18] involving a mean of 4 chromosomes [0-13] (*Figure 38*). With this high resolution array, none of the samples analyzed had no CNVs and three tumors (3%) had no LOH. Interestingly, 5 cases (16%) that had no gains, presented non-recurrent 1 (n=3), 2 (n=1) or 7 (n=1) small losses (<2.2Mb). Main CNVs in the primary HB tumors were: gains of chromosome 20 (54%), 1q (51%), 2 (48%), 8 (38%), 12 (35%), 17 (35%), and losses of 1p (22%) and 4q (22%) as shown in *Figure 39*. In contrast to CNV, LOHs

involving whole chromosomes or chromosomal arms were less frequent than punctual LOH (Figure 40). LOH were distributed in different chromosomal positions and a significant enrichment was found in 11p15, present in 15/31 (48%) of the primary tumors, none of these patients were affected by Beckwith-Wiedemann Syndrome.

The 2 recurrent samples analyzed maintained the same CNV and LOH profile from their primary tumors and interestingly, had gains of the chromosome 20 as well as LOH of chromosome 3 and 8q.

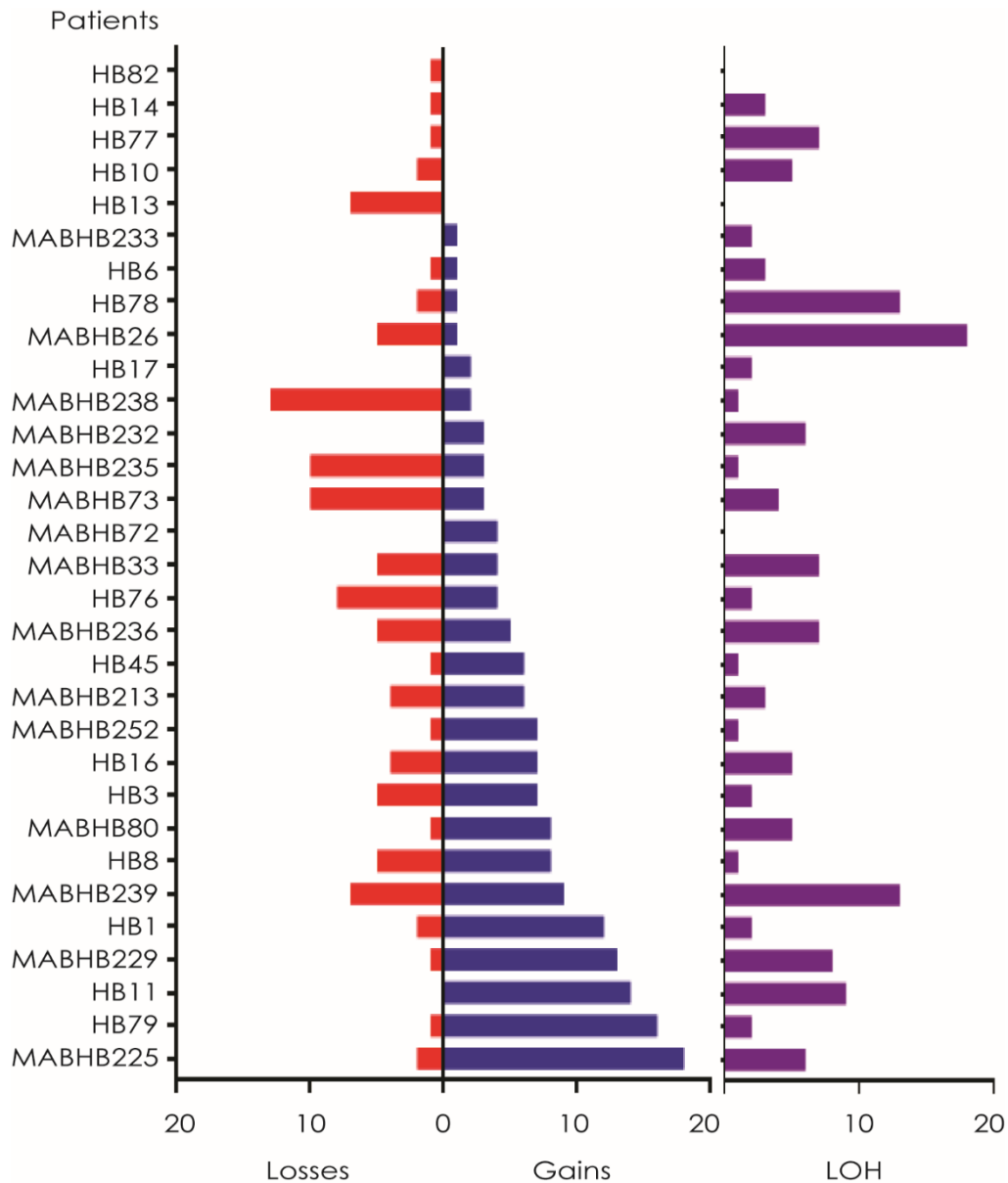


Figure 38. Number of chromosomal and allelic imbalances in primary HB tumors.

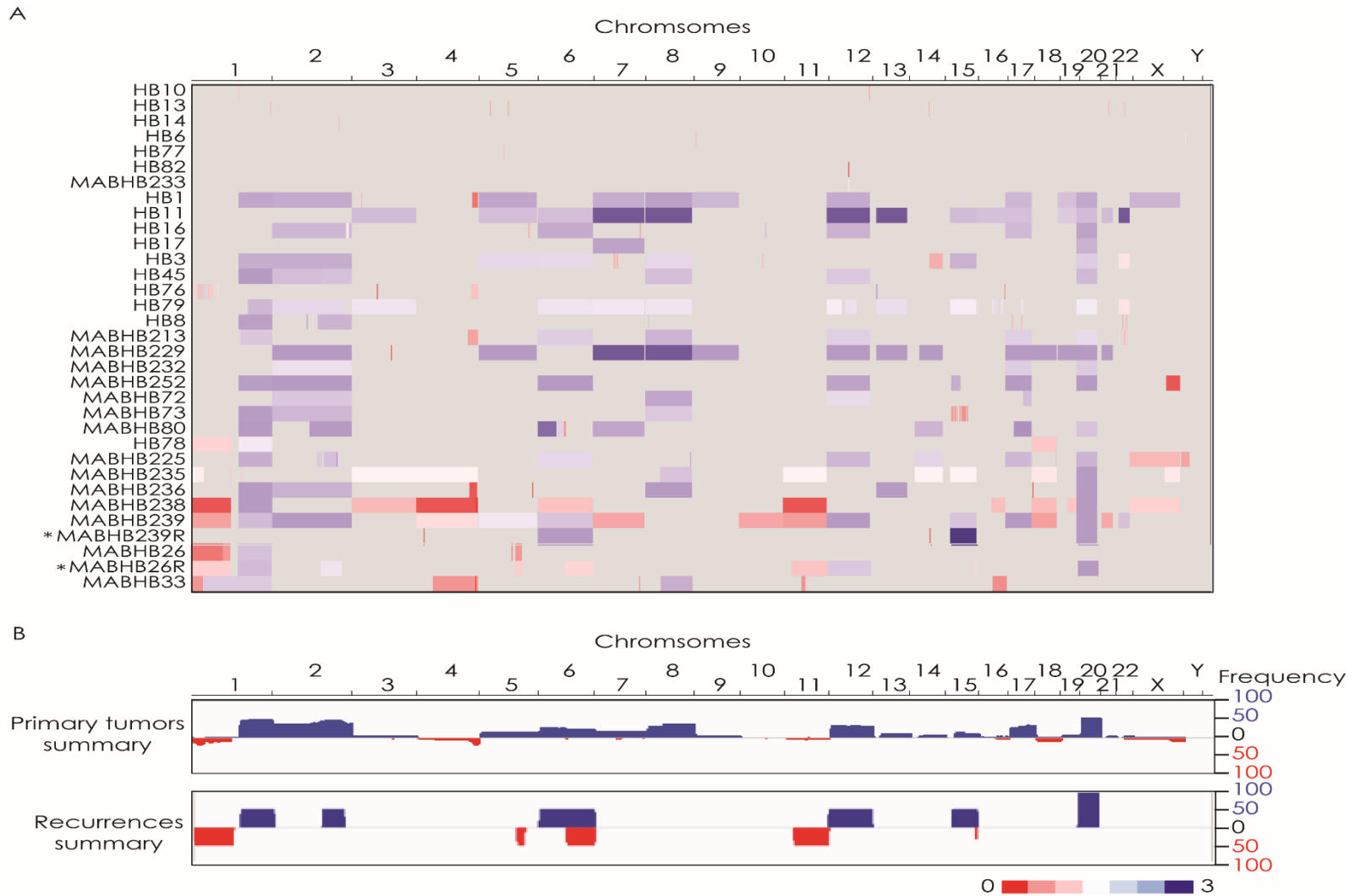


Figure 39. Copy number variations analysis in HB. Copy number variations (CNVs) in primary tumors. (*) Recurrent samples below their primary tumors (A). Frequencies of the CNVs in both primary and recurrent tumors (B). Blue, gains; red, losses; light colors represent low percentage of cells with the CNV.

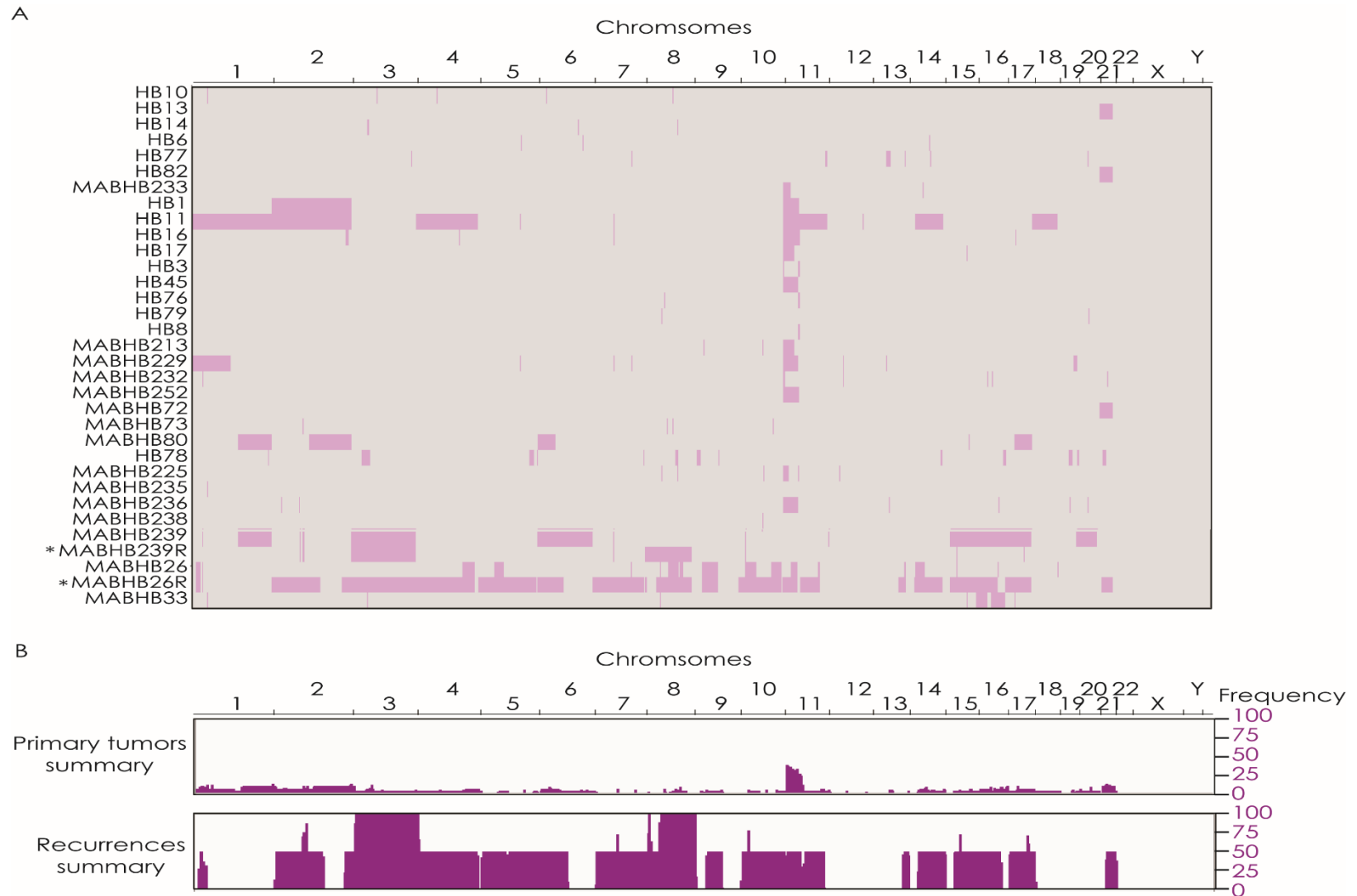


Figure 40. Allelic imbalances in HB. Regions with loss of heterozygosity (LOH) in primary tumors. * indicate recurrent samples below their primary tumors (A). Frequencies of the LOHs in both primary and recurrent tumors (B).

In order to find new oncogenes and TSGs in HB, we identified regions with CN>3 and homozygous deleted regions and studied the correlation with the mRNA level of the genes localized in these regions by using gene expression array data (data not included in the present thesis). The study of regions with CN>3, showed chromosomal gains in 4 primary tumors involving chromosomes 2, 6, 7, 8, 12, 13, 17 and 22 (Table 27). The only recurrent gains were observed on chromosomes 7 and 8. Interestingly, sample MABHB225T had a gain (CN=3.2) in chromosome 2q32.3-33.1, a 2.7kb region containing 19 genes, including the oncogene SF3B1 (Vogelstein *et al.*, 2013), however no significant increase on its mRNA level was observed (data not shown). Because the high number of genes localized in the other gained regions, we could not identify additional putative oncogenes.

Table 27. Gains with CN>3 found in primary HB tumors.

Chr	Start	End	CN state	kb	Number of HB
2q33.1	196665899	199403156	3.2	2737	1 (3%)
6p25.3-p11.2	156974	57584187	3.6	57427	1 (3%)
7p22.3-q36.3*	43360	159119707	4.0	159076	2 (6%)
8p23.3-24.3*	158048	146295771	4.0	146138	2 (6%)
12p13.33-q24.33*	173786	133777902	4.0	133604	1 (3%)
13q12.11-q34	19436286	115107733	4.0	95671	1 (3%)
17q11.1-q25.3	25270397	81041938	3.1	55771	1 (3%)
22q11.1-13.33	16888899	51197838	4.0	34309	1 (3%)

Abbreviations: Chr, chromosome; Kb, kilobases. *indicates whole-chromosome gain.

In order to find new putative tumor suppressor genes in HB we focused on homozygous deletions, and, even though they are rare events, some of them were found in 4 different samples, involving chromosomes 1, 4 and 11 (Table 28). Each deletion was seen in one single patient. Curiously, all the deleted regions with CN=0 were located in the middle of bigger deleted regions with CN=1.

One sample (MABHB26) had a homozygous deletion (CN=0.8, 20% of samples present homozygous deletion) of a 1,796 kb region in 1p21.3-21.2 containing 7 annotated genes and also including the mir137, and SNX7, which was downregulated in this sample compared to the remaining samples without the homozygous deletion (FC= -3.5). Samples MABHB33 and MABHB236 showed a homozygous deletion (CN=0) in 4q34.3 of 600kb and 2192kb respectively which contained 2 single genes, mir1305 and LINC00290; however, their expression was not significantly lower in these tumors as compared to samples without these aberrations. Lastly, we found 2 homozygous deletions in the sample MABHB238, one located in 4q35.1 of 446 kb involving 3 genes and the other at 11q25 of 113kb including one gene. The deletion localized in 4q35.1 included IRF2 gene whose expression was much lower than in NT samples and the other analyzed tumors without the homozygous copy loss according to gene expression data (FC=-9.2 and FC=-7.3 respectively).

Table 28. Homozygous deletions found in primary HB tumors. Genes reported as tumor suppressor genes or related to cancer are highlighted in bold.

Sample	Chr.	Start	End	kb	N (%)	Genes
MABHB26	1p21.3-21.2	97973580	99769188	1.795	1 (3)	DPYD, MIR137HG, MIR2682, MIR137 , LOC729987, SNX7 , LPPR5, LOC100129620, LPPR4
MABHB236	4q34.3	180180552	182372213	2192	1 (3)	LINC00290
MABHB33	4q34.3	182517467	183117920	600	1 (3)	MIR1305
MABHB238	4q35.1	185038230	185484044	446	1 (3)	ENPP6, LOC728175, IRF2
MABHB238	11q25	131382079	131495471	113	1 (3)	NTM

4.3.2.1.3 Small overlapping regions of imbalance (SORI) analysis

CNV data for each region in all samples was then compared and the SORIs defined as the minimum overlapping region involved in at least 2 samples.

A total of 186 different SORIs were identified, including 56 gains, 57 losses and 72 LOH. Number of SORIs identified at each chromosome are represented in *Figure 41*.

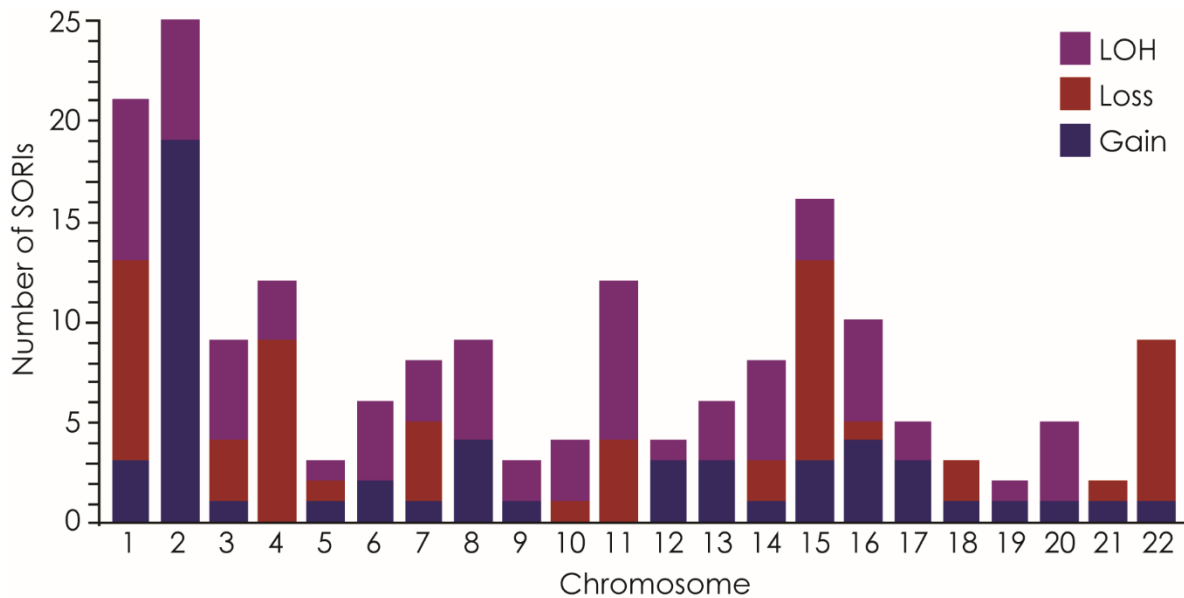


Figure 41. Number of SORIs identified per chromosome.

The different SORIs were then associated with clinical, pathological and molecular features. Interestingly, loss of the whole chromosome 4 was significantly associated with age > 3 years ($p=0.022$) and gain of chromosome 2q22.2-q23.1 was significantly associated with low levels of ALU sites editing ($p=0.012$).

The analysis of the association between the different SORIs revealed that among the top associated SORIs, loss of chromosome 11 was associated with loss of chromosomes 1 (adjusted $p=2.48 \times 10^{-6}$) and 4 (adjusted $p=8.03 \times 10^{-6}$). In addition, LOH of chromosome 10 was associated with LOH of chromosome 15 (adjusted $p=4.98 \times 10^{-6}$) and gain of chromosome 12 with gain of chromosome 17 (adjusted $p=4.03 \times 10^{-5}$).

4.3.2.4 CNV and LOH in Patient-Derived Xenografts and their primary tumors

The Cytoscan HD array data in PDXs was used to identify possible regions associated to tumor aggressiveness. First, we assessed the status of the 530,026 SNPs present in the array. The analysis revealed that $97.7 \pm 2.4\%$ of the SNPs were maintained between the primary tumor and their PDX.

Then, we compared the CNVs profile of primary tumors and their PDXs. The results showed that chromosomal alterations are, overall, well preserved in the corresponding PDXs and importantly, 78% of the CNVs in the primary tumors are maintained in the PDXs. The results of this study were published in (Nicolle *et al.*, 2016).

Main CNVs in the analyzed PDX were +20 (100%), +1q (90%), +2q (72%), +17q (72%), +8 (54%), +5q (45%), +12 (45%), -4q (45%), +13 (36%), -1p (36%), +19 (27%), +22 (27%), -11 (27%) and -21 (27%). It is interesting to highlight that all PDX and 91% (10/11) of the primary tumors analyzed had gain of chromosome 20 (Figure 42).

Regarding LOH, 63% of PDX had LOH in 11p15 and 45% in 8q11.22 (Figure 43).

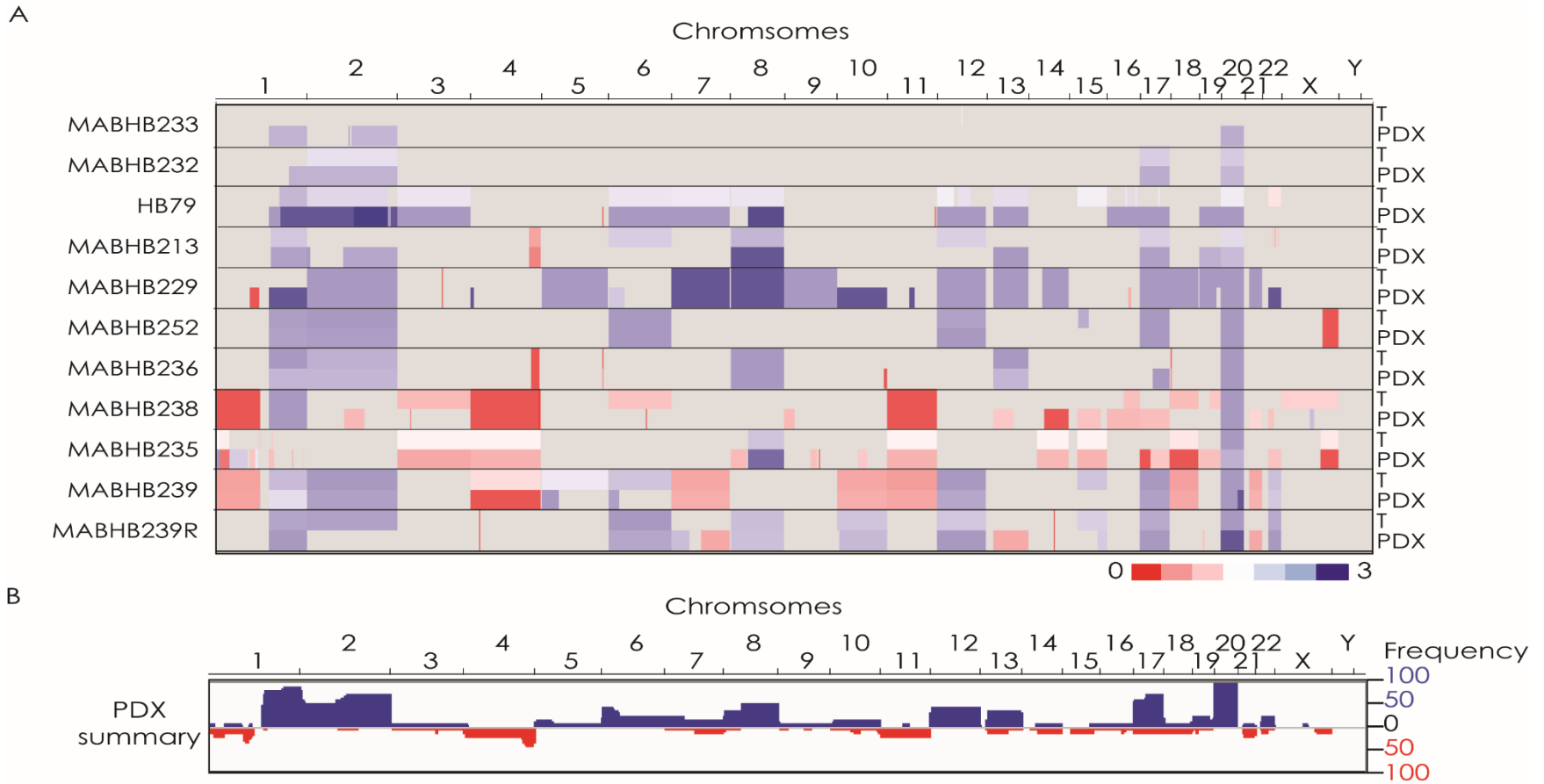


Figure 42. Copy number variations in primary HB tumors and their PDXs. Copy number variations (CNVs) in primary tumors (T) and their PDX (A). Frequencies of the CNVs in PDX (B). Blue, gains; red, losses; light colors represent low percentage of cells with the CNV.

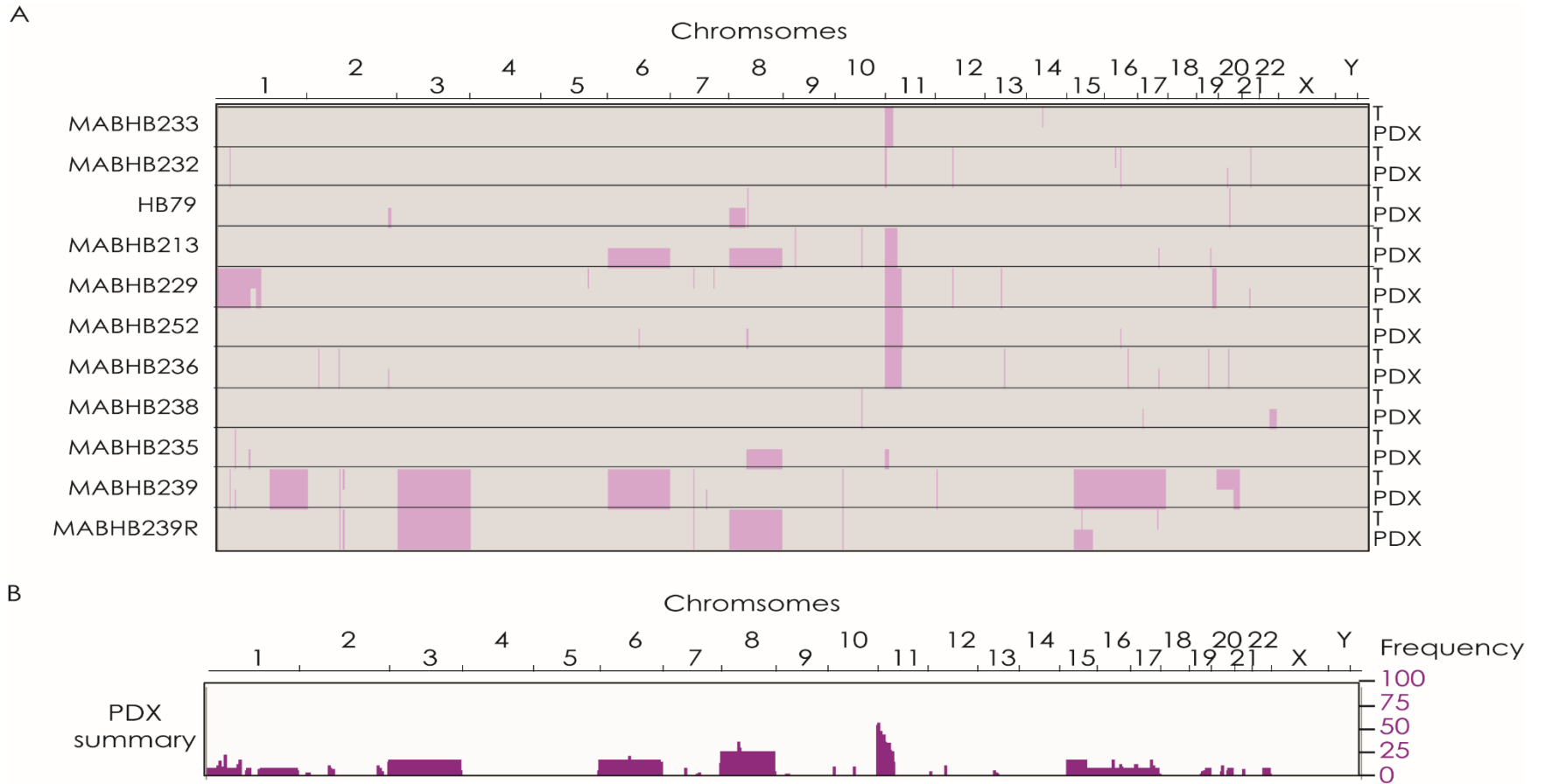


Figure 43. LOH in primary HB tumors and their PDXs. LOH in primary tumors (T) and their PDX (A). Frequencies of the LOH in PDX (B).

4.3.2.5 CNV and LOH in pHCC

The genomic study was completed with the study of a small cohort of pHCC. The main imbalances in our series of pHCC are losses of whole chromosomes or chromosomal arms, and chromosomal gains are less abundant despite affecting a high percentage of tumors. pHCC primary tumors have a mean of 5 gains [0-8], 13 losses [1-22] and 3 LOH [0-7] affecting 5 [0-8], 11 [1-17] and 3 [0-7] chromosomes respectively.

One of the 5 cases analyzed did not have any big CNV and another tumor did not show any LOH. Main CNVs in the primary pHCC tumors were: losses of chromosome 1p (80%), 14 (80%), 3 (60%), 9 (60%), 11 (60%), 16 (40%), 18 (60%), 21 (60%), 6 (40%), 13 (40%), 15 (40%) and gains of 8p (80%) and 1q (60%) (*Figure 44*). Regarding LOH, there was not an enrichment in any chromosome in pHCC.

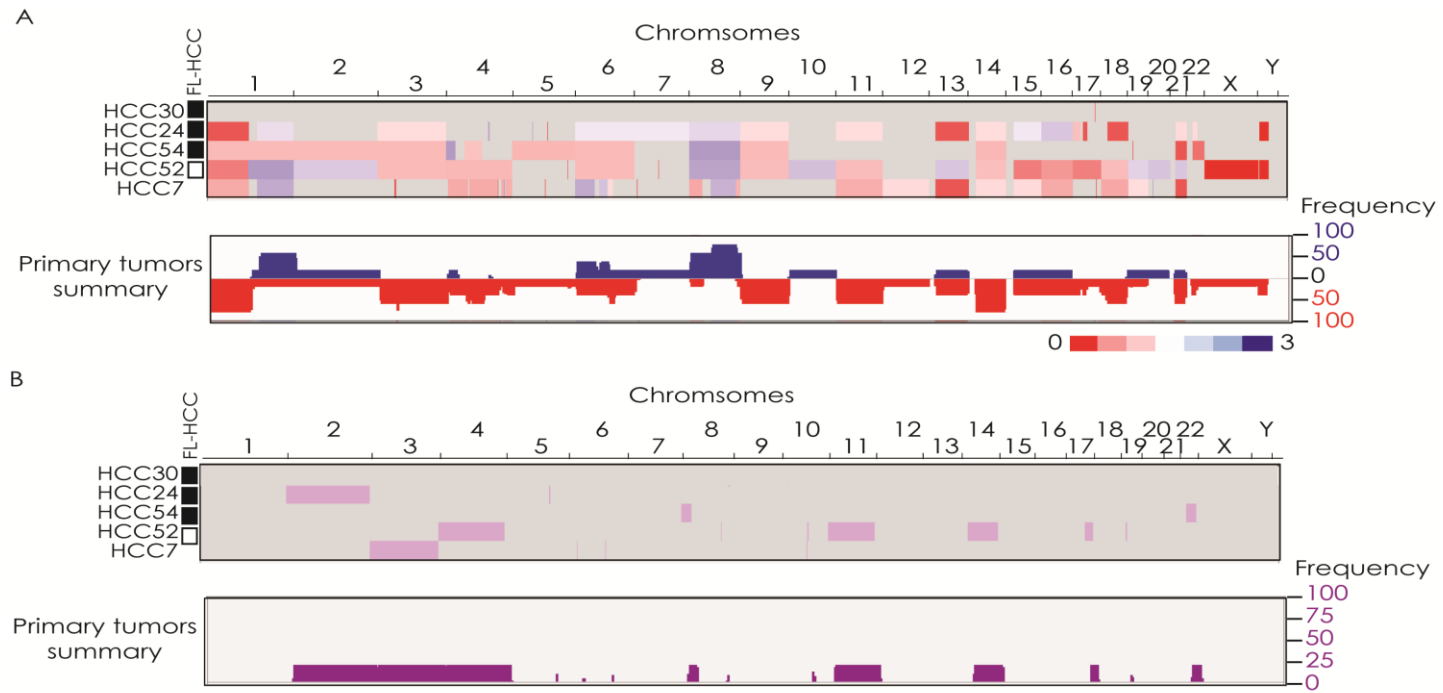


Figure 44. Copy number variations and allelic imbalances in pHCC. The upper panel represents copy number variations (CNVs) in primary tumors and the summary of frequencies. Lower panel shows the LOH and their frequencies. Blue, gains; red, losses; light colors represent low percentage of cells with the CNV; purple, LOH. Black squares indicate FL-HCC variant.

4.3.2.6 Correlation of main genomic imbalances and their impact on patient prognosis

The comparison of the chromosomal and allelic imbalances identified in HB and pHCC showed that pHCC are clearly enriched in chromosomal losses as compared the HB, which are mainly characterized by chromosomal gains and LOH in 11p15 (*Table 29*).

We performed a univariate analysis in order to find correlations between the most common CNVs and LOH in HB, PDX and pHCC and HB patients' outcome. As expected, chromosome 20 was significant. Interestingly, loss of chromosomes 4q, 11 and 18 were predictors of poor outcome for HB patients.

Table 29. Comparison of the main genomic imbalances identified in HB, PDX and pHCC and univariate analysis. *1pHCC sample had LOH of the whole chromosome 11. The univariate analysis was performed with HB patients' survival data.

CNV	HB (%)	HB-PDX (%)	pHCC (%)	Univariate analysis Log-rank p-value
+20	54	100	20	0.046
+1q	51	90	60	0.101
+2	48	72	20	0.254
+8	38	54	80 (+8q)	0.361
+12	35	45	0	0.293
+17	35	72	0	0.123
-1p	22	9	80	0.126
-4q	22	45	60	0.028
LOH 11p15	48	54	25*	0.238
-14	0	18	80	-
-3	3	9	60	-
-9	0	9	60	-
-11	9	27	60	<0.0001
-16	0	18	60	-
-18	12	18	60	0.001
-21	3	27	60	-
-6	3	0	40	-
-13	0	18	40	-
-15	0	18	40	-
LOH 3	3	18	25	-
LOH 8q	0	27	0	-

4.3.2.6 Prognostic genomic classification in HB

After the observation that PDX and pHCC, which have more aggressive behavior, showed an increased number of losses as compared to HB and giving that some of those losses are associate with poor outcome in HB patients, we aimed to classify HB tumors according to their CNV profile and to study the impact of this profile in tumor prognosis.

Thus, we defined 3 classes of HB based on their CNV profile: tumors with few and small aberrations were defined as "Stable" which showed a specific CNV profile characterized by small ($\leq 2153\text{kb}$) and scattered losses. Tumors with gains involving at least $\frac{1}{2}$ chromosomal arm but no big losses as "Gains-enriched" and tumors with big chromosomal losses involving at least $\frac{1}{2}$ chromosomal arm as "Losses-enriched" (Figure 45A).

In our cohort, 7 patients (22%) were classified as "stable" and showed only punctual alterations (number: 1-7) and interestingly, mainly losses (only 2/7 patients had gains). Any of these losses were present in more than 1 tumor. Ten patients (32%) were classified as "gain-enriched" and the main CNV showed were +20 and 2q (80%), +12, +17q, +2p (60%), +8, +7 (50%) and +1q (40%). Finally, 14 patients (45%) were classified as "loss-enriched" and were mainly characterized by -4q (50%), -1p (42%) and -18 (28%). Interestingly, the "loss-enriched" subclass showed also high incidence of gains. Although 71% of the losses-enriched tumors showed -1p, -4q and/or -18, four tumors (29%) had different losses involving at least $\frac{1}{2}$ chromosomal arm, these are: -X/Xq (2 samples), -14q (1 sample) and -15p (1 sample) (Figure 45B&D).

This genomic classification is strongly correlated with patient event free survival and patients with a stable phenotype had 100% probabilities of EFS compared to the gains-enriched with 70% and losses-enriched with 39% probabilities of EFS (log rank p-value=0.010) (Figure 45C).

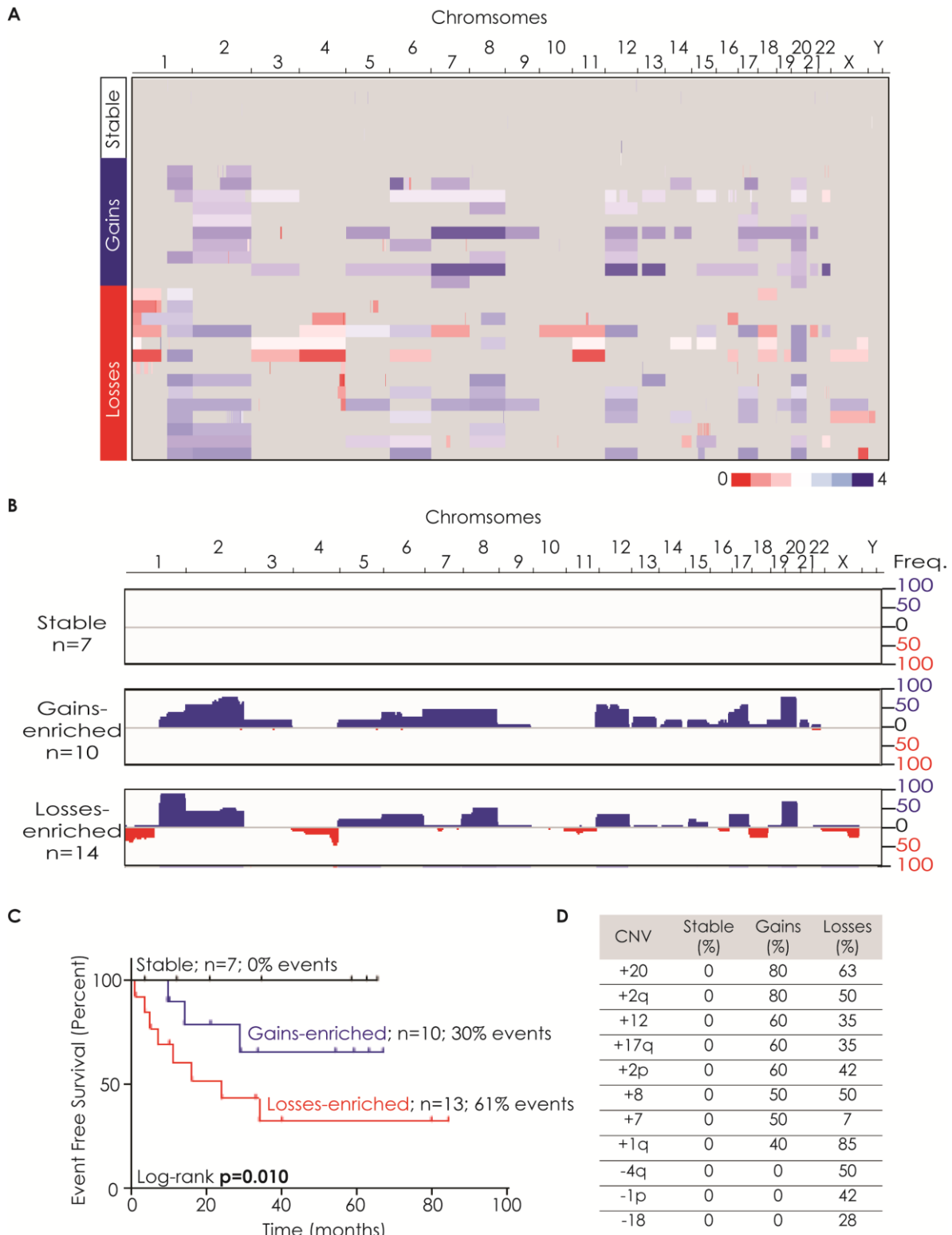


Figure 45. Genomic classification of HB. HB tumors were classified according to their CNV profile in stable, gains-enriched or losses-enriched (A). Summary of the CNVs in the 3 groups (B). Kaplan-Meier curve of the patients classified according to the genomic classification (C). Main CNV frequencies in the different groups (D).

Interestingly, the bivariate analysis showed a significant association of the genomic classification with the presence of CTNNB1 gene mutations in addition to event free survival (Table 30).

Table 30. Association of clinical, pathological and molecular data to the genomic classification of HB.

Variable		Stable N (%)	Classic N (%)	Unstable N (%)	p-value
Event Free Survival	Alive	6 (21)	7 (25)	4 (14)	0.017
	R or DOD	0 (0)	3 (11)	8 (29)	
Overall Survival	Alive	6 (21)	8 (29)	9 (32)	0.684
	DOD	0 (0)	2 (7)	3 (11)	
VPEFR ¹	No	5 (17)	8 (28)	3 (10)	0.088
	Yes	2 (7)	3 (10)	8 (28)	
Age > 3 years	No	4 (14)	9 (31)	8 (28)	0.511
	Yes	3 (10)	2 (7)	3 (10)	
Age > 8 years	No	7 (23)	10 (33)	10 (33)	0.772
	Yes	0 (0)	1 (3)	2 (7)	
AFP 100-1000ng/mL	No	5 (17)	11 (38)	11 (38)	<u>0.051</u>
	Yes	2 (7)	0 (0)	0 (0)	
AFP>10 ⁶ ng/mL	No	6 (21)	9 (31)	8 (28)	0.638
	Yes	1 (4)	2 (7)	4 (14)	
Metastasis at diagnosis	No	6 (21)	8 (29)	6 (21)	0.593
	Yes	1 (4)	3 (11)	4 (14)	
Vascular Invasion	No	5 (18)	7 (25)	4 (14)	0.302
	Yes	2 (7)	3 (11)	7 (25)	
Multifocality	No	6 (21)	9 (32)	5 (18)	0.278
	Yes	1 (4)	2 (7)	5 (18)	
16-gene signature	C1	5 (17)	5 (17)	5 (17)	0.524
	C2	2 (7)	6 (20)	7 (23)	
3 protein signature	0	2 (10)	5 (26)	3 (16)	0.840
	1, 2 or 3	2 (10)	3 (16)	4 (21)	
CTNNB1 mutations	No	5 (17)	2 (7)	2 (7)	0.033
	Yes	2 (7)	9 (30)	10 (33)	
NFE2L2 mutations	No	7 (23)	10 (33)	10 (33)	0.772
	Yes	0 (0)	1 (3)	2 (7)	
EPHB4 mutations	No	7 (23)	19 (63)	11 (37)	0.999
	Yes	0 (0)	1 (3)	1 (3)	

¹, VPEFR, presence of at least one of the following characteristics: involvement of vena cava, involvement of portal veins, extrahepatic disease, multifocal tumor, tumor rupture (Meyers *et al.*, 2017)

In order to validate the impact of the reported genomic classification on patient prognosis, we assessed it in already published genomic data obtained from 21 and 24 HB patients cohorts (Cairo *et al.*, 2008; Sumazin *et al.*, 2017). As we did for our series of patients, tumors were classified as follows: Stable, tumors without any CNV bigger than $\frac{1}{2}$ chromosomal arm; "Gains-enriched", at least one gain affecting $\frac{1}{2}$ chromosomal arm and no losses bigger than this; Losses-enriched, at least one loss involving $\frac{1}{2}$ chromosomal arm.

The results confirmed that the genomic classification previously defined is significantly correlated with patient overall survival, as stable or classic tumors had 100% of survival as compared to unstable tumors, which had 46-64% of survival (Figure 46). The unstable phenotype is also associated to multifocality (Fisher test $p=0.0237$) and metastasis at diagnosis (Fisher test $p=0.0124$) in the Cairo *et al.* cohort.

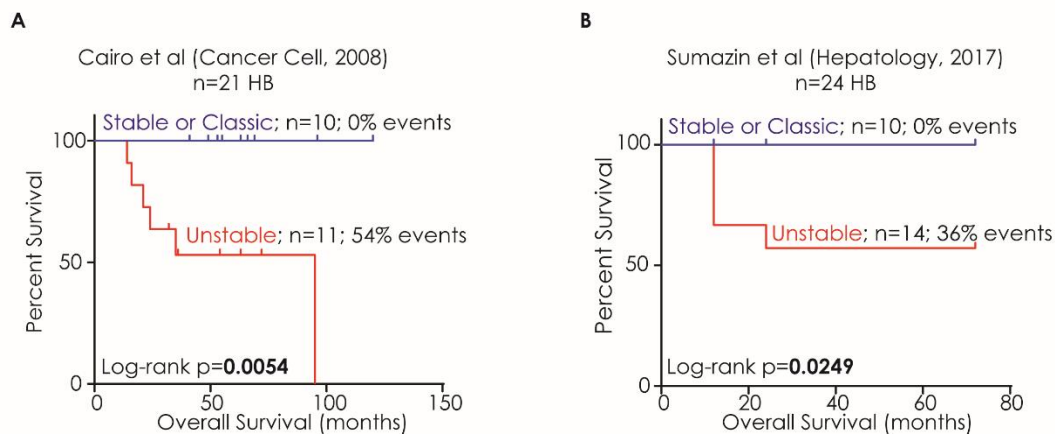


Figure 46. Genomic classification validation. The genomic classification was validated using 2 independent cohorts already published in Cairo *et al.*, 2008 (A) and Sumazin *et al.*, 2017 (B).

4.3.3 Molecular classification of HB

Interestingly, the “losses-enriched” subclass of tumors according to the genomic classification is characterized by having more features of aggressiveness, worse event free survival, higher rates of CTNNB1 mutations, higher expression of C1QBP and CKAP4, lower levels of editing and decreased nt5 BLCAP editing and ADAR2 gene expression, as well as higher expression of stem cell markers and YAP target genes (Figure 47).

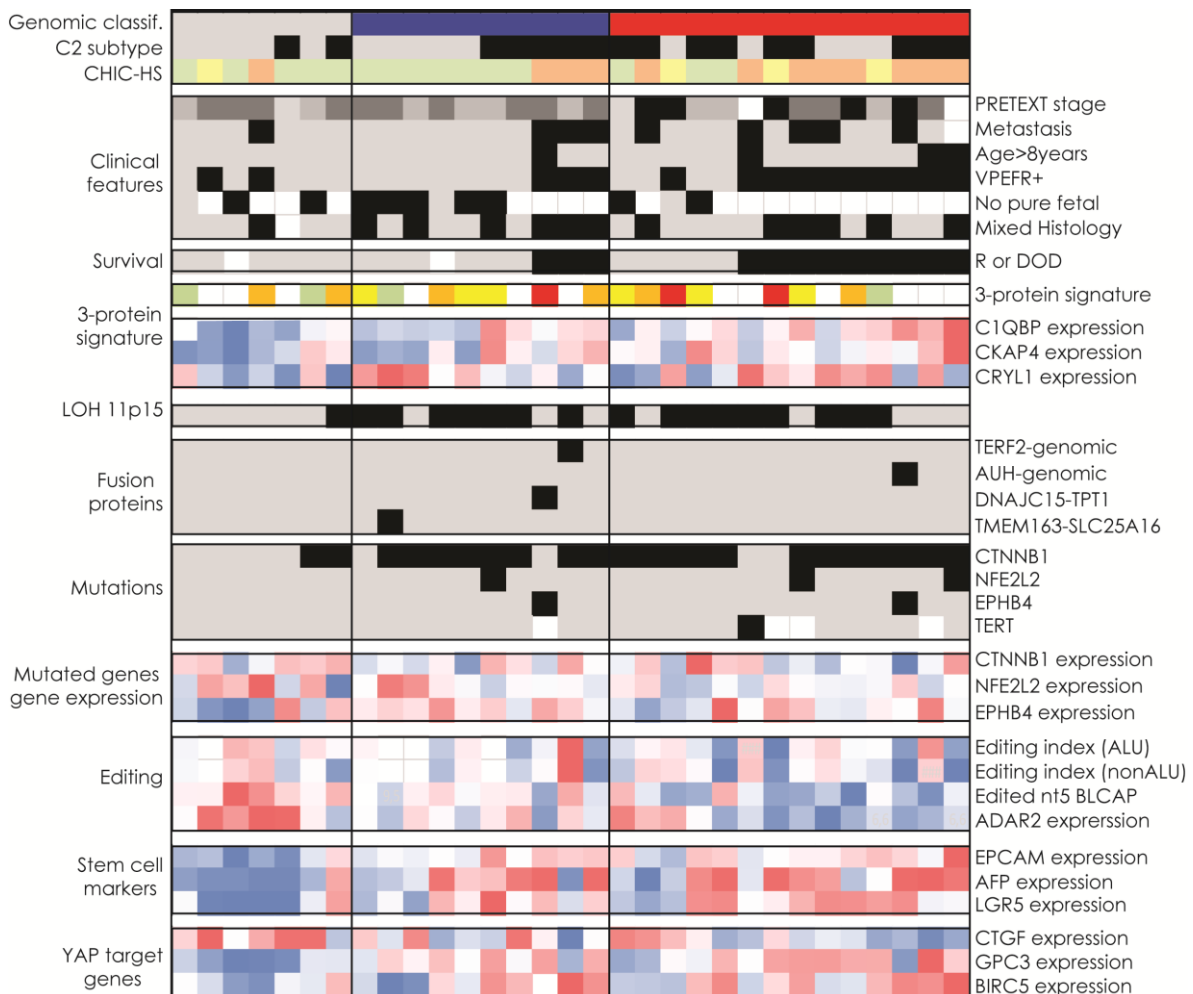


Figure 47. Molecular classification of HB. Genomic classification; grey, stable; blue, gains-enriched; red, losses-enriched; CHIC-HS: green, low risk; yellow, intermediate risk and orange, high risk. PRETEXT stage, from lighter to darker grey, PRETEXT I/II/III/IV. 3-protein signature: green, 0; yellow, 1; orange, 2 and red, 3. Black squares, yes; grey squares; no; white squares; NA. Editing index (ALU and non-ALU), RNAseq data; edited nt5 BLCAP levels, ddPCR data; ADAR2 gene expression, qPCR data. 3-protein, stem cell markers and YAP targets gene expression, array data.

5. DISCUSSION

The present thesis has contributed to the creation of the first collection of biological samples from pediatric liver tumors in Spain. Moreover, we have defined a 3-protein signature highly relevant for patient stratification and a genomic classification that increase the molecular knowledge of these tumors. The specific results of each study are discussed below.

5.1 Sample collection and creation of a biobank

Basic research of childhood liver tumors have been impaired by its rarity and the collection of tumor specimens both at diagnosis and surgery remains crucial to move forward better therapeutic strategies. Thus, the creation of the first collection of biological samples from pediatric patients with liver tumors in Spain as well as the associated clinical data is key for the study of these rare cancers and has been the basis of the studies of the present thesis. Thanks to the collaboration with multidisciplinary teams from 14 different hospitals in Spain, the proportion of pediatric patients with a liver tumor from which samples have been collected has been growing since 2009 (36%) to 2015 (100%), regardless of a considerable decrease in 2011 (23%). Nowadays, we are collecting about 80% of the cases diagnosed in Spain. Also, the establishment of solid collaborations with researchers of all over the world has allowed us to create one of the most complete series of this kind of childhood tumors.

5.2 Proteomic study

In childhood liver cancer, patient stratification is achieved by a multidisciplinary approach involving oncologists, surgeons and pathologists. This is mandatory in order to assign each patient the best treatment option. Despite the advances on pathological studies and clinical classification of this tumors, it is expected that biology will provide prognostic factors that will help defining therapy reduction in order to avoid toxicity in certain patients (López-Terrada *et al.*, 2013). With the aim to identify new prognostic biomarkers easy to apply to the clinical practice, we performed a proteomic study of HB, which, to our knowledge, is the

first ever reported in these tumors. As previously described, HB can be classified in 2 subtypes, named C1 and C2, based on a 16-gene signature. The C2 tumors represent the most aggressive form of HB, which resemble hepatic precursors of early liver development stages, show high proliferation rate, high chromosomal instability and are related to poor outcome (Cairo *et al.*, 2008). Remarkably, our proteomic data confirmed the presence of these 2 HB subtypes, reinforcing the idea that the C1 and C2 tumors are characterized by strongly different gene expression and protein profiles. This result was observed independently of the proteomic technique used. As previously reported, it is interesting to notice in C1 tumors the presence of two β -catenin target proteins (CYP2E1 and GLUL) associated to the beta-catenin program of hepatic zonation (Benhamouche *et al.*, 2006; Braeuning *et al.*, 2006; Cairo *et al.*, 2008) as well as genes related to hepatic function such as ALB and ALDH2, belonging the later to the 16-gene signature, (Cairo *et al.*, 2008). In agreement also with previous data, we found protein overexpression of MYC targets such as NPM1 and NCL in the aggressive C2 tumors. Thus, proteomic data confirmed previous findings concerning the involvement of Wnt/ β -catenin and MYC pathways in HB.

The global proteomic analysis revealed a significant deregulation of the PI3K/Akt and Hippo pathways in HB that was further confirmed by the study of the phosphorylation status of key effectors from both pathways. The over-activation of the PI3K pathway in HB tumors was evidenced by higher phosphorylation levels at Ser473 of the Serine/Threonine-kinase Akt in tumors as compared with non-tumor samples. When PI3K is stimulated by a growth factor, it catalyzes the conversion of phosphatidylinositol-4,5-triphosphate (PIP2) to phosphatidylinositol-3,4,5-triphosphate (PIP3) which acts as a second messenger to recruit AKT to the plasma membrane where it is activated by 3-phosphoinositol-dependent kinases. Once AKT is activated, it phosphorylates several growth-controlling effectors regulating synthesis, stability or subcellular localization of the cell cycle regulators Cyclin D1, p21^{CIP1}, and p27^{KIP1} (Hartmann *et al.*, 2009; Liu *et al.*, 2009). The PI3K/Akt pathway over activation has been already reported in HB (Hartmann *et al.*, 2009). Moreover, *in vitro* experiments have proved that blocking this pathway could be a good

therapeutic target for HB treatment (Venkatramani *et al.*, 2012) since its inhibition with specific inhibitors such as LY294002 (Hartmann *et al.*, 2009; Xia, Zhang and Ding, 2014) and wortmannin (Grotegut *et al.*, 2010) or the anti-proliferative compound emodin (Cui *et al.*, 2016) led to increased apoptosis and decreased proliferation of HB cells such as HepG2, Huh6 and HepT1. Although the mechanism of overactivation of the PI3K signaling pathway in HB remains unclear, it could be a consequence of the IGF2 growth factor overexpression, which signals through the PI3K pathway (Tomizawa and Saisho, 2006) rather than mutations in the PIK3CA gene, which are present in a small subset (2%) of HB tumors (Hartmann *et al.*, 2009). Evidences of PI3K-signalling deregulation have been found in other childhood tumors such as medulloblastoma (Hartmann *et al.*, 2006), neuroblastoma (Opel *et al.*, 2007; King, Yeomanson and Bryant, 2015), wilms tumor (Polosukhina *et al.*, 2017) and rhabdomyosarcoma (Petricoin *et al.*, 2007) as well as in adult cancers such as glioblastoma, endometrial, HCC, melanoma, lung, renal-cell carcinoma, ovarian and breast cancer (Vivanco and Sawyers, 2002). Several mechanisms of PI3K pathway over-activation have been described, mainly PTEN down-expression, activation mutations of the PIK3CA gene or AKT amplification.

Besides the deregulation of PI3K, we also proved the inactivation of the Hippo pathway. The Hippo pathway is a key regulator of hepatocyte differentiation and its inactivation drives to dedifferentiation and the acquisition of progenitor-like features (Yimlamai *et al.*, 2014). When activated, the Hippo pathway leads to phosphorylation of the transcriptional coactivator YAP mediated by the kinases LATS1/2 which leads to cytoplasmic localization and proteolytic degradation of YAP. Contrarily, when YAP is activated, is able to go to the nucleus where interacts with the TEAD family of transcription factors and promotes gene expression of its targets survivin (BIRC5), connective tissue growth factor (CTGF) and cyclin D1 (CCND1) (Li *et al.*, 2012; Yimlamai *et al.*, 2014). The protein profiling of HBs indicated a strong inhibition of the pathway that was further supported by increased YAP levels in tumor samples, as well its phosphorylation status. Altogether, these findings suggest that high levels of free YAP could go to the nucleus to promote transcription of its targets to induce cell proliferation. Evidence of Hippo pathway deregulations have been

found in other cancer such as ovarian, gastric, colorectal, non-small cell lung cancer, and melanoma among others (Zygulska, Krzemieniecki and Pierzchalski, 2017). Increased nuclear expression of its main effector, YAP, have been already proved in HB and in HCC, suggesting that the down regulation of this pathway is crucial for liver cancer progression (Li *et al.*, 2012).

The analysis of the differently expressed proteins in the 2 HB subtypes evidenced for the first time the over-activation eIF2 pathway in aggressive tumors. The activation of the eIF2 pathway is a consequence of the integrated stress response (ISR) which can be triggered by many cellular stresses (i.e. oncogene activation) that converge in the phosphorylation on Ser51 of the α regulatory unit of eIF2 and suppress the initiation of mRNA translation. Additionally to the reduction of the protein synthesis, EIF2 α phosphorylation (p-EIF2 α) also allows the translation of specific genes such as activating transcription factor 4 (ATF4) aiding cell survival and recovery. The final outcome of the ISR depends on the duration and intensity of the stimuli and can also lead to cell death. Thus, it is a crucial step for the cells to adapt under stress conditions and eIF2 α phosphorylation seems to be key during tumor initiation and progression (Zheng, Ye and Cao, 2014). In fact, *in vitro* models have shown that low levels of p-EIF2 α leads to malignant transformation of murine NIH 3T3 cells (Donzé *et al.*, 1995). Our results show that total eIF2 α levels are increased in aggressive C2 tumors, while its phosphorylation at Ser51 is decreased, suggesting that the pathway is activated. Interestingly, low p-EIF2 α levels have also been observed in human osteosarcoma versus normal tissue (Wimbauer *et al.*, 2012), and in non-small cell lung cancer patients, higher p-EIF2 α levels were associated with better outcome (He *et al.*, 2011). Remarkably, elevated levels of eIF2 α compared to matched non-tumor tissue have been showed by IHC in many cancer types including gastrointestinal carcinomas, bronchioloalveolar carcinomas of the lung and malignant melanoma (Zheng, Ye and Cao, 2014).

The study of differential expressed proteins between C1 and C2 tumors led as to the definition of a protein signature useful to stratify patients according to their prognosis. The protein signature identified was validated by 2 independent

techniques and includes a combination of 3 biomarkers: CKAP4, C1QBP and CRYL1. Individually, the alteration of the 3 biomarkers were associated with features of poor prognosis such as high tumor proliferative index and higher patient age at diagnosis.

Cytoskeleton associated protein 4 (CKAP4) is a transmembrane protein that is mainly located in the endoplasmic reticulum and it has a key role maintaining endoplasmatic reticulum structure (Li et al., 2013). However, it has been recently reported that it can be expressed in the cell surface membrane, where it can bind to Dickkopf-1 (DKK1) protein and their interaction can promote cell proliferation by the activation of the PI3K/Akt signaling pathway (Kikuchi, Fumoto and Kimura, 2017). Moreover, β -catenin is a target of DKK1 (Liang Chen et al., 2013), which is an antagonist of the Wnt signaling pathway. The results of our IHC study revealed that over-expression of CKAP4 at protein level occurred in 46% of HBs, 67% NOS and 80% pHCC and was significantly correlated with poor patient outcome. Although CKAP4 overexpression have not been described in HB so far, DKK1 up-regulation have already been reported in HB (Wirths et al., 2003) and HCC both in tissue (Yu et al., 2009; Tao, Liu and Liu, 2013) and in plasma (Shen et al., 2012; Yang et al., 2013; Kim et al., 2015; Fouad et al., 2016). In addition, *in vitro* experiments have demonstrated that DKK1 could promote HCC cell line invasion and metastasis (Liang Chen et al., 2013; Tao, Liu and Liu, 2013; Kim et al., 2015). Overexpression of CKAP4 has been described in other cancers such as pancreatic and lung tumors (Kimura et al., 2016). In liver cancer, CKAP4 protein has been also reported to be overexpressed in more than 50% of intrahepatic cholangiocarcinoma (ICC) as well as in more than 60% of HCCs (Li et al., 2013; Li, Tang, et al., 2014). However and in contrast to our results in HB, higher levels of CKAP4 were associated with better outcomes for both ICC and HCC patients. Additionally, the same authors showed using SMMC-7721, PLC/PRF-5, and MHCC-LM3 HCC cell lines that CKAP4 expression decreased cell proliferation and colony formation (Li, Liu, et al., 2014). The different results obtained could be explained by differences in the oncogenic pathways altered in adult and childhood liver cancer. It has been described that CKAP4 overexpressing tumors have worse outcome when DKK1 is also overexpressed (Kimura et al., 2016), and we hypothesize that the oncogenic effect of CKAP4 in HB could be mediated by the increased

expression of DKK1. It has been previously described that their interaction could lead to PI3K/Akt pathway activation (Kikuchi, Fumoto and Kimura, 2017).

Complement C1q binding protein (C1QBP), also known as hyaluronan binding protein (HABP1), is a multifunctional and multicompartamental protein involved in inflammation, infection processes, ribosome biogenesis, regulation of apoptosis, transcriptional regulation and pre-mRNA splicing. C1QBP is known to bind to C1q molecule and inhibit C1 activation thus inhibiting the first component of the serum complement system, and therefore, C1QBP could play a role in the immune evasion, angiogenesis and metastatic processes crucial for cancer development (Peerschke and Ghebrehiwet, 2014). Among its functions, it can bind coagulation factor XII leading to its autoactivation and the secreted form may enhance both extrinsic and intrinsic coagulation pathways. C1QBP can be also located in the mitochondria where it is a critical regulator of tumor metabolism by controlling the balance between oxidative phosphorylation and glycolysis. Interestingly, it has been reported that C1QBP play a role in mediating MYC-induced glutamine metabolism and that C1QBP is a direct transcriptional target of Myc (Fogal *et al.*, 2010). Our results showed that C1QBP was over expressed in 51% of HB, 33% of NOS and 80% pHCC and its overexpression in tissue but also plasma is associated with advanced tumor features. Similarly, high levels of C1QBP has been reported in several tumors including breast (Y.-B. Chen *et al.*, 2009; Yu and Wang, 2013; Niu *et al.*, 2015; Scully *et al.*, 2015; Wang *et al.*, 2015), ovarian (Yu and Wang, 2013; Yu *et al.*, 2013) endometrial (Zhao *et al.*, 2015), gastric (Gao *et al.*, 2016), prostate (Amamoto *et al.*, 2011), brain (Fogal *et al.*, 2010) and cervical cancers (Zhang *et al.*, 2017) as well as in epidermal carcinoma (Ghosh *et al.*, 2004). Moreover, *in vitro* experiments have already reported that stable C1QBP gene transfection in HepG2 HB cells leads to enhanced cell survival and tumorigenicity as well as higher expression of hyaluronan (HA). Interestingly, HA is accumulated in several human tumors and induces cell survival through the activation of AKT and β -catenin pathways (Kaul *et al.*, 2012). Beside its role as a biomarker, it could have a role as therapeutic target as antibody neutralization of cell-surface C1QBP inhibited

angiogenesis by preventing lamellapodia formation and cell migration in HUVEC cells (Kim *et al.*, 2016).

Crystallin lambda 1 (CRYL1) is an enzyme that catalyzes the dehydrogenation of L-gulonate into dehydro-L-gulonate in the uronate cycle, which is an alternative glucose metabolic pathway that accounts for about 5% of daily glucose catabolism and also is a structural protein in eye lens. In our IHC studies, we could not detect CRYL1 protein staining in 8% of HB, 16% of NOS and 60% of pHCC. Interestingly, the loss of CRYL1 expression was associated with decreased survival. The alteration of CRYL1 has been reported in HCC in which low mRNA levels are found in about 60% of HCC tissues as compared to normal liver (Chen *et al.*, 2003) but not in other cancers, . Among the causes for CRYL1 Inactivation in HCC, it has been reported so far homozygous deletion of the locus 13q12.11, histone deacetylation and promoter hypermethylation (Cheng *et al.*, 2010). Interestingly, it has been recently published that a fusion transcript involving CRYL1-IFT88 is present in 9.5% of HCC (Huang *et al.*, 2017).

In this study we have seen that the combination of these three biomarkers in the 3-protein signature, has a powerful prognostic impact and the main advantage in comparison with the 16-gene signature is that it could be easily applied into the clinical practice by performing an IHC using the non-tumor liver tissue as a reference. It is also notably that the described signature is useful to predict prognosis not only for HB patients, but also for NOS and pHCC developed in healthy liver patients, even though it cannot be used as a diagnostic signature. Although our results suggest that these 3 biomarkers may have a role in HB development and progression, functional studies are needed to uncover whether they are a cause or a consequence of the malignant transformation of HB. Currently, HB patients are stratified using the recently published CHIC-HS method in which patients are classified according to PRETEXT stage, presence of metastasis, age, AFP levels, presence of vascular invasion, extrahepatic disease, multifocal tumor and rupture at diagnosis (Meyers *et al.*, 2017). Thus, patients are classified into 4 groups: very low, low, intermediate and high risk which will receive different treatment. Importantly,

the 3-protein signature has been identified as an independent prognostic factor together with the current clinical classification. Accordingly, we have seen that it is able to improve the clinical classification having a strong impact on patient survival (EFS and OS) especially for intermediate patients. Thus, applied to those patients classified as intermediate by the CHIC-HS, it is useful to distinguish biologically aggressive tumors that could require stronger chemotherapy treatment as well as biologically less-aggressive tumors that could benefit of lower chemotherapeutic doses and consequently, have less side effects related to this treatment.

It is well known that post-chemotherapy HB specimens frequently present regressive and necrotic changes (Wang *et al.*, 2010) which apart of modify the original histology, can induce genetic alterations. For this reason, the study of pre-treatment specimens is crucial. Thus, one of the limitations of our study is the restricted number of non-treated specimens. Even though almost all the patients included in the discovery set (15/16) had received preoperative chemotherapy, the validation set included 43 pre-treatment specimens. The survival analysis classifying the patients with the clinical stratification and the 3-protein signature showed similar trends that the whole validation set together. In summary, the 3-protein signature defined could be also applied at diagnosis. In that regard, a prospective study is necessary to confirm the prognostic prediction of the 3-protein signature in diagnostic specimens of childhood patients with liver cancer.

5.3 Genomic and RNAseq study

The RNAseq and genomic study revealed that HB tumors harbour few somatic mutations mostly affecting the Catenin Beta 1 (CTNNB1) gene as well as no recurrent fusion proteins. Interestingly, these tumors can be classified according to their CNV profile, which is directly correlated with patient outcome. Thus, tumors with high incidence of chromosomal losses are more aggressive and correlate with worse patient outcome than patients with tumors with no gross chromosomal changes or mainly gains.

Fusion proteins have been identified in several pediatric tumors such as BCR-ABL1 in 3% of acute lymphoblastic leukemia (Boer and den Boer, 2017), PAX-FOXO1 fusion in 80% of alveolar rhabdomyosarcoma (Sorensen et al., 2002) or the DNAJB1-PRKACA fusion protein in around 80% of FL-HCC (Honeyman et al., 2014; Cornella et al., 2015; Darcy et al., 2015). However, so far aside from the last, no other recurrent chimeric proteins have been described in pediatric liver tumors. Our results revealed that HB and NOS tumors do not present recurrent fusion proteins. Thus we identified 4 fusion events, each of them in a single and different patient, ruling out their role in HB oncogenesis.

The mutational analysis done with the RNAseq data and the further validation study confirmed that the top mutated gene in HB is CTNNB1, confirming β -catenin mutations as a hallmark in HB (Armengol et al., 2011). The second most frequent mutated gene observed in 6% of the cases (3/52) is Nuclear Factor, Erythroid 2 Like 2 (NFE2L2). All the mutations were located in the second exon of the gene, affecting nucleotides codifying for residues that are recognized by the KEAP1/CUL3 complex for proteasomal degradation. Mutations in this domain of NFE2L2 have been already reported in HB (Eichenmüller et al., 2014). Intriguingly, the 3 cases harboring NFE2L2 mutations occurred in CTNNB1 mutated cases and confirmed previous data in both HB (Eichenmüller et al., 2014) and HCC (Guichard et al., 2012). We also identified 2 different mutations in the EPH receptor B4 (EPHB4) gene in 4% of HBs (2/52%). Alterations of this gene in liver tumors have not been

reported so far. Ephrin receptors, which represent a large family of receptor tyrosine kinases, and their ligands have key roles in several developmental processes. Particularly, the EPHB4 receptor, which binds to ephrin-B2, is crucial in vascular development and it has been reported to regulate vascularization of malignant tumors (Chen, Zhang and Zhang, 2017). Mutations of the EPHB4 gene have been already reported in glioblastoma, which correlates with increased gene expression (Masica and Karchin, 2011). Interestingly, over expression of the EPHB4 gene has been observed in breast cancer (Kumar *et al.*, 2006) and lung cancer (Ferguson *et al.*, 2015). In contrast to the EPHB4 status in breast and lung cancer, it seems to have a tumor suppressor role in colon cancer in an *in vivo* model (Dopeso *et al.*, 2009).

As a part of the characterization of our cohort, we sequenced Telomerase Reverse Transcriptase (TERT) promoter looking for mutations. A single event (146G>A) was identified in a patient with a NOS tumor. The same change have been already described in NOS (Eichenmüller *et al.*, 2014) and also in medulloblastoma (Viana-Pereira *et al.*, 2017). Interestingly, Eichenmüller *et al.* studied recurrent mutations in 15 HB tumors and 3 NOS tumors and found that TERT promoter mutations were exclusively found in the second, suggesting that TERT promoter mutation is a selective phenomenon of advanced HB with HCC-like features and that it could be used as a marker for the detection of high-risk patients.

The most interesting finding obtained from the mutational analysis is the mutation in the Bladder Cancer Associated Protein (BLCAP) RNA in 29% (9/31) of the cases. Despite mutations could not be validated at DNA level, we found them in the BLCAP RNA in both tumor and non-tumor tissue. After that, the quantification of the mutated nucleotide by ddPCR allowed us to confirm the over-representation of the edited transcript (5A>G) of BLCAP in 58% of HBs as compared to non-tumor tissue. Despite the fact that the biological role of BLCAP have not yet been discovered, It is known that BLCAP is ubiquitously expressed and also down-regulated at mRNA level in different tumors such as bladder invasive carcinoma, renal cell carcinoma and in primary cervical carcinoma (Galeano *et al.*, 2010) and for this reason is supposed to be a tumor suppressor gene. Editing in different positions of BLCAP has

already been reported, among them the 5A>G that leads to a change of amino acid (Tyr2Cys) (Levanon *et al.*, 2005; Galeano *et al.*, 2010). Interestingly, Hu *et al.* identified BLCAP over-editing of 5A>G in 40% of HCCs (Hu *et al.*, 2015).

The finding that BLCAP was in fact edited but not mutated, led us to the analysis of editing status in HB, revealing for the first time, a clear deregulation of RNA editing in this tumor. Our results revealed that, globally, HB tumors are under-edited, meaning that most of the edited sites have lower frequencies of the edited allele than the non-tumor tissue and additionally, our results showed that lower editing index leads to poor patient outcome. RNA editing is a posttranscriptional mechanism which introduces changes in the RNA sequences encoded by the genome and despite the evidence of other type of nucleotide changes, the most frequent change of nucleotide in the RNA is the substitution of an adenosine for an inosine (A→I), which is read by the translation machinery as a guanosine (G) (Nishikura, 2010). As we observed in HB, it has been already reported that most editing events occur in noncoding genes, introns and untranslated regions of specific genes, however, as it happens with BLCAP, these events also can be present in coding regions and can lead to a change of amino acid altering the protein-coding sequence of the edited gene (Peng *et al.*, 2012) and therefore contribute to the diversification of protein functions (Nishikura, 2010). Interestingly, Han *et al.*, reviewed the A→I editing profiles of more than 6000 patient samples from 17 cancer types and observed that the different cancer types show diverse editing deregulation, thus, head and neck squamous cell carcinoma, breast invasive carcinoma, thyroid carcinoma, and lung adenocarcinoma tumors presented over-editing patterns while kidney tumors presented under-editing. Curiously, some tumor types, including HCC, presented similar number of up and down-edited sites (Han *et al.*, 2015). In contrast, another study found significantly higher editing in HCC than in adjacent normal tissue (Kang *et al.*, 2015). Deregulation editing of specific genes in adult HCC have been reported, such as antizyme inhibitor 1 (AZIN1) (Leilei Chen *et al.*, 2013), aryl hydrocarbon receptor (AHR) (Nakano *et al.*, 2016), filamin B (FLNB) and coatamer protein complex subunit alpha (COPA) (Chan *et al.*, 2014), as well as in specific miRNA such as pri-miR-214 (Liu *et al.*, 2013). So, regulation of the editing

process is globally deregulated in HB as in other tumors and specific sites of editing (i.e. BLCAP) could play a role in liver tumorigenesis.

The editing mechanism is mainly regulated by specific enzymes called adenosine deaminase acting on RNA (ADAR). The ADAR enzymes convert adenosine to inosines in double-stranded RNA (dsRNA) substrates (Nishikura, 2010; Peng *et al.*, 2012). Until now, 3 ADAR enzymes have been identified, ADAR1 and ADAR2, which are broadly expressed and active and ADAR3 which is present only in the brain and seems to be inactive in *in vitro* assays and may have a regulatory role instead (Chen *et al.*, 2000). Our results showed that ADAR2 is significantly over expressed in HB as compared to non-tumor tissue and significantly correlated with BLCAP nt5 editing, while ADAR1 is not. Thus, in contrast to the observation made by Hu *et al.*, who concluded that ADAR1 was the one mediating RNA editing of BLCAP (Hu *et al.*, 2015), our results suggest that in HB the enzyme responsible could be ADAR2. However, further functional studies should be performed to confirm which enzyme is the responsible of this editing deregulation.

The high resolution array used evidenced that main CNVs in HB are gains of whole chromosomes or chromosomal arms, while losses are less frequently observed and correlate with poor patient outcome. According to our results, 100% of HBs show at least one CNV, either gain or loss, and the most frequent CNVs are +20 (54%), +1q (51%), +2 (48%), +8 (38%), +12 (35%), +17 (35%) -1p (22%) and -4q (22%). Chromosomal imbalances in HB have been extensively studied and despite the rarity of the tumor, the CNV profiles of more than 300 patients have been published and reviewed in the present thesis. Even though the different techniques used, the results of the above mentioned studies concluded that a mean of 81% of the tumors had CNVs (Steenman *et al.*, 1999; Weber *et al.*, 2000; Gray *et al.*, 2000; Hu *et al.*, 2000; Parada *et al.*, 2000; Kumon *et al.*, 2001; Mullarkey *et al.*, 2001; Surace *et al.*, 2002; Sainati *et al.*, 2002; Terracciano *et al.*, 2003; Adesina *et al.*, 2007; Suzuki *et al.*, 2008; Stejskalová *et al.*, 2009; T. T.-L. Chen *et al.*, 2009; Arai *et al.*, 2010; Eichenmüller *et al.*, 2014; Sumazin *et al.*, 2017). In our series, we are able to detect CNV in 100% of the cases; this difference could be explained by the high resolution technique used in this work compared with the techniques used in the previous reports, mainly based

on aCGH or FISH. Gain of chromosome 20 is highly enriched in our series, present in 54% of the tumors as compared to 23% in the previously described series. This enrichment could be explained by the high number of aggressive cases in our series, as chromosome 20 has been already reported as a prognostic factor for HB (Weber *et al.*, 2000; Sainati *et al.*, 2002). Gain of 8q have also been described as a prognostic factor (Weber *et al.*, 2000; Sainati *et al.*, 2002) in contrast to our results, which did not reach significance in the univariate analysis. The role of the gain of 8q in tumor aggressiveness could be connected with the overexpression of the oncogene C-MYC (Buendia, 2002) or the PLAG1 oncogene and transcriptional activator of IGF2 (Zatkova *et al.*, 2004). However, due to the fact that the whole chromosome 20 is gained, it is difficult to know which gene or genes are responsible of the oncogenic features of this chromosomal imbalance. A part of the gain of chromosome 20, the univariate analysis showed that losses of chromosomes 4, 11 and 18 are also significantly associated with worse patient outcome.

Mosaicism in our samples can be explained not only due to intra-tumor heterogeneity, but also as non-tumor cells contaminating the tumor sample as well as by the presence of infiltrating cells. Interestingly, the comparison between primary tumors and their PDX, reveals an increased % of cells carrying the CNV in the PDXs, which could be a consequence of the engraftment pressure, which leads to a positive selection of the most aggressive clones. However, this pressure is evolutionarily neutral, as it does not impact intra-tumor heterogeneity (Byrne *et al.*, 2017).

Even though we detected some gains with a CN>3, those were too big to predict which gene contained in these regions could have a role in the development of HB. On the other hand, we focused on homozygous deleted regions in order to identify tumor suppressor genes important for the development of HB. The analysis allowed us to discover several genes deleted in HB that could be important for its development, namely: mir137, previously described as tumor suppressor gene in HCC (Gao *et al.*, 2015); SNX7, that have been reported to be deleted in cisplatin-resistant ovarian cancer cells (Prasad *et al.*, 2008); LINC00290

deleted in childhood adrenocortical tumors (Letouze *et al.*, 2015); and IRF2, which have tumor suppressor functions in gastric cancer (Li *et al.*, 2016) and in hepatitis B virus-related HCC, being mutated in 5% of the tumors and is a regulator of the p53 pathway (Guichard *et al.*, 2012). Additional studies should be performed in order to uncover its role in HB tumorigenesis.

The genomic study of HB-PDX samples showed that PDX really resemble the CNV profile of their primary tumors and that most of the CNVs are enriched in PDX. Interestingly, there is an increased frequency of chromosomal losses in successfully grown PDX. Moreover, all the analyzed PDX had gains of chromosome 20, suggesting that the gain of this chromosome already reported as a characteristic of aggressive tumors (Weber *et al.*, 2000; Sainati *et al.*, 2002) makes the tumors more able to successfully engraft and grow in a new environment. All these findings actually support the idea that PDX mainly develop from aggressive tumors or tumor components (Nicolle *et al.*, 2016). Thus, PDX could be considered a good model for the study of childhood liver tumors, such as HB.

The genomic study of pHCC confirmed a much more altered chromosomal profile than HB, similar to that reported for adult HCC (Buendia, 2002). Importantly, we have seen that pHCC is characterized for highly frequent losses and less abundant gains in contrast to HB tumors. One of the analyzed cases with a fibrolamellar variant had no big CNVs. The main CNVs in our series were +8q, -1p and -14 present in 80% of patients. Interestingly, gain of 1q, that was present in 60% of the analyzed cases, has been described as an early event in adult HCC (Midorikawa *et al.*, 2009). Regarding LOH, we did not find an enrichment of a specific LOH in contrast to 11p15 in HB or what have been reported for adult HCC, in which LOH in 1p and 17q have been described in 36% and 42% of cases, respectively (Midorikawa *et al.*, 2009).

After the observation that aggressive forms of liver tumors, such as pHCC and also PDX had an enrichment of losses compared to HB, we established a genomic classification of HB based on the type (gain/loss) and length of the CNVs. Thus, we

described 3 different genomic subtypes of HB: the stable, with a specific profile characterized by small aberrations, mainly losses, scattered across the genome. Curiously, 2 cases presented CTNNB1 mutations as a unique event (no big CNV), similar seen by (Eichenmüller et al., 2014). The gains-enriched subclass was characterized by chromosomal gains, mainly affecting whole chromosomes or chromosomal arms. And finally, the loss-enriched class which includes tumors having loss of 1p or 4q or another whole chromosome lost. This classification was successfully validated with two published cohorts in which stable and classic tumors correlated with 100% of patient survival compared to unstable tumors. Despite the fact that previous reports didn't find a correlation with the number of alterations and survival (Weber et al., 2000; Sumazin et al., 2017) our genomic classification is strongly associated with patient survival and interestingly, the stable class is characterized for low incidence of CTNNB1 gene mutations, suggesting a different oncogenic mechanism of these tumors.

6. CONCLUSIONS

Proteomic study

- The proteomic profile of the tumors is different from the non-tumors and is useful to distinguish the two C1 and C2 HB subclasses, previously identified by gene expression profiling.
- Hepatoblastoma tumors have an over-activation of the PI3K/Akt pathway and an inactivation of the Hippo pathway as confirmed by differential phosphorylation of main effectors.
- Aggressive Hepatoblastoma C2 tumors have an over-activation of the EIF2 pathway.
- The defined a 3-protein signature is strongly associated with patient survival based on the altered protein expression of 3 biomarkers in tumor tissues as compared to non-tumor tissue as a reference.
- The 3-protein signature is useful for the prognostic stratification of pediatric liver cancer patients and improves the current clinical stratification. The 3-protein signature could be easily applied at the clinical practice by performing an immunohistochemistry.
- The 3-protein signature is useful to predict the prognosis of not only Hepatoblastoma patients, but also of NOS and pHCC patients. However, a validation study with an extensive cohort of patients is needed.
- Elevated plasma levels of C1QBP could be useful to detect pediatric patients with aggressive liver tumors; however, a validation in a large cohort of prospective patients is required to determine its utility in the clinical practice.

Conclusions

Genomic and RNAseq study

- RNAseq data have confirmed that Hepatoblastoma is a tumor with low mutation rate and has allowed to confirm mutations of CTNNB1 (75%), NFE2L2 (6%) and to identify mutations in a third most frequent gene, EPHB4 (4%).
- Contrarily to other pediatric tumors, RNAseq data showed that Hepatoblastoma do not have recurrent oncogenic fusion transcripts.
- We have identified for the first time a global down-regulation of RNA editing in Hepatoblastoma associated with patient outcome.
- We have also identified a specific over-editing of BLCAP mRNA in 58% of the HBs.
- Alterations in ADAR2 gene expression are associated with BLCAP RNA editing deregulation in Hepatoblastoma.
- The genomic analysis allowed as to identify chromosomal imbalances associated to poor outcome, namely gain of chromosome 20 and losses of chromosomes 4, 11 and 18.
- By comparing the genomic data (CNV and LOH) of primary tumors and their PDX, we confirmed that PDX properly resemble the tumors from which they originate and strongly support their use as a model for this disease.
- We have defined a new genomic classification in which we distinguish tumors with a stable chromosomal phenotype with scattered small chromosomal losses, tumors enriched with chromosomal gains and finally, tumors with an enrichment of large chromosomal losses.
- The tumors classified as "loss-enriched" according to the genomic classification have a poor outcome.
- The loss-enriched tumors are also associated with CTNNB1 mutations, increased expression of stem cell markers, YAP target genes and decreased levels of editing.

7. REFERENCES

- Adesina, A. M. et al. (2007)** 'FOXG1 is overexpressed in hepatoblastoma', *Human Pathology*, 38(3), pp. 400–409. doi: 10.1016/j.humpath.2006.09.003.
- Ai, J. et al. (2011)** 'Cellular Physiology and Biochemistry FLNA and PGK1 are Two Potential Markers for Progression in Hepatocellular Carcinoma', 27, pp. 207–216.
- Albrecht, S. et al. (1994)** 'Loss of Maternal Alleles on Chromosome Arm 11p in Hepatoblastoma', *Cancer Research*, 54(19), pp. 5041–5044.
- Albrethsen, J. et al. (2011)** 'Gel-based proteomics of liver cancer progression in rat', *Biochimica et Biophysica Acta - Proteins and Proteomics*. Elsevier B.V., 1814(10), pp. 1367–1376. doi: 10.1016/j.bbapap.2011.05.018.
- Alkan, C., Coe, B. P. and Eichler, E. E. (2011)** 'Genome structural variation discovery and genotyping', *Nature Reviews Genetics*, 12, pp. 363–376. doi: 10.1038/nrg2958.
- Amamoto, R. et al. (2011)** 'Mitochondrial p32/C1QBP is highly expressed in prostate cancer and is associated with shorter prostate-specific antigen relapse time after radical prostatectomy', *Cancer Science*, 102(3), pp. 639–647. doi: 10.1111/j.1349-7006.2010.01828.x.
- Arai, Y. et al. (2010)** 'Genome-Wide Analysis of Allelic Imbalances Reveals 4q Deletions as a Poor Prognostic Factor and MDM4 Amplification at 1q32.1 in Hepatoblastoma Yasuhito', *Genes, chromosomes & cancer*, 49, pp. 596–609.
- Armengol, C. et al. (2004)** 'Orthotopic Implantation of Human Hepatocellular Carcinoma in Mice : Analysis of Tumor Progression and Establishment of the BCLC-9 Cell Line Orthotopic Implantation of Human Hepatocellular Carcinoma in Mice : Analysis of Tumor Progression and Establishment', 10, pp. 2150–2157. doi: 10.1158/1078-0432.CCR-03-1028.
- Armengol, C. et al. (2011)** 'Wnt signaling and hepatocarcinogenesis: The hepatoblastoma model', *International Journal of Biochemistry and Cell Biology*. Elsevier Ltd, 43(2), pp. 265–270. doi: 10.1016/j.biocel.2009.07.012.
- Bae, J. S. et al. (2012)** 'Expression and role of epithelial cell adhesion molecule in dysplastic nodule and hepatocellular carcinoma', *International Journal of Oncology*, 41(6), pp. 2150–2158. doi: 10.3892/ijo.2012.1631.
- Benhamouche, S. et al. (2006)** 'Apc Tumor Suppressor Gene Is the "Zonation-Keeper" of Mouse Liver', *Developmental Cell*, 10(6), pp. 759–770. doi: 10.1016/j.devcel.2006.03.015.
- Bissig-Choisat, B. et al. (2016)** 'Novel patient-derived xenograft and cell line models for therapeutic testing of pediatric liver cancer.', *Journal of Hepatology*, 65(2), pp. 325–33. doi: 10.1016/j.jhep.2016.04.009.
- Boer, J. M. and den Boer, M. L. (2017)** 'BCR-ABL1 -like acute lymphoblastic leukaemia: From bench to bedside', *European Journal of Cancer*. Elsevier Ltd, 82, pp. 203–218. doi: 10.1016/j.ejca.2017.06.012.
- Boyault, S. et al. (2007)** 'Transcriptome classification of HCC is related to gene alterations and to new therapeutic targets', *Hepatology*, 45(1), pp. 42–52. doi: 10.1002/hep.21467.
- Braeuning, A. et al. (2006)** 'Differential gene expression in periportal and perivenous mouse hepatocytes', *FEBS Journal*, 273(22), pp. 5051–5061. doi: 10.1111/j.1742-4658.2006.05503.x.
- Brown, J. et al. (2000)** 'Pretreatment prognostic factors for children with hepatoblastoma - Results from the International Society of Paediatric Oncology (SIOP) Study SIOPEL 1', *European Journal of Cancer*, 36(11), pp. 1418–1425. doi: 10.1016/S0959-8049(00)00074-5.
- Buckley, J. D. et al. (1989)** 'A case-control study of risk factors for hepatoblastoma. A report from the childrens cancer study group', *Cancer*, 64(5), pp. 1169–1176. doi: 10.1002/1097-0142(19890901)64:5<1169::AID-CNCR2820640534>3.0.CO;2-I.
- Buendia, M. A. (2002)** 'Genetic alterations in hepatoblastoma and hepatocellular carcinoma: Common and distinctive aspects', *Medical and Pediatric Oncology*, 39(5), pp. 530–535. doi: 10.1002/mpo.10180.
- Byrne, A. T. et al. (2017)** 'Interrogating open issues in cancer precision medicine with patient-derived xenografts', *Nature Reviews Cancer*. Nature Publishing Group, 17(4), pp. 254–268. doi: 10.1038/nrc.2016.140.
- Cairo, S. et al. (2008)** 'Hepatic Stem-like Phenotype and Interplay of Wnt/ β -Catenin and Myc Signaling in Aggressive Childhood Liver Cancer', *Cancer Cell*. doi: 10.1016/j.ccr.2008.11.002.
- Cairo, S. et al. (2010)** 'Stem cell-like micro-RNA signature driven by Myc in aggressive liver cancer', *Proceedings of the National Academy of Sciences*, 107(47), pp. 20471–20476. doi: 10.1073/pnas.1009009107.
- Cartier, F. et al. (2017)** 'New tumor suppressor microRNAs target glypican-3 in human liver cancer', *Oncotarget*, 8(25), pp. 41211–41226. doi: 10.18632/oncotarget.17162.
- Casamassimi, A. et al. (2017)** 'Transcriptome profiling in human diseases: New advances and

References

- perspectives', *International Journal of Molecular Sciences*, 18(8). doi: 10.3390/ijms18081652.
- Cavenee, W. K. et al. (1983)** 'Expression of recessive alleles by chromosomal mechanisms in retinoblastoma', *Nature*, 305(5937), pp. 779–84.
- Chan, T. H. M. et al. (2014)** 'A disrupted RNA editing balance mediated by ADARs (Adenosine DeAminases that act on RNA) in human hepatocellular carcinoma', *Gut*, 63(5), pp. 832–843. doi: 10.1136/gutjnl-2012-304037.
- Chen, C. X. et al. (2000)** 'A third member of the RNA-specific adenosine deaminase gene family, ADAR3, contains both single- and double-stranded RNA binding domains.', *RNA (New York, N.Y.)*, 6(5), pp. 755–67. doi: 10.1017/S1355838200000170.
- Chen, J. et al. (2003)** 'Human CRYL1, a novel enzyme-crystallin overexpressed in liver and kidney and downregulated in 58% of liver cancer tissues from 60 Chinese patients, and four new homologs from other mammals', *Gene*, 302(1–2), pp. 103–113. doi: 10.1016/S0378-1119(02)01095-8.
- Chen, J. C. et al. (1998)** 'Hepatocellular Carcinoma Clinical Review and Comparison', 33(9), pp. 1350–1354.
- Chen, J. C. et al. (2005)** 'Comparison of childhood hepatic malignancies in a hepatitis B hyper-endemic area', *World Journal of Gastroenterology*, 11(34), pp. 5289–5294.
- Chen, L. et al. (2013)** 'DKK1 promotes hepatocellular carcinoma cell migration and invasion through β -catenin/MMP7 signaling pathway.', *Molecular cancer*, 12, p. 157. doi: 10.1186/1476-4598-12-157.
- Chen, L. et al. (2013)** 'Recoding RNA editing of AZIN1 predisposes to hepatocellular carcinoma', *Nature Medicine*, 19(2), pp. 209–216. doi: 10.1038/nm.3043.
- Chen, M. et al. (2011)** 'Promoter Hypermethylation Mediated Downregulation of FBP1 in Human Hepatocellular Carcinoma and Colon Cancer', 6(10). doi: 10.1371/journal.pone.0025564.
- Chen, S.-C. et al. (2015)** 'Hepatoma-derived growth factor/nucleolin axis as a novel oncogenic pathway in liver carcinogenesis', *Oncotarget*, 6(18), pp. 16253–16270. doi: 10.18632/oncotarget.3608.
- Chen, T. T.-L. et al. (2009)** 'Establishment and Characterization of a Cancer Cell Line Derived From an Aggressive Childhood Liver Tumor', *Pediatric Blood and Cancer*, 53, pp. 1040–1047. doi: 10.1002/pbc.22187.
- Chen, Y.-B. et al. (2009)** 'Increased expression of hyaluronic acid binding protein 1 is correlated with poor prognosis in patients with breast cancer.', *Journal of surgical oncology*, 100(5), pp. 382–6. doi: 10.1002/jso.21329.
- Chen, Y., Zhang, H. and Zhang, Y. (2017)** 'Targeting receptor tyrosine kinase EphB4 in cancer therapy', *Seminars in Cancer Biology*. Elsevier, (June), pp. 0–1. doi: 10.1016/j.semcancer.2017.10.002.
- Cheng, I. K.-C. et al. (2010)** 'Reduced CRYL1 expression in hepatocellular carcinoma confers cell growth advantages and correlates with adverse patient prognosis', *The Journal of pathology*, 220, pp. 348–360. doi: 10.1002/path.2644.
- Chiorean, L. et al. (2015)** 'Benign liver tumors in pediatric patients - Review with emphasis on imaging features.', *World journal of gastroenterology*, 21(28), pp. 8541–61. doi: 10.3748/wjg.v21.i28.8541.
- Chong, C. et al. (2008)** 'Decreased Expression of UK114 Is Related to the Differentiation Status of Human Hepatocellular Carcinoma', 17(March), pp. 535–543. doi: 10.1158/1055-9965.EPI-07-0506.
- Cibulskis, K. et al. (2013)** 'Sensitive detection of somatic point mutations in impure and heterogeneous cancer samples', *Nature Biotechnology*. Nature Publishing Group, 31(3), pp. 213–219. doi: 10.1038/nbt.2514.
- Cornella, H. et al. (2015)** 'Unique genomic profile of fibrolamellar hepatocellular carcinoma', *Gastroenterology*, 148(4), pp. 806–18. doi: 10.1053/j.gastro.2014.12.028.
- COSMIC: Catalogue Of Somatic Mutations In Cancer** (no date).
- Craig, J. et al. (1980)** 'Fibrolamellar carcinoma of the liver: a tumor of adolescents and young adults with distinctive clinico-pathologic features', *Cancer*, 46(2), pp. 372–379.
- Crist, W. M.- and Larry, K. E. (1991)** 'Common solid tumors childhood_Med progress_rev_1991', *The New England Journal of Medicine*.
- Cui, Y. et al. (2016)** 'Involvement of PI3K/Akt, ERK and p38 signaling pathways in emodin-mediated extrinsic and intrinsic human hepatoblastoma cell apoptosis', *Food and Chemical Toxicology*. Elsevier Ltd, 92, pp. 26–37. doi: 10.1016/j.fct.2016.03.013.
- Curia, M. C. et al. (2008)** 'Sporadic childhood hepatoblastomas show activation of beta-catenin, mismatch repair defects and p53 mutations', *Modern pathology: an official journal of the United States and Canadian Academy of Pathology, Inc*, 21(1), pp. 7–14. doi: 10.1038/modpathol.3800977.
- Czauderna, P. et al. (2002)** 'Hepatocellular Carcinoma in Children: Results of the First Prospective Study of the International Society of Pediatric Oncology Group', *Journal of Clinical Oncology*. doi: 10.1200/JCO.2002.06.102.

- Czauderna, P. et al. (2014)** 'Hepatoblastoma state of the art: pathology, genetics, risk stratification, and chemotherapy.', *Current opinion in pediatrics*, 26(1), pp. 19–28. doi: 10.1097/MOP.000000000000046.
- Dannenberg, L. O. et al. (2006)** 'Differential regulation of the alcohol dehydrogenase 1B (ADH1B) and ADH1C genes by DNA methylation and histone deacetylation', *Alcoholism: Clinical and Experimental Research*, 30(6), pp. 928–937. doi: 10.1111/j.1530-0277.2006.00107.x.
- Darbari, A. et al. (2003)** 'Epidemiology of primary hepatic malignancies in U.S. children', *Hepatology*, 38(3), pp. 560–566. doi: 10.1053/jhep.2003.50375.
- Darcy, D. G. et al. (2015)** 'The genomic landscape of fibrolamellar hepatocellular carcinoma: whole genome sequencing of ten patients', *Oncotarget*, 6(2), pp. 755–770. doi: 10.18632/oncotarget.2712.
- DeBaun, M. R. and Tucker, M. a (1998)** 'Risk of cancer during the first four years of life in children from The Beckwith-Wiedemann Syndrome Registry.', *The Journal of pediatrics*, 132(3 Pt 1), pp. 398–400. doi: 10.1016/S0022-3476(98)70008-3.
- Donzé, O. et al. (1995)** 'Abrogation of translation initiation factor eIF-2 phosphorylation causes malignant transformation of NIH 3T3 cells.', *The EMBO journal*, 14(15), pp. 3828–3834.
- Dopeso, H. et al. (2009)** 'The receptor tyrosine kinase EPHB4 has tumor suppressor activities in intestinal tumorigenesis', *Cancer Research*, 69(18), pp. 7430–7438. doi: 10.1158/0008-5472.CAN-09-0706.
- Dupain, C. et al. (2017)** 'Relevance of Fusion Genes in Pediatric Cancers: Toward Precision Medicine', *Molecular Therapy - Nucleic Acids*. Elsevier Ltd., 6(March), pp. 315–326. doi: 10.1016/j.omtn.2017.01.005.
- Eddelbuettel, D. (2013)** 'Seamless R and C++ Integration with Rcpp.', in: Springer New York.
- Eichenmüller, M. et al. (2009)** 'Blocking the hedgehog pathway inhibits hepatoblastoma growth', *Hepatology*, 49(2), pp. 482–490. doi: 10.1002/hep.22649.
- Eichenmüller, M. et al. (2014)** 'The genomic landscape of hepatoblastoma and their progenies with HCC-like features', *Journal of Hepatology*, 61(6), pp. 1312–1320. doi: 10.1016/j.jhep.2014.08.009.
- Emre, S., Umman, V. and Rodriguez-Davalos, M. (2012)** 'Current concepts in pediatric liver tumors', *Pediatric Transplantation*, 16(6), pp. 549–563. doi: 10.1111/j.1399-3046.2012.01704.x.
- Esteller, M. (2011)** 'Epigenetic changes in cancer', *F1000 Biology Reports*, (3), p. 9. doi: 10.3410/B3-9.
- Ferguson, B. D. et al. (2015)** 'Novel EPHB4 Receptor Tyrosine Kinase Mutations and Kinomic Pathway Analysis in Lung Cancer.', *Scientific reports*. Nature Publishing Group, 5, p. 10641. doi: 10.1038/srep10641.
- Fogal, V. et al. (2010)** 'Mitochondrial p32 Protein Is a Critical Regulator of Tumor Metabolism via Maintenance of Oxidative Phosphorylation', *Molecular and Cellular Biology*, 30(6), pp. 1303–1318. doi: 10.1128/MCB.01101-09.
- Fouad, Y. M. et al. (2016)** 'Clinical significance and diagnostic value of serum dickkopf-1 in patients with hepatocellular carcinoma', *Scandinavian Journal of Gastroenterology*, 51(9), pp. 1133–1137. doi: 10.3109/00365521.2016.1172337.
- von Frowein, J. et al. (2011)** 'MicroRNA-492 is processed from the keratin 19 gene and up-regulated in metastatic hepatoblastoma', *Hepatology*, 53(3), pp. 833–842. doi: 10.1002/hep.24125.
- Fuchs, J. et al. (1996)** 'Successful transplantation of human hepatoblastoma into immunodeficient mice', *Journal of Pediatric Surgery*, 31(9), pp. 1241–1246. doi: 10.1016/S0022-3468(96)90242-0.
- Fuchs, J. et al. (2002)** 'Pretreatment prognostic factors and treatment results in children with hepatoblastoma: A report from the German cooperative pediatric liver tumor study HB 94', *Cancer*, 95(1), pp. 172–182. doi: 10.1002/cncr.10632.
- Galeano, F. et al. (2010)** 'Human BLCAP transcript: New editing events in normal and cancerous tissues', *International Journal of Cancer*, 127(1), pp. 127–137. doi: 10.1002/ijc.25022.
- Gao, H. et al. (2016)** 'Elevated HABP1 protein expression correlates with progression and poor survival in patients with gastric cancer', *OncoTargets and Therapy*, 9, pp. 6711–6718. doi: 10.2147/OTT.S114756.
- Gao, M. et al. (2015)** 'Inhibition of cell proliferation and metastasis of human hepatocellular carcinoma by miR-137 is regulated by CDC42', *Oncology Reports*, 34(5), pp. 2523–2532. doi: 10.3892/or.2015.4261.
- García-Miguel, P. and López Santamaría, M. (2005)** 'Estado actual del diagnóstico y tratamiento del hepatoblastoma Purificación', *Clinical and Translational Oncology*, 7(7), pp. 328–34.
- Garzon, R., Marcucci, G. and Croce, C. M. (2010)** 'Targeting MicroRNAs in Cancer: Rationale, Strategies and Challenges', *Nature Reviews Drug Discovery*, 9(10), pp. 775–589. doi: doi:10.1038/nrd3179.
- Ghosh, I. et al. (2004)** 'Differential expression of Hyaluronic Acid Binding Protein 1 (HABP1)/P32/C1QBP during progression of epidermal carcinoma.', *Molecular and Cellular Biochemistry*, 267, pp. 133–9.
- Graham, R. P. et al. (2015)** 'DNAJB1-PRKACA is specific for fibrolamellar carcinoma', *Modern Pathology*. Nature Publishing Group, 28(6), pp. 822–829. doi: 10.1038/modpathol.2015.4.
- Gray, S. G., Eriksson, T., et al. (2000)** 'Altered expression of members of the IGF-axis in

References

- hepatoblastomas.', *British journal of cancer*, 82(9), pp. 1561–1567. doi: 10.1054/bjoc.1999.1179.
- Gray, S. G., Kytölä, S., et al. (2000)** 'Comparative genomic hybridization reveals population-based genetic alterations in hepatoblastomas.', *British journal of cancer*, 83(8), pp. 1020–5. doi: 10.1054/bjoc.2000.1390.
- Greenman, C. et al. (2007)** 'Patterns of somatic mutation in human cancer genomes', *Nature*, 446(7132), pp. 153–158. doi: 10.1038/nature05610.
- Grotegut, S. et al. (2010)** 'Hepatocyte growth factor protects hepatoblastoma cells from chemotherapy-induced apoptosis by AKT activation', *International Journal of Oncology*, 36, pp. 1261–1267. doi: 10.3892/ijo.
- Grovas, A. et al. (1997)** 'The National Cancer Data Base report on patterns of childhood cancers in the United States', *Cancer*, 80, pp. 2321–32.
- Guichard, C. et al. (2012)** 'Integrated analysis of somatic mutations and focal copy-number changes identifies key genes and pathways in hepatocellular carcinoma', *Nature Genetics*. Nature Publishing Group, 44(6), pp. 694–698. doi: 10.1038/ng.2256.
- Haas, J. E. et al. (1989)** 'Histopathology and Prognosis in Childhood Hepatoblastoma and Hepatocarcinoma', *Cancer*, 64, pp. 1082–1095.
- Haas, J., Feusner, J. and Finegold, M. (2011)** 'Small cell undifferentiated histology in hepatoblastoma may be unfavorable.', *Cancer*, 92(12), pp. 3130–4.
- Han, L. et al. (2015)** 'The Genomic Landscape and Clinical Relevance of A-to-I RNA Editing in Human Cancers', *Cancer Cell*. Elsevier Inc., 28(4), pp. 515–528. doi: 10.1016/j.ccell.2015.08.013.
- Hanahan, D. and Weinberg, R. A. (2000)** 'The hallmarks of cancer.', *Cell*, 100(1), pp. 57–70. doi: 10.1007/s00262-010-0968-0.
- Hanahan, D. and Weinberg, R. A. (2011)** 'Hallmarks of cancer: The next generation', *Cell*. Elsevier Inc., 144(5), pp. 646–674. doi: 10.1016/j.cell.2011.02.013.
- Harada, N. et al. (2002)** 'Lack of tumorigenesis in the mouse liver after adenovirus-mediated expression of a dominant stable mutant of β -catenin', *Cancer Research*, 62(7), pp. 1971–1977.
- Hartmann, W. et al. (2000)** 'p57(KIP2) is not mutated in hepatoblastoma but shows increased transcriptional activity in a comparative analysis of the three imprinted genes p57(KIP2), IGF2, and H19', *American Journal of Pathology*, 157(4), pp. 1393–1403. doi: 10.1016/S0002-9440(10)64652-4.
- Hartmann, W. et al. (2006)** 'Phosphatidylinositol 3'-kinase/AKT signaling is activated in medulloblastoma cell proliferation and is associated with reduced expression of PTEN', *Clinical Cancer Research*, 12(10), pp. 3019–3027. doi: 10.1158/1078-0432.CCR-05-2187.
- Hartmann, W. et al. (2009)** 'Activation of phosphatidylinositol-3'-kinase/AKT signaling is essential in hepatoblastoma survival.', *Clinical Cancer Research*, 15(14), pp. 4538–4545. doi: 10.1158/1078-0432.CCR-08-2878.
- Harvey, J. et al. (2008)** 'Germline APC mutations are not commonly seen in children with sporadic hepatoblastoma', *J.Pediatr.Gastroenterol.Nutr.*, 47(5), pp. 675–677. doi: 10.1097/MPG.0b013e318174e808.
- Hashimoto, T. et al. (2010)** 'TMPRSS13, a type II transmembrane serine protease, is inhibited by hepatocyte growth factor activator inhibitor type 1 and activates pro-hepatocyte growth factor', *FEBS Journal*, 277(23), pp. 4888–4900. doi: 10.1111/j.1742-4658.2010.07894.x.
- He, J. et al. (2016)** 'Regulatory network analysis of genes and microRNAs in human hepatoblastoma', pp. 4099–4106. doi: 10.3892/ol.2016.5196.
- He, Y. et al. (2011)** 'The role of PKR/eIF2 α signaling pathway in prognosis of Non-Small cell lung cancer', *PLoS ONE*, 6(11), p. e24855. doi: 10.1371/journal.pone.0024855.
- Hirschman, B. A., Pollock, B. H. and Tomlinson, G. E. (2005)** 'The spectrum of APC mutations in children with hepatoblastoma from familial adenomatous polyposis kindreds', *Journal of Pediatrics*, 147, pp. 263–6. doi: 10.1016/j.jpeds.2005.04.019.
- Hishiki, T. et al. (2011)** 'Outcome of hepatoblastomas treated using the Japanese Study Group for Pediatric Liver Tumor (JPLT) protocol-2: Report from the JPLT', *Pediatric Surgery International*, 27(1), pp. 1–8. doi: 10.1007/s00383-010-2708-0.
- Hoffman, R. (1999)** 'Orthotopic metastatic mouse models for anticancer drug discovery and evaluation: a bridge to the clinic.', *Investigational New Drugs*, 17(4), pp. 343–59.
- Honda, S. et al. (2008)** 'The methylation status of RASSF1A promoter predicts responsiveness to chemotherapy and eventual cure in hepatoblastoma patients', *International Journal of Cancer*, 123(5), pp. 1117–1125. doi: 10.1002/ijc.23613.
- Honeyman, J. N. et al. (2014)** 'Detection of a Recurrent DNAJB1-PRKACA Chimeric Transcript in Fibrolamellar Hepatocellular Carcinoma', 343(6174), pp. 1010–1014. doi: 10.1126/science.1249484.

- Hoshida, Y. and Toffanin, S. (2010)** 'Molecular classification and novel targets in hepatocellular carcinoma: recent advancements', *Seminars in liver disease*, 30(1), pp. 35–51. doi: 10.1055/s-0030-1247131.Molecular.
- Hu, J. et al. (2000)** 'Comparative Genomic Hybridization Analysis of Hepatoblastoma', 201 (June 1999), pp. 196–201.
- Hu, X. et al. (2015)** 'RNA over-editing of BLCAP contributes to hepatocarcinogenesis identified by whole-genome and transcriptome sequencing', *Cancer Letters*. Elsevier Ireland Ltd, 357(2), pp. 510–519. doi: 10.1016/j.canlet.2014.12.006.
- Hu, Y. et al. (2004)** 'Genetic alterations in doxorubicin-resistant hepatocellular carcinoma cells: A combined study of spectral karyotyping, positional expression profiling and candidate genes', pp. 1357–1364.
- Huang, X. et al. (no date)** 'αB-Crystallin complexes with 14-3-3ζ to induce epithelial-mesenchymal transition and resistance to sorafenib in hepatocellular carcinoma Xiao-Yong', pp. 1–57.
- Huang, Y. et al. (2017)** 'Transcriptome profiling identify a recurrent CRYL1-IFT88 chimeric transcript in hepatocellular carcinoma.', *Oncotarget*, 8(25), pp. 40693–40704. doi: 10.18632/oncotarget.17244.
- Ikeda, H., Matsuyama, S. and Tanimura, M. (1997)** 'Association between hepatoblastoma and very low birth weight: A trend or a chance?', *Journal of Pediatrics*, 130(4), pp. 557–560. doi: 10.1016/S0022-3476(97)70239-7.
- De Ioris, M. et al. (2008)** 'Hepatoblastoma with a low serum alpha-fetoprotein level at diagnosis: the SIOPEL group experience.', *European Journal of Cancer*, 44(4), pp. 545–50. doi: 10.1016/j.ejca.2007.11.022.
- Ishikawa, T. et al. (2011)** 'Molecular targeting of CSN5 in human hepatocellular carcinoma: a mechanism of therapeutic response', pp. 1–10. doi: 10.1038/onc.2011.126.
- Jeng, Y. M. et al. (2000)** 'Somatic mutations of β-catenin play a crucial role in the tumorigenesis of sporadic hepatoblastoma', *Cancer Letters*, 152(1), pp. 45–51. doi: 10.1016/S0304-3835(99)00433-4.
- Jia, D. et al. (2014)** 'Exome sequencing of hepatoblastoma reveals novel mutations and cancer genes in the Wnt pathway and ubiquitin ligase complex', *Hepatology*, 60(5), pp. 1686–1696. doi: 10.1002/hep.27243.
- Kanda, M. et al. (2011)** 'Promoter Hypermethylation of Fibulin 1 Gene Is Associated With Tumor Progression in Hepatocellular Carcinoma', 579(October 2010), pp. 571–579. doi: 10.1002/mc.20735.
- Kang, L. et al. (2015)** 'Genome-wide identification of RNA editing in hepatocellular carcinoma', *Genomics*. Elsevier B.V., 105(2), pp. 76–82. doi: 10.1016/j.ygeno.2014.11.005.
- Kasai, M. and Watanabe, I. (1970)** 'Histologic classification of liver-cell carcinoma in infancy and childhood and its clinical evaluation. A study of 70 cases collected in Japan', *Cancer*, 25(3), pp. 551–563. doi: 10.1002/1097-0142(197003)25:3<551::AID-CNCR2820250309>3.0.CO;2-5.
- Katzenstein, H. M. et al. (2002)** 'Hepatocellular carcinoma in children and adolescents: Results from the Pediatric Oncology Group and the Children's Cancer Group intergroup study', *Journal of Clinical Oncology*, 20(12), pp. 2789–2797. doi: 10.1200/JCO.2002.06.155.
- Katzenstein, H. M. et al. (2003)** 'Fibrolamellar hepatocellular carcinoma in children and adolescents', *Cancer*, 97(8), pp. 2006–2012. doi: 10.1002/cncr.11292.
- Kaul, R. et al. (2012)** 'Overexpression of hyaluronan-binding protein 1 (HABP1/p32/gC1qR) in HepG2 cells leads to increased hyaluronan synthesis and cell proliferation by up-regulation of cyclin D1 in AKT-dependent pathway', *Journal of Biological Chemistry*, 287(23), pp. 19750–19764. doi: 10.1074/jbc.M111.266270.
- Khan, R. et al. (2013)** 'Protein expression profiling of nuclear membrane protein reveals potential biomarker of human hepatocellular carcinoma', pp. 1–12.
- Kikuchi, A., Fumoto, K. and Kimura, H. (2017)** 'The Dickkopf1-CKAP4 axis creates a novel signaling pathway and may represent a molecular target for cancer therapy', *British Journal of Pharmacology*. doi: 10.1111/bph.13863.
- Kim, B.-C. et al. (2016)** 'Antibody neutralization of cell-surface gC1qR/HABP1/SF2-p32 prevents lamellipodia formation and tumorigenesis.', *Oncotarget*, 7(31), pp. 49972–49985. doi: 10.18632/oncotarget.10267.
- Kim, S. U. et al. (2015)** 'Serum dickkopf-1 as a biomarker for the diagnosis of hepatocellular carcinoma', *Yonsei Medical Journal*, 56(5), pp. 1296–1306. doi: 10.3349/ymj.2015.56.5.1296.
- Kim, T. M. et al. (2008)** 'Clinical implication of recurrent copy number alterations in hepatocellular carcinoma and putative oncogenes in recurrent gains on 1q', *International Journal of Cancer*, 123(12), pp. 2808–2815. doi: 10.1002/ijc.23901.
- Kimura, H. et al. (2016)** 'CKAP4 is a Dickkopf1 receptor and is involved in tumor progression', *Journal of*

References

- Clinical Investigation*, 126(7), pp. 2689–2705. doi: 10.1172/JCI84658.
- Kimura, O. et al. (2010)** 'Characterization of the epithelial cell adhesion molecule (EpCAM)+ cell population in hepatocellular carcinoma cell lines', *Cancer Science*, 101(10), pp. 2145–2155. doi: 10.1111/j.1349-7006.2010.01661.x.
- King, D., Yeomanson, D. and Bryant, H. E. (2015)** 'PI3King the lock: targeting the PI3K/Akt/mTOR pathway as a novel therapeutic strategy in neuroblastoma.', *Journal of pediatric hematology/oncology*, 37(4), pp. 245–51. doi: 10.1097/MPH.0000000000000329.
- Knudson, A. G. (1971)** 'Mutation and Cancer: Statistical Study of Retinoblastoma', *Proceedings of the National Academy of Sciences*, 68(4), pp. 820–823. doi: 10.1073/pnas.68.4.820.
- Koch, A. et al. (1999)** 'Childhood hepatoblastomas frequently carry a mutated degradation targeting box of the β -catenin gene', *Cancer Research*, 59(2), pp. 269–273.
- Koch, A. et al. (2004)** 'Mutations and elevated transcriptional activity of conductin (AXIN2) in hepatoblastomas', *Journal of Pathology*, 204(5), pp. 546–554. doi: 10.1002/path.1662.
- Koh, K. N. et al. (2011)** 'Prognostic Implications of Serum Alpha-Fetoprotein Response During Treatment of Hepatoblastoma', *Pediatric Blood and Cancer*, 57, pp. 554–560. doi: 10.1002/pbc.23069.
- Kumar, S. R. et al. (2006)** 'Receptor tyrosine kinase EphB4 is a survival factor in breast cancer.', *The American journal of pathology*. American Society for Investigative Pathology, 169(1), pp. 279–293. doi: 10.2353/ajpath.2006.050889.
- Kumon, K. et al. (2001)** 'Frequent increase of DNA copy number in the 2q24 chromosomal region and its association with a poor clinical outcome in Hepatoblastoma: cytogenetic and comparative genomic hybridization analysis', *Japanese Journal of Cancer Research*, pp. 854–862.
- Kurahashi, H. et al. (1995)** 'Biallelic Inactivation of the APC Gene in Hepatoblastoma', 55, pp. 5007–5011.
- Lai, K. K. Y. et al. (2011)** 'Extracellular matrix dynamics in hepatocarcinogenesis: A comparative proteomics study of PDGFC transgenic and Pten null mouse models', *PLoS Genetics*, 7(6). doi: 10.1371/journal.pgen.1002147.
- Letouze, E. et al. (2015)** 'SNP Array Profiling of Childhood Adrenocortical Tumors Reveals Distinct Pathways of Tumorigenesis and Highlights Candidate Driver Genes', 97(March), pp. 1284–1293. doi: 10.1210/jc.2012-1184.
- Levanon, E. Y. et al. (2005)** 'Evolutionarily conserved human targets of adenosine to inosine RNA editing', *Nucleic Acids Research*, 33(4), pp. 1162–1168. doi: 10.1093/nar/gki239.
- Li, H. et al. (2012)** 'Deregulation of Hippo kinase signalling in Human hepatic malignancies', *Liver International*, 32(1), pp. 38–47. doi: 10.1111/j.1478-3231.2011.02646.x.
- Li, M. hong et al. (2013)** 'Expression of cytoskeleton-associated protein 4 is related to lymphatic metastasis and indicates prognosis of intrahepatic cholangiocarcinoma patients after surgery resection', *Cancer Letters*. Elsevier Ireland Ltd, 337(2), pp. 248–253. doi: 10.1016/j.canlet.2013.05.003.
- Li, R. et al. (2012)** 'Chloride intracellular channel 1 is an important factor in the lymphatic metastasis of hepatocarcinoma', *Biomedicine et Pharmacotherapy*. Elsevier Masson SAS, 66(3), pp. 167–172. doi: 10.1016/j.biopha.2011.10.002.
- Li, S. X., Liu, L. juan, et al. (2014)** 'CKAP4 inhibited growth and metastasis of hepatocellular carcinoma through regulating EGFR signaling', *Tumor Biology*, 35(8), pp. 7999–8005. doi: 10.1007/s13277-014-2000-3.
- Li, S. X., Tang, G. S., et al. (2014)** 'Prognostic significance of cytoskeleton-associated membrane protein 4 and its palmitoyl acyltransferase DHHC2 in hepatocellular carcinoma', *Cancer*, 120(10), pp. 1520–1531. doi: 10.1002/cncr.28593.
- Li, X. et al. (2009)** 'Dermatopontin is expressed in human liver and is downregulated in hepatocellular carcinoma.', *Biochemistry Biokhimiia*, 74, pp. 979–85.
- Li, Y. et al. (2016)** 'MicroRNA-520c enhances cell proliferation, migration, and invasion by suppressing IRF2 in gastric cancer', *FEBS Open Bio*, 6(12), pp. 1257–1266. doi: 10.1002/2211-5463.12142.
- Litten, J. B. and Tomlinson, G. E. (2008)** 'Liver Tumors in Children', *The Oncologist*, 13, pp. 812–820. doi: 10.1634/theoncologist.2008-0011.
- Liu, H. et al. (2003)** 'Characterization of Reduced Expression of Glycine N-Methyltransferase in Cancerous Hepatic Tissues Using Two Newly Developed Monoclonal Antibodies', pp. 87–97. doi: 10.1159/000068083.
- Liu, M. et al. (2014)** 'A cancer-related protein 14-3-3 ζ is a potential tumor-associated antigen in immunodiagnosis of hepatocellular carcinoma'. doi: 10.1007/s13277-013-1555-8.
- Liu, P. et al. (2009)** 'Targeting the phosphoinositide 3-kinase (PI3K) pathway in cancer', *Nat. Rev. Drug. Discov.*, 8(8), pp. 627–644. doi: 10.1038/nrd2926.Targeting.

- Liu, T. et al. (2013)** '14-3-3 e Overexpression Contributes to Epithelial- Mesenchymal Transition of Hepatocellular Carcinoma', 8(3), pp. 1–12. doi: 10.1371/journal.pone.0057968.
- Liu, W. H. et al. (2013)** 'ADAR2-mediated editing of miR-214 and miR-122 precursor and antisense RNA transcripts in liver cancers', *PLoS ONE*, 8(12), pp. 1–10. doi: 10.1371/journal.pone.0081922.
- Llovet, J. M. et al. (2016)** 'Hepatocellular carcinoma', *Nature Reviews Disease Primers*, 2, pp. 1–23. doi: 10.1038/nrdp.2016.18.
- López-Terrada, D. et al. (2009)** 'Histologic subtypes of hepatoblastoma are characterized by differential canonical Wnt and Notch pathway activation in DLK+ precursors', *Human Pathology*. Elsevier Inc., 40(6), pp. 783–794. doi: 10.1016/j.humpath.2008.07.022.
- López-Terrada, D. et al. (2013)** 'Towards an international pediatric liver tumor consensus classification: proceedings of the Los Angeles COG liver tumors symposium', *Modern Pathology*, (February 2013), pp. 472–491. doi: 10.1038/modpathol.2013.80.
- Lu, Y. et al. (2013)** 'Thioredoxin-Like Protein 2 Is Overexpressed in Colon Cancer and Promotes Cancer Cell Metastasis by Interaction with Ran', 19(9), pp. 899–911. doi: 10.1089/ars.2012.4736.
- Lucito, R. et al. (2003)** 'Representational Oligonucleotide Microarray Analysis: A High-Resolution Method to Detect Genome Copy Number Variation', pp. 2291–2305. doi: 10.1101/gr.1349003.
- Luo, J.-H. et al. (2006)** 'Transcriptomic and genomic analysis of human hepatocellular carcinomas and hepatoblastomas.', *Hepatology (Baltimore, Md.)*, 44(4), pp. 1012–24. doi: 10.1002/hep.21328.
- Magrelli, A. et al. (2009)** 'Altered microRNA Expression Patterns in Hepatoblastoma Patients.', *Translational oncology*, 2(3), pp. 157–163. doi: http://dx.doi.org/10.1593/tlo.09124.
- Maibach, R. et al. (2012)** 'Prognostic stratification for children with hepatoblastoma: The SIOPEL experience', *European Journal of Cancer*, 48, pp. 1543–1549. doi: 10.1016/j.ejca.2011.12.011.
- Malogolowkin, M. H. et al. (2006)** 'Intensified platinum therapy is an ineffective strategy for improving outcome in pediatric patients with advanced hepatoblastoma', *Journal of Clinical Oncology*, 24(18), pp. 2879–2884. doi: 10.1200/JCO.2005.02.6013.
- Malouf, G. G. et al. (2014)** 'Transcriptional profiling of pure fibrolamellar hepatocellular carcinoma reveals an endocrine signature', *Hepatology*, 59(6), pp. 2228–2237. doi: 10.1002/hep.27018.
- Martinez-Quetglas, I. et al. (2016)** 'IGF2 Is Up-regulated by Epigenetic Mechanisms in Hepatocellular Carcinomas and Is an Actionable Oncogene Product in Experimental Models', *Gastroenterology*. Elsevier Ltd, 151(6), pp. 1192–1205. doi: 10.1053/j.gastro.2016.09.001.
- Masica, D. L. and Karchin, R. (2011)** 'Correlation of Somatic Mutation and Expression Identifies Genes Important in Human Glioblastoma Progression and Survival', *Cancer Re*, 71(13), pp. 4550–4561. doi: 10.1158/0008-5472.CAN-11-0180.Correlation.
- McLaughlin, C. C. et al. (2006)** 'Maternal and infant birth characteristics and hepatoblastoma', *American Journal of Epidemiology*, 163(9), pp. 818–828. doi: 10.1093/aje/kwj104.
- Megger, D. A. et al. (2013)** 'Proteomic Differences Between Hepatocellular Carcinoma and Nontumorous Liver Tissue Investigated by a Combined Gel-based and Label-free Quantitative Proteomics Study', pp. 2006–2020. doi: 10.1074/mcp.M113.028027.
- Merajver, S. D. et al. (1995)** 'Germline BRCA1 Mutations and Loss of the Wild-Type Allele in Tumors from Families with Early Onset Breast and Ovarian Cancer', *Clinical Cancer Research*, 1(5), pp. 539–544.
- Meyers, R. L. et al. (2017)** 'Risk-stratified staging in paediatric hepatoblastoma: a unified analysis from the Children's Hepatic tumors International Collaboration', *The Lancet Oncology*. Elsevier Ltd, 18(1), pp. 122–131. doi: 10.1016/S1470-2045(16)30598-8.
- Miao, J. et al. (2003)** 'Sequence variants of the Axin gene in hepatoblastoma', *Hepatology Research*, 25(2), pp. 174–179. doi: 10.1016/S1386-6346(02)00264-4.
- Midorikawa, Y. et al. (2009)** 'Allelic imbalances and homozygous deletion on 8p23.2 for stepwise progression of hepatocarcinogenesis', *Hepatology*, 49(2), pp. 513–522. doi: 10.1002/hep.22698.
- Mokkapat, S. et al. (2014)** 'β-Catenin activation in a novel liver progenitor cell type is sufficient to cause hepatocellular carcinoma and hepatoblastoma', *Cancer Research*, 74(16), pp. 4515–4525. doi: 10.1158/0008-5472.CAN-13-3275.
- Mullarkey, M. et al. (2001)** 'Genetic abnormalities in a pre and post-chemotherapy hepatoblastoma', *Cytogenetics and Cell Genetics*, 95, pp. 9–11.
- Murawski, M. et al. (2016)** 'Hepatocellular carcinoma in children: Does modified platinum-and doxorubicin-based chemotherapy increase tumor resectability and change outcome? Lessons learned from the SIOPEL 2 and 3 studies', *Journal of Clinical Oncology*, 34(10), pp. 1050–1056. doi: 10.1200/JCO.2014.60.2250.
- Nagai, H. et al. (2003)** 'Hypermethylation associated with inactivation of the SOCS-1 gene, a JAK/STAT inhibitor, in human hepatoblastomas', 48(2), pp. 65–9.

References

- Nakano, M. et al. (2016)** 'RNA editing modulates human hepatic aryl hydrocarbon receptor expression by creating MicroRNA recognition sequence', *Journal of Biological Chemistry*, 291(2), pp. 894–903. doi: 10.1074/jbc.M115.699363.
- Nault, J. C. et al. (2013)** 'High frequency of telomerase reverse-transcriptase promoter somatic mutations in hepatocellular carcinoma and preneoplastic lesions', *Nature Communications*. Nature Publishing Group, 4(May), pp. 1–6. doi: 10.1038/ncomms3218.
- Negroni, L. et al. (2014)** 'Integrative Quantitative Proteomics Unveils Proteostasis Imbalance in Human Hepatocellular Carcinoma Developed on Nonfibrotic Livers', *Molecular & Cellular Proteomics*, 13(12), pp. 3473–3483. doi: 10.1074/mcp.M114.043174.
- Nicolle, D. et al. (2016)** 'Patient-derived mouse xenografts from pediatric liver cancer predict tumor recurrence and advise clinical management', *Hepatology*, 64(4), pp. 1121–1135. doi: 10.1002/hep.28621.
- Nishikura, K. (2010)** 'Functions and regulation of RNA editing by ADAR deaminases', *Annu Rev Biochem*, 79, pp. 321–349. doi: 10.1146/annurev-biochem-060208-105251.
- Niu, M. et al. (2015)** 'Elevated expression of HBP1 is correlated with metastasis and poor survival in breast cancer patients.', *American journal of cancer research*, 5(3), pp. 1190–8. Available at: <http://www.pubmedcentral.nih.gov/articlerender.fcgi?artid=4449446&tool=pmcentrez&rendertype=abstract>.
- Nusse, R. and Lim, X. (1997)** *The Wnt Homepage*.
- O'Brien, W., Finlay, J. L. and Gilbert-Barnes, E. F. (1989)** 'Patterns of antigen expression in Hepatoblastoma and Hepatocellular carcinoma in childhood', *Pediatric Hematology and Oncology*, 6, pp. 361–365.
- Oda, H. et al. (1996)** 'Somatic Mutations of the APC Gene in Sporadic Hepatolastomas', *Cancer Research*, 56, pp. 3320–3323.
- Olson, P. et al. (2009)** 'MicroRNA dynamics in the stages of tumorigenesis correlate with hallmark capabilities of cancer', *Genes and Development*, 23(18), pp. 2152–2165. doi: 10.1101/gad.1820109.
- Opel, D. et al. (2007)** 'Activation of Akt Predicts Poor Outcome in Neuroblastoma', *Cancer Res*, 67(2), pp. 735–45. doi: 10.1158/0008-5472.CAN-06-2201.
- Ortega, J. et al. (2000)** 'Randomized comparison of cisplatin/vincristine/fluorouracil and cisplatin/continuous infusion doxorubicin for treatment of pediatric hepatoblastoma: A report from the Children's Cancer Group and the Pediatric Oncology Group.', *Journal of Clinical Oncology* 2, 18(14), pp. 2665–75. doi: 10.1200/JCO.2000.18.14.2665 *Journal of Clinical Oncology* 18, no. 14 (July 2000) 2665–2675.
- Pan, Y. et al. (2013)** 'Glyoxylate reductase/hydroxypyruvate reductase: A novel prognostic marker for hepatocellular carcinoma patients after curative resection', *Pathobiology*, 80(3), pp. 155–162. doi: 10.1159/000346476.
- Parada, L. A. et al. (2000)** 'Cytogenetics of hepatoblastoma: Further characterization of 1q rearrangements by fluorescence in situ hybridization: An international collaborative study', *Medical and Pediatric Oncology*, 34(3), pp. 165–170. doi: 10.1002/(SICI)1096-911X(200003)34:3<165::AID-MPO1>3.0.CO;2-T.
- Paradis, V. (2013)** 'Multidisciplinary Treatment of Hepatocellular Carcinoma', in Vauthe, J. N. and Brouquet, A. (eds) *Recent Results in Cancer Research*, pp. 21–33. doi: 10.1007/978-3-642-16037-0_2.
- Patil, M. A. et al. (2005)** 'Array-based comparative genomic hybridization reveals recurrent chromosomal aberrations and Jab1 as a potential target for 8q gain in hepatocellular carcinoma', *Carcinogenesis*, 26(12), pp. 2050–2057. doi: 10.1093/carcin/bgi178.
- Peerschke, E. I. B. and Ghebrehiwet, B. (2014)** 'CC1qR/CR and gC1qR/p33: Observations in cancer', *Molecular Immunology*. Elsevier Ltd, 61(2), pp. 100–109. doi: 10.1016/j.molimm.2014.06.011.
- Peng, S. et al. (2008)** 'Aberrant expression of the glycolytic enzymes aldolase B and type II hexokinase in hepatocellular carcinoma are predictive markers for advanced stage, early recurrence and poor prognosis', pp. 1045–1053.
- Peng, Z. et al. (2012)** 'Comprehensive analysis of RNA-Seq data reveals extensive RNA editing in a human transcriptome', *Nature Biotechnology*. Nature Publishing Group, 30(3), pp. 253–260. doi: 10.1038/nbt.2122.
- Perilongo, G. et al. (2004)** 'Risk-adapted treatment for childhood hepatoblastoma: Final report of the second study of the International Society of Paediatric Oncology - SIOPEL 2', *European Journal of Cancer*, 40(3), pp. 411–421. doi: 10.1016/j.ejca.2003.06.003.
- Perilongo G, Shafford E, P. J. L. T. S. G. of the I. S. of P. O. (2000)** 'SIOPEL trials using preoperative chemotherapy in hepatoblastoma.', *Lancet Oncology*.

- Petricoin, E. F. et al. (2007)** 'Phosphoprotein pathway mapping: Akt/mammalian target of rapamycin activation is negatively associated with childhood rhabdomyosarcoma survival', *Cancer Research*, 67(7), pp. 3431–3440. doi: 10.1158/0008-5472.CAN-06-1344.
- Pinkel, D. and Albertson, D. G. (2005)** 'Array comparative genomic hybridization and its applications in cancer.', *Nature genetics supplement*, 37(May), pp. S11–7. doi: 10.1038/ng1569.
- Piskol, R., Ramaswami, G. and Li, J. B. (2013)** 'Reliable identification of genomic variants from RNA-seq data', *American Journal of Human Genetics*. The American Society of Human Genetics, 93(4), pp. 641–651. doi: 10.1016/j.ajhg.2013.08.008.
- Polosukhina, D. et al. (2017)** 'Functional KRAS mutations and a potential role for PI3K/AKT activation in Wilms tumors', *Molecular Oncology*, 11(4), pp. 405–421. doi: 10.1002/1878-0261.12044.
- Prasad, M. et al. (2008)** 'High Definition Cytogenetics and Oligonucleotide aCGH Analyses of Cisplatin-Resistant Ovarian Cancer Cels', *Genes, chromosomes & cancer*, 47, pp. 427–436. doi: 10.1002/gcc.20547.
- Prokurat, A. et al. (2002)** 'Transitional liver cell tumors (TLCT) in older children and adolescents: A novel group of aggressive hepatic tumors expressing beta-catenin', *Medical and Pediatric Oncology*, 39, pp. 510–518. doi: 10.1002/mpo.10177.
- Pu, C. et al. (2009)** '[Retrospective analysis of maternal and infant birth features of hepatoblastoma patients].', *Zhonghua Gan Zang Bing Za Zhi*, 17(6), pp. 459–61.
- Qin, X. et al. (2013)** 'High-throughput screening of tumor metastatic-related differential glycoprotein in hepatocellular carcinoma by iTRAQ combines lectin-related techniques', *Medical Oncology*, 30(1). doi: 10.1007/s12032-012-0420-8.
- R Peris Bonet et al. (2016)** 'Registro Español de Tumores Infantiles. Cáncer infantil en España. Estadísticas 1980 - 2015', pp. 1–75. Available at: http://www.uv.es/rnti/pdfs/Informe_RETI-SEHOP_1980-2015.pdf.
- Raucci, R. et al. (2011)** 'Biochimica et Biophysica Acta Structural and functional studies of the human selenium binding protein-1 and its involvement in hepatocellular carcinoma', *BBA - Proteins and Proteomics*. Elsevier B.V., 1814(4), pp. 513–522. doi: 10.1016/j.bbapap.2011.02.006.
- Reti-Sehop (2014)** 'Cáncer Infantil En España', pp. 1–6.
- Pellanda, H (2013)** 'Betaine homocysteine methyltransferase (BHMT) -dependent remethylation pathway in human healthy and tumoral liver', 51(3), pp. 617–621. doi: 10.1515/ccim-2012-0689.
- Robinson, M. and Oshlack, A. (2010)** 'A scaling normalization method for differential expression analysis of RNA-seq data', *Genome biology*, 11(3), pp. 1–9. doi: 10.1186/gb-2010-11-3-r25.
- Ruck, P. et al. (2000)** 'Ep-CAM in malignant liver tumours.', *The Journal of pathology*, 191(1), pp. 102–3. doi: 10.1002/(SICI)1096-9896(200005)191:1<102::AID-PATH542>3.0.CO;2-X.
- Rumbajan, J. M. et al. (2013)** 'Comprehensive analyses of imprinted differentially methylated regions reveal epigenetic and genetic characteristics in hepatoblastoma.', *BMC cancer*, 13, p. 608. doi: 10.1186/1471-2407-13-608.
- Rusolo, F. et al. (2013)** 'Evaluation of Selenite Effects on Selenoproteins and Cytokine in Human Hepatoma Cell Lines', (ii), pp. 2549–2562. doi: 10.3390/molecules18032549.
- Ryland, G. L. et al. (2015)** 'Loss of heterozygosity: what is it good for?', *BMC Medical Genomics*. BMC Medical Genomics, 8(1), p. 45. doi: 10.1186/s12920-015-0123-z.
- Sainati, L. et al. (2002)** 'Fluorescence in situ hybridization improves cytogenetic results in the analysis of hepatoblastoma', *Cancer Genetics and Cytogenetics*, 134(1), pp. 18–20. doi: 10.1016/S0165-4608(01)00586-6.
- Sakamoto, L. H. T. et al. (2010)** 'MT1G hypermethylation: A potential prognostic marker for hepatoblastoma', *Pediatric Research*, 67(4), pp. 387–393. doi: 10.1203/PDR.0b013e3181d01863.
- Salari, K., Tibshirani, R. and Pollack, J. R. (2009)** 'DR-Integrator: A new analytic tool for integrating DNA copy number and gene expression data', *Bioinformatics*, 26(3), pp. 414–416. doi: 10.1093/bioinformatics/btp702.
- Schmid, I. and Schweinitz, D. Von (2017)** 'Pediatric hepatocellular carcinoma: challenges and solutions', *Journal of Hepatocellular Carcinoma*, 4, pp. 15–21. doi: 10.2147/JHC.S94008.
- Schulze, K. et al. (2015)** 'Exome sequencing of hepatocellular carcinomas identifies new mutational signatures and potential therapeutic targets', *Nature Genetics*, 47(5), pp. 505–511. doi: 10.1038/ng.3252.
- von Schweinitz, D. et al. (1997)** 'Efficiency and toxicity of ifosfamide, cisplatin and doxorubicin in the treatment of childhood hepatoblastoma. Study Committee of the Cooperative Paediatric Liver Tumour Study HB89 of the German Society for Paediatric Oncology and Haematology', *European journal of cancer (Oxford, England: 1990)*, 33(8), pp. 1243–1249. Available at: [papers3://publication/uid/C5AA8603-7EB5-4548-B8B7-64E66EED6B81](https://pubmed.ncbi.nlm.nih.gov/94008/).

References

- Scotting, P. J., Walker, D. A. and Perilongo, G. (2005)** 'Childhood solid tumours: a developmental disorder', *Nat Rev Cancer*, 5(6), pp. 481–488. doi: 10.1038/nrc1633.
- Scully, O. J. et al. (2015)** 'Complement component 1, q subcomponent binding protein is a marker for proliferation in breast cancer', *Experimental Biology and Medicine*, 240(7), pp. 846–853. doi: 10.1177/1535370214565075.
- Shen, Q. et al. (2012)** 'Serum DKK1 as a protein biomarker for the diagnosis of hepatocellular carcinoma: A large-scale, multicentre study', *The Lancet Oncology*. Elsevier Ltd, 13(8), pp. 817–826. doi: 10.1016/S1470-2045(12)70233-4.
- Shih, Y. L. et al. (2007)** 'SFRP1 suppressed hepatoma cells growth through Wnt canonical signaling pathway', *International Journal of Cancer*, 121(5), pp. 1028–1035. doi: 10.1002/ijc.22750.
- Sia, D. et al. (2013)** 'Intrahepatic cholangiocarcinoma: pathogenesis and rationale for molecular therapies', *Oncogene*. Nature Publishing Group, 32(41), pp. 4861–4870. doi: 10.1038/onc.2012.617.
- Simon, E. P. et al. (2015)** 'Transcriptomic characterization of fibrolamellar hepatocellular carcinoma', *Proceedings of the National Academy of Sciences*, 112(44), pp. E5916–E5925. doi: 10.1073/pnas.1424894112.
- Sorensen, P. H. B. et al. (2002)** 'PAX3-FKHR and PAX7-FKHR gene fusions are prognostic indicators in alveolar rhabdomyosarcoma: A report from the Children's Oncology Group', *Journal of Clinical Oncology*, 20(11), pp. 2672–2679. doi: 10.1200/JCO.2002.03.137.
- Sorenson, E. C. et al. (2017)** 'Genome and transcriptome profiling of fibrolamellar hepatocellular carcinoma demonstrates p53 and IGF2BP1 dysregulation', *PLoS ONE*, 12(5), pp. 1–17. doi: 10.1371/journal.pone.0176562.
- Spector, L. G. and Birch, J. (2012)** 'The epidemiology of hepatoblastoma', *Pediatric Blood and Cancer*. doi: 10.1002/pbc.24215.
- Spector, L. G., Feusner, J. H. and Ross, J. A. (2004)** 'Hepatoblastoma and low birth weight [1]', *Pediatric Blood and Cancer*, 43(6), p. 706. doi: 10.1002/pbc.20122.
- Stasio, M. D. I. et al. (2011)** 'A possible predictive marker of progression for hepatocellular carcinoma', (14), pp. 1247–1251. doi: 10.3892/ol.2011.378.
- Steenman, M. et al. (1999)** 'Comparative genomic hybridization analysis of hepatoblastomas: additional evidence for a genetic link with Wilms tumor and rhabdomyosarcoma', *Cytogenetics and Cell Genetics*, 86, pp. 157–161.
- Stejskalová, E. et al. (2009)** 'Cytogenetic and array comparative genomic hybridization analysis of a series of hepatoblastomas.', *Cancer genetics and cytogenetics*, 194(2), pp. 82–7. doi: 10.1016/j.cancergencyto.2009.06.001.
- Sumazin, P. et al. (2017)** 'Genomic analysis of hepatoblastoma identifies distinct molecular and prognostic subgroups', *Hepatology*, 65(1), pp. 104–121. doi: 10.1002/hep.28888.
- Sun, S. et al. (2010)** 'Circulating Lamin B1 (LMNB1) Biomarker Detects Early Stages of Liver Cancer in Patients research articles', *Journal of proteome research*, 1, pp. 70–78.
- Surace, C. et al. (2002)** 'Fluorescent in situ hybridization (FISH) reveals frequent and recurrent numerical and structural abnormalities in hepatoblastoma with no informative karyotype', *Medical and Pediatric Oncology*, 39(5), pp. 536–539. doi: 10.1002/mpo.10181.
- Suzuki, M. et al. (2008)** 'Whole-genome profiling of chromosomal aberrations in hepatoblastoma using high-density single-nucleotide polymorphism genotyping microarrays', *Cancer Science*, 29(3), pp. 564–570. doi: 10.1111/j.1349-7006.2007.00710.x.
- Tan, G. S. et al. (2014)** 'Novel Proteomic Biomarker Panel for Prediction of Aggressive Metastatic Hepatocellular Carcinoma Relapse in Surgically Resectable Patients', *Journal of proteome research*.
- Tan, L. et al. (2016)** 'Distinct set of chromosomal aberrations in childhood hepatocellular carcinoma is correlated to hepatitis B virus infection', *Cancer Genetics*. Elsevier Inc., 209(3), pp. 87–96. doi: 10.1016/j.cancergen.2015.12.010.
- Tanaka, Y., Inoue, T. and Horie, H. (2013)** 'International pediatric liver cancer pathological classification: Current trend', *International Journal of Clinical Oncology*, 18(6), pp. 946–954. doi: 10.1007/s10147-013-0624-8.
- Taniguchi, K. et al. (2002)** 'Mutational spectrum of β -catenin, AXIN1, and AXIN2 in hepatocellular carcinomas and hepatoblastomas', *Oncogene*, 21(31), pp. 4863–4871. doi: 10.1038/sj.onc.1205591.
- Tao, J. et al. (2015)** 'Induction of Hepatocarcinogenesis in Mice', 147(3), pp. 690–701. doi: 10.1053/j.gastro.2014.05.004.Activation.
- Tao, Y. M., Liu, Z. and Liu, H. L. (2013)** 'Dickkopf-1 (DKK1) promotes invasion and metastasis of hepatocellular carcinoma', *Digestive and Liver Disease*, 45(3), pp. 251–257. doi: 10.1016/j.dld.2012.10.020.

- Terracciano, L. M. et al. (2003)** 'Comparative genomic hybridization analysis of hepatoblastoma reveals high frequency of X-chromosome gains and similarities between epithelial and stromal components', *Human Pathology*, 34(9), pp. 864–871. doi: 10.1016/S0046-8177(03)00351-4.
- The GATK Best Practices for variant calling on RNAseq, in full detail (2014)**. Available at: <http://gatkforums.broadinstitute.org/gatk/discussion/3892/the-gatk-best-practices-for-variant-calling-on-rnaseq-in-full-detail>.
- Tian, S. Y. et al. (2014)** 'Expression of leucine aminopeptidase 3 (LAP3) correlates with prognosis and malignant development of human hepatocellular carcinoma (HCC)', *International Journal of Clinical and Experimental Pathology*, 7(7), pp. 3752–3762.
- Tomizawa, M. and Saisho, H. (2006)** 'Signaling pathway of insulin-like growth factor-II as a target of molecular therapy for hepatoblastoma', *World Journal of Gastroenterology*, 12(40), pp. 6531–6535.
- Tomlinson, G. E. et al. (2005)** 'Cytogenetic Evaluation of a Large Series of Hepatoblastomas : Numerical Abnormalities with Recurring Aberrations Involving 1q12 – q21', 184(April), pp. 177–184. doi: 10.1002/gcc.20227.
- Tomlinson, G. E. and Kappler, R. (2012)** 'Genetics and epigenetics of hepatoblastoma', *Pediatric Blood and Cancer*, 59, pp. 785–792. doi: 10.1002/pbc.24213.
- Trobaugh-Lothario, A. D. et al. (2009)** 'Small Cell Undifferentiated Variant of Hepatoblastoma: Adverse Clinical and Molecular Features Similar to Rhabdoid Tumors', *Pediatric Blood and Cancer*, 52, pp. 328–334. doi: DOI 10.1002/pbc.21834.
- Tsang, T. Y. et al. (2009)** 'Mechanistic study on growth suppression and apoptosis induction by targeting hepatoma-derived growth factor in human hepatocellular carcinoma HepG2 cells', *Cell Physiol Biochem*, 24, pp. 253–262. doi: 10.1159/000233250.
- Venkatramani, R. et al. (2012)** 'Current and future management strategies for relapsed or progressive hepatoblastoma', *Pediatric Drugs*, 14(4), pp. 221–232. doi: 10.2165/11597740-000000000-00000.
- Viana-Pereira, M. et al. (2017)** 'Study of hTERT and Histone 3 Mutations in Medulloblastoma', *Pathobiology*, 84(2), pp. 108–113. doi: 10.1159/000448922.
- Vivanco, I. and Sawyers, C. L. (2002)** 'The phosphatidylinositol 3-Kinase–AKT pathway in human cancer', *Nature Reviews Cancer*, 2(7), pp. 489–501. doi: 10.1038/nrc839.
- Vogelstein, B. et al. (2013)** 'Cancer Genome Landscapes', *Science*, 339(6127), pp. 1546–1558. doi: 10.1126/science.1235122.Cancer.
- Wang, J. et al. (2015)** 'Elevated expression of HABP1 is a novel prognostic indicator in triple-negative breast cancers.', *Tumour biology: the journal of the International Society for Oncodevelopmental Biology and Medicine*, 36(6), pp. 4793–9. doi: 10.1007/s13277-015-3131-x.
- Wang, L. L. et al. (2010)** 'Effects of neoadjuvant chemotherapy on hepatoblastoma: a morphologic and immunohistochemical study.', *The American journal of surgical pathology*, 34(3), pp. 287–99. doi: 10.1097/PAS.0b013e3181ce5f1e.
- Ward, S. C. et al. (2010)** 'Fibrolamellar carcinoma of the liver exhibits immunohistochemical evidence of both hepatocyte and bile duct differentiation.', *Modern pathology*. Nature Publishing Group, 23(9), pp. 1180–90. doi: 10.1038/modpathol.2010.105.
- Waxman, S. and Wurmbach, E. (2007)** 'De-regulation of common housekeeping genes in hepatocellular carcinoma.', *BMC genomics*, 8(1), p. 243. doi: 10.1186/1471-2164-8-243.
- Weber, R. G. et al. (2000)** 'Characterization of genomic alterations in hepatoblastomas. A role for gains on chromosomes 8q and 20 as predictors of poor outcome.', *The American journal of pathology*, 157(2), pp. 571–8. doi: 10.1016/S0002-9440(10)64567-1.
- Weeda, V. B. et al. (2013)** 'Fibrolamellar variant of hepatocellular carcinoma does not have a better survival than conventional hepatocellular carcinoma - Results and treatment recommendations from the Childhood Liver Tumour Strategy Group (SIOPEL) experience', *European Journal of Cancer*, 49(12), pp. 2698–2704. doi: 10.1016/j.ejca.2013.04.012.
- Wei, X. et al. (2015)** 'Chloride intracellular channel 1 participates in migration and invasion of hepatocellular carcinoma by targeting maspin', *Journal of Gastroenterology and Hepatology*, 30, pp. 208–216. doi: 10.1111/jgh.12668.
- Wei, Y. et al. (2000)** 'Activation of beta-catenin in epithelial and mesenchymal hepatoblastomas.', *Oncogene*, 19(4), pp. 498–504. doi: 10.1038/sj.onc.1203356.
- Weinberg, A. and Finegold, M. (1983)** 'Primary hepatic tumors of childhood.', *Human Pathology*, 14(6), pp. 512–37.
- Wimbauer, F. et al. (2012)** 'Regulation of interferon pathway in 2-methoxyestradiol-treated osteosarcoma cells', *BMC Cancer*. BioMed Central Ltd, 12(1), p. 93. doi: 10.1186/1471-2407-12-93.
- Wirhth, O. et al. (2003)** 'Overexpression of human Dickkopf-1, an antagonist of wingless/WNT signaling,

References

- in human hepatoblastomas and Wilms' tumors.', *Laboratory Investigation*, 83(3), pp. 429–34.
- Wu, D. (2010)** 'GSK3: a multifaceted kinase in Wnt signaling Dianqing', *Trends in Biochemical Sciences*, 35(3), pp. 161–168. doi: 10.1016/j.tibs.2009.10.002.
- Xia, Z., Zhang, N. and Ding, D. (2014)** 'Proliferation and migration of hepatoblastoma cells are mediated by IRS-4 via PI3K/Akt pathways', *International Journal of Clinical and Experimental Medicine*, 7(10), pp. 3763–3769.
- Xin, H. et al. (2014)** 'Establishment and characterization of 7 novel hepatocellular carcinoma cell lines from patient-derived tumor xenografts', *PLoS ONE*, 9(1), pp. 1–9. doi: 10.1371/journal.pone.0085308.
- Yamashita, T. et al. (2008)** 'EpCAM and α -fetoprotein expression defines novel prognostic subtypes of hepatocellular carcinoma', *Cancer Research*, 68(5), pp. 1451–1461. doi: 10.1158/0008-5472.CAN-07-6013.
- Yamashita, T. et al. (2009)** 'EpCAM-Positive Hepatocellular Carcinoma Cells Are Tumor-Initiating Cells With Stem/Progenitor Cell Features', *Gastroenterology*. AGA Institute American Gastroenterological Association, 136(3), p. 1012–1024.e4. doi: 10.1053/j.gastro.2008.12.004.
- Yang, H. et al. (2013)** 'Dickkopf-1: as a diagnostic and prognostic serum marker for early hepatocellular carcinoma.', *The International Journal of Biological Markers*, 28(3), pp. 286–97. doi: 10.5301/ijbm.5000015.
- Yang, Z. et al. (2015)** 'Upregulation of heat shock proteins (HSPA12A, HSP90B1, HSPA4, HSPA5 and HSPA6) in tumour tissues is associated with poor outcomes from HBV-related early-stage hepatocellular carcinoma', *International Journal of Medical Sciences*, 12(3), pp. 256–263. doi: 10.7150/ijms.10735.
- Yimlamai, D. et al. (2014)** 'Hippo pathway activity influences liver cell fate', *Cell*. Elsevier Inc., 157(6), pp. 1324–1338. doi: 10.1016/j.cell.2014.03.060.
- Yoshida, K. et al. (2006)** 'Hepatoma-derived growth factor is a novel prognostic factor for hepatocellular carcinoma.', *Annals of surgical oncology*, 13(2), pp. 159–167. doi: 10.1245/ASO.2006.11.035.
- Yu, B. et al. (2009)** 'Elevated expression of DKK1 is associated with cytoplasmic/nuclear β -catenin accumulation and poor prognosis in hepatocellular carcinomas', *Journal of Hepatology*. European Association for the Study of the Liver, 50(5), pp. 948–957. doi: 10.1016/j.jhep.2008.11.020.
- Yu, G. and Wang, J. (2013)** 'Significance of hyaluronan binding protein (HABP1/P32/gC1qR) expression in advanced serous ovarian cancer patients', *Experimental and Molecular Pathology*, 94(1), pp. 210–215. doi: 10.1016/j.yexmp.2012.06.007.
- Yu, H. et al. (2013)** 'Elevated expression of hyaluronic acid binding protein 1 (HABP1)/P32/C1QBP is a novel indicator for lymph node and peritoneal metastasis of epithelial ovarian cancer patients', *Tumor Biology*, 34(6), pp. 3981–3987. doi: 10.1007/s13277-013-0986-6.
- Yu, Z. et al. (2014)** 'Using a yeast two-hybrid system to identify FTCD as a new regulator for HIF-1 α in HepG2 cells', *Cellular Signalling*. Elsevier Inc., 26(7), pp. 1560–1566. doi: 10.1016/j.cellsig.2014.03.016.
- Zarzosa, P. et al. (2017)** 'Patient-derived xenografts for childhood solid tumors: a valuable tool to test new drugs and personalize treatments', *Clinical and Translational Oncology*, 19(1), pp. 44–50. doi: 10.1007/s12094-016-1557-2.
- Zatkova, A. et al. (2004)** 'Amplification and overexpression of the IGF2 regulator PLAG1 in hepatoblastoma.', *Genes, chromosomes & cancer*, 39(2), pp. 126–37. doi: 10.1002/gcc.10307.
- Zen, Y. et al. (2014)** 'Childhood hepatocellular carcinoma: A clinicopathological study of 12 cases with special reference to EpCAM', *Histopathology*, 64(5), pp. 671–682. doi: 10.1111/his.12312.
- Zha, R. et al. (2014)** 'Genome-Wide Screening Identified That miR-134 Acts as a Metastasis Suppressor by Targeting Integrin β 1 in Hepatocellular Carcinoma', 9(2), p. e87665. doi: 10.1371/journal.pone.0087665.
- Zhang, H. et al. (2014)** 'Genetic variations in IDH gene as prognosis predictors in TACE-treated hepatocellular carcinoma patients', *Medical oncology (Northwood, London, England)*, 31(11), p. 278. doi: 10.1007/s12032-014-0278-z.
- Zhang, J. et al. (2015)** '[Association of chromosome 17q copy number variation with overall survival of patients with hepatocellular carcinoma and screening of potential target genes].', *Zhonghua Yi Xue Yi Chuan Xue Za Zhi*, 32(5), pp. 615–9. doi: 10.3760/cma.j.issn.1003-9406.2015.05.002.
- Zhang, M. et al. (2017)** 'Hyaluronic acid binding protein 1 overexpression is an indicator for disease-free survival in cervical cancer', *International Journal of Clinical Oncology*, 22(2), pp. 347–352. doi: 10.1007/s10147-016-1077-7.
- Zhang, S. et al. (2013)** 'Chloride intracellular channel 1 is overexpression in hepatic tumor and correlates with a poor prognosis', *Acta pathologica, microbiologica et immunologica scandinavica*, 6(Clic), pp. 1047–1053. doi: 10.1111/apm.12093.

- Zhang, T. et al. (2013)** 'The Contributions of HIF-Target Genes to Tumor Growth in RCC', *PLoS ONE*, 8(11), pp. 1–13. doi: 10.1371/journal.pone.0080544.
- Zhao, J. et al. (2015)** 'Overexpression of HABP1 correlated with clinicopathological characteristics and unfavorable prognosis in endometrial cancer', *Tumor Biology*, 36(2), pp. 1299–1306. doi: 10.1007/s13277-014-2761-8.
- Zheng, Q., Ye, J. and Cao, J. (2014)** 'Translational regulator eIF2a in tumor', *Tumor Biology*, 35(7), pp. 6255–6264. doi: 10.1007/s13277-014-1789-0.
- Zhou, S. et al. (2017)** 'Glypican 3 as a Serum Marker for Hepatoblastoma', *Scientific Reports*, 7(April), p. 45932. doi: 10.1038/srep45932.
- Zimmermann, A. (2005)** 'The emerging family of hepatoblastoma tumours: From ontogenesis to oncogenesis', *European Journal of Cancer*, 41(11), pp. 1503–1514. doi: 10.1016/j.ejca.2005.02.035.
- Zsiros, J. et al. (2013)** 'Dose-dense cisplatin-based chemotherapy and surgery for children with high-risk hepatoblastoma (SIOPEL-4): A prospective, single-arm, feasibility study', *The Lancet Oncology*, 14(9), pp. 834–842. doi: 10.1016/S1470-2045(13)70272-9.
- Zsiros, J. et al. (2010)** 'Successful treatment of childhood high-risk hepatoblastoma with dose-intensive multiagent chemotherapy and surgery: Final results of the SIOPEL-3HR study', *Journal of Clinical Oncology*, 28(15), pp. 2584–2590. doi: 10.1200/JCO.2009.22.4857.
- Zygulska, A. L., Krzemieniecki, K. and Pierzchalski, P. (2017)** 'Hippo pathway - brief overview of its relevance in cancer', *Journal of Physiology and Pharmacology*, 68(3), pp. 311–335.

8. ACKNOWLEDGEMENTS

Acknowledgements

Agraïments

Agradecimientos

Gràcies a la meua directora de tesi, la Dra Carolina Armengol, per haver-me donat la oportunitat d'iniciar-me en la recerca i de participar en un projecte tan especial com aquest.

Gràcies a tota la gent del grup: les dels inicis, Sonia i Isa, que em van acompanyar durant els meus primers mesos al lab. A la Laura, gràcies per tota la teva feina i pel teu suport, un plaer haver format el “*Pipet girls team*” amb tu! Als del final: Kim, Juan i Montse. I a totes les estudiants que han aportat el seu granet de sorra: Orfhlaith, Vicky, Samara, Fiorela i especialment a la María per la seva implicació des del minut zero i per tots els moments viscuts al *lab* i totes les converses al tren i al bus (fins i tot quan conduïa la kamikaze!).

A tota la gent del servei de digestiu, començant pel Dr Ramon Planas que em va donar la oportunitat de formar-ne part. En Ramon Bartolí, per estar sempre disposat a donar-me un cop de ma, sobretot amb la burocràcia del ciber. A la Marga, l'Helena, la Rosa. A tots els d'inflamatòria, en especial en Josep, la Vio i l'Arce, per tots els bons moments viscuts al *lab* i als congressos, per la vostra ajuda i la vostra simpatia. Gràcies!

A todos los miembros del Grupo Español para el Estudio de los Tumores Hepáticos Infantiles y a todos los que forman parte de esta red: del Hospital Vall d'Hebron, Tino Sábado, Marta Garrido, a Gabriela Guillén y José Andrés Molino por dejarme ver muy de cerca su increíble trabajo, a Aroa Soriano; del Hospital de La Paz, Laura Guerra, Diego Plaza, Yasmina Mozo, Manuel López de Santamaría, Francisco Hernández; Maria Elena Mateos... por su esfuerzo y dedicación, porque a pesar de su carga de trabajo somos capaces de obtener muestras de muchísimos pacientes. Sin vuestro trabajo, sería imposible realizar el nuestro. ¡Gracias!

Infinites gràcies a tots els pacients i als seus pares, que en un moment tan delicat, van decidir apostar per la recerca i confiar en nosaltres, pensant que la seva participació desinteressada en el projecte podria servir, algun dia, per ajudar a altres nens i nenes. Tot el nostre esforç és per a ells.

I would like to thank Dr. Marie-Annick Buendia and Dr. Stefano Cairo for their contribution to this work, both with samples and ideas.

Moltíssimes gràcies a la Lara Nonell i a la Magda Arnal del Servei d'Anàlisi de Microarrays de l'IMIM, per tota la feina feta, però sobretot, per la paciència i per apropar-me una mica més al món de l'estadística i la bioinformàtica!

Quiero agradecer a Mikel Azkargorta su impecable trabajo en el estudio proteomico y su inagotable paciencia resolviendo nuestras dudas y repitiendo los

Acknowledgements

análisis las veces que hacía falta. Extiendo el agradecimiento a Felix Elortza por su dedicación al proyecto.

I would like to thank Llovet's lab, Dr JM Llovet, Daniela Sia, Olga Kuchuk and also Nicholas Akers and Bojan Losic for the incredible work done with RNAseq data.

A la Mar Mallo, gràcies per totes les hores invertides en el projecte i per les tardes d'estiu davant de l'ordinador analitzant els Cytoscans. Amb la teva infinita paciència vaig a aprendre a interpretar els *allele peaks* i (encara que semblava impossible) a passar-m'ho bé fent-ho!

A l'equip d'Immunitat Innata: vull agrair a la Dra Maria Rosa Sarrias, per les seves crítiques constructives i per tot el temps dedicat, directa o indirectament, al projecte. A Lucía, por haber sido como mi hermana mayor del lab en los duros inicios. A la Gemma, companya des del principi, compartint penes i alegries i l'estrès dels group meetings, qui ens hauria dit que acabaríem fent presentacions en anglès com xurros?! I per aquesta recta final que ens farà una mica més lliures!. A Cris, ¡qué bien me habría ido conocerte antes! Por tu ayuda, por desprender pasión por la ciencia por todos tus poros, por tu motivación, y sobre todo, por haberme hecho descubrir el mejor restaurante thai de Amsterdam, ¡Gracias! A l'Erica per tot l'esforç i pel teu bon caràcter, gràcies!

A la Laia Pérez i la Irian del Banc de tumors. Per estar sempre atentes a qualsevol HCC i per fer possible tot el que us demanàvem, gràcies.

Si fa uns anys m'haguessin dit que acabaria a Can Ruti fent el doctorat i vivint a Barcelona, hauria pensat que qui ho deia no em coneixia gens. Però aquí estic, feliç de que la vida fes aquest gir. Aquests 4 anys i mig no han estat fàcils, però tornaria a començar encara que només fos per tornar a conèixer la gent que m'ha acompanyat. Sou la canya.

Gracias a mis chochipeguis, Vanesa, Noemí y Sara, por haberme enseñado a reírme de todo y de todos, empezando conmigo. Vosotras iniciasteis en mí un cambio, y lo sabéis. ¿Cómo podría olvidar nuestros desayunos, meriendas, cenas, confesiones importantes en el Magic o nuestro viaje a Madrid? Ah! Gracias Noemí por haberme convertido en tita de Dennis, ¡qué preciosidad!

A l'Alfonsina, la mallorquina més alegre que va venir a Badalona per obrir-me al món. No puc ni enumerar tot el que hem viscut aquests anys i tot el que he après al teu costat. *Si deixes sortir totes les teves pors tindràs més espai per viure tots els teus somnis.* Gràcies!

Gràcies a l'Anna, per la teva alegria i optimisme. Perquè un esdeveniment molt especial ens ha unit encara més i espero que només sigui el principi de moltes més partides a vuit mans (i nits de càmping, qui sap).

Gracias también a las niñas (y niño) de la comida, Marian, Laura y Jon, por todas las conversaciones, risas y recetas compartidas. Por hacer que la hora de la comida fuera un momento de desconexión muy necesario. I especialment a l'Eva

i la Gisela, per haver-me escoltat i pels vostres consells, per haver-me ajudat a veure una sortida quan semblava impossible, gràcies!

A tota la gent que, d'una manera o altra, m'ha fet més fàcil i agradable l'experiència: a l'Alba, per la companyia al japonès i pels breaks en els inicis; a la Jovita, font inesgotable de consells i bon humor; a l'Eudald, pels milers de vegades que vam veure caure la nit des del japonès; en Nacho, última incorporació al japonès però que t'has fet estimar des del minut zero; a en Vicenç, la Vera, la Sara C, i la Sara B, pel vostre bon rotllo, pels sopars i pels consells; a Ana, una de las mejores cosas que me llevaré del IGTP aunque solo coincidimos un año; a Raquel, la investigadora-joyera-fotógrafa más graciosa, creativa y genial del mundo; a Kerrie, por los buenos momentos en el *lab* y los machaques en el gym. A todos/as vosotros/as, Gràcies!!

A mi Maribel, la cara y el corazón del IGTP. Eres la pieza que hace que todo funcione, gracias.

No em puc oblidar de la gent del ICO, en Pepe pel seu bon rotllo i per la seva ajuda fent *pellets*! I a la Cris, per ser tan genial, gràcies!

I, encara que impliqui anar molt enrere en el temps, gràcies a la Júlia i la Hortènsia, vosaltres vau fer que sentís més que curiositat per la biologia i la bioquímica, i que em decidís a començar una carrera que m'ha portat fins aquí.

A la Marina, la de tota la vida. Per tants anys d'amistat i confiança absoluta, perquè malgrat la distància sempre t'he sentit molt a prop, gràcies!

Gràcies a la Marta i l'Anna per demostrar-me que les amistats de la Universitat són inacabables. Encara que estiguem repartides pel territori, les nostres trobades de converses eternes fan que sembli que ens haguéssim vist ahir. Per totes les hores a la biblioteca, treballs, pràctiques, nits al Cercle, Girona, Londres, Madrid, Catalunya Nord i sobretot, pel vostre suport en EL pitjor moment, gràcies!

Gràcies a la Carla, en Kinki i en Christian. Per tot el vostre suport aquests anys, per interessar-vos per com avançava la tesi tot i semblar-vos tant estrany de què us parlava, pels dinars i sopars al König que han evolucionat fins a les festes a Palol. Per infinites anècdotes, moments, riures, balls, barbacoes. Per una amistat que no té preu.

A en Jaume, per escoltar-me, aconsellar-me i donar-me suport, gràcies.

A la mama, gràcies per inculcar-me el valor del treball i de l'esforç des de ben petita.

Al papa, gràcies per ensenyar-me que res és impossible, a tenir esperança, a ser tossuda i perseverant, a no rendir-me.

A la Carme i en Pau, per haver-me acollit i tractat com una filla. Per tot el seu suport i comprensió, gràcies! A en Pau i la Sira, per ser-hi sempre, per escoltar-me, per ajudar-me quan ho he necessitat, gràcies!

Acknowledgements

A l'Ona i en Josep, els nens més preciosos del planeta, que algun dia ja no seran tan nens i estic segura que es convertiran en grans persones. Per deixar-me fer-me gran al seu costat i aprendre amb ells, per l'alegria i l'amor que em donen, gràcies!

A en Miki, gràcies per haver-me tractat com una germana des del primer moment. Per haver-me acollit, aconsellat i acompanyat.

I als meus pilars:

A la Sílvia, pel teu suport. Per ajudar-me i fer-me costat sense dir-me el que havia de fer. Per ser forta, intel·ligent, perseverant. Per ser un exemple a seguir. Per donar-me motius per sentir-me afortunada. Per ser la millor germana que podria tenir. Sense el teu suport no hauria arribat ni a mig camí d'on soc avui. Gràcies.

A en Raül, per haver-me acompanyat en aquest camí i haver escollit quedar-te al meu costat fins i tot en els pitjors moments. Per creure en mi quan ni jo mateixa ho feia i fer-m'ho saber. Per la confiança, l'humor i l'amor. Per ser-hi sempre. Tot i que una paraula em sembla poc per dir-te com d'agraïda em sento, GRÀCIES.